**Univerzita Karlova v Praze**

**Přírodovědecká fakulta**

Studijní program: Geologie

**Bc. Filip Scheiner**

# Carbon and Oxygen Stable Isotope Ratio from Foraminiferal Tests as a Key to the Paleoenvironmental Interpretations in the Middle Miocene of the Carpathian Foredeep (Central Paratethys)

# Stabilní izotopy uhlíku a kyslíku ve schránkách foraminifer jako klíč k interpretaci paleoprostředí ve středním miocénu karpatské předhlubně (Centrální Paratetyda)

Diplomová práce

Vedoucí práce: doc. RNDr. Katarína Holcová CSc.

Praha 2015

**Prohlášení:**

Prohlašuji, že jsem závěrečnou práci zpracoval samostatně a že jsem uvedl všechny použité informační zdroje a literaturu. Tato práce ani její podstatná část nebyla předložena k získání jiného nebo stejného akademického titulu.

V Praze, 29.4 2015

Podpis

## Poděkování:

Chtěl bych poděkovat Grantové agentuře UK (GAUK) za financování projektu číslo 222214, jehož součástí je i tato práce. Dále bych rád poděkoval katedře Ústavu geologie a paleontologie rovněž za finanční pomoc této práci. Velký dík patří školitelce a vedoucí práce doc. RNDr. Kataríně Holcové CSc. za cenné připomínky, postřehy a všechen věnovaný čas. Dále bych rád poděkoval Mgr. Rastislavu Milovskému PhD., za provedení geochemických analýz a seznámení s použitou technologií. Dále bych rád poděkoval svým přátelům za poskytnuté připomínky ohledně jazykové stránky práce.

# Abstract

The (Lomnice) LOM-1 borehole records a nutrient-rich quiet environment of the outer shelf to upper bathyal in the Mid Badenian (sensu Hohenegger *et al.* (2014)) of the Carpathian Foredeep. The LOM-1 borehole is rich of a fossil content with a relatively good preservation. The studied section can be correlated with the interval from 14.6 Ma (the FO of *Orbulina* spp.) to 13.42 Ma (the LO of *Sphenolithus heteromorphus*) which agrees with the beginning of the "Middle Miocene Climate Transition".

The foraminifera for the carbon and oxygen stable isotope analysis were picked from the fraction 0.063-2 mm. The suitability for the stable isotope analysis was carefully evaluated based on the inner wall preservation. The isotopic analysis was done for fifteen samples with total 373 tests analyzed. Each analysis was performed from exactly one test. The following foraminiferal genera from different paleobiotops were used for the isotope analysis: *Globigerina bulloides*; *Orbulina universa, Praeorbulina glomerosa*; *Globigerinoides* spp.; *Uvigerina* spp.; *Heterolepa dutemplei*; *Cibicidoides* spp.; *Gyroidinoides* spp. and *Melonis pompilioides* to document the isotopic signal for the superficial and bottom waters. The oxygen and carbon isotope analysis from foraminiferal tests were used for the verification of the paleoecologic interpretations by Holcová *et al.* (submitted). The Benthic foraminiferal oxygen index was applied on the studied section.

The isotopic analysis results together with the benthic foraminiferal oxygen index were used for a detailed interpretation of the paleoenvironment in each sample. The interpretation documents the large variability and rapid changing of the paleoecological parameters, throughout the LOM-1 borehole. The observed relationship between the isotopic signal of *Melonis pompilioides* and *Gyroidinoides* spp. enabled the discussion about the ecologic preference of these particular species. Compared with the other isotopic studies in the Badenian of the Central Paratethys, the isotopic values show no global trends as reported by Báldi (2006) and Peryt (2013). Based on the isotopic signal of *G. bulloides* and *Orbulina universa,* the span of paleotemperatures was calculated. This span shows a good agreement with the paleotemperatures reported by Grunert *et al.* (2010) and Peryt (2013).

Keywords: carbon and oxygen stable isotopes; Central Paratethys; foraminifera; Mid Badenian; paleoecology; Carpathian Foredeep

# Abstrakt

Vrt Lomnice 1 (LOM-1) reprezentoval prostředí vnějšího šelfu až horního batyálu ve středním bádenu (dle Hohenegger *et al.* (2014)) karpatské předhlubně. Vrt Lomnice 1 je bohatý na fosilní materiál s dobrým stupněm zachování. Studovaný interval může být korelován s intervalem od 14,6 milionů let (na základě prvního výskytu rodu *Orbulina* spp.) do 13,42 milionů let (poslední výskyt druhu *Sphenolithus heteromorphus*), což koresponduje s počátkem středně miocénních změn označovaných jako „Middle Miocene Climate Transition".

Foraminifery pro analýzy stabilních izotopů uhlíku a kyslíku byly vybrány z frakce 0.063-2 mm. Vhodnost jednotlivých vzorků pro izotopické analýzy byla pečlivě zvážena na základě studia zachování vnitřní struktury schránky. Bylo analyzováno patnáct vzorků s celkem 373 jednotlivými schránkami, přičemž každá schránka reprezentuje právě jednu analýzu. Devět taxonů foraminifer vybraných na izotopické analýzy (*Globigerina bulloides*; *Orbulina universa, Praeorbulina glomerosa*; *Globigerinoides* spp.; *Uvigerina* spp.; *Heterolepa dutemplei*; *Cibicidoides* spp.; *Gyroidinoides* spp. a *Melonis pompilioides*) dokumentuje na základě odlišných biotopů izotopický signál povrchových, tak spodních vod. Výsledné izotopické analýzy byly použity k ověření interpretací paleoprostředí navrhovaných Holcovou *et al.* (sumitted).

Obsah kyslíku na mořském dně se vyjadřuje pomocí indexu nazývaného „Benthic foraminiferal oxygen index". V literatuře je navrženo několik způsobů výpočtu tohoto indexu. Testování třech možností výpočtu ukázalo minimální rozdíly v hodnotě indexu.

Výsledky izotopických analýz spolu s hodnotami „Benthic foraminiferal oxygen index" byly použity pro detailní interpretaci paleoprostředí v každém ze vzorků. Výsledná interpretace dokumentuje velkou variabilitu a rychlé změny paleoekologických parametrů ve vrtu LOM-1. Pozorovaný vztah mezi druhem *Melonis pompilioides* a rodem *Gyroidinoides* spp. umožnil diskuzi ohledně ekologických preferencí těchto dvou druhů. V porovnání s ostatními izotopickými studiemi z bádenu Centrální Paratetydy tyto výsledky nevykazují globální trendy, které publikovali Báldi (2006) a Peryt (2013). Na základě izotopického signálu z druhů *Globigerina bulloides* a *Orbulina universa* byla vypočítána paleoteplota. Vypočítaný rozsah paleoteplot se shoduje s rozsahy paleoteplot, které publikovali Grunert *et al.* (2010) a Peryt (2013).

Klíčová slova: stabilní izotopy uhlíku a kyslíku; Centrální Paratethyda; foraminifera; střední báden; paleoekologie; karpatská předhlubeň

# Table of content

# 1. Introduction

The first part of this study provides a complex overview of carbon and oxygen stable isotopes including basic knowledge of carbon and oxygen isotopes, fractionation, determination of isotopic ratios and a detailed description of the particular mechanisms affecting the global cycles of carbon and oxygen. It focuses in detail on different mechanisms controlling the isotopic ratios fixed in the foraminiferal tests. The following chapter is devoted to the Middle Miocene of the Central Paratethys. It provides basic information about the paleogegraphical context and complete stratigraphic summary of the Middle Miocene of the Central Paratethys. The Badenian period was characterized in detail including the biostratigraphical correlation, subdivision of the Badenian, paleogeography and paleoclimatology.

The LOM-1 borehole was chosen for the carbon and oxygen stable isotopic analysis due to the good preservation of fossil assemblages. The LOM-1 is rich in a fossil content, with a minimal taphonomic alteration of microfossil assemblages. The LOM-1 was studied by Holcová *et al.* (submitted) by using a multiproxy approach, thus in the end both studies could be compared. The suitability for the stable isotope analysis of carbon and oxygen was evaluated based on the inner wall structure preservation. The following foraminiferal genera from different paleobiotops were used for the isotope analysis: *Globigerina bulloides*; *Orbulina universa, Praeorbulina glomerosa*; *Globigerinoides* spp.; *Uvigerina* spp.; *Heterolepa dutemplei*; *Cibicidoides* spp.; *Gyroidinoides* spp. and *Melonis pompilioides.* Fifteen samples with 373 tests in total were analyzed. The analysis was performed by Geologický ústav SAV, Banská Bystrica, Slovakia. The overall external precision of 0.04‰ for $\delta^{13}C$ and 0.08‰ for $\delta^{18}O$ was reached for our analyses. The Benthic foraminiferal oxygen index was used in various models throughout the LOM-1 borehole.

Based on the isotopic analysis of foraminiferal tests and the benthic foraminiferal oxygen index data, the detailed interpretation of the paleoenvironment was done for each sample. This interpretation documents the large variability and rapid changing of the paleoecological parameters throughout the LOM-1 borehole. The results and interpretation was compared with the interpretation proposed by Holcová *et al.* (submitted). The isotopic data showed an interesting relationship between the isotopic signal of *Melonis pompilioides* and *Gyroidinoides* spp. The results were also compared with the other isotopic studies in the Badenian by Báldi (2006) and Peryt (2013). Based on the isotopic signal of *G. bulloides* and *Orbulina universa,* the range of paleotemperatures was calculated.

# 2. Isotopes

## 2.1. History

Analyses of stable oxygen and carbon isotopes from foraminiferal shells have played an important role in paleoceanography since the late fifties (e.g. Emiliani, 1955). Shackleton and Opdyke correlated the isotope stratigraphy with magnetic stratigraphy in 1973 and thus dated 22 recognizable isotopic stages. Analyzing the records Shackleton and Opdyke (1973) also demonstrated an important finding that the signal reflects fluctuations in global ice volume predominantly, while the temperature plays a secondary role. Their work started a widespread use of records in global stratigraphic correlations (Imbrie *et al.*, 1984b, 1992). Shackleton (1977a) studied downcore variations of records and showed their significance and a possible potential in studying water mass movement and paleoproductivity. He also postulated a connection between climatically induced changes in the terrestrial biosphere with observed carbonate dissolution cycles and the flux of dissolved $CO_2$ in the oceans (Sen Gupta, 1999).

## 2.2. Isotopes introduction

The mass of an atom is the function of the proton number and the neutron number as well. Several possible numbers of neutrons can combine with a given number of protons to form a stable nucleus. This phenomenon produces different isotopes of the same element, i.e. the atoms that have the same atomic number but different masses. For example, helium has 2 stable isotopes: $^{3}He$ and $^{4}He$. Both $^{3}He$ and $^{4}He$ have 2 protons and a matching number of electrons, but $^{4}He$ has 2 neutrons while $^{3}He$ has only 1. All isotopes of a given element contain, without exception, the same number and arrangement of electrons. The mass differences between different isotopes are particularly important in light elements. Molecules vibrate with a fundamental frequency which depends on the mass of the isotopes which they are composed of. The differences in the dissociation energy of the light and heavy isotopes show that the bonds formed by light isotopes are weaker than those bonds formed by heavy isotopes. The molecules comprised of the light isotopes react more easily than the molecules comprised of the heavy isotopes (White, 2013).

There are three stable isotopes of oxygen - $^{16}O$, $^{17}O$ and $^{18}O$. Relative natural abundances are 99.76% for $^{16}O$, 0.04% for $^{17}O$ and 0.20% for $^{18}O$. Any research on oxygen stable isotopes ratio concerns $^{18}O/^{16}O$ ratios. There are two stable isotopes of carbon - $^{12}C$ with a relative natural abundance of 98.89% and $^{13}C$ with a relative natural abundance of 1.11%. Partitioning of isotopes between substances is called fractionation. If $R_A$ and $R_B$ are the heavy/light isotope ratios for any two isotopes (e.g. $^{13}C/^{12}C$) in exchanging chemical compounds A and B, then the fractionation factor is defined as $\alpha_{A\text{-}B} = R_A/R_B$. Fractionation results from isotopic

exchange reactions and kinetic effects. These are so called “equilibrium isotope fractionation” processes and these processes are strictly temperature dependent. Kinetic effects cause deviations from equilibrium due to different rates of reaction for the various isotopic species. Important kinetic effects are also associated with diffusion (Sen Gupta, 1999).

The absolute abundances of minor isotopes (e.g. $^{18}O$ and $^{13}C$) cannot be precisely determined. It is possible to get quantitative estimates by comparing results for a known external standard (*std*) with those for the unknown sample (*sam*). These differences are defined as - $\delta_{sam}‰=10^3 \times (R_{sam} - R_{std})/R_{std}$. A positive δ value indicates enrichment in the heavy isotope relative to the standard and conversely a negative δ value indicates depletion relative to the standard (Sen Gupta, 1999).

The stable isotopes of oxygen and carbon in carbonates are analyzed by mass spectrometric determination of the mass ratios of carbon dioxide ($CO_2$) obtained from the sample by reaction of carbonate with phosphoric acid - $CaCO_3 + H_3PO_4 \leftrightarrow CaHPO_4 + CO_2 + H_2O$ (McCrea, 1950), with reference to a standard $CO_2$ of known isotopic composition. The standard for both oxygen and carbon in carbonates, is referred to as PDB (Pee Dee Belemnite), having $\delta\ ^{18}O = 0$ and $\delta\ ^{13}C = 0$, by definition (Epstein *et al.*, 1953). The PDB standard (no longer available) is a guard from *Belemnitella americana*, a cretaceous belemnite from Pee Dee Formation in North Carolina, USA (Friedman and O’Neil, 1977; Sen Gupta, 1999).

Various international standards have been running against PDB for comparative purposes up to present days. The final results of any research are required to be $\delta^{13}C$ and $\delta^{18}O$ relative to VPDB (Vienna PDB standard – international standard identical to PDB); (Swart *et al.,* 1991; Sen Gupta, 1999).

# 2.3. Oxygen Isotopes

## 2.3.1. Oxygen isotope ratio in seawater

Seawater $\delta^{18}O$ is in connection with the hydrological cycle (see Fig. 1) consisting of evaporation, atmospheric vapour transport and conversely return of freshwater to the ocean via precipitation and runoff, or iceberg melting. Furthermore, a long-term freshwater storage (e.g. ice sheets, also aquifers) significantly affects seawater $\delta^{18}O$. Any seasonal sea ice formation and melting impose strong local variability. The spatial $\delta^{18}O$ distribution in the oceans depends on mixing and advection of water masses from different source regions (Sen Gupta, 1999).

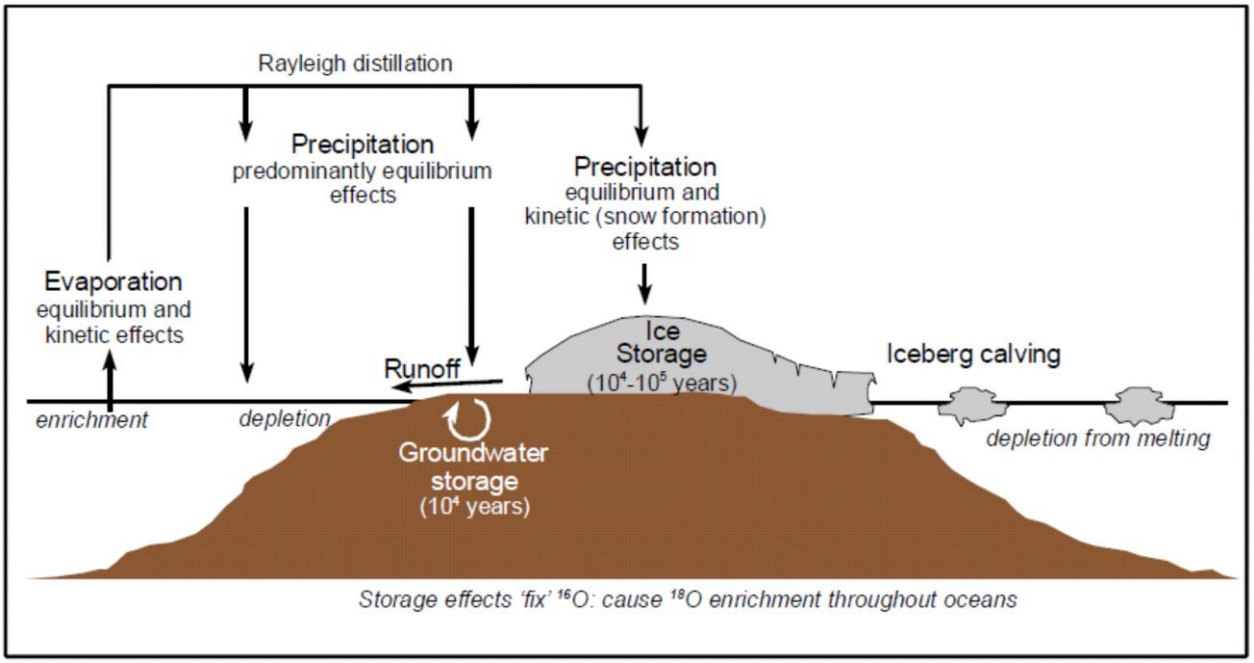


**Figure 1.** The hydrological cycle influences on oxygen isotope ratio. Effects on seawater are described in italics. From: Sen Gupta (1999)

## 2.3.2. Evaporation

Isotopic exchange at the sea-air interface is given by - $H_2{}^{16}O_{liquid} + H_2{}^{18}O_{vapor} \leftrightarrow H_2{}^{18}O_{liquid} + H_2{}^{16}O_{vapor}$. Because of higher vapour pressures, the lighter molecular species are preferentially enriched in the vapour phase (see Fig. 1). The fractionation factor for equilibrium exchange is $\alpha_{1\text{-}v} = [{}^{18}O/{}^{16}O]_l / [{}^{18}O/{}^{16}O]_v$. The most common used relationship between $\alpha_{1\text{-}v}$ and temperature is $\alpha_{1\text{-}v} = \exp\{(1.137T^{-2}) \times 10^3 - (0.4156T^{-1}) - 2.0667 \times 10^{-3}\}$, with $T$ in Kelvin. This relationship illustrates a decrease in fractionation with increasing temperature (Majoube, 1971; Sen Gupta, 1999). The $\delta^{18}O$ difference between seawater and vapor equals $10^3$ ln(α)‰ which at 20°C amounts to 9.8‰. The equilibrium enrichment factor ε equals α-1 and it is reported as a ‰ value (Sen Gupta, 1999).

There is also a kinetic fractionation linked with molecular diffusion within the boundary layer between the water-air interface and the turbulent region where no further fractionation occurs (Gonfiantini, 1986; Sen Gupta, 1999). The magnitude of the kinetic enrichment depends on relative air humidity in the turbulent region, changing by about 0.7‰ for every 5% change in relative humidity (Gonfiantini, 1986), and to a lesser extent on roughness of the water-atmosphere interface (Merlivat and Jouzel, 1979; Sen Gupta, 1999). Preferential uptake of lighter isotopes during evaporation increases $\delta^{18}O$ values in the remaining surface waters (Sen Gupta, 1999).

## 2.3.3. Precipitation and atmospheric water transport

Condensation acts in the opposite way towards evaporation (see Fig. 1). The kinetic effects are negligible and droplets are near equilibrium with atmospheric vapour (Ehhalt and Knott, 1965; Stewart, 1975). The first precipitation has a similar $\delta^{18}O$ to the original seawater, while longer pathways from the source region (= more rain out) cause increasing depletion in vapour and new precipitation. Successive condensations during the transport towards colder regions cause a relationship of 0.69‰°$C^{-1}$ between $\delta^{18}O$ of precipitation and temperature (between - 40°C and + 15°C); (Sen Gupta, 1999). High latitude precipitation is significantly more depleted than precipitation in the tropics (reaching -60‰ or less in Antarctica; (Lorius, 1983; Rozanski *et al.*, 1993). Above +15°C, the so called "amount effect" is dominant, with 1.5‰ depletion in the $\delta^{18}O$ of precipitation for every 100 mm increase in rainfall (Dansgaard, 1964; Craig and Gordon, 1965; Jouzel *et al.*, 1975; Stewart, 1975; Rozanski *et al.*, 1982, 1993; Merlivat and Jouzel, 1979; Sen Gupta, 1999).

Changes in $\delta^{18}O$ of precipitation affect the oceanic surface waters by direct addition of fresh water or addition via run-off. Arid areas show the evaporative surface water $\delta^{18}O$ enrichment. The regions in proximity to a river mouth are affected by the volumetrically weighted average of isotopic composition of precipitation over the catchment area. High-latitude rivers import freshwater with generally lower $\delta^{18}O$ values than low- latitude rivers (e.g. McKenzie: $\delta^{18}O$ ~ -20‰, Paraná: $\delta^{18}O$ ~ -4‰); (Rohling and Bigg, 1998; Sen Gupta, 1999).

The long-term storage of precipitation causes two main delayed responses. Calving icebergs from continental ice sheets are the main source of imported freshwater with fossil isotopic signatures. Similarly, but to a lesser extent, aquifers may also accumulate old waters with fossil isotopic signatures (not as old as in continental ice sheets; aquifers - $10^4$ years vs. continental ice sheets - $10^5$ years) and contribute to an import of water with fossil isotopic signatures (Sen Gupta, 1999).

## 2.3.4. Glacial ice-volume

Besides the delayed return of fossil signals, there is a long-term storage in glacial ice sheets and in major aquifers which also affects the global $\delta^{18}O$ budget (see Fig. 1). Storage time-scales (in the order of $10^4$ - $10^5$ years) exceed those of ocean ventilation (in the order of $10^3$ years). Due to this fact, the storage effects influence $\delta^{18}O$ values both in surface and deep waters. The most important fluctuations are related to the volume of glacial ice sheets. Ice sheets are built up by high latitude precipitation at very low temperatures and record extremely low $\delta^{18}O$ values. Preferential sequestration of $\delta^{16}O$ in ice sheets leaves the oceans enriched in $\delta^{18}O$. At the same time, a build up of ice volume lowers the global sea level. The relationship between sea level lowering and mean oceanic $\delta^{18}O$ increase approximates 0.012 ± 0.001‰$m^{-1}$ (Aharon, 1983; Labeyrie *et al.*, 1987; Shackleton, 1987; Fairbanks, 1989; Sen Gupta, 1999).

## 2.3.5. Sea ice freezing and melting

Newly formed sea ice is 2.57 ± 0.10‰ enriched relative to seawater $\delta^{18}O$ (Macdonald *et al.*, 1995). This difference causes a significant seasonal fluctuation associated with ice formation and melting (Strain and Tan, 1993). These seasonal influences do not necessarily cancel out in the long term, because due to sea ice formation there is an increase in surface-water salinity and this may lead to convection and transport of existing surface waters into the ocean interior (Rohling and Bigg, 1998; Sen Gupta, 1999). Large errors may arise in interpretations near sea-ice margins if these effects are overlooked (Sen Gupta, 1999).

## 2.3.6. Advection

Advection and mixing of water masses from different source areas are important for the basic $\delta^{18}O$ composition at any site. Each source area consists of a basin or region, where surface waters are imprinted with a characteristic $\delta^{18}O$ composition by the freshwater cycle (e.g. freezing/melting of sea ice, etc). This pre-set composition is like a conservative property for the newly formed watermass (if does not come into a contact with any further sources); (Weiss *et al.*, 1979; Fairbanks, 1982; Paren and Potter, 1984; Kipphut, 1990; Frew *et al.*, 1995). The $\delta^{18}O$ of a mixing endmember is a volumetrically weighted average of the $\delta^{18}O$ compositions of its components. Any change in the relative proportions or isotopic compositions of the mixing components affects the basic endmember $\delta^{18}O$ (Sen Gupta, 1999).

## 2.4. Oxygen isotope ratio in foraminiferal carbonate

The equilibrium fractionation between water and the various carbonate species ($CaCO_3$, $H_2CO_3$, $HCO_3^-$, $CO_3^{2-}$) determine an important temperature influence on the $\delta^{18}O$ of foraminiferal carbonate. Several processes cause deviations from equilibrium, both in planktonic and benthic foraminifera (Fairbanks and Wiebe, 1980; Duplessy *et al.*, 1981; Bouvier-Soumagnac and Duplessy, 1985; Woodruff *et al.*, 1980; Vincent *et al.*, 1981; Wefer and Berger, 1991; Sen Gupta, 1999).

### 2.4.1. Equilibrium fractionation

The overall reaction for precipitation of carbonate is - $Ca_2^+ + 2HCO_3^- \leftrightarrow CaCO_3 + CO_2 + H_2O$. Between 0°C and 500°C, the equilibrium fractionation factor $\alpha_{c\text{-}w}$ between calcite and water changes according to $\alpha_{c\text{-}w} = \exp\{(2.78T^{-2}) \times 10^3 - 3.39 \times 10^{-3}\}$, with $T$ in Kelvin (O'Neil *et al.*, 1969). The $\delta^{18}O$ change with temperature is more pronounced at low temperatures (up to 0.25‰°$C^{-1}$) than at higher temperatures (around 0.2‰°$C^{-1}$); (Kim and O'Neil, 1997).

Since temperature decreases with increasing depth in the surface ocean, vertical migrations influence the equilibrium fractionation. Many planktonic foraminiferal species show a $\delta^{18}O$ increase with growth that suggests calcification in deeper, colder waters (Emiliani, 1954; Berger, 1971; Emiliani, 1971; Berger *et al.*, 1978; Fairbanks *et al.*, 1982; Bouvier-Soumagnac and Duplessy, 1985; Kroon and Darling, 1995).

### 2.4.2. Deviations from equilibrium $\delta^{18}O$ in foraminiferal calcite

There are five main causes of disequilibrium: the ontogenetic effect; the symbiont photosynthesis effect; the respiration effect; the gametogenic calcite effect and the effect of changes in [$CO_3^{2-}$] (carbonate ion concentration). These various effects may operate in opposite ways. They are all essential for planktonic foraminifera, but many of them also for benthic foraminifera (Duplessy *et al.*, 1970; Woodruff *et al.*, 1980; Vincent *et al.*, 1981; Wefer and Berger, 1991; Sen Gupta, 1999).

## 2.4.3. Ontogenetic effect

With constant $\delta^{18}O$ of water and constant temperature (laboratory conditions), *Globigerina bulloides* documents a progressive $\delta^{18}O$ increase of up to 0.8‰ with shell development - juvenile chambers are strongly depleted (around 1.15‰ $\delta^{18}O$), while the final chamber is less depleted (around 0.30‰ $\delta^{18}O$), relative to equilibrium (Spero and Lea, 1996). The mass-balanced average of the individual chambers gives a whole-shell depletion of around 0.7‰ $\delta^{18}O$. A similar trend of increasing values through ontogeny was observed in $\delta^{13}C$, an explanation was offered in terms of an incorporation of metabolic (respired) $CO_2$ during calcification. The higher metabolic rates in juveniles would cause the strongest depletions, while adults gradually trend towards equilibrium (Sen Gupta, 1999).

The $\delta^{18}O$ trend is corroborated, to some extent, by reports of a size-dependent trend in *Globigerina bulloides* (Kroon and Darling, 1995). However, the trend in real ocean results appears to be smaller than that one observed under laboratory conditions. Reduced signal could be caused by vertical migrations from deeper, cooler waters during early life stages to shallow, warmer waters during later life stages (Spero and Lea, 1996; Bemis *et al.*, 1998; Sen Gupta, 1999).

## 2.4.4. Symbiont photosynthesis

*Globigerinoides sacculifer*, which is photosynthetic symbiont-bearing planktonic foraminifera, reflects no variations in shell $\delta^{18}O$ with ontogeny within the size range 350 – 850 μm (Spero and Lea, 1993). However, a distinct chamber $\delta^{18}O$ decrease is documented with increasing irradiance levels (Spero and Lea, 1993). A similar but weaker decrease with increasing irradiance occurs in photosynthetic symbiont-bearing *Orbulina universa* (Spero, 1992; Spero and Lea, 1993; Spero *et al.,* 1997). Increased growth rates were observed with increasing light intensities, corroborating observations of light-enhanced calcification rates under elevated irradiance (Ter Kuile and Erez, 1984). Decreasing $\delta^{18}O$ skeletal values with increasing growth rates were also repored by McConnaughey, (1989a) and Wefer and Berger, (1991); (Sen Gupta, 1999).

## 2.4.5. Respiration

Respiration does cause $\delta^{18}O$ depletion (Lane and Doyle, 1956). Relative to ambient dissolved oxygen, the oxygen used in respiration is depleted by 21‰ in near-shore, shallow waters (Kroopnick, 1975), and 11‰ in the deep ocean (Grossman, 1987). The $\delta^{18}O$ of ambient dissolved oxygen in surface waters commonly ranges around +24 to +26‰ (SMOW); (Kroopnick *et al.*, 1972; Kroopnick, 1975). Utilization of depleted respiratory products during calcification (Belanger *et al.*, 1981; Grossman, 1987) might cause skeletal $\delta^{18}O$ depletion (Sen Gupta, 1999).

## 2.4.6. Gametogenic calcite

Several planktonic foraminiferal species deposit an additional layer of calcite on the surface of their shells at the end of their life-cycle (Bé, 1980; Duplessy *et al.*, 1981; Deuser, 1987; Spero and Lea, 1993; Bemis *et al.*, 1998). *Globigerinoides sacculifer* secretes an additional calcite layer over a period of up to 16 hours before gamete release (Bé, 1980), and its gametogenic calcite layer comprises 18 to 28% of the shell mass (Bé, 1980; Duplessy *et al.*, 1981); (around 26% in *Orbulina universa*; (Bouvier- Soumagnac and Duplessy, 1985)). Specimens covered by gametogenic calcite are called thick-walled (conversely, specimens with no such layer are called thin-walled). Gametogenic calcite is $\delta^{18}O$ enriched relative to earlier (thin-walled) stages of the shell (Sen Gupta, 1999).

It is thought that the early stages of foraminifera calcify at distinct disequilibrium in warm shallow waters, whereas the gametogenic calcite layer is deposited in colder waters as foraminifera sinks, before releasing the gametes (at the end of the life cycle) at depths up to several hundreds of meters, possibly near equilibrium (Duplessy *et al.*, 1981; Bouvier-Soumagnac and Duplessy, 1985; Kroon and Darling, 1995; Sen Gupta, 1999).

## 2.4.7. Carbonate ion concentrations

Specimens of *Orbulina universa* were subjected to variations of [$CO_3^{2-}$] at constant alkalinity, under both low and high irradiance conditions. A constant $\delta^{18}O$ offset between the high and low irradiance experiments was documented, while the ratio of change in shell $\delta^{18}O$ with change in [$CO_3^{2-}$] remained similar for both cases. Another experiment observed a change in shell $\delta^{18}O$ with [$CO_3^{2-}$] variations in *Globigerina bulloides* (which bears no symbionts); (Spero *et al.*, 1997). Spero *et al.* (1997) concluded that foraminiferal $\delta^{18}O$ decreases with increasing [$CO_3^{2-}$]. The magnitude of this response is species-specific, and symbiont photosynthesis plays no role. It supported observations on inorganic precipitates, suggesting common, abiological, kinetic fractionation effect (McCrea, 1950; McConnaughey, 1989b; Usdowski and Hoefs, 1993; Spero *et al.,* 1997; Sen Gupta, 1999).

## 2.4.8. Aragonite versus calcite

Some benthic foraminifera construct their test from aragonite rather than calcite (e.g. *Hoeglundina elegans*). *Hoeglundina elegans* is enriched relative to the equilibrium value for calcite by 0.78 ± 0.19‰ (Grossmann, 1984a). This findings agree with observations (constant temperature) that inorganically precipitated aragonite is about 0.6‰ enriched relative to inorganically precipitated calcite, while theoretical calculations suggests an enrichment of 0.79‰ (Tarutani *et al.,* 1969). The temperature dependence of the aragonite-water fractionation is similar to that of the calcite water fractionation (Grossman and Ku, 1986; Sen Gupta, 1999).

# 2.5. Carbon isotopes

## 2.5.1. Carbon isotopes and the global carbon cycle

There are two main carbon reservoirs – organic matter and sedimentary rocks. The organic carbon cycle pivots around $CO_2$ fixation into organic biomass through photosynthesis – $CO_2 + H_2O$ + energy (sunlight) → $CH_2O + O_2$ (see Fig. 2), in both the marine and the terrestrial biospheres. Respiration under the presence of oxygen follows the reverse reaction. The organic carbon cycle acts on a wide range of time scales, from daytime (photosynthesis) and night-time (respiration) within plants to cycles in the order of $10^8$ years (sedimentary rocks); (Sen Gupta, 1999).

Weathering of most types of rocks draws down $CO_2$ from the atmosphere (see Fig. 2). The weathering reaction for calcsilicates is – $CaSiO_3 + CO_2 \rightarrow CaCO_3 + SiO_2$. The $CaCO_3$ dissociates in water, utilizing more $CO_2$. Long-term cycles of orogeny and weathering (of order $10^8$ years), therefore, cause fluctuations of atmospheric $CO_2$ concentrations which also equilibrate with total dissolved inorganic carbon in the oceans (Sen Gupta, 1999).

The inorganic carbon pool in the oceans is controlled by carbonate reactions. Most of the $CO_2$ in water is contained in $HCO_3^-$ (the bicarbonate ion), due to $H_2O + CO_2 \leftrightarrow H^+ + HCO_3^-$, while a further reaction may dissociate according to $HCO_3^- \leftrightarrow H^+ + CO_3^{2-}$. At normal seawater pH of 7.8–8.3, $HCO_3^-$ dominates and there are small amounts of $CO_3^{2-}$. The total dissolved inorganic carbon (DIC) consists of $HCO_3^-$, $CO_3^{2-}$ and dissolved $CO_2$. Calcium carbonate, biogenic and abiogenic, interacts with the inorganic carbon via the precipitation/dissolution reaction - $2HCO_3^- + Ca^{2+} \leftrightarrow CaCO_3 + CO_2 + H_2O$ (Sen Gupta, 1999).

The average $\delta^{13}C$ of the carbonate reservoir is around 0‰, while the organic carbon reservoir averages around -25‰ (Hoefs, 1997); (see Fig. 2). Extremely depleted values have methane in the form of gas-hydrates (clathrates; continental slope environment) with typical values ranging between -35‰ and -80‰. The seepage of these clathrates may cause $\delta^{13}C$ depletions in infaunal benthic Foraminifera (Wefer *et al.*, 1994; Sen Gupta, 1999).

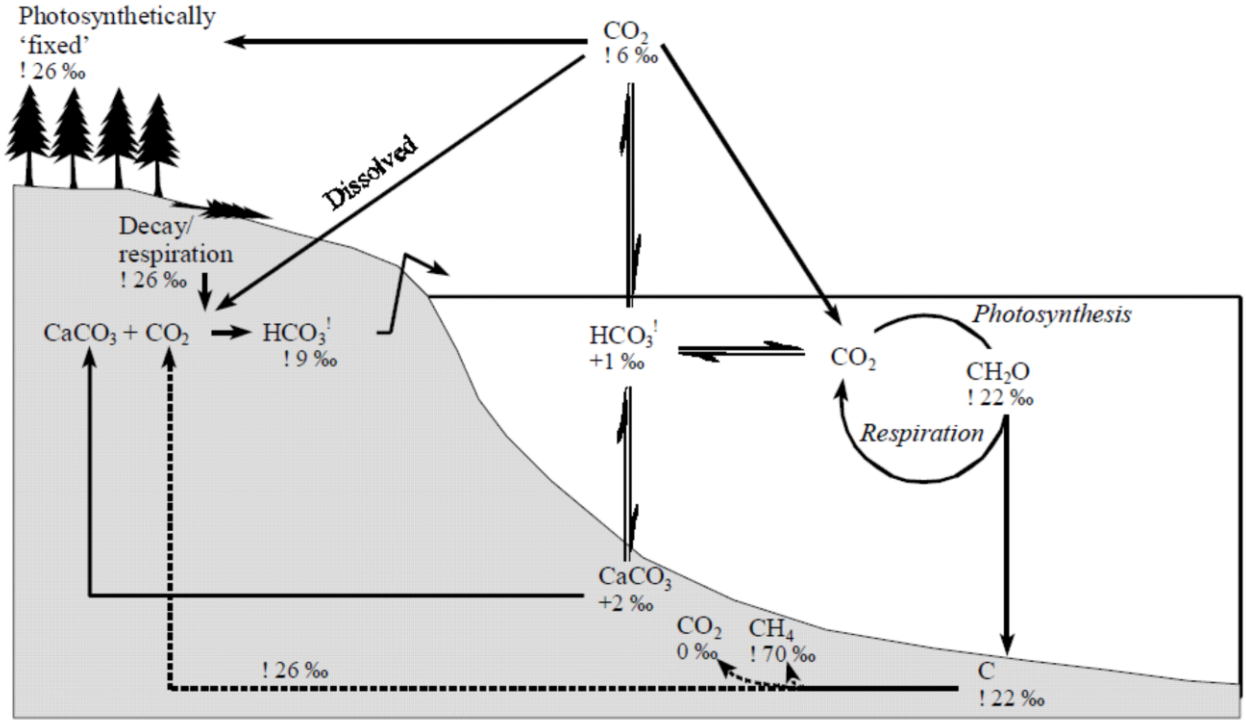


**Figure 2.** Interactions between the terrestrial and marine organic and inorganic carbon cycles, with general mean carbon isotope values. From: Sen Gupta (1999)

## 2.5.2. Carbon isotopes in seawater

## 2.5.2.1. Photosynthesis, respiration, lateral $\delta^{13}C$ gradients

Photosynthesis is strongly discriminative in favour of $^{12}C$, and marine phytoplankton forms organic matter with $\delta^{13}C$ values of -20‰ to -23‰ relative to ambient water. Photosynthesis is restricted to the euphotic layer. The dissolved carbon in surface waters is relatively enriched in $^{13}C$ due to the preferential uptake of $^{12}C$ during photosynthesis. This enrichment affects surface water $HCO_3^-$ and the newly formed carbonates. Within the mixed layer, this effect offsets the enrichment of water due to photosynthesis (see Fig. 3); (Sen Gupta, 1999).

Lateral gradients in deep water $\delta^{13}C$ may be used to trace the history of deep water from its source area. The deep water $\delta^{13}C$ reflects time of exposure to organic matter decay; the amount of organic matter decayed within the deep water (export production); and the rapidity of organic matter decay (temperature dependent - respiration rates approximately double for each 10°C temperature increase; (Swart, 1983)). Geographic shifts of deep water $\delta^{13}C$ sources greatly affect the world ocean's surface-deep gradients (Sen Gupta, 1999).

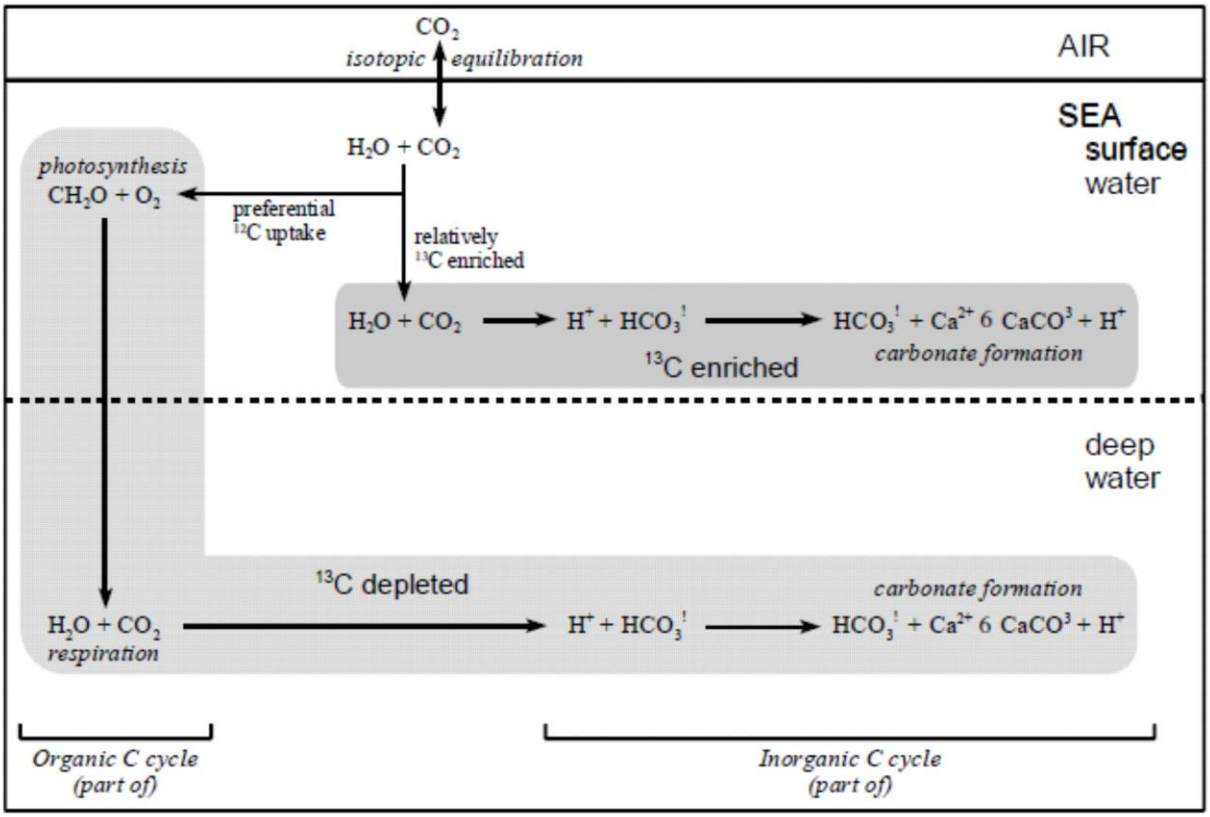


**Figure 3.** The generation of surface-deep carbon isotope gradient due to export production and interactions between the marine organic and inorganic cycles. From: Sen Gupta (1999)

## 2.5.2.2. Interactions with $\delta^{13}C$ of atmospheric $CO_2$

Major changes in $\delta^{13}C$ of atmospheric $CO_2$ will be recorded in the marine cycles. Interactions between $\delta^{13}C$ of atmospheric $CO_2$ and the marine reservoir depend on two main influences. The first influence is spatial variability in the equilibration between atmospheric $CO_2$ and dissolved inorganic carbon. This influence is caused by the temperature dependence of equilibrium exchange. The dissolved inorganic carbon (DIC) in sea water is $\delta^{13}C$ enriched relative to atmosphere, but with increasing temperature the fracionation becomes weaker. Warm, low latitude sea water $\delta^{13}C_{DIC}$ will be less enriched than those in cold, high latitude sea water if sufficient time for equilibration is allowed (Kroopnick *et al.* 1977; Lynch-Stieglitz and Fairbanks, 1994). The second influence is geographically widespread temporal variability in the $\delta^{13}C$ of atmospheric $CO_2$. Potential cause of change was a shift in terrestrial vegetation with differences in photosynthetic pathways.[1] $C_3$ plants become much more $\delta^{13}C$ depleted than $C_4$ plants (Kelly *et al.*, 1993). $C_4$ plants reduced the mean relative atmospheric $^{13}C$ enrichment caused by terrestrial plants. It is presumed that in the late Miocene there was an increase in dominance of $C_4$ plants (grasses) relative to $C_3$ plants (Leavitt, 1993). The late Miocene shift to lower $\delta^{13}C$ values in marine carbonates was explained by this signal (Derry and France-Lanord. 1996; Sen Gupta, 1999).

## 2.5.3. Carbon isotope ratios in foraminiferal carbonate

## 2.5.3.1. Equilibrium fractionation

Temperature independent relationship between the $\delta^{13}C$ values of equilibrium carbonate and bicarbonate is - $\delta^{13}C_{eqcarb} = \delta^{13}C_{HCO3^-} + 1$ (Romanek *et al.*, 1992). There is an older equation, $\varepsilon_{c\text{-}b}$ (‰) = $10.51 - 29810T^{-1}$, with $T$ in Kelvin, c – calcite versus b – bicarbonate (Grossman, 1984b). Aragonite shows a weak inverse relationship with temperature (Grossman, 1984b; Grossman and Ku, 1986; Wefer and Berger, 1991).

Carbonate $\delta^{13}C$ equilibrium is reported relative to the $\delta^{13}C$ of total dissolved inorganic carbon (the $\delta^{13}C$ of $\Sigma CO_2 = \delta^{13}C_{DIC}$), rather than relative to the $\delta^{13}C$ of bicarbonate. The value for $\delta^{13}C_{DIC}$ can be analytically determined, or estimated from apparent oxygen utilization rates (Kroopnick, 1974; Kroopnick 1985). However, the $\delta^{13}C$ of bicarbonate can only be obtained indirectly from calculations (Kroopnick, 1985; Sen Gupta, 1999).

[1] **$C_3$ plants** – e.g. trees; follow the Calvine-Benson cycle; show a non-linear fractionation linked with photorespiration; typical values around -28‰ $\delta^{13}C$ **$C_4$ plants** – grasses; follow the Hatch-Slack pathway; absence of photorespiration and the associated isotopic fractionations; evolutionary more advanced; typical values around -12‰ $\delta^{13}C$ (Swart, 1983).

## 2.5.3.2. Differential depth habitat and microhabitat effect

The differences among the preferred depths and changes in depth of calcification during the growth of different planktonic foraminiferal species may cause $\delta^{13}C$ deviations from surface water equilibrium. It is caused by the steep $\delta^{13}C_{DIC}$ gradient between the surface and the thermocline (Kroopnick *et al.*, 1972; Garlick, 1974; Kroopnick 1985; Tan, 1989). The covariation between decreasing $\delta^{13}C$ and increasing $\delta^{18}O$ with growth in several planktonic foraminiferal species suggests that the calcification at later growth stages occurs well below the mixed layer (Bouvier-Soumagnac and Duplessy, 1985). Regarding benthic foraminiferal species, it is essential to view species's preferred living depth and/or microhabitat and the context of ambient pore water $\delta^{13}C$ (Woodruff *et al.*, 1980; Belanger *et al.*, 1981; Grossman, 1984a.b; 1987; McCorkle *et al.*, 1985; Zahn *et al.*, 1986; Wefer and Berger, 1991; Loubere *et al.*, 1995). Pore water $\delta^{13}C$ gradients may reach 1‰ depletion per cm depth within sediment due to decomposition of sedimentary organic matter (Grossman, 1984a,b; McCorkle *et al.*, 1985; Grossman, 1987). There are additional intraspecific controls of depletion and mechanisms of food supply within the sediment (Zahn *et al.*, 1986; Loubere, 1997); (Sen Gupta, 1999).

# 2.6. Deviations from equilibrium $\delta^{13}C$ in foraminiferal carbonate

Disequilibrium in foraminiferal $\delta^{13}C$ may be caused by – utilization of metabolic $CO_2$ during the shell formation; photosynthetic activity of symbionts; growth rate and variations in carbonate ion concentrations in ambient waters. The effects are not separate, and thus there could be strong overlaps (Sen Gupta, 1999).

## 2.6.1 Respiratory $CO_2$ (so called "vital" effects)

As vital effects we can consider the incorporation of isotopically light metabolic $CO_2$ into the carbonate skeleton. The magnitude of this effect is proportional to the amount of metabolic $CO_2$ within the organism's internal $CO_2$ pool, which reflects the ability for gas exchange with ambient water (Erez, 1978).

Large variation in $\delta^{13}C$ of food used by *Orbulina universa* and *Globigerina bulloides* cause only negligible shifts in shell $\delta^{13}C$ (Spero and Lea, 1993, 1996; Ortiz *et al.*, 1996). The major cause for shell $\delta^{13}C$ fluctuations is not food $\delta^{13}C$, but metabolic rates controlled by temperature (Ortiz *et al.*, 1996). Also photosynthetic symbiont-bearing larger foraminifera shift to very low $\delta^{13}C$ values in the reproductive period (Wefer and Berger, 1991).

## 2.6.2 Symbiont photosynthesis

*Globigerinoides sacculifer* documents elevated utilization of $^{12}CO_2$ by photosynthetic symbionts, which increases the calcifying microenvironment in $H^{13}CO_3^-$ and thus produces $\delta^{13}C$ enriched chambers (Spero and Lea, 1993). A similar relationship was observed in *Orbulina universa* however, the relationship disappears during prevented photosynthetic activity (Spero and Williams, 1988). *Globigerinoides sacculifer* shift slightly $\delta^{13}C$ values below equilibrium at low light levels, which suggest suppressed photosynthetic effects and that some respired $CO_2$ gets incorporated into the shell mass (to a proportion 0 – 3% of shell carbon); (Spero and Lea, 1993). Similar values were observed for *Orbulina universa* (Spero, 1992).

## 2.6.3. Changes with growth

Most foraminifera experience major physiological changes during growth. *Orbulina universa* and *Globigerinella aequilateralis* document increasing symbiont density together with increasing test size, which in turn increases rate of photosynthesis so that each new chamber shows an increased $\delta^{13}C$ values (Faber *et al.*, 1985; Spero and Parker, 1985; Spero *et al.*, 1991). An analysis of whole-shell $\delta^{13}C$ gives integrated value of all individual chambers and will therefore be different for the same species of different sizes (Spero *et al.*, 1991). However, *Orbulina universa* shows a progressive increase in $\delta^{13}C$ in the natural environment, which suggest possible migration to deeper habitats with lower light intensity during growth and thus may cause progressive $\delta^{13}C$ depletion which may cause partial offset of the $\delta^{13}C$ enrichment due to increased symbiont density (Ravelo and Fairbanks, 1995); (Sen Gupta, 1999).

In non-symbiont bearing species, a change with size is expected in the depletion caused by contamination $\delta^{13}C$ of shell with metabolic or respiratory $CO_2$. Depletions should be strongest in small, juvenile specimens from early life stages with higher metabolic rates, decreasing towards equilibrium in adult stages, with lower metabolic rates (Berger *et al.*, 1978; Wefer and Berger, 1991); (Sen Gupta, 1999).

Deep-sea benthic foraminifera show no significant change in skeletal $\delta^{13}C$ values with size (Vincent *et al.,* 1981; Dunbar and Wefer, 1984; Grossman, 1984, 1987; Wefer and Berger, 1991); (Sen Gupta, 1999).

## 2.6.4. Carbonate ion concentration

Foraminiferal $\delta^{13}C$ decreases with increasing [$CO_3^{2-}$], similarly to $\delta^{18}O$ values. The signal magnitude is species-specific, and symbiont photosynthesis plays no role (Spero *et al.*, 1997; McCrea, 1950); (Sen Gupta, 1999).

## 2.6.5. Aragonite versus calcite

The aragonitic benthic foraminifer *Hoeglundina elegans* shows constant $\delta^{13}C$ values with depth and an increase of $\delta^{13}C_{DIC}$ with depth at studied area (Grossman, 1984a). It shows a negative temperature dependence of bicarbonate-aragonite fractionation (Grossman, 1984b; Grossman and Ku, 1986). However, fractionations associated with aragonite formation remain poorly understood (Sen Gupta, 1999).

# 3. Central Paratethys

## 3.0.1. Introduction

The Central Paratethys represents a chain of Oligocene to Miocene epeiric seas with presumed oscillations of paleoecological parameters and episodic communications with the oceanic realms (Indian Ocean; Atlantic Ocean; Mediterranean); (see Fig. 4). It is expected that marked paleoecological either geochemical oscillations were present. It represented a very specific marine domain which has no exact equivalent in the present days.

## 3.0.2. Paleogeography and geodynamical settings

During the Cenozoic Era, the African plate moved towards the Eurasian plate with a quite northwards shift and a counterclockwise rotation which involved several microplates in the Mediterranean area (Kováč *et al.,* 1998b; Márton *et al.,* 2003, 2006; Seghedi *et al.,* 2004).

Consequently, the Eurasian paleogeography went through dramatic changes. From vast marine areas interrupted only by archipelagos, it started to shift into dry land. This process of continentalisation was accompanied by the rise of the Alpidic chains which intensively changed and structured the topography. Around the Eocene/Oligocene boundary, the African plate moved northward which resulted into the subduction of the Europian plate under the African plate, and thus the final disintegration of the (Western) Tethys Ocean (Báldi, 1980; Harzhauser *et al.,* 2002; Harzhauser and Piller, 2007; Piller *et al.,* 2007).

The chain of epeiric seas called the Paratethys Sea spread during its maximum extent from the Rhône Basin in France towards Inner Asia. It came into existence during the latest Eocene and Early Oligocene (Eocene/Oligocene boundary) due to the rising of Alpidic chains which acted as geographic barriers (Rögl, 1998). The rising archipelago consisted of the Alps, Dinarids, Hellenids, Pontids, and the Anatolian Massif. Due to this change in paleogeography and topography, the newly formed Paratethys Sea was partitioned into three large geotectonic units which underwent different environmental histories because of the different timing of geotectonic events and also global sea-level fluctuations (see Fig. 4); (Popov *et al.,* 2004; Piller *et al.,* 2007).

The western part consists of the Western and the Central Paratethys and to the east up to inner Asia spreads the larger Eastern Paratethys. The Western Paratethys comprises the Rhône Basin in France and Alpine Foreland Basins of Switzerland, Germany and Upper Austria (Seneš, 1961). The Central Paratethys spreads from Bavaria to Moldavia as the Eastern Alpine - Carpathian Foreland basins. The Eastern Paratethys comprises the Euxinian (Black Sea), the Caspian and Aral Sea basins (Nevesskaja *et al.,* 1993); (Piller *et al.,* 2007). Related to the changes in paleogeography is a complex pattern of changing seaways and landbridges between the Paratethys sea and the Mediterranean Sea, the North Sea and as well as the western Indo-Pacific ocean (see Fig. 4); (Rögl, 1998, 1999).

# 3. 1. Miocene stratigraphy – Central Paratethys (see Fig. 6)

# 3.2. Latest Oligocene – Early Miocene

## 3.2.1. Egerian (~ 25 - 21 Ma)

The Egerian regional stage spans from the Late Oligocene to a large part of the Aquitanian (Báldi and Seneš, 1975). The stratotype of the Egerian stage was defined at Eger in northern Hungary (Báldi, 1975). It is characterized by mainly siliciclastic depositional regime which goes from the Kiscellian and continues to the Egerian. The carbonate sedimentation is only minor throughout the Egerian. If it is present, mixed carbonate–siliciclastic systems predominated by corallinaceans, bryozoans and larger foraminifers (e.g. miogypsinids) are typical for the Egerian (Kaiser *et al.,* 2001; Harzhauser and Piller, 2007).

In the Late Oligocene, the Paratethys was a huge west to east oriented sea. Normal marine conditions were present due to connections to Western Tethys Ocean. The other connection towards the North Sea Basin was initiated via the Rhine Graben and also a connection to the Venetian Basin opened in the southwest (see Fig. 4); (Rögl, 1998; Reichenbacher, 2000). However, this “transeuropean” connection ceased during the Late Egerian (Reichenbacher, 2000). In the western part of Paratethys, different freshwater environments and paralic basins developed (Barthelt, 1989; Berger, 1996). The seaways into the Western Tethys Ocean via partly submerged Alpine nappes remained open (Wagner, 1996; Steininger and Wessely, 2000).

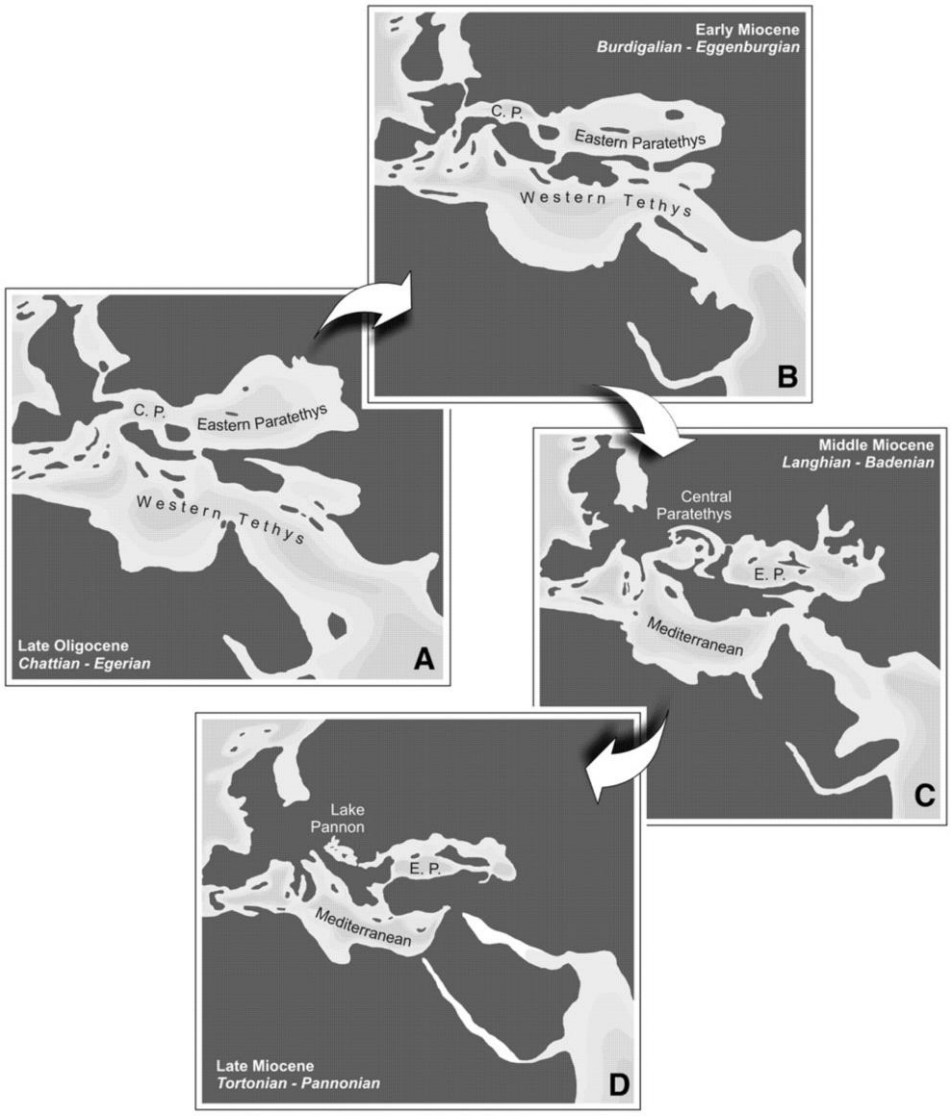


**Figure 4.** The paleogeographic maps of the Paratethys Sea realm. (C.P. = Central Paratethys; E.P. = Eastern Paratethys); A: new connections with the North Sea and the Western Tethys; B: the Central Paratethys - a west–east oriented deep basin, connections into the Rhône Basin; C: the Carpathian chain starts to structure; connections to the Eastern Paratethys unstable then became broad, passable (during the late Badenian and the Sarmatian); D: the Eastern Paratethys still connects with the Mediterranean Sea; the Central Paratethys – vanished, brackish Lake Pannon took the place. Modified after: Harzhauser and Piller, (2007)

## 3.2.2. Eggenburgian (~ 21 – 18 Ma)

The Eggenburgian regional stage spans from the Late Miocene stage Aquitanian to a great part of the Burdigalian. The stratotype of the Eggenburgian is located in Austria at Loibersdorf NW from Viena (Steininger, 1971; Harzhauser and Piller, 2007). The biostratigraphy of this stage is strongly based on its characteristic mollusc fauna (Steininger and Seneš, 1971). Sandy and pellitic sedimentation dominates in the lower Eggenburgian. Carbonates are rare, patchy and often of mixed siliciclastic–carbonate type. The shallow marine corallinacean rhodonite carpets admixed with fine to medium sand is a typical example (Steininger, 1971). In deep-neritic to bathyal settings typical grey calcareous clays with intercalations of sands, the so-called “Schlier” developed. Only in the Outer Carpathians, we could find a relic Flysch with turbidite sequences (Báldi, 1998; Popov *et al.,* 2004; Harzhauser and Piller, 2007).

There were broad connections into the Eastern Paratethys which allowed migration of early Eggenburgian mollusc faunas (Rögl, 1998). Also, the western seaway via Alpine foreland started to open during the initial Eggenburgian (see Fig. 4.). The sea successively invaded the foreland from the west connecting to the Central Paratethys during the Eggenburgian (Berger, 1996). This marine pathway of the Paratethys via the Alpine Foredeep into the Rhône Basin, which was newly established, coincided with a second flow from the Eastern Mediterranean (Martel *et al.,* 1994). It is reflected in the meso and macrotidally controlled deposits (throughout the Alpine Foreland Basins) lasting from the late Eggenburgian to the middle Ottnangian (Allen *et al.,* 1985; Faupl and Roetzel, 1990).

## 3.2.3. Ottnangian (~ 18 – 17 Ma)

The stratotype of the Ottnangian regional stage is at Ottnang in Upper Austria (Rögl *et al.,* 1973). The revision of the Ottnangian stratotype was done by Grunert *et al.* (2010). For the lower Ottnangian a normal marine development is characteristic. Sedimentation is dominated by siliciclastics with widespread tidal-influenced deposits and the characteristic sandy/silty “Schlier” sediments (Faupl and Roetzel, 1990). Carbonates are scarce and correspond in composition to the late Eggenburgian corallinaceam–bryozoans limestone type. Corals are rare aside from few patchy colonies and no carpets or reefs were observed (Harzhauser and Piller, 2007; Piller *et al.,* 2007).

However, uplift of the Alpine Foreland Basin caused the cessation of the western connection (Rögl, 1998). Due to this event the fluvial–lacustrine environments of the Upper Freshwater Molasse became established in the western Alpine Foreland Basin (Berger, 1996). The sea-level fall during the Early Miocene global sea-level change of TB 2.1. cycle (Haq *et al.,* 1988) was the beginning of the isolation of the Paratethys from the Mediterranean Sea during the late Ottnangian. No real marine environments are known from the

Carpathian-Pannonian–Dinaride domain and brackish to fresh water sedimentary environments prevailed except for the Northern Alpine Foreland Basin and its continuation into the Polish foredeep (Kováč *et al.,* 2004). During the late Ottnangian and the synchronous Kotsakhurian in the Eastern Paratethys biogeographic relations between the Paratethys and the Mediterranean Sea ceased. This crisis is reflected in the nearshore settings by brackish water conditions and a sudden evolutionary peak resulting in a large number of endemic genera (so-called "*Rzehakia* fauna"); (Steininger, 1973; Harzhauser and Piller, 2007; Piller *et al.,* 2007).

## 3.2.4. Karpatian (~ 17 – 16.3 Ma)

The stratotype of the regional stage Karpatian is based on a section Slup in Moravia, Czech Republic and it is equivalent to the late Burdigalian (Cicha *et al.,* 1967). A new version and revision of the Karpatian stratotype was done by Brzobohatý *et al.* (2003). The Karpatian stage starts with a transgression in the Central Paratethys area associated with the sea-level rise at the beginning of the late Early Miocene during the global 3rd order sea-level cycle of TB 2.2., and a reorganisation of palaeogeographic patterns (Haq *et al.,* 1988; Rögl *et al.,* 2003). The sediments are represented mainly by terrestrial, alluvial, fluvial and deltaic deposits at the base of the Karpatian then rapidly turn into the overlying strata of marine, neritic to shallow bathyal sediments. The predominated sediments are green-blue and grey pelites, silty calcareous shales in the offshore environments and clayey sand in marginal areas (Rögl *et al.,* 2003; Harzhauser and Piller, 2007).

In the early Karpatian, there are similarities with the Ottnangian. The hydrodynamic regime was cool-temperate water masses with high amounts of siliceous fossils (Rögl *et al.,* 2003). The carbonate production was very low throughout the Central Paratethys and suboxic bottom conditions in the basins and also upwelling regime is suggested based on planktonic foraminifera (Cicha *et al.,* 2003). In the late Karpatian, a general warming trend appeared and a new broad connection with the Mediterranean Sea was established via the Slovenian "Trans-Tethyan Trench Corridor" (Bistricic and Jenk, 1985). This seaway enabled a free faunal exchange between the Central Paratethys and the Mediterranean area (Harzhauser and Piller, 2007). There was also a dramatic tectonic turnover in the Central Paratethys area leading to a change from W–E trending basins towards intra-mountain basins (Rögl, 1998; Kováč *et al.,* 2003). The formation of evaporites in the Rumanian part of the Carpathian Foredeep and in the Transylvanian Basin reflects poor or absent connection with the Eastern Paratethys during the late Early Miocene (Harzhauser and Piller, 2007).

The boundary between Karpatian/Badenian (Burdigalian/Langhian) is characterised by a significant sea-level drop (Haq *et al.,* 1988; Hardenbol *et al.,* 1998), expressed as a hiatus traceable throughout the Central Paratethys (Rögl *et al.,* 2002). The top of the Lower Miocene in the Paratethyan basins is marked by erosional surfaces or by an angular discordance between the Lower and Middle Miocene strata, and is called the “Styrian unconformity” (Latal and Piller, 2003).

# 3.3. Middle Miocene

## 3.3.1. Badenian (16.3 - 12.7 Ma)

### 3.3.1.1. Correlation

The stratotype of the Badenian is the locality Baden-Soos, south of Vienna. The base of the Badenian is defined with the FO (first occurrence) of *Praeorbulina* (see Table 2), (Papp and Cicha, 1978) following a transgression due to the Styrian tectonic phase (Stille, 1924) and the sea level lowstand at the Bur 4/Lan 1 sequence boundary (Latal and Piller, 2003; Strauss *et al.,* 2006). The biostratigraphic subdivision of the Badenian is traditionally based on planktonic foraminifera (*Orbulina suturalis, Velapertina indigena, Globigerinoides quadrilobatus, Globorotalita druryi, Globorotalia peripheroronda, Globoquadrina altispira),* smaller benthic foraminifera (*Uvigerina grilli, U. macrocarinata, U. venusta, U. brunnensis, Pappina parkeri, P. Neudorfensis*) and larger benthic foraminifera (*Borelis haueri, B. melo melo, Planostegina* group *costata, P. giganteoformis, Amphistegina mammila*) as well as on other groups (e.g. calcareous nannoplankton, palynology, molluscs etc.); (Cicha *et al.,* 1998).

Several fossil groups (gastropods, foraminifera) increase dramatically in diversity at the onset of the Badenian. Almost 505 gastropod taxa, and up to 82 taxa of foraminifera have their FO’s at the onset of the Badenian. This event is called the “Early Badenian Build-up Event (EBBE)” (Harzhauser and Piller, 2007).

A subdivision of the Badenian (see Table 2) is based on significant paleoecologic and paleogeographic changes reflected in the composition of the biota (Papp *et al.,* 1978; Kováč *et al.,* 2004). The lower Badenian is represented by the "*Lagenidae* Zone", the middle Badenian by the *"Spiroplectammina* Zone", and the upper Badenian by the *"Bulimina/Bolivina* Zone" (Grill, 1943). However, this subdivision is outdated and is currently considered invalid. In the eastern Central Paratethys and the Carpathian Foredeep, additional three substages were established, Moravian for the lower, Wielician for the middle, and Kosovian for the upper Badenian (Piller *et al.,* 2007). Characteristic deposits are the evaporites of the Wielician substage (Papp *et al.,* 1978), which occur in the Carpathian Foredeep (Peryt, 2001) and also in the Transylvanian Basin (Krézsek and Filipescu, 2005).

The Badenian is the acme of the carbonate production in the Paratethys realm. There are also present highly fossiliferous offshore clays. Corallinacean limestones are quite common throughout the Miocene, but the only coral reef phase of the Central Paratethys occurs during the Badenian. Early Badenian reefs are fairly diverse (Friebe, 1993; Riegl and Piller, 2002; Erhart and Piller, 2004). By the Late Badenian a variety of carbonate facies were still present (Dullo, 1983), but a change in the coral reefs had occurred. In the southern Central Paratethys (e.g., Vienna Basin, Styrian Basin), the complex reefs were replaced by coral carpets, dominated by *Porites, Tarbellastraea, Caulastrea, Acanthastrea,* and *Stylocora* (Piller and Kleemann, 1991; Riegl and Piller, 2000, 2002). This shift in the reef structure and diversity is linked to the climatic deterioration which was triggered by the global Middle Miocene Climate Transition (Shevenell *et al.,* 2004).

The early Badenian can be correlated with the early Langhian of the Mediterranean Based on the FO of *Praeorbulina* (see Table 2) in the Styrian Basin, the Vienna Basin and the Alpine Foreland Basin (Rögl *et al.,* 2002). The lowermost Badenian is correlated, in terms of calcareous nannoplankton to NN4 zone (see Table 2) based on the occurrence of *Helicosphaera ampliaperta* and *Sphenolithus heteromorphus* (Rögl *et al.,* 2002; Spezzaferri *et al.,* 2002, 2004). Higher up the NN5 zone is reflected by the presence of *Helicosphaera waltrans* together with *S. heteromorphus* (Rögl *et al.,* 2002). The base of the Badenian can be correlated to the global sea level cycle TB 2.3. of Haq *et al.* (1988), and Bur 5/Lan 1 of Hardenbol *et al.* (1998); (Kováč *et al.,* 2004; Strauss *et al.,* 2006). The top of lower Badenian is marked by an unconformity pointing to a sea level drop of more than 120 m (Kreutzer, 1986; Weissenbäck, 1996; Harzhauser and Piller, 2007). In many marginal settings e.g. the Alpine Foreland Basin, we also could trace this unconformity representing the sea level drop (Mandic *et al.,* 2002; Mandic, 2004; Kroh *et al.,* 2003). This event was triggered by an expansion of the East Antarctic ice sheet (Flower and Kennett, 1993; Shevenell *et al.,* 2004) and corresponds to the Lan 2/Ser 1 sequence boundary of Hardenbol *et al.* (1998).

The second Badenian cycle (middle Badenian) is an expression of the global sea level cycle TB 2.4. of Haq *et al.* (1988). Characteristic transgressive and regressive sedimentary structures are observed in seismic studies in the Vienna Basin (Kreutzer, 1986; Strauss *et al.,* 2006). In the Carpathian Foreland basins and in the Transylvanian Basin, the evaporitic phase, which is known as the Wielician crisis (Steininger *et al.,* 1978; Kasprzyk, 1999; Chira, 2000) starts and correlates to the Lan 2/Ser 1 lowstand of Hardenbol *et al.* (1998). In the western parts of the Central Paratethys, corallinacean platforms with frequent caliche formation and vadose leaching are characteristic for this cycle (Dullo, 1983; Schmid *et al.,* 2001). The occurrence of *Sphenolithus heteromorphus* places middle Badenian sediments in NN 5 nannoplankton zone (Piller *et al.,* 2007).

The third Badenian cycle (Late Badenian) is biostratigraphically dated by the onset of NN6 nannoplankton zone (Hudáčková *et al.,* 2000; Kováč *et al.,* 2004). The base of this biozone is defined by the LO (last occurrence) of *Sphenolithus heteromorphus* (see Table 2) and corresponds to the Langhian/Serravallian boundary in the Mediterranean calibrated by Foresi *et al.* (2002a) at 13.59 Ma (see also Gradstein and Ogg, 2004; Gradstein *et al.,* 2004; Lourens *et al.,* 2004). The Langhian/Serravallian boundary roughly correlates to the middle/upper Badenian boundary, and a correlation with the global cycle TB 2.5. of Haq *et al.* (1988) is possible (Piller *et al.,* 2007).[2] Late Badenian is characterised by the deposition of dysoxic pelites in basinal settings in the entire Central Paratethys area which indicates stratified water body during the late Badenian (Hudáčková *et al.,* 2000).

In contrast to this subdivision of the Badenian, Hohenegger *et al.* (2014) defined a new subdivision (see Table 1) which put aside the stray division according to "*Foraminifera*" zones". Hohenegger *et al.* (2014) redefined the primary subdivision for the Lower Badenian where considerable shortcomings were reported according to authors (e.g. Hohenegger *et al.*, 2009). They detected a large interval between the uppermost Karpatian and the base of the lower "*Lagenidae* zone" (the former base of the Badenian - correlated with the NN4/NN5 boundary at 14.91 Ma). Detailed investigations of the detected interval showed a paleoenviromental change which is documented by stable isotopes, shallow benthic foraminifera and occurrence of planktonic foraminifera *Praeorbulina sicana* together with a marked change in nannofossil composition at 16.3 Ma. Hohenegger *et al.* (2014) suppose that the Styrian Tectonic Phase caused this change. Based on this fact and magnetostratigraphic data, they placed the base of the Badenian at 16.303 Ma (does not coincide with the Burdigalian/Langhian boundary at 15.974 Ma). The interval named the Early Badenian spans between 16.303 Ma and 15.032 Ma and largely corresponds to the 3rd order sea-level cycle TB 2.3 (Haq *et al.*, 1988); (Hohenegger *et al.*, 2014).

[2] Considering the dating and the magnitude of this cycle gives possible correlation with the global cycle TB 2.5. of Haq *et al.* (1988); (Piller *et al.,* 2007).

The lower "*Lagenidae* zone" of the newly defined Mid Badenian starts at 15.032 Ma (belonging to the NN5 Zone) which is at the top of polarity Chron C5Bn.2n., and ends at 14.24 Ma which is due to the short cooling event in the Middle Miocene transition curve. The upper "*Lagenidae* zone" of the newly defined Mid Badenian spans from 14.24 to 13.982 Ma. The age is based on calibration of the stratotype belonging to the upper "*Lagenidae* zone" in the southern Vienna Basin (Hohenegger and Wagreich, 2012).

The Langhian/Serravallian boundary with the significant $\delta^{18}O$ increase at 13.82 Ma, Hohenegger *et al.* (2014) links it with the end of the Mid Badenian and beginning of the Late Badenian. The Badenian/Sarmatian boundary is placed at the top of the polarity Chron C5Ar2n at 12.829 Ma, and this boundary possibly reflects a sequence boundary of cycle TB 2.5 (Hohenegger *et al.*, 2014).

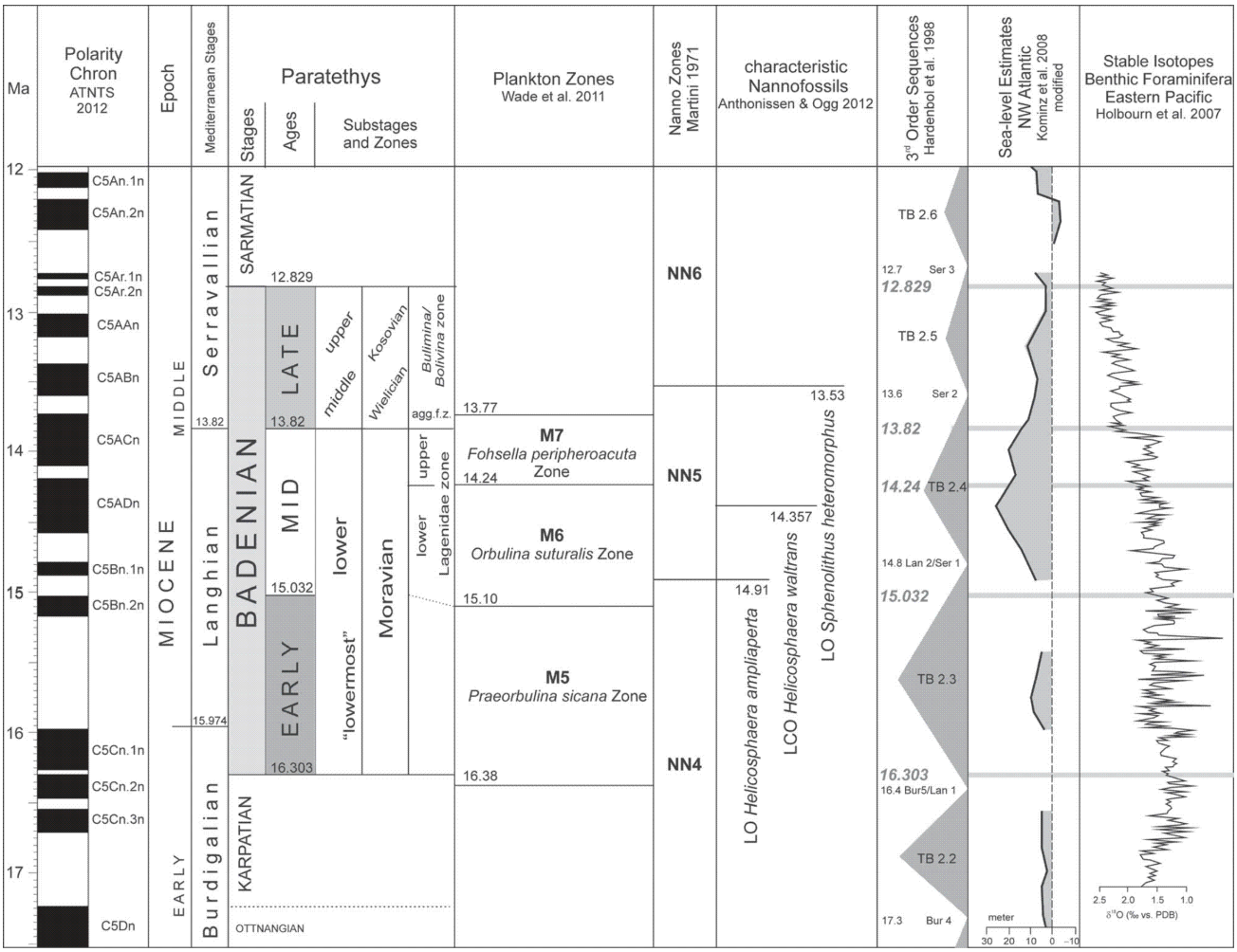


**Table 1.** Timing of the Badenian according to Hohenegger *et al.,* (2014). From: Hohenegger *et al.* (2014)

This division into the Early, Mid and Late Badenian also correlates with the global 3rd level cycles TB 2.3, TB 2.4 and TB 2.5, with durations in the order of 1 million years. The informal division of the Badenian into the lower and upper "*Lagenidae* zone", the "*Spiroplectammina* zone" and the "*Bulimina/Bolivina* zone" is restricted to the Vienna Basin and Hohenegger *et al.* (2014) correlate it to the global plankton zones by Wade *et al.* (2011). The *Praeorbulina sicana* zone marks the Early Badenian, *Orbulina suturalis* and *Fohsella peripheroacuta* zone marks the Mid Badenian, and *Velapertina indigena* zone marks the Late Badenian. The new subdivision also correlates with the paleoclimatic evolution of the Middle Miocene. The Early Badenian corresponds approximately to the "Middle Miocene Climate Optimum", the Mid Badenian to "Middle Miocene Climate Transition" and the Late Badenian corresponds to the initial part of the "Middle Miocene Icehouse"; (Hohenegger *et al.*, 2014).

However, this subdivision has not been fully accepted by scientific community, yet. For more details see Hohenegger *et al.* (2014) and Hohenegger and Wagreich (2012) and references therein.

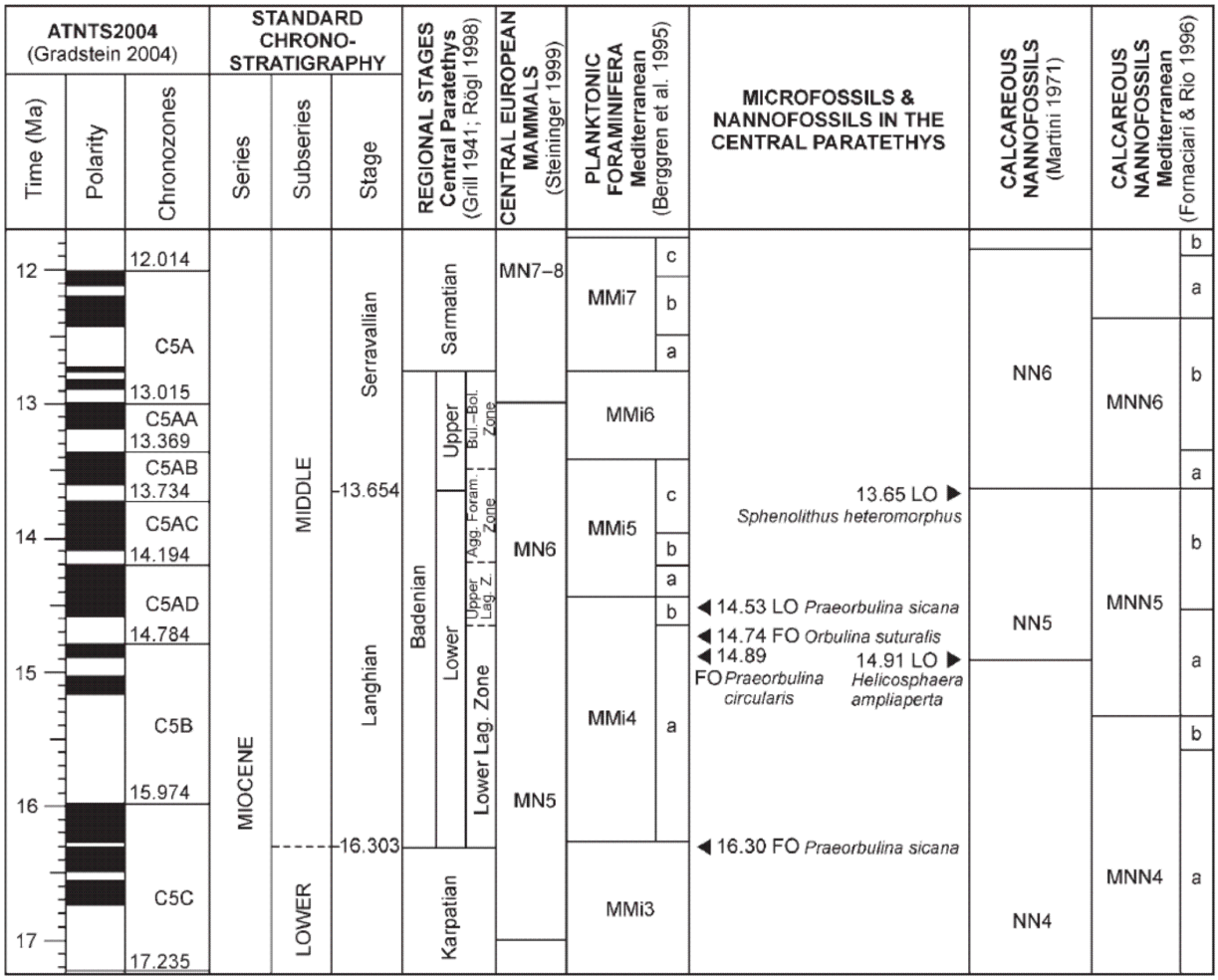


**Table 2.** The biostratigraphy of the Badenian in the Central Paratethys basins. Zones of Martini (1971) in the Paratethys were recalibrated according to Gradstein *et al.* (2004). From: Kováč *et al.* 2007

## 3.3.1.2. Paleogeography

During the early Badenian the "Trans-Tethyan Trench Corridor" via Slovenia was still open and connected the Mediterranean Sea to the Pannonian basin system (see Fig. 4). The connections into eastern directions are problematic.[3] Highly probable is a repeated re-opening of the Tethyan gateway between the Mediterranean Sea and the Indo-Pacific during the Langhian (early Badenian) (Rögl, 1998a; Popov *et al.,* 2004) and into the Serravallian (Jones, 1999); (see Fig. 5). During the middle Badenian the eastern seaways were sealed. The only water supply for the Central Paratethys was via the "Trans-Tethyan Trench Corridor", (see Fig. 5). This gateway was closed in the Late Badenian (Piller *et al.,* 2007). The Central Paratethys then depended on the connection to the Eastern Paratethys via today's western Black Sea area (see Fig. 5). However, faunistic differences exclude the Eastern Paratethys as passage into the west (Studencka *et al.,* 1998). The seaway between the Black Sea plate and the Pontids might have acted as a gateway (Rögl, 1998a).[2]

The dramatic change in marine biota occurs at the Badenian/Sarmatian boundary. Almost 588 LO's (last occurrence) of gastropods and 121 LO's of foraminifers are recorded. This event is called the "Badenian Sarmatian Extinction Event" (BSEE); (Harzhauser and Piller, 2007). It was triggered by a strong restriction of the open ocean connections of the Central Paratethys (Rögl, 1998a). It corresponds to the Ser 3 sequence boundary of Hardenbol *et al.* (1998) and the beginning of cycle TB 2.6. of Haq *et al.* (1988); (Kováč *et al.,* 1999, 2004; Harzhauser and Piller, 2004b; Strauss *et al.,* 2006). The Badenian/Sarmatian boundary is possibly related to the glacio-eustatic isotope event MSi-3 at 12.7 Ma (Abreu and Haddad, 1998).

## 3.3.1.3. Paleoclimatic situation

The Badenian climate can be reffered as fairly uniform. For example, the new subdivision of the Badenian sensu Hohenegger *et al.* (2014) correlates well with the general paleoclimatic evolution of the Central Paratethys throughout the Badenian (see chapter 3.3.1.1.).

[3] Rögl (1998a) and Steininger and Wessely (2000) postulate an open connection into the Eastern Paratethys while Studencka *et al.* (1998) and Popov *et al.* (2004) indicate a land barrier between both seas. Also Rögl (1998a) discussed a marine pathway between the southern margin of the Black Sea plate and the Pontids, connecting the Eastern Mediterranean with the Central Paratethys (Piller *et al.,* 2007). There is no clear evidence that would favour one theory over the other.

The Lower Badenian is characterized by highly diversified mollusc fauna and very typical is the algal limestone deposition (Studencka *et al.*, 1998; Filipescu, 2001a; Harzhauser *et al.*, 2003). The maximum of diversity is in foraminiferal genera in the Lower Badenian (Cicha *et al.*, 1998; Ćorić *et al.,* 2004), and all these aspects reflect a stable subtropical marine environment. The faunal associations are quite similar throughout the Paratethys realm. There is only a slight N-S gradient expressed by a decreasing of diversity of some coldfishes (Brzobohatý *et al.*, 2007) and by maximum of thermophylic taxa in the southern basins which are missing to the north/northeast (Harzhauser *et al.*, 2003; Kováč *et al.*, 2007). Also, the occurrence of coral structures is limited to the southern basins with only small exceptions (The Polish Carpathian Foredeep). The foraminiferal species *Amphistegina* and *Planostegina* have their mass occurrence in the Lower Badenian, and point to subtropical conditions as well. Their distribution is restricted by 20°C summer isotherms (modern distribution), (Rögl and Brandstätter, 1993; Kováč *et al.*, 2007). The salinity crisis in the eastern regions of the Central Paratethys is attributed to the sea regression rather than to the climatic change (Czapowski, 1994; Bąbel, 2004).

In the Central Paratethys a climatic cooling is indicated by planktonic foraminiferal data (Bicchi *et al.*, 2003) at the end of the early Badenian, however, the microfauna' assemblages response is pointing to the cooling event first in the late Badenian. From the uppermost part of the "*Lagenidae* zone", we can also observe a slight increase in moderate-water fishes (Brzobohatý *et al.*, 2007) and ostracods (Jiříček, 1983) that can support the foraminiferal data. A biogeographical differentiation between basins started to become more prominent during the late Badenian. It is characterized by the absence of thermophilic fauna in the northern part of the Central Paratethys regions. The decreasing in surface water temperature is supported by less diversified planktonic foraminiferal assemblages and significant reduction of density of warm-water planktonic foraminiferal species (Bicchi *et al.*, 2003). In the northern parts of the Central Paratethys, this development is also supported by the occurrence of boreal ostracod genera *Cluthia* and *Pseudocythere* (Szczechura, 1997). There is also an absence of warm-water bivalve taxa (giant scallops *Gigantopecten* and *Flabellipecten*, cockles *Cardium indicum*, *C. kunstleri* and *Megacardita*). These taxa were commonly found in the early Badenian throughout the Central Paratethys and in the Late Badenian these taxa were restricted to the southern basins (Studencka *et al.*, 1998; Studencka, 1999); (Kováč *et al.*, 2007).

In the Central Paratethys terrestrial ecosystems the landscape evolution played the pivotal role. The uplift of the Carpathian mountain chain and evolution of steep landscape and adjacent lowlands caused the altitudinal zonation. For the early Badenian characteristic vegetation is zonal vegetation with evergreen broadleaved forests supplemented by azonal vegetation (e.g. swamps). In the late Badenian a higher proportion of extrazonal (=mountain; *Picea*, *Abies*, *Tsuga*, *Cedrus*) vegetation was present. The subtropical climate with changes at the early/late Badenian boundary is confirmed in both terrestrial and aquatic ecosystems.

In pollenspectra, an increased proportion of the arctoterciary taxa (*Quercus*, *Ulmus, Carya*) is documented and conversely thermophilous taxa (*Fagaceae; Platycarya, Engelhardia, Myrica, Distylium*) are less frequent. Herbs are represented mainly by the halophytes (*Chenopodiaceae*). In the Badenian/Sarmatian boundary, swamp elements (*Taxodiaceae, Myricaceae, Nyssaceae*) become common (Kováčová *et al.*, 2011). For more details see Kováčová *et al.* (2011) and references therein.

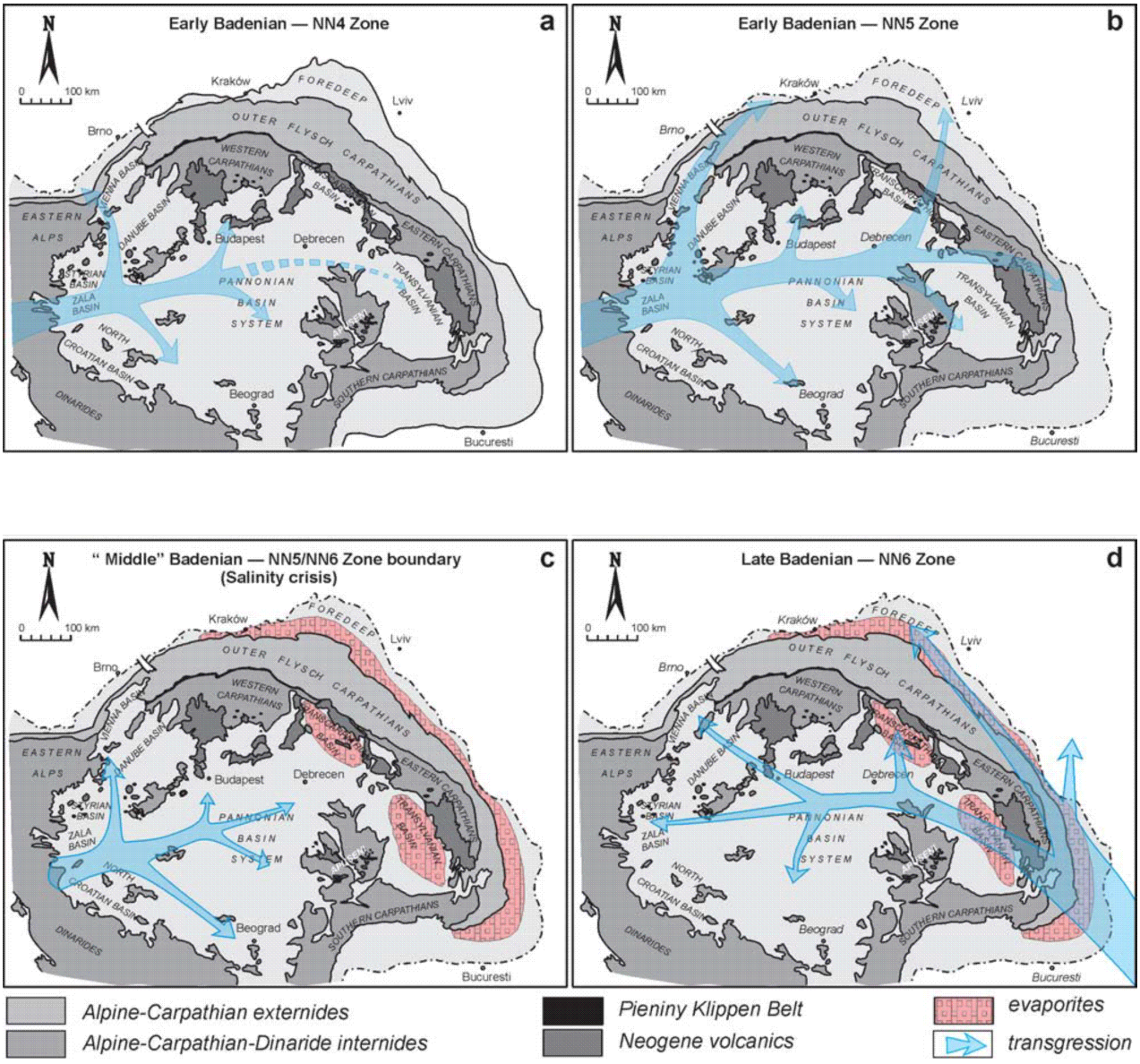


**Figure 5.** (a; b; c; d) Central Paratethys Sea connections during the Badenian. From: Kováč *et al.* (2007)

## 3.3.2. Sarmatian (12.7 – 11.6 Ma)

The stratotype of the Sarmatian is located in the northern Vienna basin at the Nexing section (Papp and Steininger, 1974). Fine-siliciclastic sedimentation dominates in the lower Sarmatian. The broad spectrum of Badenian reefal structures completely vanished within the entire Paratethys Sea at the Badenian/Sarmatian boundary. Carbonates are very rare and only represented by allochtonous build-ups formed by polychaetes and bryozoans (Harzhauser and Piller, 2004a,b). The outcropping fine-siliciclastic sediments were deposited on tidal flats or in estuaries. In sections which reflects open water conditions diatomites with marine diatoms may occur (Harzhauser and Piller, 2004a,b). Marls and silty clays then represent the offshore deposits. In the late Sarmatian the sedimentation in the Central Paratethys switched from siliciclastic to carbonatic. Oolites and coquina-dominated sands spread in nearshore settings and on shallow shoals (Harzhauser and Piller, 2004a,b). The early Sarmatian polychaete–bryozoan build-ups disappeared and were replaced by unique foraminiferal build-ups contributed by the sessile foraminiferal genus *Sinzowella* (Harzhauser and Piller, 2007).

In the Eastern Paratethys the Sarmatian analogue in the regional stages are Volhynian and Bessarabian. The Paratethys became nearly completely sealed off at this time and the Central Paratethys was only connected to the Eastern Paratethys. A narrow marine connection into the Mediterranean Sea formed in the east due to tectonic movements along the Dead Sea fault system (Steininger and Wessely, 2000).

# 3.4. Late Miocene

## 3.4.1. Pannonian (11.6 – 6.1 Ma)

The stratotype of the Pannonian regional stage is defined at Vösendorf in the southern Vienna Basin (Papp, 1985a). The Pannonian represents the ongoing degree of continentalisation in the central and south-eastern Europe which resulted into the restriction of the aquatic realm of the Central Paratethys area to the Pannonian basins system and formation of the Lake Pannon at about 11.6 Ma in the place of the relic Paratethys Sea (see Fig. 4). The brackish to freshwater lake was encircled by the Alps, the Carpathians and the Dinarids. Grey-blue clays and marls are typical deposits in basinal settings whilst deltaic gravel, sand, whitish marls and lignites accumulated along the coasts of the Lake Pannon (Harzhauser and Piller, 2007). Oolites and bryozoans buil-ups are frequent in the late Bessarabian stage of the Eastern Paratethys (Pisera, 1996), conversely in the Lake Pannon there are no equivalents (Harzhauser and Piller, 2007). During the late Pannonian, the northwestern part of the Lake Pannon (e.g. Vienna

Basin) turned into floodplain environment as a consequence of the retreat of the coastline (Magyar *et al.,* 1999; Harzhauser and Tempfer, 2004). The southern and central part of the Lake Pannon remained as a several hundred metres deep sub-basin complex filled by prodelta turbidites and prograding deltaic deposits (Popov *et al.,* 2004). The southern coastline along the northern Dinarids was quite stable throughout the Pannonian (Magyar *et al.,* 1999; Popov *et al.,* 2004).

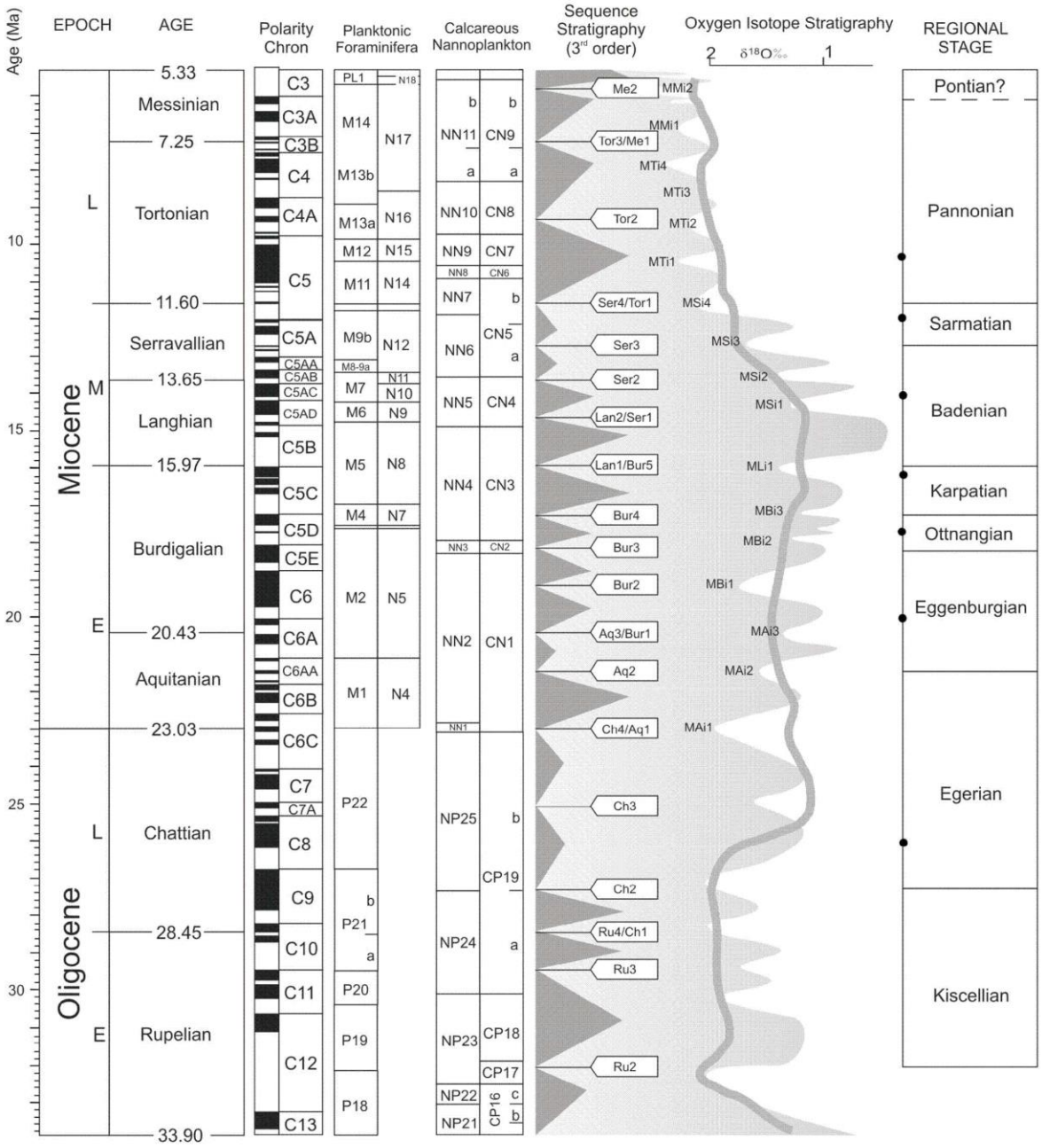


**Figure 6.** Oligocene – Miocene geochronology; geomagnetic polarity chrons; biozonations of planktonic foraminifers and calcareous nannoplankton (all Lourens *et al.*, 2004); sequence stratigraphy and sea level curve (Hardenbol *et al.*, 1998); oxygen isotope stratigraphy (Abreu and Haddad, 1998); the black dots (the right column) indicate the stratigraphic position of the holostratotypes of the regional stages. From: Piller *et al.* (2007)

# 4. Material and methods

The Borehole LOM-1 has represented a convenient material for our study of stable isotopes as geochemical proxies. The borehole LOM-1 was drilled as a part of project GAČR 205/09/0103 therefore the material was available. Another aspect was that LOM-1 is rich of fossil content with relatively good preservation (preservation is crucial in the stable isotope analysis) and apparently represents some very specific environment within the Carpathian Foredeep. In addition, there was reported a minimal taphonomic alteration of microfossil assemblages. It was also studied by Holcová *et al.* (submitted) by using multiproxy approach including sedimentology, gammaspectrometry, biostratigraphy and paleoecology (foraminifera, calcareous nannoplankton, otholiths) thus LOM-1 was perfect for our cause because in the end both studies could be compared and one could confirm or contradict the other.

## 4.1. Locality

The cored shallow borehole was drilled near the town Lomnice (see Fig. 7), referred to as the borehole LOM-1 (GPS location 49°23.945'N and 016°24.542'E, 382 m a.s.l.). The borehole was drilled within the GAČR 205/09/0103 project.

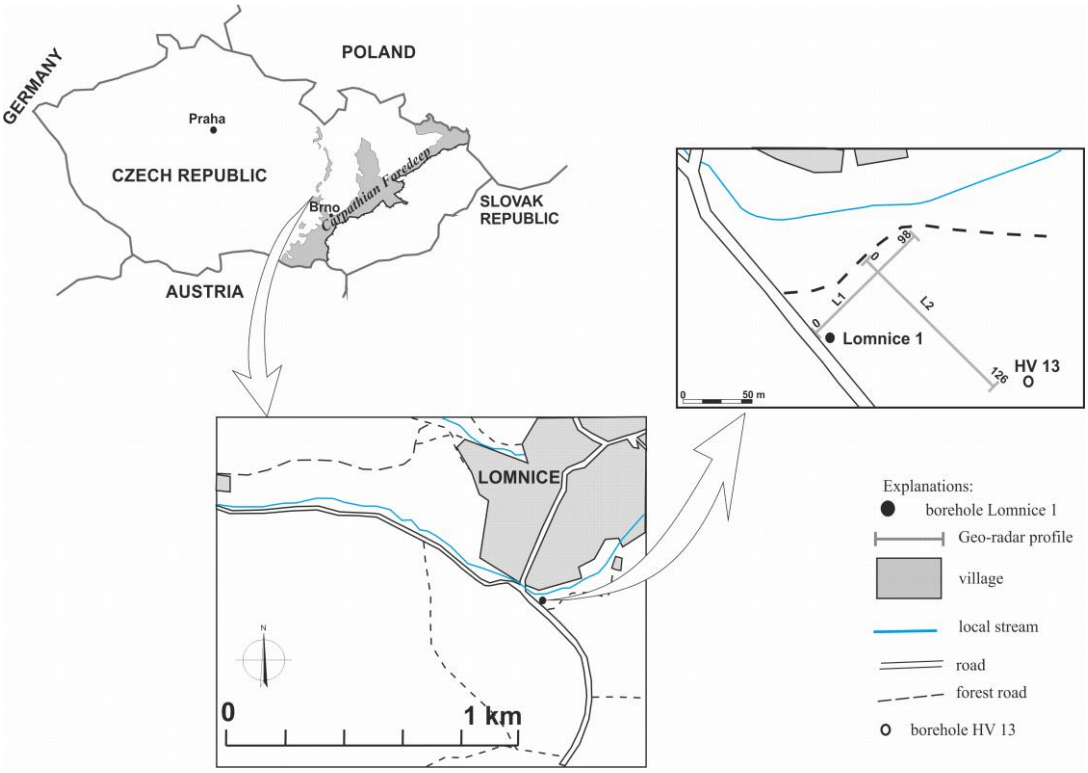


**Figure 7.** Map with the localization of the borehole Lomnice, LOM-1. From: Holcová *et al.* (submitted)

## 4.1.2. Geological settings

The Miocene deposits from the wider vicinity of Lomnice are only known as isolated erosional relics. Their exact areal extent is poorly known because of thick Quaternary cover. These deposits are a part of the Carpathian Foredeep, which represents a peripheral foreland basin formed on the loaded eastern margins of the Bohemian Massif due to the tectonic emplacement of the Carpathian thrust wedge. Marine sedimentation in this western sector of the Carpathian Foredeep commenced in the Egerian to Early Eggenburgian and continued into the Mid Badenian. The studied section is formed by the youngest marine deposits. In the early Middle Miocene, the basin geometry was reorganised by the northward (NW- to NNW-oriented) structural contraction of the Carpathian orogenic wedge and so Badenian deposits of the foreland basin represent a distinct period of the basin evolution (Nehyba and Šikula, 2007). Parastratotype of the Moravian is situated at locality Borač in Lomnice – Tišnov relict (Papp *et al.*, 1978).

Miocene deposits at Lomnice are represented by calcareous clays, sandy clays, quartzose sands, calcareous sands and algal limestones (Hudec, 1986). They lie on the Pre-Neogene basement formed by the metamorphic rocks of the Svratka unit of the Moravian Zone (Precambrian), (Mísař *et al.*, 1983). Stratigraphical and paleontological studies about these localities were published by Procházka in the end of the nineteenth century (e.g. Procházka, 1892a, b, 1893, 1899). He interpreted the deposits as marine ones, deposited along very irregular coastline with numerous bays and islands, with an important role of a basement relief. Novák (1975) and Zdražílková (1985) studied the Lower Badenian limestones in the area and speculated about their deposition in a narrow sea bay with important input of terrigenous material. Based on the study of otoliths, Brzobohatý (1975) interpreted the normal salinity conditions and deposition likely in the shallower neritic (infralitoral) environment. *Scleractinia* from this locality were studied by Hladil (1976). Hamršmíd (1985) described the trace fossil *Helicotaphrichnus commensalis* from the locality Lomnice.

## 4.1.3. Biostratigraphical correlation

Traditionally, the stratigraphical position of the deposits was based mainly on the study of gastropoda and corrals. Lower Badenian age is confirmed by occurrences of *Turritella spirata, Nassa restitutiana, Mitra scrobiculata* and *Anachis moravica* (e.g. Hudec, 1986).

The biostratigraphical correlation (see Fig. 8) of the section is based on the first and last occurrences of planktonic foraminifera and calcareous nannoplankton index species (Gradstein *et al.*, 2012). The succession of the bioevents follows well the successions in the Mediterranean area (Di Stefano *et al.*, 2008; Abdul Azis *et al.*, 2008; Hüsing *et al.*, 2010), where the LO of *Praeorbulina* spp. is an indefinable event which may be observed above the LO of *Helicosphaera waltrans*. The same succession of bioevents was described in the Carpathian Foredeep by Švábenická (2002) and also in the borehole RY-1 Rybníček (Kopecká, 2012) and OV-1 Oslavany (Nehyba, personal communication); (Holcová *et al.*, submitted).

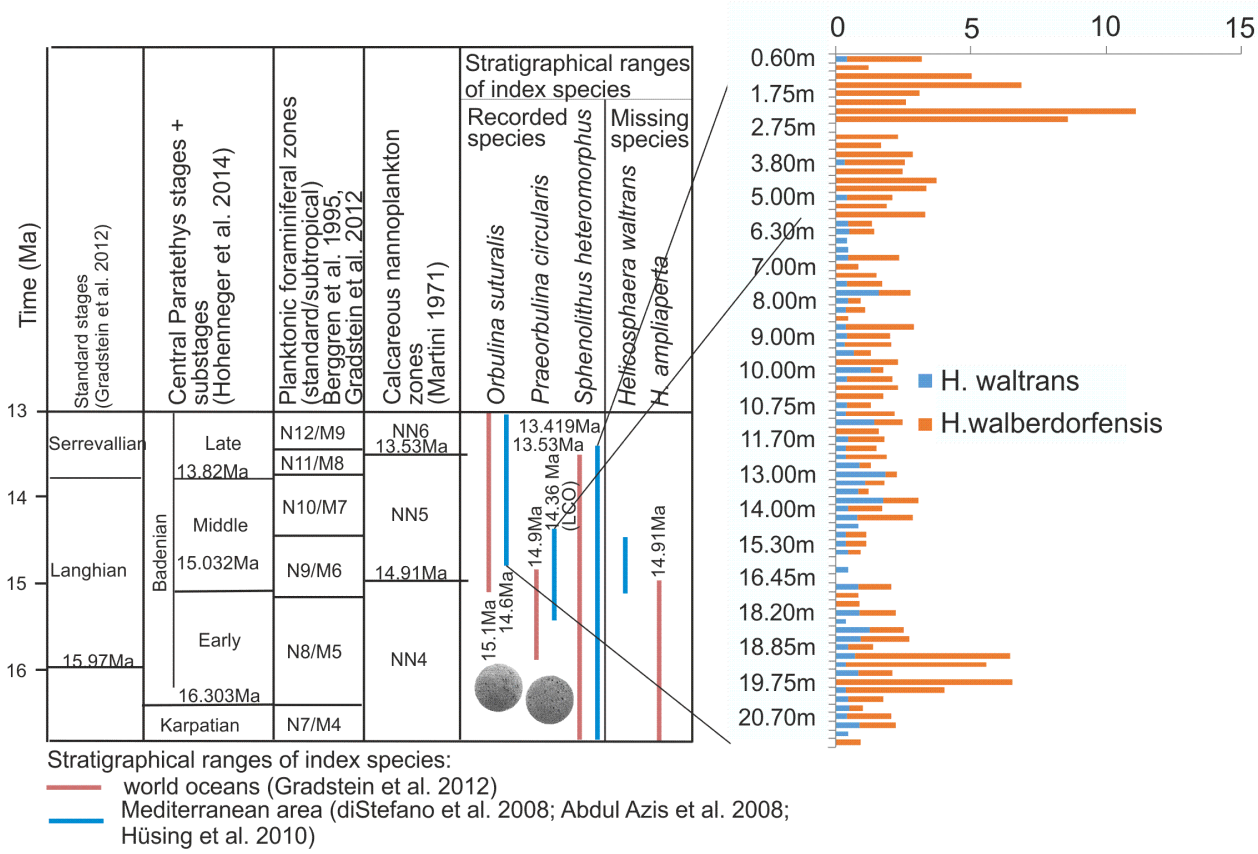


**Figure 8.** Stratigraphical ranges of index species. In the right part of the picture, there is a gradual decrease of relative abundances of *Helicosphaera waltrans* in comparison with the abundances of *Helicosphaera walberdorfensis* which is shown here. From: Holcová *et al.* (submitted)

From the index species, *Praeorbulina* (the last occurrence (LO) 14.9 Ma: Gradstein *et al.*, 2012; Mediterranean area: latterly: Abdul Azis *et al.*, 2008), *Orbulina* (the first occurrence (FO) 15.1 Ma: Gradstein *et al.*, 2012; Mediterranean 14.6 Ma: Abdul Azis *et al.*, 2008; Hüsing *et al.*, 2010) and *Sphenolithus heteromorphus* (LO 13.53 Ma Gradstein *et al.*, 2012, Mediterranean area 13.419 Ma: Abdul Azis *et al.*, 2008; Hüsing *et al.*, 2010) were recorded during the whole interval and *Helicosphaera ampliaperta* (the LO 14.91 Ma; Gradstein *et al.*, 2012) is missing. The top of the continual occurrence of *Helicosphaera waltrans* (the LCO (Last Common Occurrence) at 14.357 Ma in the Mediterranean area: Abdul Azis *et al.*, 2008) is recorded around the level 6.0 m. The gradual decrease of its relative abundances in comparison with abundances of *Helicopshaera walberdorfensis* is shown at Fig. 8. The LOM section can be correlated with the interval 14.6 Ma (the FO of *Orbulina* spp. in Mediterranean) to 13.42 Ma (the LO of *Sphenolithus heteromorphus*), though the upper boundary is probably older (Holcová *et al.*, submitted).

## 4.1.4. Previous research results

The previous research was done by Holcová *et al.* (submitted). The team of authors processed the same material and their researches in biostratigraphy and paleoecology based on foraminifera, calcareous nannoplankton and otoliths plus sedimentological research (see Fig. 9). Their conclusions are summarized further.

The borehole LOM-1 represents an environment of an outer shelf to upper bathyal. The litology mainly consists of monotonous clayey silts which are typical for the proximal parts of peripheral foreland basin. Specificity of this section, in comparison with other Moravian localities, is documented by high abundances of benthic foraminiferal high-nutrient markers such as *Nonion* spp. and *Uvigerina* spp. as well as planktonic foraminiferal species *Globigerina bulloides* and *Globigerina praebulloides*. These foraminiferal species require a high nutrient input, better of a marine origin, produced during phytoplankton blooms which are often triggered by an upwelling regime. However, the significant role of the terrigenous nutrient input can be interpreted from the common occurrence of the opportunistic foraminiferal taxa *Cibicidoides* spp. (Holcová *et al.,* submitted).

↓ **Figure 9.** The summarizing picture of the major faunal trends/changes, paleoenvironmental interpretation, gammespectrometrical curve and litofacial profile in the LOM-1 section. From: Holcová *et al.* (submitted)

m of LOM-1
Lithology
Lithofacies
Th
U
K
Th/U
Th/K
1 2 3 4
shallowing
hypoxy at floor
cooling
oscillation of nutrient input and oxygen at the sea floor
maximum of nutrients
oscillation of nutrient input and oxygen at the sea floor
Benthic foraminifera
Bulimina diversified
oscillations of high-nutrient, hypoxis and lagenids
lagenids low diversity
Sphaeroi-dina
oscillations of hypoxis and lagenids
Uvigerina + Cibicidoides
Sphaeroidina + Cibicidoides + Pullenia
Diatoms
no diatoms
abundant diatoms
rare diatoms
no diatoms
Planktonic foraminifera
diversified
Globigerinoides Globigerinella
small Globigerina T. quinqueloba
decrease Globigerinoides increase T. qiunqueloba through oscillations
G-noides G-nella
small Globigerina T. quinqueloba
Globorotalids
Globigerinoides + Globigerinella + globoraliids
Calcareous nannoplankton
R. minuta
C. pelagicus
variegated R. minuta + C. pelagicus
peaks of C. pelagicus
variegated R. minuta + R.. haqii
peaks of R. haqii
R. minuta
R. minuta + U. jafari
R. haqii + U. jafari
Otoliths
LCO of Helicosphaera waltrans
dominant myctophid otoliths (< Diaphus)
most abundant otoliths
peak of Vinciguerria
high diversity, deepest assemblage
low diversity
neritic taxa increas
shallowest assemblages
no stomii-forms
highest diversity
peak of Gadiculus argenteus
Interpretation
shallowing
increased hypoxy and nutrients at the sea floor
seasonally changes mixed/stratified layer
variegated, short-time oscillations
cooling, instable (seasonality + interannual variations) stress in superficial layer
warm low nutrients
cold, decrease nutrient increase oxygen
cooling, instability
increased hypoxy at the sea floor
pulse of eutrophic (?cold) water (14,16 m)
???sesonal coastal upwelling
rapid warming ( deepening)
seasonal oscillations of nutrient and oxygen con increase of nutrients

The studied section can be subdivided into seven intervals (see Fig. 9). This confirms a rather cyclical character of Middle Miocene sedimentation in the Central Paratehys which was triggered by Milankovitch cycles. Each cycle starts with rapid warming and continues with gradual cooling. The seasonal succession of assemblages was interpreted mainly from co-occurrence of planktonic foraminiferal species which is specific for different seasons. The season with colder, mixed water was followed by a season with stratification of water column consisting of oligotrophic and warm upper layer and low oxic condition at sea floor. Occurrence of the small oxyphilic opportunistic foraminiferal taxa *Cibicidoides* spp. is pointing to a terrestrial input of nutrients. However, *Epistominella* spp. and *Cassidulina* spp. as markers of the terrigenous nutrient input are missing. In addition, the seasonal upwelling cannot be excluded during the deposition of the lower part of studied section. (Holcová *et al.,* submitted).

From oscillations of Thorium (Th), Uranium (U) and Kalium (K) values (gammaspectrometry), (see Fig. 9) and relative abundances of high-nutrient/oligotrophic markers together with warm/cold water and stress markers an interannual variations of nutrient content, temperature and/or salinity are expected (Holcová *et al.,* submitted).

The turnover connected with initiation of the “Middle Miocene Climate Transition” is recorded above the LO (last occurrence) of *Helicosphaera waltrans* (Holcová *et al.*, 2015). This is in agreement with previous observations in the Carpathian Foredeep. The changes mentioned above include cooling, decrease of nutrients, a probable increase of salinity of superficial water and increase of seasonality. The high numbers of otoliths of cryophilic fish species *G. argenteus argenteus* are also indicative for cooling (Holcová *et al.,* submitted).

## 4.2.1. Methods

The borehole LOM-1 was drilled in the length of 21.5 meters and was sampled after 25 cm. The Miocene sediments are present in the interval from 0.5 m to 21.5 m. The LOM-1 samples were washed out and wet sieved into the fraction of 0.063 - 2 mm. After that Foraminifera were picked up under the light microscope from this fraction.

The suitability for the stable isotope analysis of carbon and oxygen was evaluated based on the inner wall structure preservation. This is a really important step, because analyzing the inappropriate samples could cause a total distortion of results. Such results are completely wrong and their interpretation is a mistake.

At first, each sample was floated in distilled water, to get to uplift tests with no mineral filling. After that, for each sample around thirty specimens of various species were picked up (the number of species was as high as possible; it depended strongly on the character of each sample; multiple test of each species). These species (tests respectively) were analyzed by SEM (scanning electron microscope) at first as a whole set and after that the specimens were crushed under the light microscope and analyzed under the SEM again to see more details and to get a better view on the inner wall structure characteristics. The inner wall, in ideal case, should not show any signs of the slightest recrystallization. It is visible as a crystal coating on the inner wall or as diagenetic calcite crystals (differences in the arrangement of crystals) on the wall sections (see Fig. 10; appendix 1). The ideal sample has got a smooth inner wall structure with no signs of minor recrystallization, both on the surface and cross-sectional (see Fig. 10). From each sample, twenty five to thirty tests were analyzed. Multiple tests of the same species (three per species in most cases) were chosen. Samples were analyzed as a whole set to get the best possible results.

Based on the previous characteristics, fifteen samples were chosen as suitable for the stable isotope analysis. They were 4.5 m; 8.5 m; 9 m; 10 m; 11 m; 11.3 m; 11.7 m; 12.6 m; 14.25 m; 14.5 m; 16.5 m; 16.75 m; 18 m; 19.2 m; 19.25 m (appendix 5).

From each of these samples around twenty to thirty specimens (varying throughout the samples, based on the characteristics of each particular sample), their tests respectively, were picked up for the stable isotope analysis. In this step, however, only multiple tests of the particular species were chosen. The species were chosen carefully based on their “usability” for stable isotope studies. It depends primarily on the level of knowledge about the life of the particular species and of course on the life strategy itself. As the primary target for our analysis, these species were chosen: (see Fig. 11) *Globigerina bulloides, Orbulina universa, Praeorbulina glomerosa*, *Globigerinoides* spp., *Uvigerina* spp., *Heterolepa dutemplei, Gyroidinoides* spp*., Melonis pompilioides* and *Cibicidoides* spp. Each sample contained specific assemblages therefore it is not usual that all the marked species are present in each sample. Sometimes, in samples with lower diversity, other possibly interesting species were only chosen to supplement the set. From the marked species, five tests of each present species were picked up in each sample (if it was possible) to capture the variability of the isotopic values either for the individual tests. At the same time, we tried to pick up the tests of approximately the same size to minimize any differences caused by the ontogenetic development. Each analysis represents exactly one test from the sample.

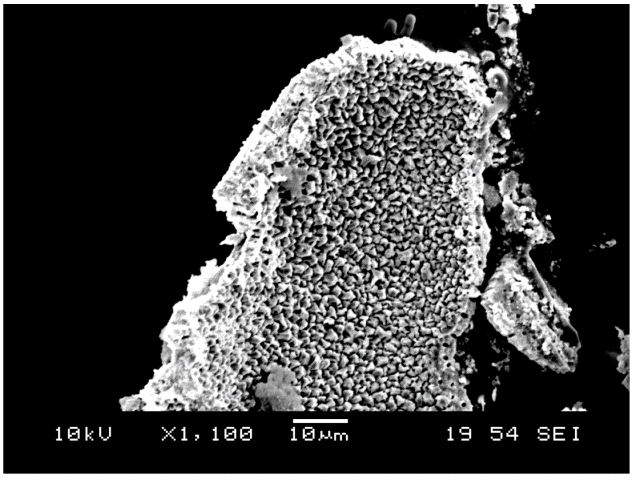


**A:recrystallization of inner wall structure**

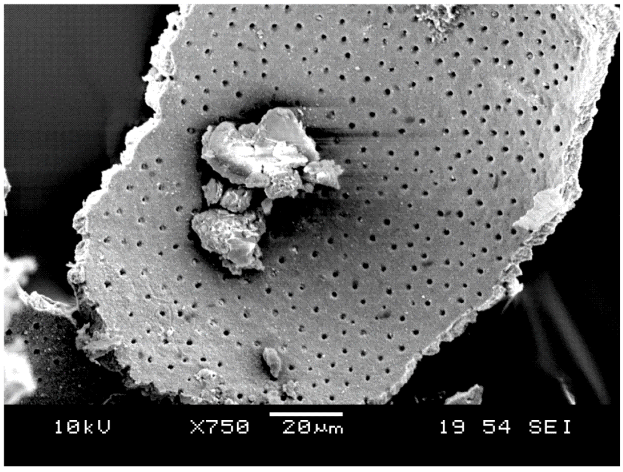


**B:well-preserved inner wall structure**

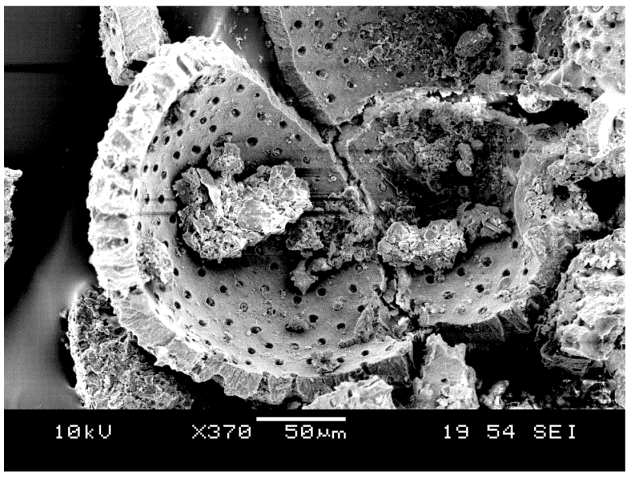


**C:well-preserved inner wall structure**

**Figure 10.** Inner wall preservation: A: a clearly visible crystal coating on the inner wall thus inappropriate for analysis; B + C: smooth inner walls with no signs of recrystallization.

The target species were chosen based on their ecological preferences to document the different biotops and niche in the water column and at sea floor (see Fig. 11): *Globigerina bulloides* - quite cold-water, high-nutrient, shallow dweller (Schiebel *et al.*, 1997; Hemleben *et al.*, 1989); *Orbulina universa, Praeorbulina glomerosa*. - warm-water, oligotrophic, shallow dweller; the same is valid for *Globigerinoides* spp. (Bé, 1977; Reynolds and Thunell, 1985; Hemleben *et al.*, 1989; Chapman, 2010; Schiebel and Hemleben, 2005); *Uvigerina* spp. - low-oxic, infaunal (Miller and Lohman, 1982; Jorrisen *et al.*, 1992; Murray, 2006), *Heterolepa dutemplei* and *Cibicidoides* spp. - high-oxic, epifaunal (Kaiho, 1994; Murray, 2006); *Gyroidinoides* spp. – epifaunal (Murray, 2006) and *Melonis pompilioides*-infaunal (Caralp, 1989; Hermelin, 1992; Sjoerdsma and van der Zwaan, 1992; Sen Gupta and Machain-Castillo, 1993; Miao and Thunell, 1993; Rathburn and Corliss, 1994).

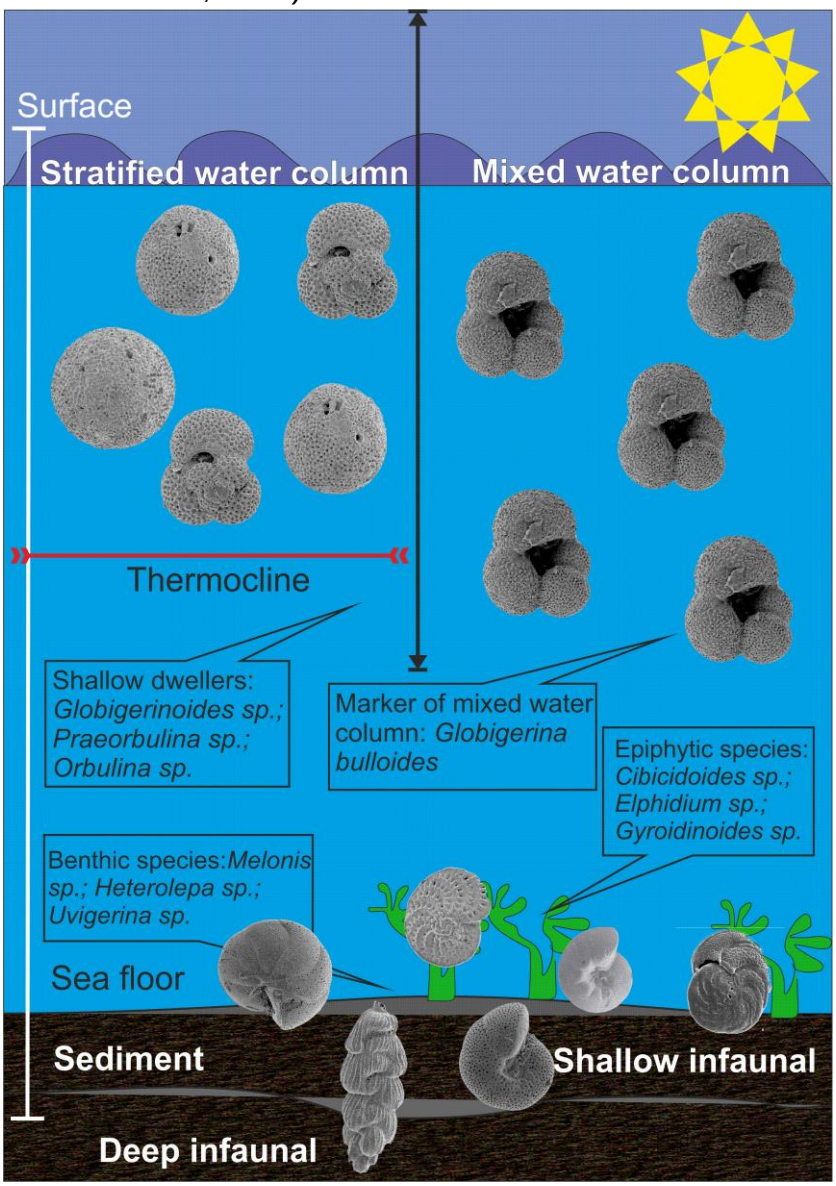


**Figure 11.** The life positions and habitat of the marked foraminiferal species used for the stable isotope analysis.

## 4.2.2. Stable isotope analysis

The analysis of stable isotopes of carbon and oxygen were performed by Dr. R. Milovský, Geologický ústav SAV, Banská Bystrica, Slovakia. The laboratory is equipped with the Thermo Scientific Kiel IV Carbonate Device (see Fig. 12) coupled to the Thermo Scientific 10kV MAT 253 Mass Spectrometer. All isotopic data were reported in ‰ relative to VPDB related to the ATC1 standard.

The KIEL IV Carbonate Device uses the principle of the individual acid bath (see Fig. 13) for conversion of carbonates to $CO_2$. The storage, transfer and chemical reaction of phosphoric acid at elevated temperatures are operated under full temperature control (temperature controlled oven +/- 0.1°C, absolutely dry conditions). The system uses 105% dry phosphoric acid. The borosilicate septum-free vials are used for the phosphorolysis of the carbonates. All the released $CO_2$ is transferred and processed in an all-metal sealed cryogenic trapping system (see Fig. 13). The reaction of carbonates with phosphoric acid produces $CO_2$ and $H_2O$ and traces of water contained in the nominally anhydrous phosphoric acid (104% of $H_3PO_4$ = 0.25 mol $H_2O$/L $H_3PO_4$), plus non-condensable gases (e.g. $N_2$, $O_2$) from impurities in the sample. The cryogenic trapping system consists of a temperature controlled first trap with associated valves, an ultra-high vacuum system, pressure gauge and a microvolume. In the first step, $CO_2$ and $H_2O$ are trapped into the first automated liquid nitrogen trap at -190 °C while any non-condensable gases are removed. The $CO_2$ is then released at -90 °C for the transfer into the microvolume, while the water is completely retained in the first trap. The microvolume is heated to +30 °C releasing the $CO_2$ via a dedicated stainless steel capillary to the changeover valve and into the IRMS (mass spectrometer) for $\delta^{13}C$ and $\delta^{18}O$ analysis. In parallel, the water is removed from the gas cleaning and trapping system by baking the first trap and evacuating all valves and gas lines. Based on the pressure of the released $CO_2$ the software defines the portion of $CO_2$ being transferred into the microvolume. This assures the optimal sample gas pressure in the Isotope Ratio MS. In parallel, the reference gas bellow in the dual inlet is pre-adjusted to the expected inlet pressure (modified from: www.thermoscientific.com; 12. 4 2015).

An overall external precision of 0.04‰ for $\delta^{13}C$ and 0.08‰ for $\delta^{18}O$ is reached for the samples greater than 20 µg. For samples with weight smaller than 10 µg an overall external precision is of 0.05‰ for $\delta^{13}C$ and 0.1‰ for $\delta^{18}O$ (modified from: www.thermoscientific.com; 12. 4 2015).

There were fifteen samples (mentioned above; see appendix 3; 5) and 348 single tests for analysis were taken from these samples. In addition, 25 tests were picked up to supplement the previous 348. In total, 373 tests were analyzed. Not all analysis were successful because of the initial problems with instrumental technique and several analyzes were not included in the conclusions due to unreliable data values mainly caused by very low weight of the analyzed sample (sample = test mentioned here). The weight limit was around 9-10 µg per test.

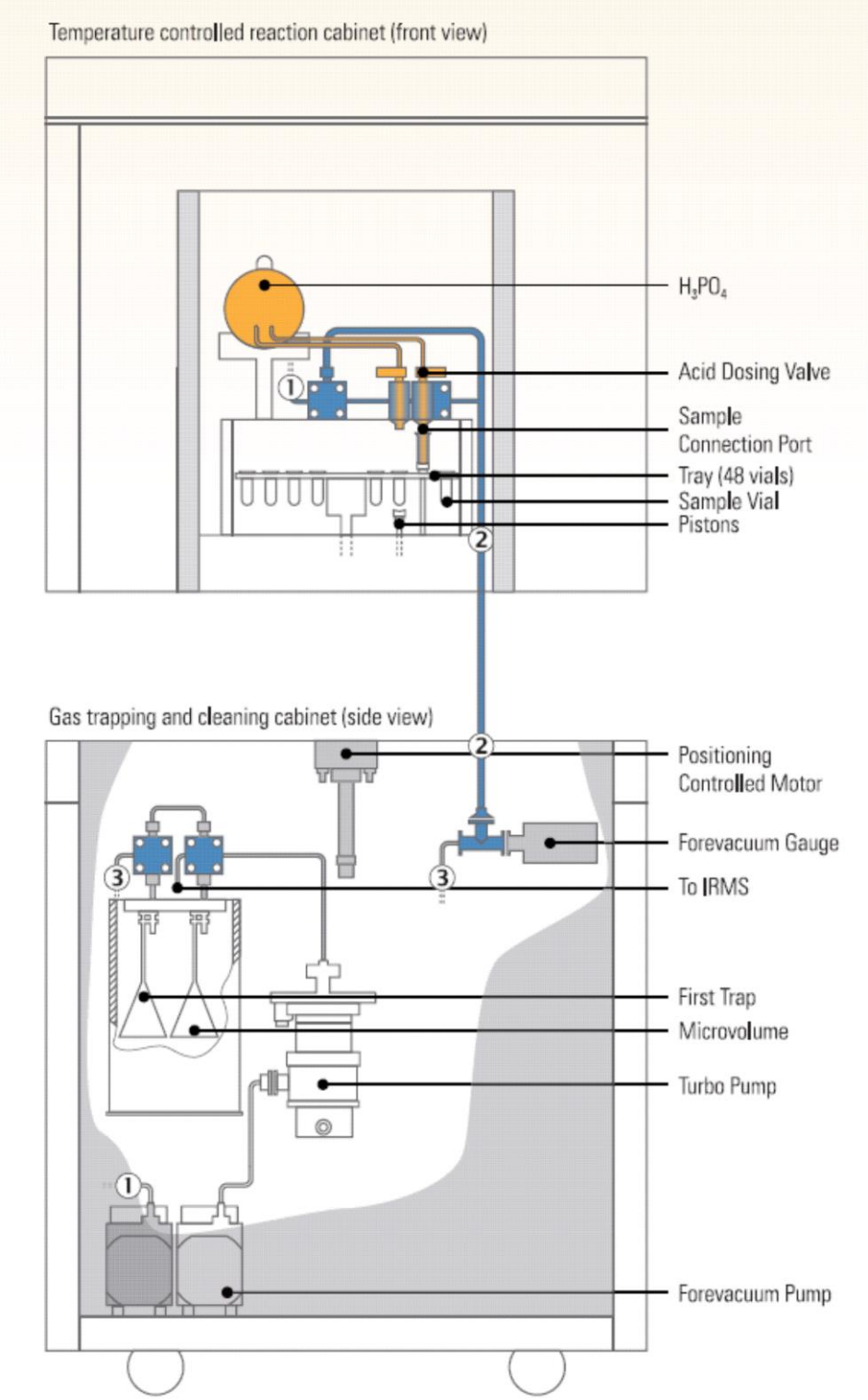


**Figure 12.** The inside views of the temperature controlled reaction cabinet (top) and the gas trapping and cleaning cabinet (bottom) show: 1) The connection to four vacuum pumps for vial pre-evacuation; 2) The connection of the reaction region and first trap; 3) The connection to the high vaccum region for the first trap and microvolume evacuation; From: www.thermoscientific.com; 12. 4 2015

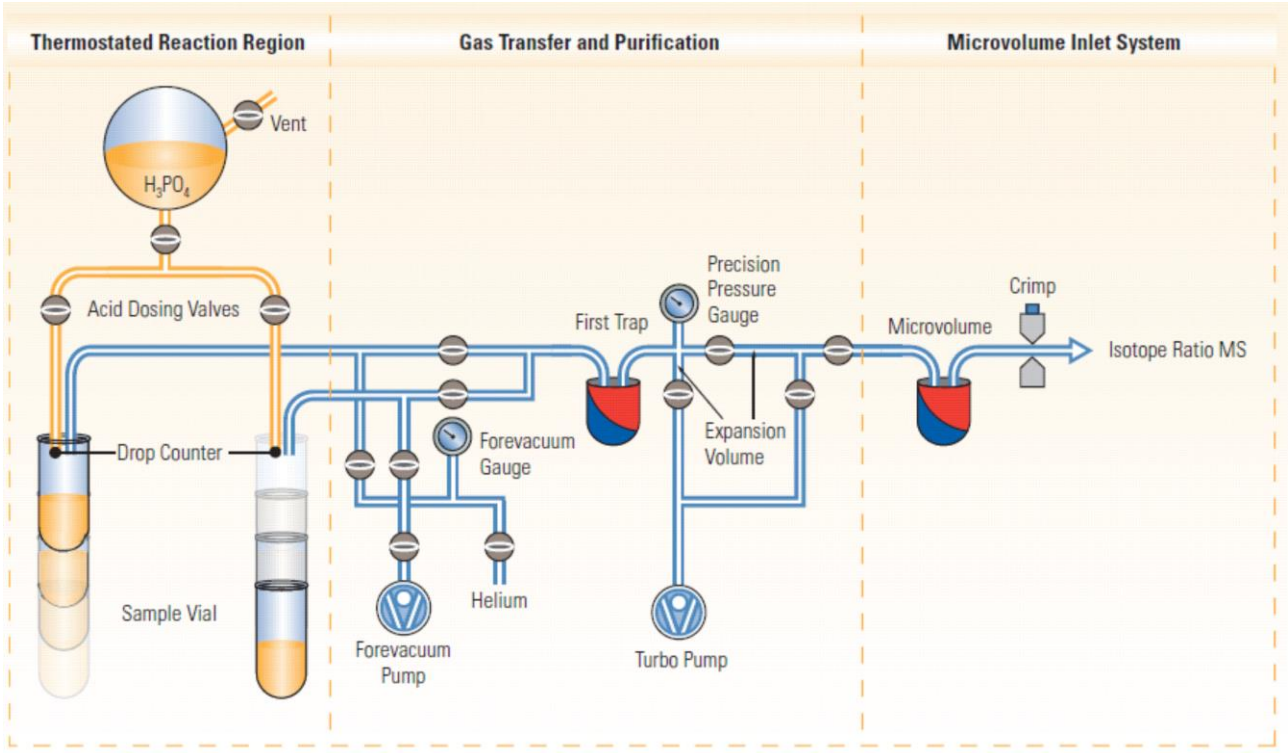


**Figure 13.** Schematic of the KIEL IV Carbonate Device. From: www.thermoscientific.com; 12. 4 2015

## 4.2.3. Benthic foraminiferal oxygen index (BFOI)

The Benthic foraminiferal oxygen index (BFOI) was developed by Kaiho (1994, 1999). BFOI expresses the amount of dissolved oxygen in bottom waters on the basis of the composition of benthic foraminiferal assemblages. The variations in the abundances of oxygen-sensitive morphologic groups may reflect changes in the dissolved oxygen content. Kaiho (1994) divided the calcareous benthic foraminifera into three groups: (i) dysoxic (0.1 – 0.3 mL/L $O_2$), (ii) suboxic (0.3 – 1.5 mL/L $O_2$) and (iii) oxic (>1.5 mL/L $O_2$). The foraminifera were divided on the basis of relation between the specific morphological characteristics, oxygen levels and foraminiferal microhabitat. (i) The dysoxic indicators are characterized by e.g. thin wall (e.g. *Globobulimina* spp., *Chilostomella* spp., *Bolivina* spp., *Fursenkoina* spp.); small; flat or elongate-tapered morphotypes; high porosity tests; infaunal dwelling but living in both epifaunal – infaunal life position. (ii) The oxic indicators are characterized by e.g. thick wall; large tests; epifaunal; absent in low oxygen conditions; planoconvex, biconvex, rounded trochospiral and sphaerical test shapes (e.g. *Cibicidoides, Nuttalides, Globocassidulina*). (iii) Kaiho (1994) divided the suboxic indicators into three subgroups. The first one is characterized by small specimens of oxic indicators. The second group is between the morphological extremes of oxic and disoxic indicators (*Lenticulina, Dentalina, Nodosaria*), large ornamented species (e.g. *Bulimina, Stilostomella*); rounded planispiral, flat ovoid,

and sphaerical forms; small and thin-walled, planoconvex and biconvex, trochospiral forms (e.g. *Uvigerina, Oridorsalis, Gyroidina, Gyroidinoides, Hoeglundina*). The third group consist of the species which have thin walls but their microhabitats are between the first two groups (e.g. *Bulimina aculeata, Nonionella* spp., *Elphidium excavatum*); (Kaiho, 1994, 1999). For furthermore details see Kaiho (1994, 1999).

The BFOI mathematical formula is {[*O*/(*O*+*D*)] x 100}; *O* and *D* are numbers of specimens of oxic and disoxic foraminifera. The values range between 100 and 0. When *O* = 0 and *D*+*I* > 0 (I is the number of specimens of suboxic indicators), the equation is {[*I*/(*I*+*D*)] - 1} x 50, and the values ranging between 0 and -50. The following five dissolved oxygen conditions are recognized (see Table 3.): anoxic (0 – 0.1 mL/L $O_2$), dysoxic (0.1 – 0.3 mL/L $O_2$), suboxic (0.3 – 1.5 mL/L $O_2$), low oxic (1.5 – 3.0 mL/L $O_2$) and high oxic (3.0 – 6.0 + mL/L $O_2$); (Kaiho, 1994).

Dissolved oxygen conditions recognized using calcareous benthic foraminifera and their characteristics (Kaiho 1994)

| Oxygen condition | Oxygen level (mL/L) | Oxygen index | Calcareous benthic foraminifera characteristics |
|---|---|---|---|
| High oxic | 3.0 - 6.0+ | 50 - 100 | Dysoxic, suboxic and high ratios of oxic indicators |
| Low oxic | 1.5 - 3.0 | 0 - 50 | Dysoxic, suboxic and low ratios of oxic indicators |
| Suboxic | 0.3 - 1.5 | -40 - 0 | Disoxic and high ratios of suboxic indicators |
| Dysoxic | 0.1 - 0.3 | -50 - (-40) | Disoxic and low ratios or barren of suboxic indicators |
| Anoxic | 0.0 - 0.1 | -55 | Barren of calcareous benthic foraminifera |

**Table 3.** Explanation of BFOI values, dissolved oxygen conditions and their characteristics. From: Kaiho (1994)

Three separate calculations were used in this study. Three models were used due to different positioning of various species in particular groups (dysoxic, oxic and suboxic group), (see appendix 4). The first BFOI calculation followed Kaiho (1994) and his classification of species. However, Kaiho (1994) developed his classification based on modern foraminiferal species with known ecological preferences. In the Central Paratethys, these ecological preferences are not entirely known for many foraminiferal species and the ecological preferences are mainly derived from actuoecology of related species or their modern equivalents. To use a calculation following Kaiho (1994) a reclassification of the Central Paratethys species with no modern equivalent was done sensu Kaiho's (1994) description of dysoxic, oxic and suboxic groups. As the main character, the morphological description and relation to the modern equivalents of species were chosen as described above.

The second calculation followed Báldi (2006) classification of benthic species. Báldi (2006) used various morphologic criteria at the species level to associate the species with inbenthic and epibenthic microhabitat. An attention was also paid to the association of endemic and extinct foraminiferal species with the inbenthic and epibenthic microhabitat. This classification also followed ecologic observations of Kouwenhoven and Van der Zwaan (2006) which appeared after Kaiho (1994). The positioning of *Lenticulina* group, *Uvigerina* group, *Melonis pompilioides* and *Pullenia bulloides* are the main differences from Kaiho's (1994) classification. Kaiho (1994) places all the mentioned groups and species to suboxic group of species but conversely Báldi (2006) considers *Lenticulina* group as oxic species (strictly epibenthic microhabitat), *Uvigerina* group with *Melonis pompillioides* and *Pullenia bulloides* as dysoxic species (infaunal microhabitat sensu Báldi (2006)). To see the different positioning of particular species see appendix 4. For furthermore details about the differences in classification and positioning/microhabitat of species see Báldi (2006).

Finally the third calculation was based on my own proposal for classification of species to oxic, suboxic and disoxic categories. The *Lenticulina* group was divided based on the morphological characteristics. Large ornamented species (*Lenticulina inornata*) were considered as oxic group of species while smaller species with not such a distinctive ornamentation were considered as suboxic group. The same was done for *Uvigerina* group where the ornamentation and sculptation were the main feature for dividing the group into the dysoxic species (see appendix 4) while *Uvigerina semiornata* was placed in the suboxic species. *Pullenia bulloides* and *Melonis pompilioides* were considered as suboxic species because it seems that the nutrient availability is the main factor controlling their relative abundances (e.g. Sen Gupta and Machain-Castillo, 1993; Miao and Thunell, 1993; Rathburn and Corliss, 1994). For furthermore details about positioning of particular species see appendix 4.

Likewise, see appendix 4 for differences in the individual calculations (plotted graphs). All three models were calculated following Kaiho's (1994) mathematical formula as described above.

# 5. Results and interpretation

## 5.1 Stable Isotope analysis of $\delta^{13}C/^{12}C$ and $\delta^{18}O/^{16}O$

Fifteen samples were analyzed from the interval 19.25 m – 4.50 m for stable isotopes. In this chapter, the results are presented for the individual samples from the bottom to the top of the LOM-1 borehole. Each sample is discussed separately. Original data of the stable isotopic analysis of $\delta^{13}C/^{12}C$ and $\delta^{18}O/^{16}O$ are presented in appendix 2. The separate data with plotted graphs for each sample are presented in appendix 3. The X – axis represents $\delta^{18}O/^{16}O$ while the Y – axis represents $\delta^{13}C/^{12}C$. All values are in ‰ relative to VPDB related to the ATC1 standard.

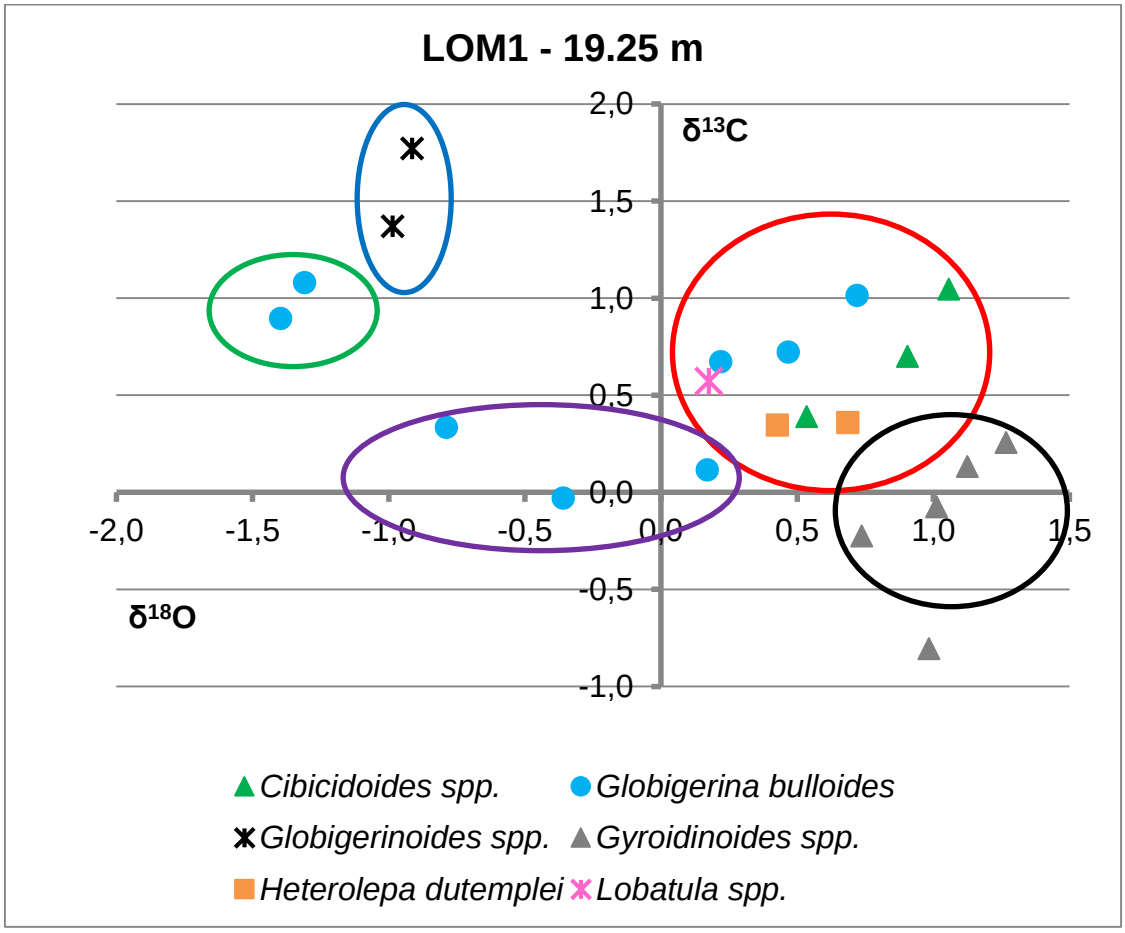


**Figure 14.** Oxygen and carbon isotope values for foraminifera from the sample 19.25 m.

The blue cluster (Fig. 14) of isotopic values for *Globigerinoides* spp. specimens (warm water, oligotrophic shallow-dweller (Bé, 1977; Reynolds and Thunell, 1985; Hemleben *et al.*, 1989; Chapman, 2010; Schiebel and Hemleben, 2005) indicates a stratified water column with oligotrophic conditions within the warm upper water layer. The warm upper water layer is represented by the negative oxygen values and represents a summer season. The green cluster (Fig. 14) of isotopic values for *G. bulloides* specimens (rather cold-water, high-nutrient, shallow dweller (Schiebel *et al.*, 1997; Hemleben *et al.*, 1989)) with positive carbon values and relatively low oxygen values demonstrates a seasonal instability probably of high precipitation rather than freshwater input, because there are no low carbon values within this cluster. The violet cluster (Fig. 14) of isotopic values for *G. bulloides* specimens' shows slightly lower carbon values which point to high nutrient availability. Oxygen isotopes show the temperature difference against the red and green clusters. The violet cluster demonstrates a well mixed water column with no apparent stratification. The red cluster (Fig. 14) represents isotopic values for separate population of *G. bulloides* which is displayed together with epifaunal *Cibicidoides* spp. and *Heterolepa dutemplei* specimens. Carbon and oxygen values in *G. bulloides* are very similar as in epifaunal species although epifaunal species shows slightly higher positive oxygen values which is in accordance with slightly cooler conditions of the bottom water. The red cluster points to a well mixed water column with a low nutrient availability which is documented by positive values of carbon isotope. This cluster probably reflects a bloom of *G. bulloides*. *Lobatula* spp. (Fig. 14) is considered to be closely related to *Cibicidoides* spp. (based on molecular data (Schweizer *et al.*, 2009)). The position of the isotopic signal for *Lobatula* spp. is corroborating this close relationship, because there is only a minor difference between the isotopic signal of *Lobatula* spp. and *Cibicidoides* spp. The black cluster (Fig. 14) represents *Gyroidinoides* spp. specimens. However, ecologic preferences of *Gyroidinoides* spp. are poorly known. Carbon values are slightly higher pointing to a low nutrient availability at the sea floor. Positive oxygen isotope values point to cooler temperatures of the bottom water.

The BFOI index indicates low oxic conditions of the bottom water in this sample. The blue cluster demonstrates a stratified water column with oligotrophic conditions and temperature stratification within a summer season. This season is probably reflected by the black cluster at the sea floor. On the other hand, the reflection of a season with high precipitation and no significant stratification of the water column is displayed by the violet and green clusters. The red cluster points to season with a well mixed water column with a low nutrient availability at the sea floor.

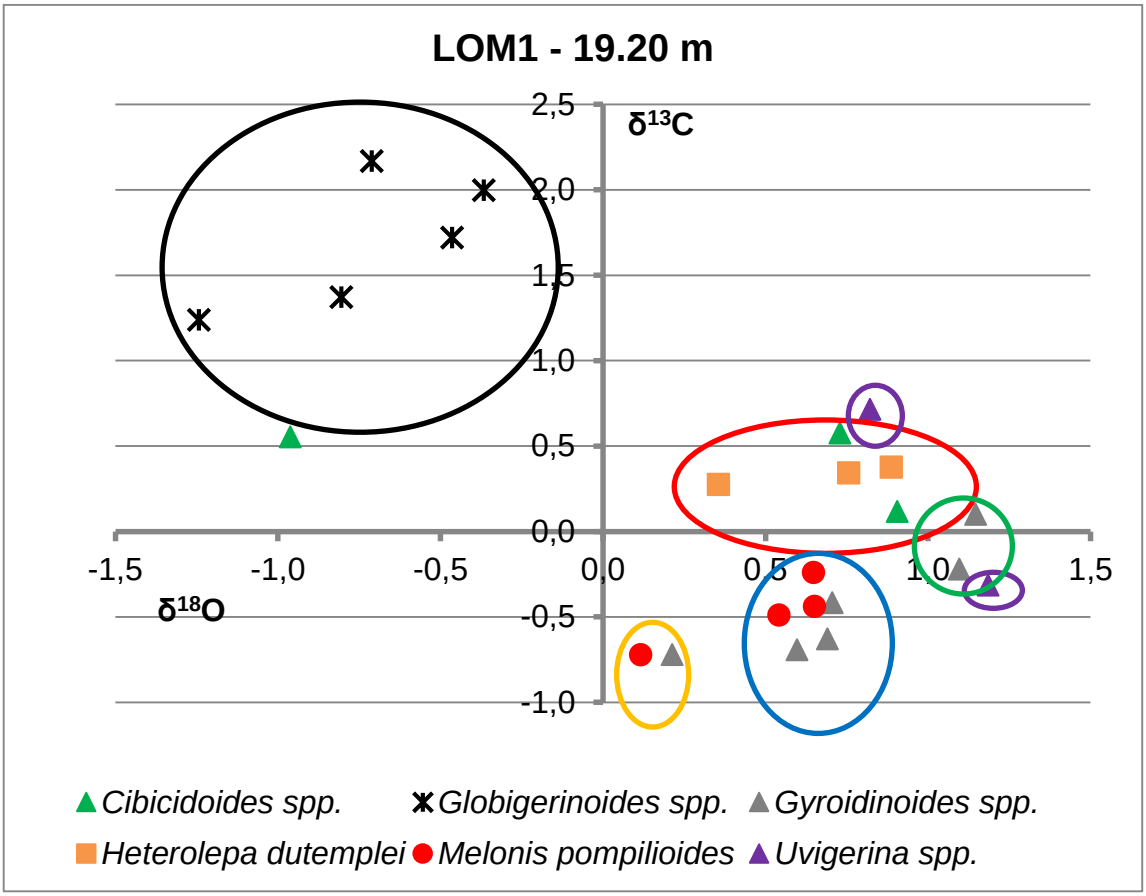


**Figure 15.** Oxygen and carbon isotope values for foraminifera from the sample 19.20 m.

The black cluster (Fig. 15) shows isotopic values for *Globigerinoides* spp. specimens pointing to a stratified water column with oligotrophic conditions of the warm upper water layer. This cluster probably reflects a summer season. The red cluster (Fig. 15) demonstrates isotopic values for epifaunal species *Heterolepa dutemplei* and *Cibicidoides* spp. specimens with positive oxygen values pointing to the cooler bottom water. The isotopic values of *Cibicidoides* spp. (Fig. 15) with high negative oxygen value of -1 was disregarded, because this isotopic response is very unlikely for this species. Such shift could be caused by diagenetic alteration or it could be a redeposition. The violet cluster (Fig. 15) displays isotopic values for two specimens of *Uvigerina* with a quite different isotopic signal. However, *Uvigerina* group was not determined at the species level and such phenomenon could be explained by different ecologic strategy (which could be quite different) and microhabitats of different *Uvigerina* species. The blue cluster (Fig. 15) represents isotopic values for *Melonis pompilioides* specimens (high nutrient; (Caralp, 1989; Hermelin, 1992; Sjoerdsma and van der Zwaan, 1992; Sen Gupta and Machain-Castillo, 1993; Miao and Thunell, 1993; Rathburn and Corliss, 1994)) together with *Gyroidinoides* spp. specimens. *Melonis pompilioides* trend to have slightly higher carbon values than *Gyroidinoides* spp., if both species are present together. However, *Melonis pompilioides* seems to be a high nutrient seasonal aspect (Caralp, 1989; Hermelin, 1992; Sjoerdsma and van der Zwaan, 1992;

Sen Gupta and Machain-Castillo, 1993; Miao and Thunell, 1993; Rathburn and Corliss, 1994; Jorissen *et al.*, 1995). While *Melonis pompilioides* is not present, *Gyroidinoides* spp. trend to have slightly higher carbon values (the green cluster). The orange cluster (Fig. 15) reflects isotopic values for *Melonis pompilioides* together with *Gyroidinoides* spp. This cluster shows slightly lower oxygen values than the blue cluster which indicates warmer temperature of the bottom water.

The BFOI indicates low oxic conditions of the bottom water in this sample. A summer season with a stratified water column, temperature stratification and the oligotrophic warm upper water layer is displayed by the black, red and green clusters. The blue and orange clusters also points out to seasonal nutrient availability at the sea floor.

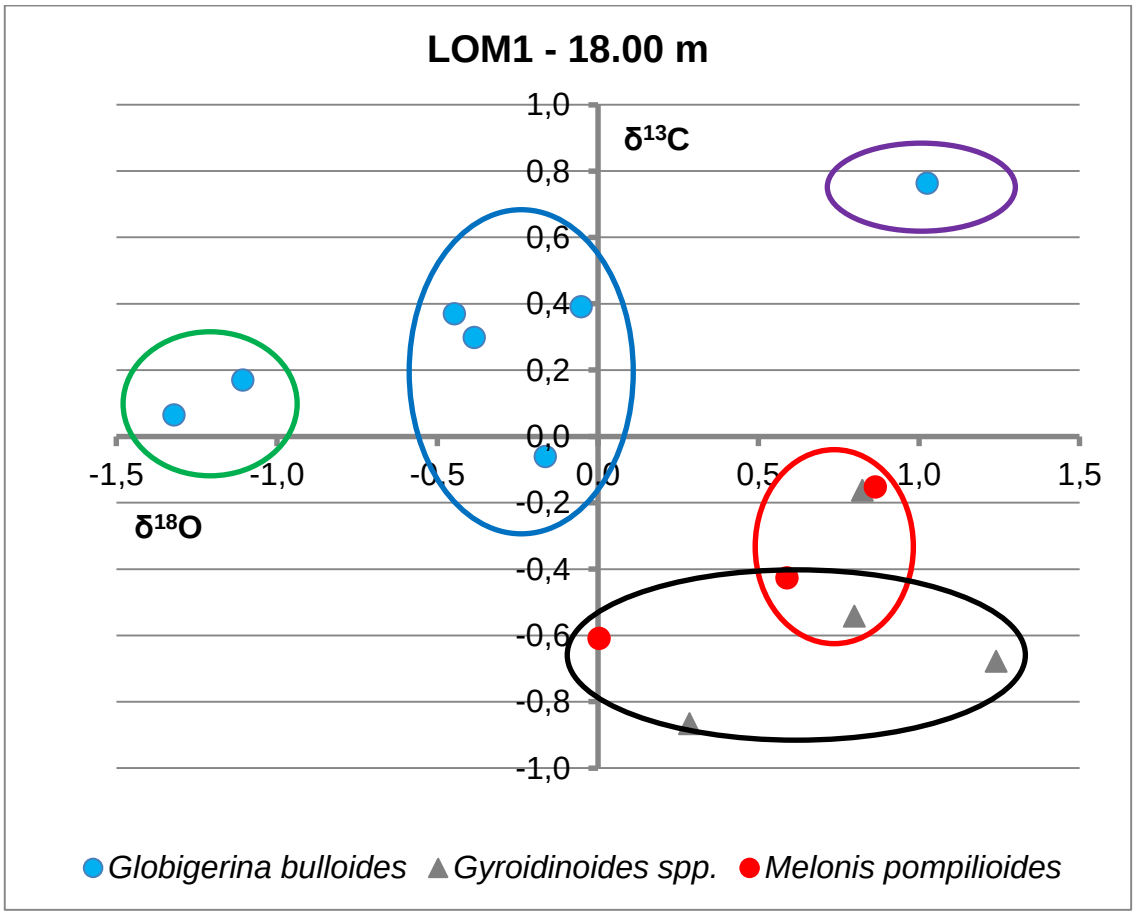


**Figure 16.** Oxygen and carbon isotope values for foraminifera from the sample 18.00 m.

The blue cluster (Fig. 16) represents isotopic values for *G. bulloides* specimens with low carbon values indicating a high nutrient availability. This cluster probably reflects a bloom of *G. bulloides*. The green cluster (Fig. 16) of isotopic values for *G. bulloides* specimens has higher negative values of oxygen isotopes which points to a high precipitation or freshwater input which shifts oxygen towards more negative values. There are no oligotrophic markers such *Globigerinoides* spp.

present here. The isotopic values of *G. bulloides* marked by the violet ring (Fig. 16) show higher carbon values pointing to a rather low nutrient availability within the mixed water column. The red cluster (Fig. 16) represents isotopic values for *Melonis pompilioides* specimens together with *Gyroidinoides* spp. specimens. Both species show similar trend as mentioned in previous sample. The black cluster (Fig. 16) of isotopic values for *Melonis pompilioides* together with *Gyroidinoides* spp. displays a span of oxygen values. This span points to the changing temperature of the bottom water throughout the seasons.

The BFOI indicate suboxic conditions of the bottom water in this sample. Surely no significant stratification of the water column is present here. The *G. bulloides* populations indicate rather the mixed water column model. The different blooms (the violet cluster and the blue cluster) of *G. bulloides* are present. The red and black clusters show a relative nutrient availability at the sea floor. However, the temperature of the bottom water seems to change throughout the seasons. Also a reflection of a high precipitation or freshwater input is documented by the green cluster.

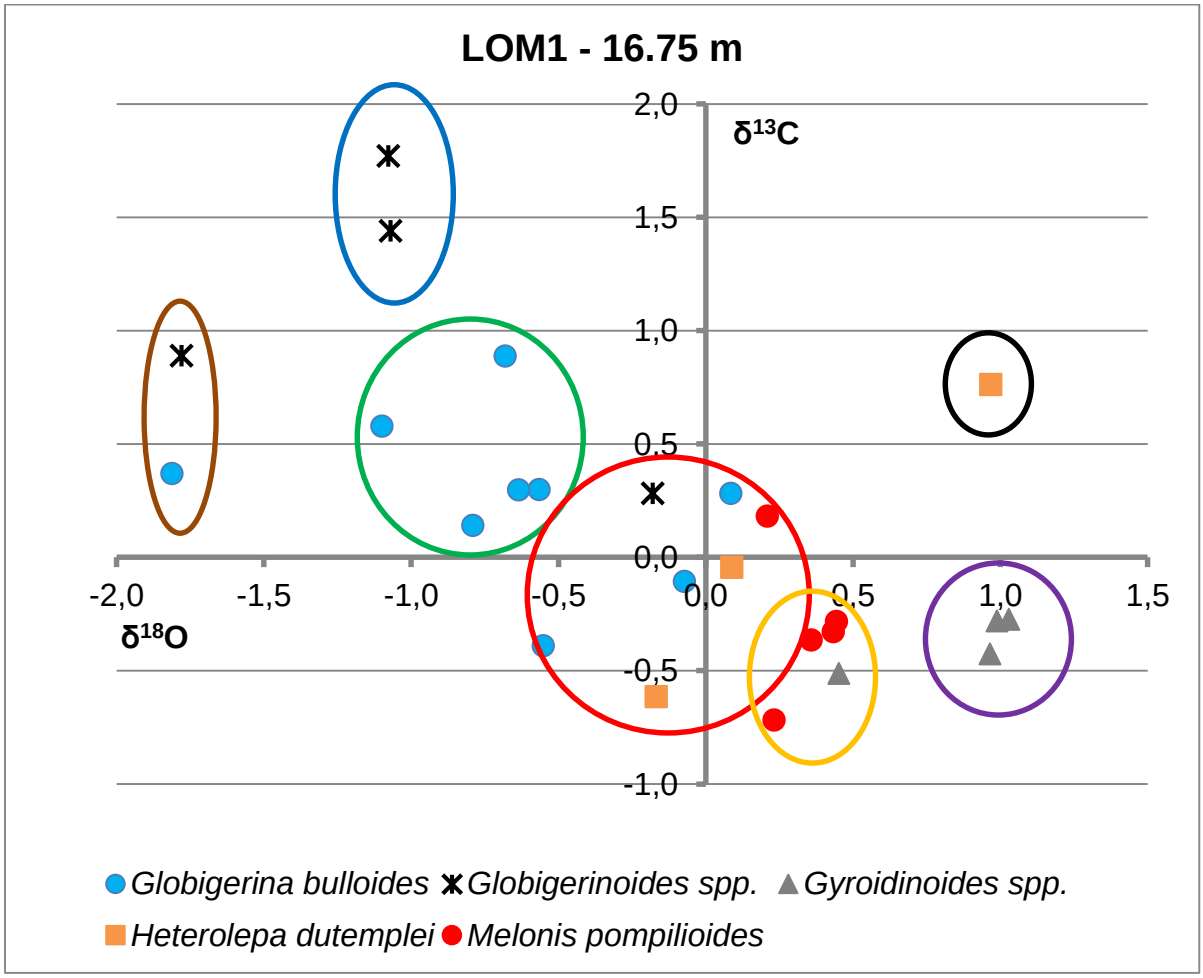


**Figure 17.** Oxygen and carbon isotope values for foraminifera from the sample 16.75 m.

The blue cluster (Fig. 17) of isotopic values for *Globigerinoides* spp. specimens points to the seasonal stratification of the water column with oligotrophic conditions within a summer season. The isotopic values of *Globigerinoides* spp. specimen (Fig. 17) near zero (in the red cluster but does not belong here) seem to be an error possibly caused by a diagenetic alteration, because such isotopic response is extremely unlikely for this species. The brown cluster (Fig. 17) of isotopic values for *Globigerinoides* spp. specimens and *G. bulloides* specimens demonstrates high negative oxygen values which represent a record of an episodic high precipitation or freshwater input which shifts oxygen towards negative values. The green cluster (Fig. 17) of isotopic values for *G. bulloides* specimens points to a mixed water column. This cluster probably reflects a bloom of *G. bulloides*. The isotopic values of *Heterolepa dutemplei* marked by the black ring (Fig. 17) display slightly higher positive carbon values which indicate a less nutrient availability at the sea floor. High positive oxygen values indicate the temperature stratification pointing to cooler water at the sea floor. The violet cluster (Fig. 17) represents isotopic values for *Gyroidinoides* spp. specimens and the orange cluster shows *Gyroidinoides* spp. together with *Melonis pompilioides* specimens. As mentioned above, *Melonis pompilioides* seems to be a high nutrient seasonal aspect (Caralp, 1989; Hermelin, 1992; Sjoerdsma and van der Zwaan, 1992; Sen Gupta and Machain-Castillo, 1993; Miao and Thunell, 1993; Rathburn and Corliss, 1994; Jorissen *et al.*, 1995). *Melonis pompilioides* displays slightly higher carbon values than *Gyroidinoides* spp. (the orange cluster). However, oxygen isotopes slightly differ from these two clusters which indicate a warmer temperature of the bottom water in the orange cluster. If *Melonis pompilioides* is truly a seasonal aspect then the orange cluster represents a slightly different season than the violet one. The red cluster (Fig. 17) clearly documents a well mixed water column indicated by very similar isotopic values in *G. bulloides* specimens and *Heterolepa dutemplei* specimens. The high nutrient availability is demonstrated by negative carbon values in specimens of *Heterolepa dutemplei* and *G. bulloides*. Fytodetritus or a terrigenous nutrient input could cause such depletion in carbon isotope values in specimens of *G. bulloides* together with *Heterolepa dutemplei* while *Melonis pompilioides* specimen exhibits positive values. The brown cluster, as mentioned above, points to precipitation or a freshwater input which can be a source of a terrigenous nutrient input reflected by this pattern. However, a seasonal upwelling regime cannot be excluded from this pattern.

The BFOI index indicates low oxic conditions of the bottom water in this sample. The record of a summer season with a well stratified water column, oligotrophic conditions and temperature stratification is displayed by the blue, black, violet cluster. The second record is an episode with a high precipitation or a freshwater input which is reflected by the brown cluster. The orange cluster shows a seasonal nutrient availability at the sea floor. Finally, the red cluster demonstrates a well stratified water column with a high nutrient availability. A seasonal upwelling regime cannot be excluded here, although it could be caused by a high nutrient input of terrigenous origin. Also a bloom of *G. bulloides* is present (the green cluster).

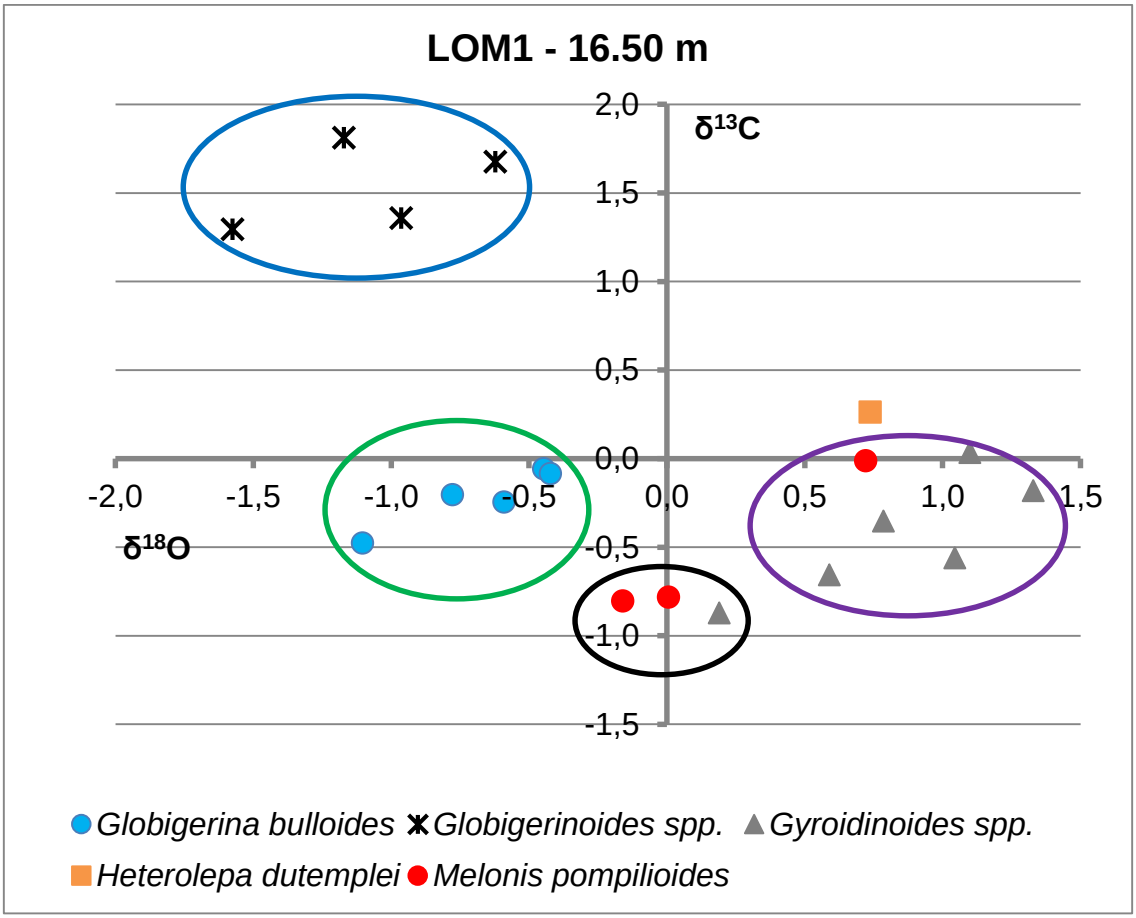


**Figure 18.** Oxygen and carbon isotope values for foraminifera from the sample 16.50 m.

The blue cluster (Fig. 18) of isotopic values for *Globigerinoides* spp. specimens indicates a stratified water column with oligotrophic conditions in the warm upper water layer representing a summer season. The isotopic values of *Heterolepa dutemplei* together with the violet cluster (Fig. 18) of isotopic values for *Melonis pompilioides* and *Gyroidinoides* spp. specimens points to the temperature stratification reflected by positive oxygen values showing cooler bottom water. Conversely, the isotopic values of *Globigerinoides* spp. specimens with high negative oxygen values demonstrate a warmer upper water layer. The violet cluster (Fig. 18) shows isotopic values for *Melonis pompilioides* together with *Gyroidinoides* spp. specimens reflecting relatively stable conditions at the sea floor. The green cluster (Fig. 18) of isotopic values for *G. bulloides* specimens displays negative carbon values which point to a probably terrigenous nutrient input, thus the carbon values are shifted towards negative values. However, no apparent shift in oxygen values is present to support any freshwater input or high precipitation. These facts reflect a mixed water column or no significant stratification . The green cluster probably reflects a bloom of *G. bulloides*. The black cluster (Fig. 18) of isotopic values for *Melonis pompilioides* specimens and *Gyroidinoides* spp. documents a shift to negative oxygen values which reflect no significant temperature stratification

of the water column. Slightly higher negative carbon values may point to a higher nutrient availability at the sea floor.

The BFOI indicates suboxic conditions of the bottom water in this sample. Apparently, a seasonal variability is presented here. A summer season with a well stratified water column with the temperature stratification, relatively oligotrophic warm upper water layer and stable conditions at the sea floor is present (the blue and violet clusters). On the other hand, there is a reflection of a season with a mixed water column (or no significant stratification of water masses), no temperature stratification and a high nutrient availability. The nutrient source seems to be of terrigenous origin.

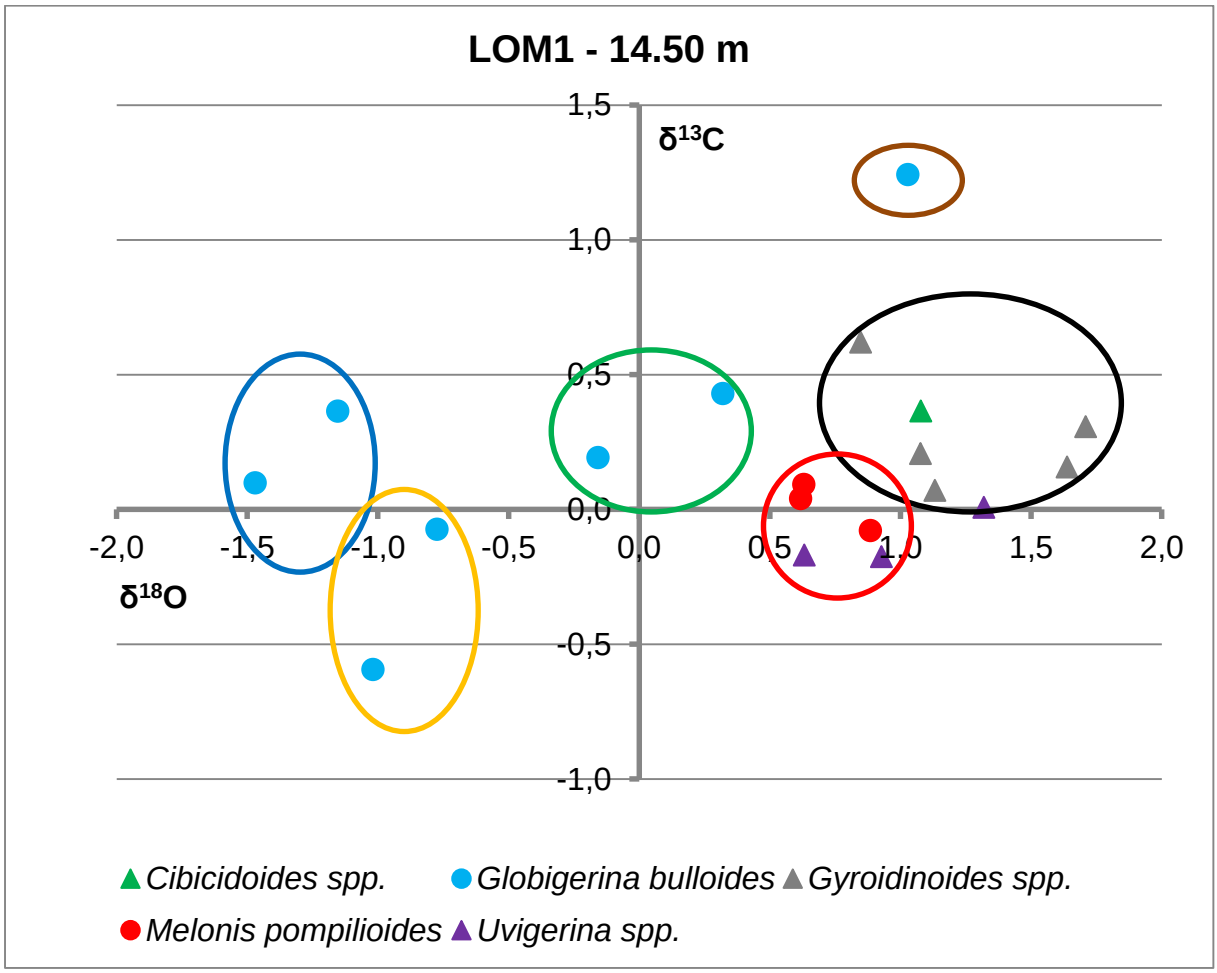


**Figure 19.** Oxygen and carbon isotope values for foraminifera from the sample 14.50 m.

The blue cluster (Fig. 19) of isotopic values for *G. bulloides* specimens displays high negative oxygen values and points to an increased freshwater input or precipitation. The orange cluster (Fig. 19) of isotopic values for *G. bulloides* specimens has negative carbon values which could indicate a terrigenous nutrient input. This fact corresponds to the increased precipitation or freshwater input as it was documented by the blue cluster. The isotopic values of *G. bulloides* (Fig. 19)

marked by the brown ring show high positive carbon values which point to a low nutrient availability. The oxygen is shifted towards positive values. This specimen surely represents a different population. This shift in oxygen could be caused by cooler water within the mixed water column, but it is contrary to the lower nutrient availability reflected by carbon isotopes, because cooler waters are generally nutrient rich. However, this disproportion may be caused by the $\delta^{18}O$ increase with a shell development in *G. bulloides* (Spero and Lea, 1996). The green cluster (Fig. 19) of isotopic values for *G. bulloides* specimens demonstrates a mixed water column. This cluster probably represents a bloom of *G. bulloides*. Carbon values point to a nutrient availability within the mixed water column. The oxygen values are slightly shifted towards positive values. This shift could be explained by no significant temperature stratification of the water column and it indicates slightly cooler water. However, the nutrient availability was not as high as in the orange cluster which represents a high nutrient availability probably linked with precipitation, a freshwater input. The black cluster (Fig. 19) displays isotopic values of *Gyroidinoides* spp. specimens together with *Cibicidoides* spp. *Cibicidoides* spp. isotopic values are within the typical position for this species. Nevertheless, *Gyroidinoides* spp. specimens reflect an interesting shift towards positive carbon values. This indicates a low nutrient availability at the sea floor. This shift supports low nutrient conditions within the water column as shown by the brown marked *G. bulloides*. The red cluster (Fig. 19) shows isotopic values for *Melonis pompilioides* specimens together with *Uvigerina* specimens. As mentioned above, the differences in *Uvigerina* group can be caused by different life strategies of particular species. *Melonis pompilioides* specimens show a slight shift towards positive carbon values. *Uvigerina* specimens also have slightly higher carbon values indicating a relatively low nutrient environment within the sediment.

The BFOI indicates low oxic/high oxic conditions of the bottom water depending on the model used in this sample. This sample represents several different seasons. The mixed water column with relatively oligotrophic conditions at the sea floor and cooler water masses is reflected by the black cluster. An episode of a high precipitation and consequential nutrient input is represented by the blue and orange clusters. The results clearly show the instability within the water column. The cooler, oligotrophic seasons are interrupted by high precipitation events. However, no stratified water column indicators are present and oxygen isotopes point to cooler temperatures and carbon isotopes to rather low nutrient conditions.

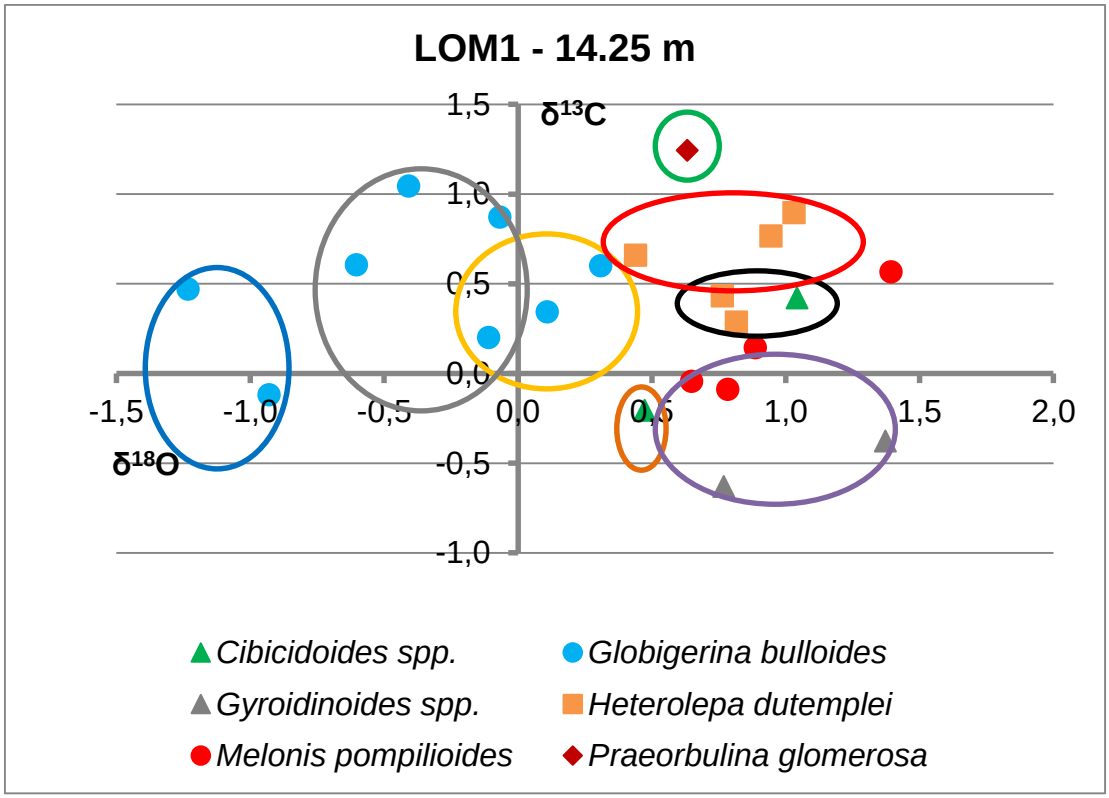


**Figure 20.** Oxygen and carbon isotope values for foraminifera from the sample 14.25 m.

The isotopic values of *Praeorbulina glomerosa* marked by the green ring (Fig. 20) (warm-water, oligotrophic, shallow dweller (Bé, 1977; Reynolds and Thunell, 1985; Hemleben *et al.*, 1989; Chapman, 2010; Schiebel and Hemleben, 2005)) display high positive carbon values which correspond well with the stratified water column model and oligotrophic conditions. The oxygen shift towards higher positive values points to increased salinity of the warm upper water layer in a summer season. However, it could be a redeposition, because no other oligotrophic markers are present (e.g. *Orbulina, Globigerinoides*). The isotopic values of *Heterolepa dutemplei* specimens in the red cluster (Fig. 20) reflect a shift towards positive carbon values. This indicates a low nutrient availability at the sea floor. The low nutrient availability is displayed by the isotopic values of *Melonis pompilioides* specimens which are not included in any of the clusters. The carbon values are high which can corroborate a low nutrient availability at the sea floor. The isotopic values of *G. bulloides* specimens in the grey cluster (Fig. 20) have high positive carbon values pointing to a lower nutrient availability within the mixed water column. The oxygen values show a temperature stratification reflecting warmer water masses. This cluster probably represents a bloom of *G. bulloides*. The blue cluster (Fig. 20) demonstrates isotopic values for *G. bulloides* specimens with high negative oxygen values which indicate a high precipitation or freshwater input. The slightly low carbon values point to a probable terrigenous origin of the nutrient input. The orange cluster (Fig. 20) of isotopic values for *G. bulloides* specimens has high positive oxygen values. This cluster reflects a mixed water

column and colder water masses. Carbon values are slightly lower than in the grey cluster which points to a higher nutrient availability. This cluster probably reflects a different bloom of *G. bulloides* than the grey cluster. The isotopic values of *Cibicidoides* spp. marked by the brown ring show a shift to negative carbon values. This shift could reflect a high nutrient availability, probably of a terrigenous origin. This shift also supports the blue cluster of *G. bulloides* specimens pointing to a high precipitation or freshwater input. The black cluster (Fig. 20) of isotopic values for *Heterolepa dutemplei* specimens and *Cibicidoides* spp. displays the temperature stratification indicating cooler water at the sea floor. This fact is based on the positive oxygen values. This group is within the typical position for epifaunal species. The violet cluster (Fig. 20) reflects isotopic values for *Melonis pompilioides* specimens together with *Gyroidinoides* spp. specimens. *Melonis pompilioides* specimens have higher carbon values than *Gyroidinoides* spp. specimens as mentioned above. This cluster points to a nutrient availability at the sea floor.

The BFOI indicates high oxic conditions of the bottom water in this sample. There is a record of a summer season with a stratified water column, oligotrophic conditions both in the water column and at the sea floor, and with increased salinity in the warm uppermost water layer (the green marked Praeorbulina glomerosa, probably the red and black clusters and unmarked *Melonis pompilioides* specimens). Contrary to this, a season with a stratified water column, nutrient availability and episodic high precipitation or freshwater input is present (the orange, grey, violet and blue cluster).

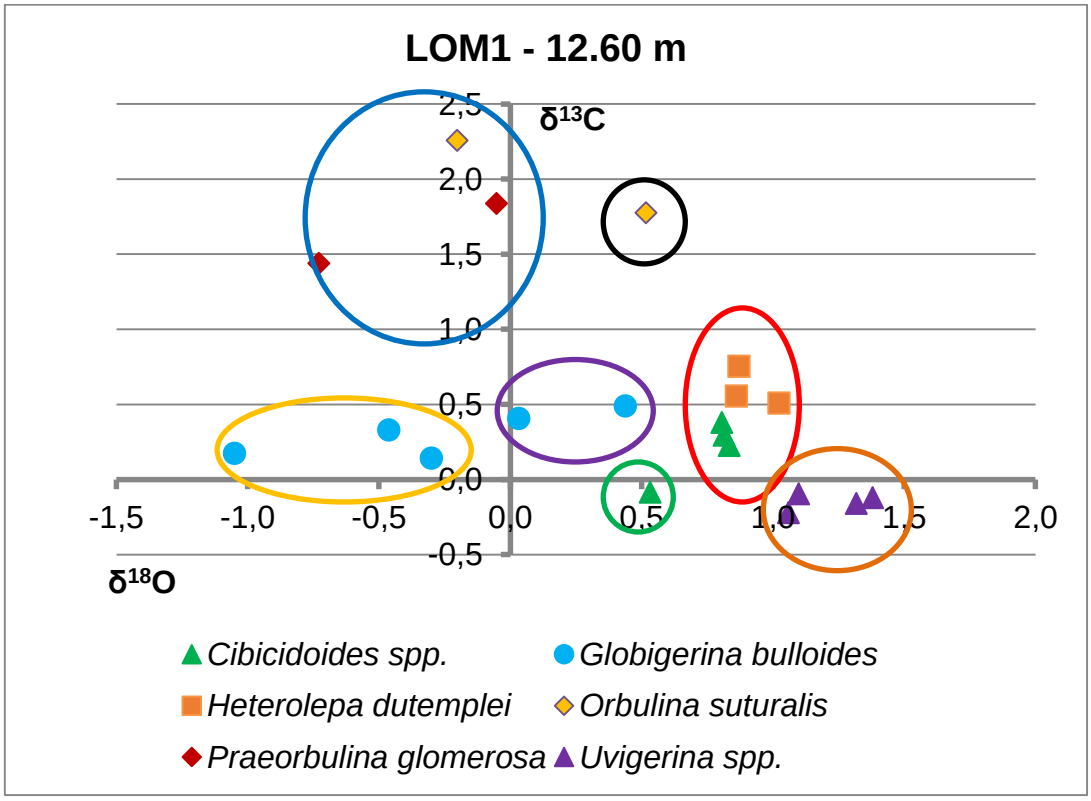


**Figure .21.** Oxygen and carbon isotope values for foraminifera from the sample 12.60 m.

The blue cluster (Fig. 21) shows isotopic values for *Orbulina suturalis* and *Praeorbulina glomerosa* specimens which both are markers of the stratified water column with rather oligotrophic conditions within a summer season. The isotopic values of *Orbulina universa* marked by the black ring (Fig. 21) demonstrate a shift towards positive oxygen values. This indicates higher salinity in the upper water layer during a part of the summer season. The violet cluster (Fig. 21) of isotopic values for *G. bulloides* specimens displays a slight shift towards more positive oxygen values. This cluster indicates a mixed water column with no apparent stratification. Oxygen isotopes document a cooler temperature of the mixed water column. The orange cluster (Fig. 21) of isotopic values for *G. bulloides* specimens reflects slightly lower carbon values which documents an increase in nutrient availability. The specimen around -1 oxygen value may document some minor freshwater input, because it has slightly higher negative oxygen value. This cluster is probably a reflection of a bloom of *G. bulloides*. The isotopic values of *Cibicidoides* spp. specimen marked by the green ring displays a slight shift of carbon to negative value. This shift points to a high nutrient availability. The oxygen isotope indicates no apparent temperature stratification comparing the violet cluster. The red cluster (Fig. 21) of isotopic values for *Heterolepa dutemplei* specimens and *Cibicidoides* spp. specimens demonstrates minimal scattering of isotopic values which reflect relatively stable conditions with no major fluctuations at the sea floor. The brown cluster (Fig. 21) of isotopic values for *Uvigerina* specimens also shows minimal scattering. This position corresponds well to infaunal microhabitat which is presumed for this species (Murray, 2006). This minimal scattering document relatively stable conditions within the sediment, because no significant shifts are present here.

The BFOI indicates high oxic environment at the bottom water in this sample. This sample reflects at least two seasons. A summer season with a stratified water column, oligotrophic conditions and increased salinity within the warm uppermost water layer (the black marked *Orbulina suturalis*, probably the blue, red and brown clusters). Contrary to this, a record of a season with a mixed water column with no apparent temperature stratification and relatively increased nutrient availability is present (the green marked *Cibicidoides* spp., the violet and the orange clusters).

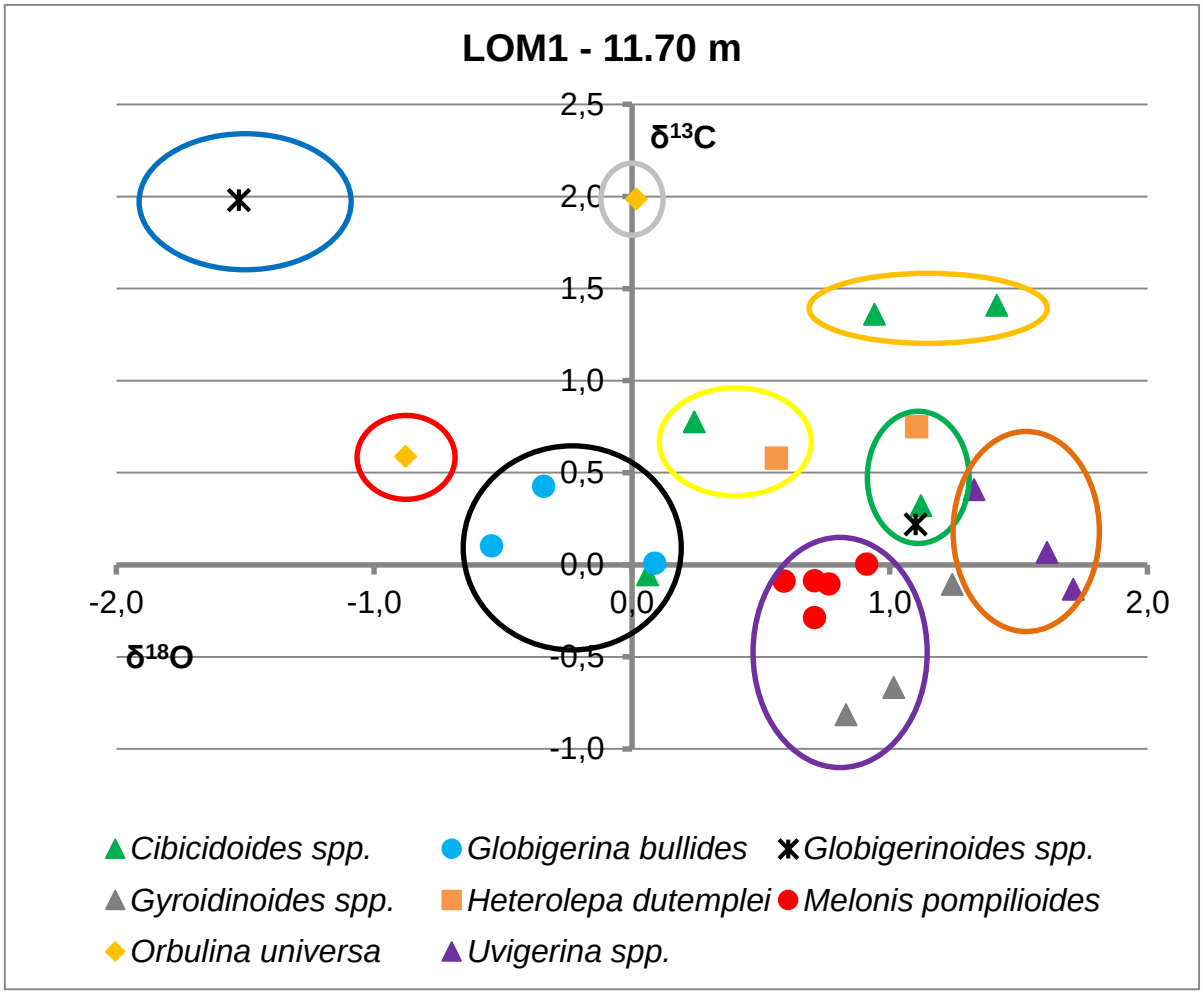


**Figure 22.** Oxygen and carbon isotope values for foraminifera from the sample 11.70 m.

*Globigerinoides* spp. specimen isotopic values marked by the blue ring (Fig. 22) show high positive carbon values and high negative oxygen values which indicate a stratified water column with oligotrophic conditions in the warm upper water layer. *Globigerinoides* spp. specimen isotopic values which are partly inside the green cluster reflect an isotopic response that is very unlikely for this species and apparently represents some diagenetic alteration. The isotopic values of *Orbulina suturalis* marked by the grey ring (Fig. 22) point to a stratified water column with oligotrophic conditions in the warm upper water layer. The oxygen is shifted to more positive values. The oxygen isotopes reflect higher salinity in the uppermost water layer within a summer season. The isotopic values of *Orbulina suturalis* specimen marked by the red ring (Fig. 20) displays a significant shift towards negative carbon and oxygen values than the grey marked specimen. This shift could be caused by a rather higher nutrient availability within a part of a summer season. However, the oxygen values are not as highly shifted towards negative carbon values, but it may be caused by freshwater input or high precipitation. The orange cluster (Fig. 22) of isotopic values for *Cibicidoides* spp. specimens documents a shift towards positive carbon values indicating a low nutrient availability at the sea floor.

The oxygen isotopes reflect positive values consistent with cooler temperatures at the sea floor. The green cluster (Fig. 22) represents isotopic values for *Heterolepa dutemplei* together with *Cibicidoides* spp. within the typical position for epifaunal species. The oxygen isotopes point to a cooler temperature of the bottom water. The yellow cluster (Fig. 22) again demonstrates isotopic values for *Heterolepa dutemplei* with *Cibicidoides* spp. with slightly higher positive carbon values pointing to a lower nutrient availability but not as much as the orange cluster. The oxygen isotopes shift slightly towards lower values which indicate a warmer temperature of the bottom water. The violet cluster (Fig. 22) displays isotopic values for *Melonis pompilioides* specimens together with *Gyroidinoides* spp. specimens. *Melonis pompilioides* specimens show higher carbon values than *Gyroidinoides* spp. specimens when present together as mentioned above. *Melonis pompilioides* specimens reflect minimal scattering thus represent a relatively stable environment at the sea floor. However, as mentioned before, *Melonis pompilioides* seems to be indicating high nutrient periods (Caralp, 1989; Hermelin, 1992; Sjoerdsma and van der Zwaan, 1992; Sen Gupta and Machain-Castillo, 1993; Miao and Thunell, 1993; Rathburn and Corliss, 1994; Jorissen *et al.*, 1995). The brown cluster (Fig. 22) represents isotopic values for specimens of *Uvigerina* spp. which display a shift to more positive carbon values. However, it could be caused by different life strategies of particular species as mentioned before. Otherwise, the position reflects rather lower nutrient availability in the infaunal microhabitat. The black cluster (Fig. 22) shows isotopic values for *G. bulloides* specimens and *Cibicidoides* spp. specimen. The carbon values reflect a shift to lower values which point to a high nutrient availability. The oxygen isotopes document variability in the temperature within the mixed water column. This cluster probably reflects a bloom of *G. bulloides*.

The BFOI indicates suboxic conditions of the bottom water in this sample. This sample represents several seasons. There is a record of a summer season with a stratified water column, oligotrophic conditions and with a possible high saline warm upper water layer. The temperature stratification is present (the grey, red marked *Orbulina suturalis*, the blue marked *Gyroidinoides* spp., and the orange and brown clusters). The conditions at the sea floor reflect a low nutrient availability. On the other hand, a season with a mixed water column, high nutrient availability at the sea floor is displayed by the violet and the black clusters. However, the origin or the source of the nutrient input cannot be precisely determined, because there is no clear isotopic evidence of any high precipitation or freshwater input. These facts clearly points to the variability of the environment especially at the sea floor. The yellow and the green clusters somehow may reflect the transitions between different seasons.

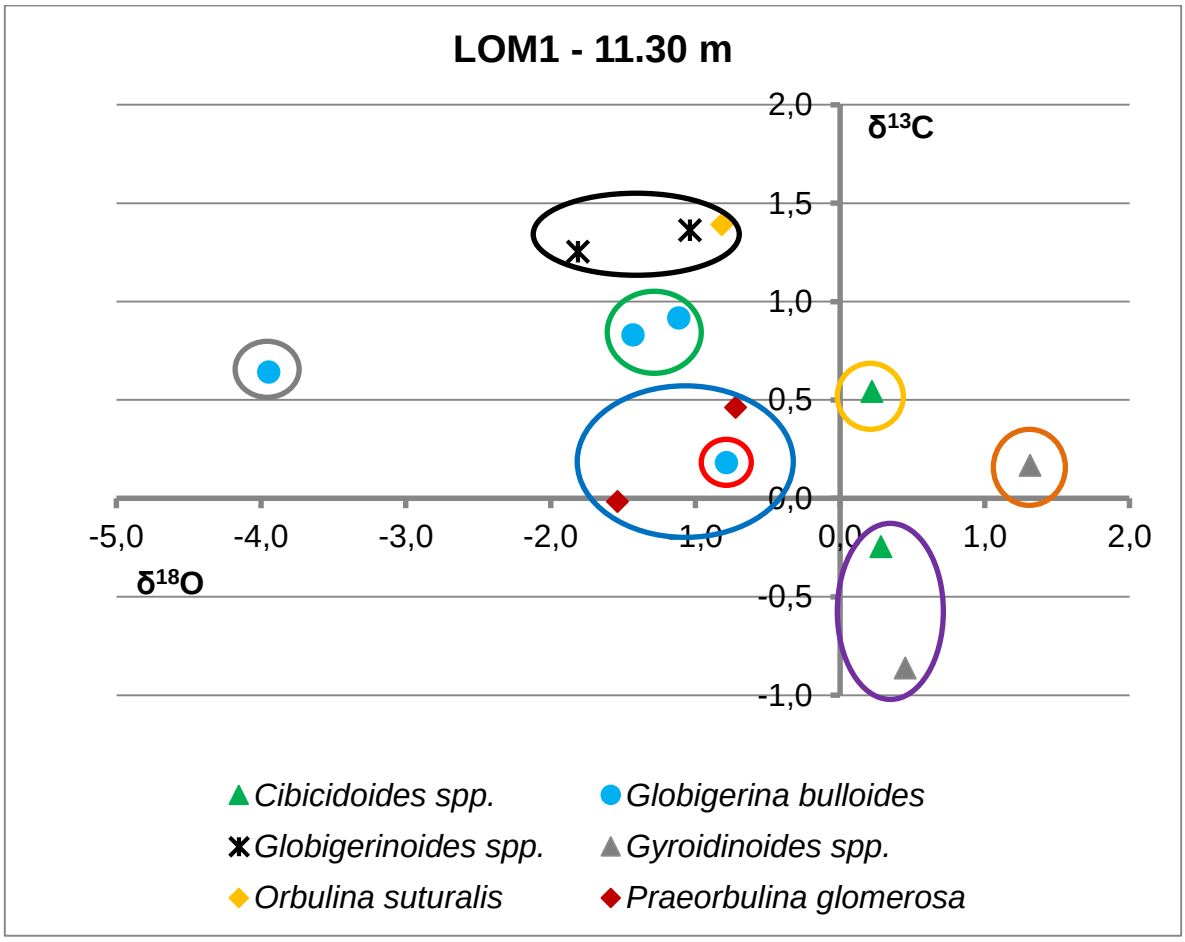


**Figure 23.** Oxygen and carbon isotope values for foraminifera from the sample 11.30 m.

The black cluster (Fig. 23) of isotopic values for *Globigerinoides* spp. specimens and *Orbulina universa* has relatively high negative oxygen values. These oxygen values document a stratified water column with oligotrophic conditions within the warm upper water layer. The high temperatures are indicated by the oxygen values. This cluster is a reflection of a summer season. The blue cluster (Fig. 23) of isotopic values for *Praeorbulina glomerosa* specimens shows a notable shift towards low carbon values. The low carbon values can be explained by a high nutrient availability but it does not fit with the presumed microhabitat of this species. The difference from *Orbulina* is quite notable, because the warm-water, oligotrophic, shallow dweller life habitat for both genera is expected (Bé, 1977; Reynolds and Thunell, 1985; Hemleben *et al.*, 1989; Chapman, 2010; Schiebel and Hemleben, 2005). This cluster could represent some transition between two different seasons but it could be also a redeposition. *G. bulloides* specimen marked by the red ring (Fig. 23) displays a shift to low carbon values which point to a high nutrient availability. *G. bulloides* specimen marked by the grey ring (Fig. 23) demonstrates high negative oxygen values of - 4 and rather positive carbon values. This is very unlikely for this species and could be

probably caused by a diagenetic alteration. The green cluster (Fig. 23) of isotopic values for *G. bulloides* specimens reflects higher positive carbon values indicating a slightly low nutrient availability within the water column. The oxygen isotope points to a warmer water within the mixed water column. This cluster probably represents a bloom of *G. bulloides*. The violet cluster (Fig. 23) displays isotopic values for *Cibicidoides* spp. specimen together with *Gyroidinoides* spp. specimen. Both are shifted towards more negative carbon values which document a high nutrient environment at the sea floor. However, the nutrient origin or source cannot be precisely determined. The isotopic values of *Cibicidoides* spp. specimen marked by the orange ring (Fig. 23) demonstrate a shift to lower oxygen values indicating a warmer temperature at the sea floor. The carbon values are relatively high which points to a low nutrient availability at the sea floor. The isotopic values of *Gyroidinoides* spp. specimen marked by the brown ring (Fig. 23) show positive oxygen values which point to a cooler temperature at the sea floor. The carbon isotope shows positive values which indicate a low nutrient availability at the sea floor.

The BFOI indicates low oxic/suboxic conditions of the bottom water in this sample. This sample reflects several different seasons. A summer season with a stratified water column, oligotrophic conditions and the warm upper water layer is reflected by the black cluster and the orange and the brown marked specimens. The violet cluster represents a rather high nutrient environment of the mixed water column with little temperature stratification. Apart from that, the green cluster probably reflects a bloom of *G. bulloides*. At last, the blue cluster of *Praeorbulina glomerosa* and *G. bulloides* specimen marked by the red ring could represent some transitional environment between two different seasons or it could be a redeposition. This clearly documents an increasing instability of the water column. However, the origin of the nutrient input cannot be precisely determined.

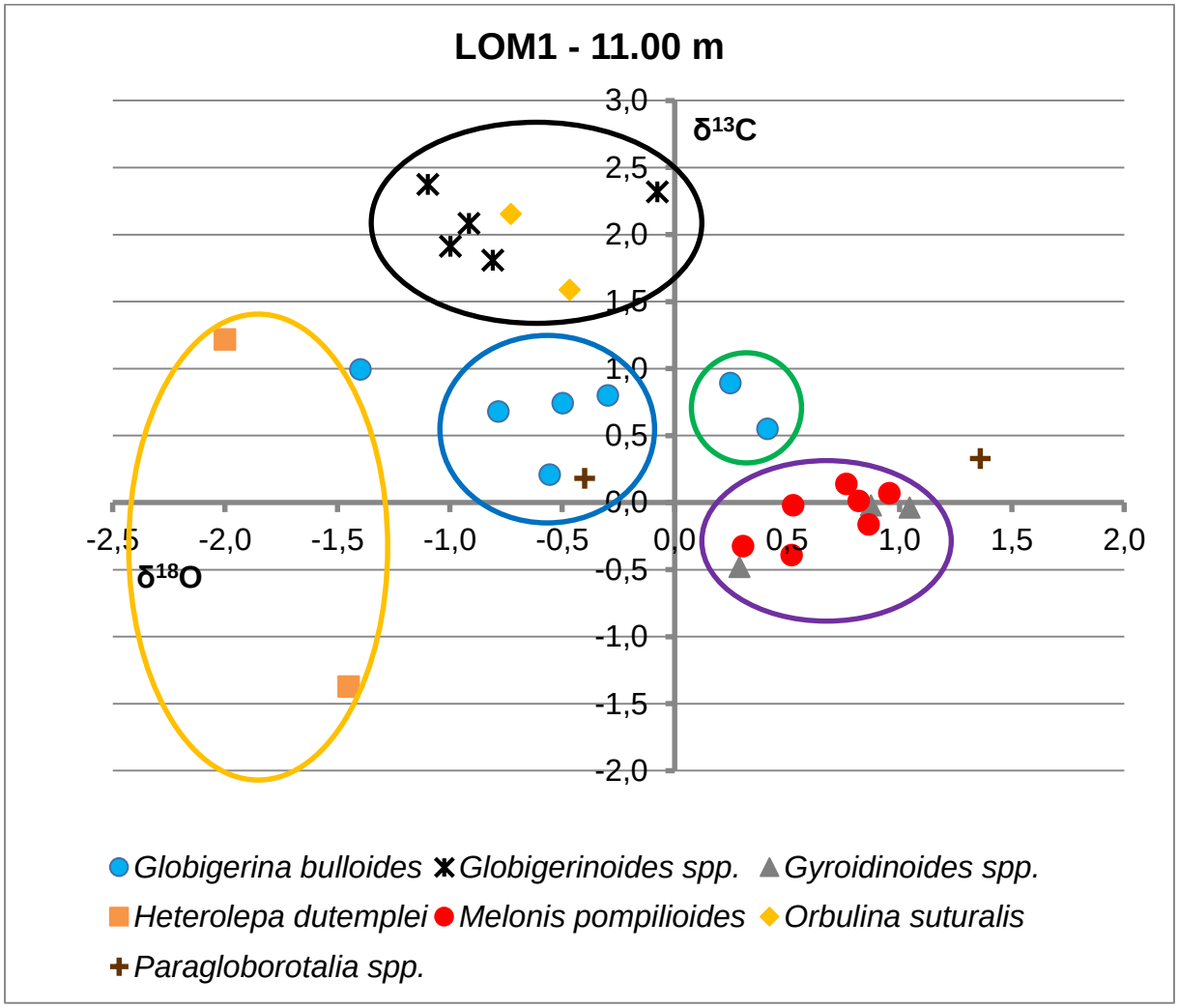


**Figure 24.** Oxygen and carbon isotope values for foraminifera from the sample 11.00 m.

The black cluster (Fig. 24) of isotopic values for *Globigerinoides* spp. specimens and *Orbulina suturalis* specimens indicate oligotrophic conditions and a warm temperature within the upper water layer documented by the negative oxygen values. A slight shift to positive values as seen in one *Globigerinoides* spp. specimen can be caused by increased salinity in the uppermost water layer. This cluster reflects a stratified water column within a summer season. The availability of $\delta^{13}C$ is documented by the high carbon values. The orange cluster (Fig. 24) of isotopic values for *Heterolepa dutemplei* specimens displays an unexpected range of values. Both reflect high negative oxygen values which are inconsistent with the presumed isotopic signal of this epifaunal species. Moreover, there is a huge difference between the carbon values. Without any further review, this cannot be reasonably interpreted. *Paragloboratalia* spp. specimens (Fig. 24) reflect an inconsistent response. Picking them for an isotope analysis was a test how this species signal

would perform. For any further interpretation this species is not suitable. The violet cluster (Fig. 24) demonstrates isotopic values for *Melonis pompilioides* specimens together with *Gyroidinoides* spp. specimens. As mentioned above, *Melonis pompilioides* shows slightly higher carbon values than *Gyroidinoides* spp., if present together. *Melonis pompilioides* seems to be an aspect with the preference of a high nutrient availability (Caralp, 1989; Hermelin, 1992; Sjoerdsma and van der Zwaan, 1992; Sen Gupta and Machain-Castillo, 1993; Miao and Thunell, 1993; Rathburn and Corliss, 1994; Jorissen *et al.*, 1995). The green cluster (Fig. 24) of isotopic values for *G. bulloides* specimens reflects higher positive oxygen values which points to a mixed water column with no temperature stratification and rather cooler water within the water column. This probably reflects a bloom of *G. bulloides*. The blue cluster (Fig. 24) of isotopic values for *G. bulloides* specimens document lower oxygen values indicating warmer water within the mixed water column. No significant stratification is present here. This reflects a different bloom than the green cluster. The lonely *G. bulloides* specimen isotopic values display a shift to lower oxygen values. This shift probably points to a high precipitation.

The BFOI indicates a high oxic environment of the bottom water in this sample. This sample represents several periods or seasons. A summer season with a stratified water column and oligotrophic conditions within the warm upper water layer with a possible high saline uppermost water layer is reflected by the black cluster. The violet cluster shows a nutrient availability at the sea floor. However, no hypoxic conditions are indicated, thus the nutrient influx had to be balanced with the amount of consumed nutrients. The blue cluster probably reflects a bloom of *G. bulloides* indicating warmer temperatures within the mixed water column whereas the green cluster points to a different bloom of *G. bulloides* documenting slightly cooler conditions within the water column. Both demonstrate a mixed water column or a water column with no apparent stratification.

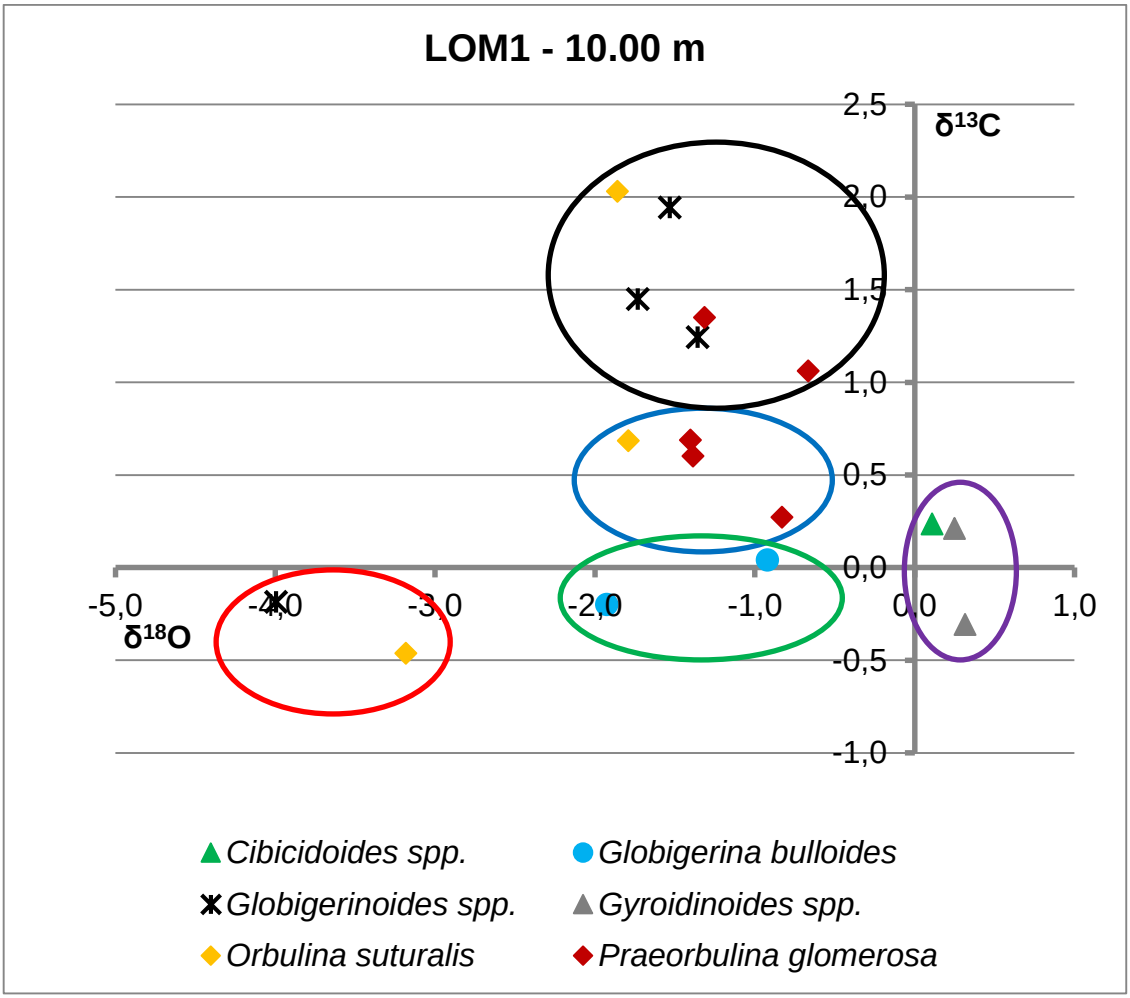


**Figure 25.** Oxygen and carbon isotope values for foraminifera from the sample 10.00 m.

The black cluster (Fig. 25) shows isotopic values for *Globigerinoides* spp. specimens together with *Orbulina suturalis* and *Praeorbulina glomerosa* specimens. This cluster points to a stratified water column with oligotrophic conditions within the warm upper water layer. The warmer temperature within the upper water layer is documented by negative oxygen values. The blue cluster (Fig. 25) represents isotopic values for *Orbulina suturalis* specimens together with *Praeorbulina glomerosa* specimens. A slight shift of carbon to lower values indicates a higher nutrient availability than in the black cluster. The oxygen isotopes point to the warm upper water layer. This cluster can represent the beginning or end of a summer season with a higher nutrient availability while the black cluster reflects a summer season in its course when more oligotrophic conditions prevail. The red cluster (Fig. 25) of isotopic values for *Globigerinoides* spp. specimen and *Orbulina suturalis* specimen displays an extreme shift of oxygen towards negative values. Carbon isotope is also shifted towards lower values. This is caused by a high precipitation and freshwater input, probably by some catastrophic climatic event. The green cluster (Fig. 25) of isotopic values for *G. bulloides* specimens documents

a negative shift in carbon values. Carbon values point to a high nutrient availability within the mixed water column. The specimen with higher negative oxygen values could reflect an episode with a high precipitation or freshwater input. This cluster probably reflects a bloom of *G. bulloides*. The violet cluster (Fig. 25) represents isotopic values for *Cibicidoides* spp. and *Gyroidinoides* spp. specimens. The shift to slightly lower oxygen values points to a warmer temperature at the sea floor.

The BFOI indicate a low oxic environment of the bottom water in this sample. This sample records climatic events (the red cluster) of the high precipitation and freshwater input. On the other hand, a summer season with a stratified water column and rather oligotrophic conditions is documented by the black and the blue clusters. The green cluster probably shows a bloom of *G. bulloides* indicating no apparent stratification of the water column.

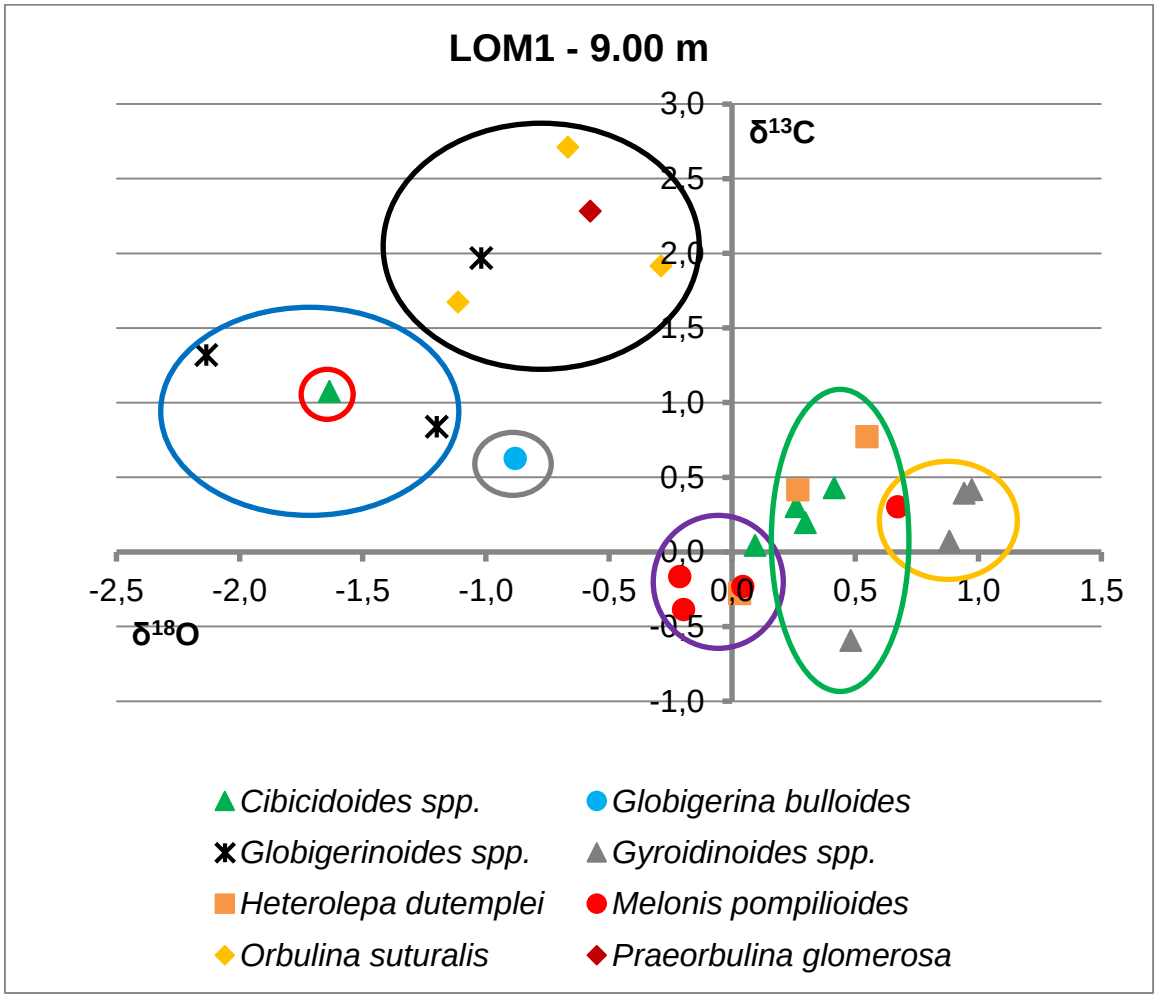


**Figure 26.** Oxygen and carbon isotope values for foraminifera from the sample 9.00 m.

The blue cluster (Fig. 26) represents isotopic values for *Globigerinoides* spp. specimens with a shift to lower carbon values which could indicate a nutrient availability within the upper water layer. The oxygen isotopes are shifted towards negative values. This reflects a probably high precipitation rather than a freshwater input, because the carbon values are not so low. The black cluster (Fig. 26) shows isotopic values for *Globigerinoides* spp. specimen, *Orbulina suturalis* specimens and *Praeorbulina glomerosa* specimen pointing to a stratified water column with an oligotrophic environment within the warm upper water layer. This cluster probably reflects a summer season. The lonely specimen of *G. bulloides* marked by the grey ring (Fig. 26) displays a shift to lower oxygen values. This shift indicates the warmer water within the mixed water column. *Cibicidoides* spp. specimen marked by the red ring (Fig. 26) reflects a shift to a very unlikely position for this species. This shift is probably caused by a diagenetic alteration or it is a redeposited specimen. The green cluster demonstrates isotopic values for *Cibicidoides* spp. specimens and *Heterolepa dutemplei* specimens (Fig. 26) within the typical position for epifaunal species. *Gyroidinoides* spp. specimen included to this cluster documents a higher nutrient availability at the sea floor, possibly within the shallow infaunal microhabitat. The orange cluster (Fig. 26) represents isotopic values for *Melonis pompilioides* specimen together with *Gyroidinoides* spp. specimens with a slight shift towards higher carbon values. The carbon values point to a low nutrient environment at the sea floor which can correspond to a summer season. The positive oxygen values point to cooler bottom water. The violet cluster (Fig. 26) shows isotopic values for *Melonis pompilioides* specimens together with *Heterolepa dutemplei* specimens and *Cibicidoides* spp. This cluster shows relatively low carbon values indicating a degradation of organic matter at the sea floor. The oxygen isotopes especially in *Melonis pompilioides* specimens are shifted towards negative values which indicate a warmer temperature at the bottom water.

The BFOI indicates low oxic/high oxic conditions of the bottom water depending on the model used in this sample. This sample reflects a summer season with a stratified water column and oligotrophic conditions within the warm upper water layer (the black cluster). At the sea floor, it seems that stable conditions (the green cluster) were replaced by a low nutrient availability (the orange cluster) within the possible summer season. However, the events of a probably high precipitation were present (the blue cluster). The violet cluster and *G. bulloides* specimen marked by the grey ring represent a mixed water column or a water column with no significant vertical stratification and with a relatively high nutrient availability at the sea floor (the violet cluster).

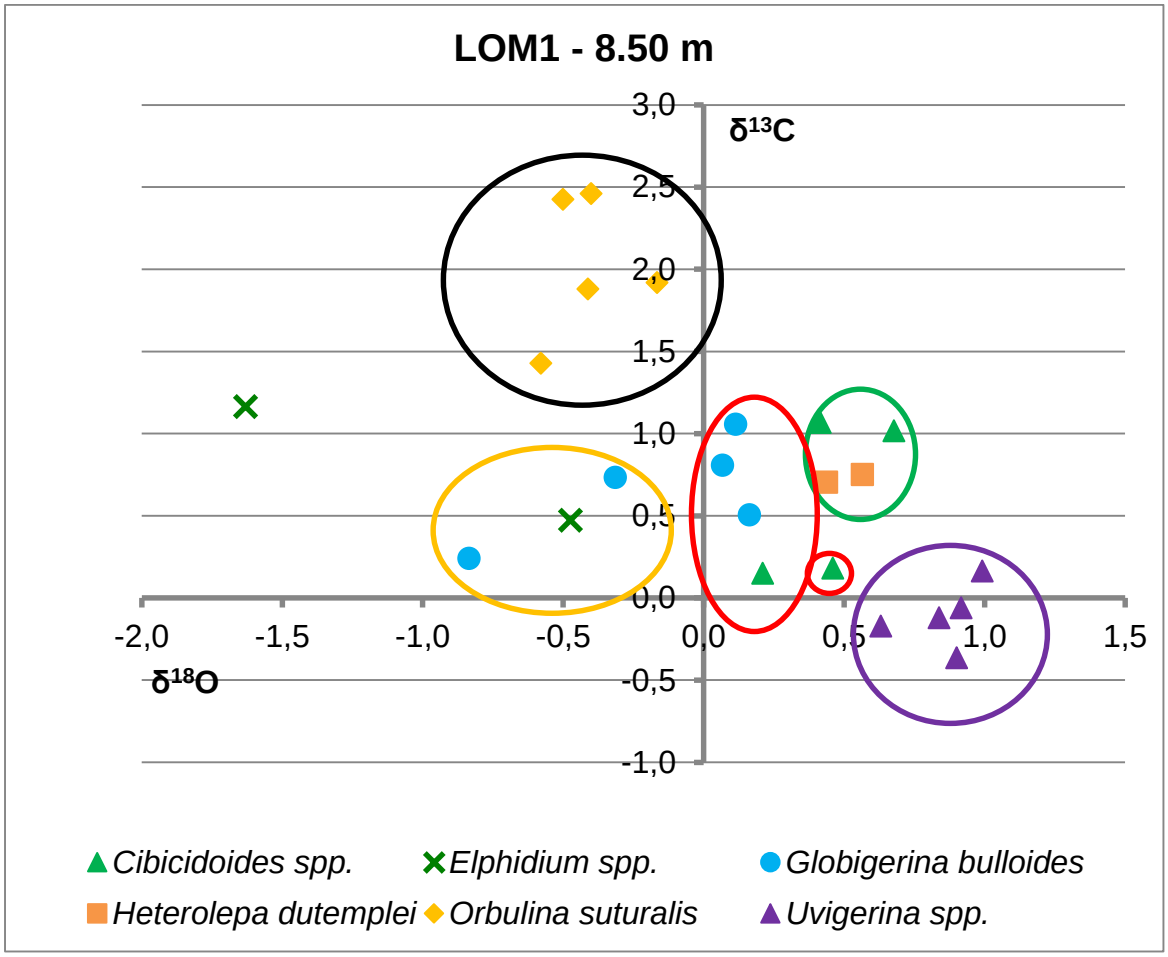


**Figure 27.** Oxygen and carbon isotope values for foraminifera from the sample 8.50 m.

The black cluster (Fig. 27) demonstrates isotopic values for *Orbulina suturalis* specimens indicating oligotrophic conditions within the warm upper water layer. The oxygen isotopes show only a slight shift towards negative values which could be caused by increased salinity in the uppermost water layer. This facts clearly points to a stratified water column within a summer season. High carbon values also point to $\delta^{13}C$ availability within the upper water layer. *Elphidium* spp. (epifaunal; attached to seagrasses) were picked up to test the isotopic response of this species. However, this species is long-lived with a presence of symbionts, thus it is not suitable for any further interpretation. The inappropriateness is documented by an inconsistent isotopic signal (Fig. 27) as shown in this sample. The orange cluster (Fig. 27) of isotopic values for *G. bulloides* specimens displays a slight shift towards negative oxygen values. This shift documents warmer water within the water column with no significant stratification. This cluster probably reflects a bloom of *G. bulloides*. The red cluster (Fig. 27) represents isotopic values for *G. bulloides* specimens and *Cibicidoides* spp. specimen indicating a mixed water column with no temperature stratification. *Cibicidoides* spp. specimen reflects slightly lower carbon values indicating a high nutrient availability at the sea floor. This cluster probably represents a separate bloom of *G. bulloides* than the orange cluster. However, a seasonal

upwelling regime cannot be excluded from this pattern. The violet cluster (Fig. 27) demonstrates isotopic values for *Uvigerina* group. These values typically reflect the presumed deep infaunal life position. The oxygen isotopes point to cooler bottom water, while carbon values reflect a nutrient availability within the sediment. The green cluster (Fig. 27) of isotopic values for *Cibicidoides* spp. specimens and *Heterolepa dutemplei* specimens displays slightly higher carbon values which point to a rather low nutrient environment at the sea floor.

The BFOI indicates low oxic/high oxic conditions of the bottom water depending on the model used in this sample. This sample represents several different seasons. A summer season with a stratified water column and oligotrophic conditions of the warm upper water layer is reflected by the black, green and violet clusters. On the other hand, a season with a well stratified water column and high nutrient availability is reflected by the red cluster. The red cluster may also indicate a seasonal upwelling regime. There is a separate bloom of *G. bulloides* documented by the orange cluster.

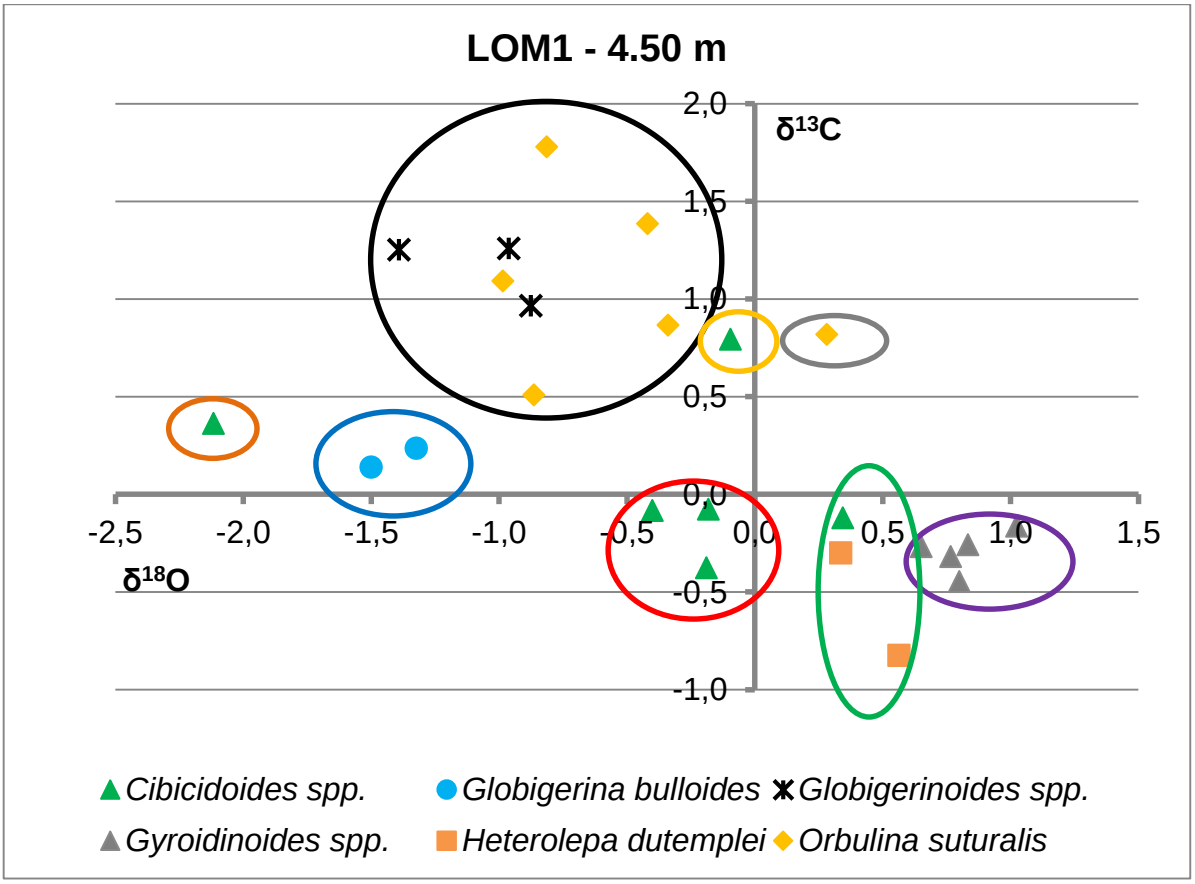


**Figure 28.** Oxygen and carbon isotope values for foraminifera from the sample 4.50 m.

The black cluster (Fig. 28) demonstrates isotopic values for *Globigerinoides* spp. specimens together with *Orbulina suturalis* specimens indicating a stratified water column with oligotrophic conditions. The high positive carbon values points to the $\delta^{13}C$ availability within an upper water layer. The negative oxygen values

document warm water within the shallow water masses. *Orbulina suturalis* specimen isotopic values marked by the grey ring (Fig. 28) reflect a positive shift in the oxygen values which point to increased salinity in the uppermost water layer during the hottest period. *Cibicidoides* spp. specimen isotopic values marked by the brown ring (Fig. 28) display high negative oxygen values. This is very unlikely for this epifaunal species thus it could be probably caused by a diagenetic alteration. The blue cluster (Fig. 28) of isotopic values for *G. bulloides* specimens document a shift to lower oxygen values and also a slight shift to lower carbon values which probably points to a high precipitation or freshwater input. This could be the source of nutrients for the green and the red clusters of epifaunal species. The negative oxygen values reflect cooler water within the water column. This probably represents a bloom of *G. bulloides*. The red cluster (Fig. 28) displays isotopic values for *Cibicidoides* spp. specimens with lower carbon values indicating a high nutrient environment at the sea floor. The oxygen reflects a shift towards negative values which could document warmer bottom water or lower salinity levels of the bottom water. The green cluster (Fig. 28) demonstrates isotopic values for *Cibicidoides* spp. specimen and *Heterolepa dutemplei* specimens with a shift to lower carbon values indicating a high nutrient availability at the sea floor. The oxygen isotopes display positive values pointing to a cooler temperature of the bottom water. The isotopic values for *Cibicidoides* spp. specimen marked by the orange ring (Fig. 28) document high carbon values indicating a low nutrient environment at the sea floor. The oxygen isotopes are shifted towards negative values pointing to warmer bottom water or lower salinity level. The violet cluster (Fig. 28) of isotopic values for *Gyroidinoides* spp. specimens represents positive oxygen values indicating a cooler temperature at the sea floor. The carbon isotopes are within the typical position and reflect the shallow infaunal microhabitat.

The BFOI indicates low oxic conditions of the bottom water in this sample. This sample records several different seasonal or interannual changes of water masses circulations and the nutrient input. A summer season with a stratified water column and oligotrophic conditions is documented by the black cluster. *Orbulina suturalis* marked by the grey ring documents a possible increase in salinity in the uppermost water layer. At the sea floor, the violet cluster reflects a cooler environment with a relative nutrient availability. On the other hand, the blue cluster reflects a bloom of *G. bulloides* indicating a mixed water column and higher precipitation or freshwater input. The green cluster demonstrate a relatively nutrient rich environment at the sea floor and points to cooler or more saline bottom water than the red cluster. Conversely, the red cluster displays a high nutrient environment of warm or less saline bottom water. *Cibicidoides* spp. specimen which is marked by the orange ring documents rather oligotrophic warmer or less saline water at the sea floor. Clearly, there is a great instability within the water column. It may be caused by the beginning of shallowing, thus the high instability and many different patterns are reflected. These patterns probably points to lowering of salinity by a freshwater input and influx of nutrients to the system and even alteration of the bottom water. However, a summer season with its vertical stratification seems to be still present.

# 5.2. Benthic foraminifera oxygen index (BFOI)

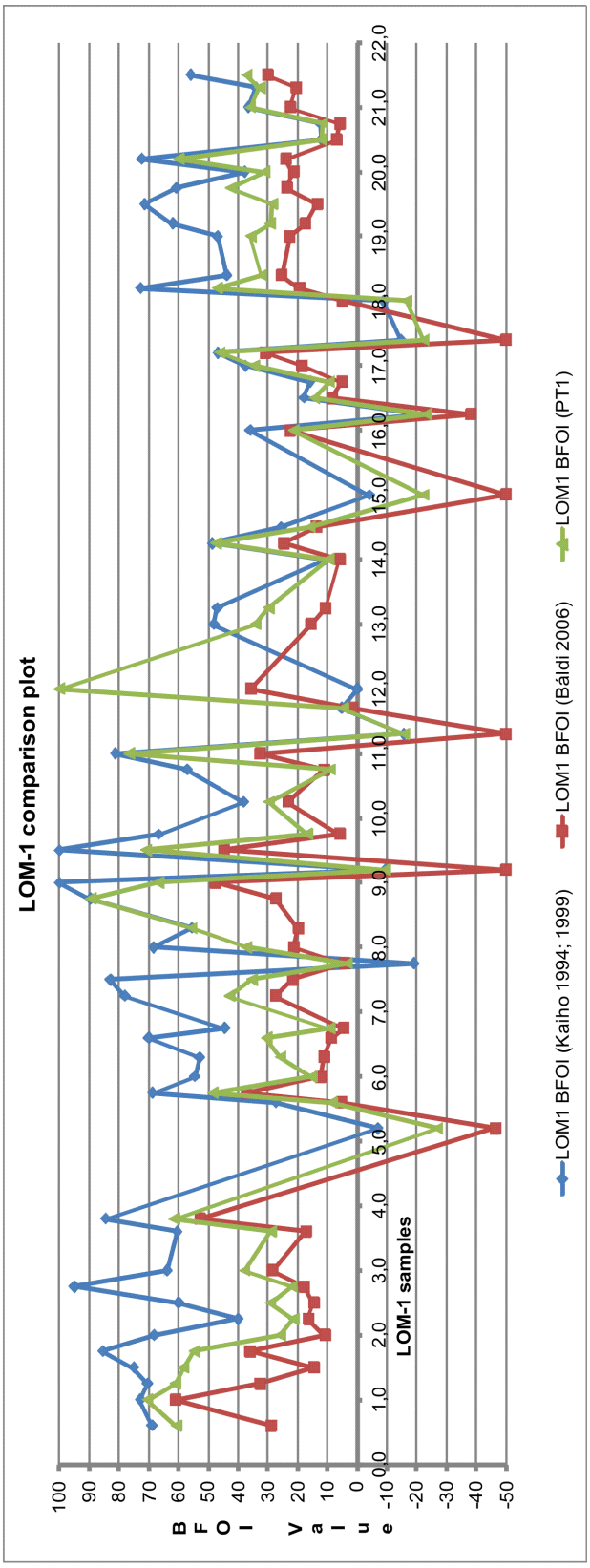


The three separate calculations of BFOI demonstrate almost similar results in general. All three curves show a relatively similar shape with minimal differences but there is a notable shift between all three curves (see Fig. 29). The biggest difference is within the 12.0 m and 13.0 m interval (see Fig. 29).

However, a closer look to the magnitude of differences is essential. The shifts between the values of different models are usually within the magnitude of twenty/thirty. BFOI, however, changes its interpretation results within the magnitude of forty or fifty. This clear disproportion documents that most of the shifts between the three models will not affect the final results of interpretation of the bottom water condition.

Another aspect is that Kaiho (1994) created this calculation for modern benthic foraminiferal species with known ecological characteristics. In fossil material, a reclassification based mainly on morphological criteria and actuoecology of related species is used to determine the ecologic characteristics for particular species. This can produce many misinterpretations in the ecological characteristics of particular species. Moreover, a high specificity of environment such as in the Central Paratethys can considerably affect the ecological characteristics of species.

**Figure 29.** Comparison of all three models of BFOI for LOM-1 borehole. Notice a certain shift between the different models but also notice very similar waveforms of each model. For more details about particular models see appendix 4.

The differences between all three models are described in chapter 4.2.3. As a major factor, the position of *Melonis pompilioides* and *Pullenia bulloides* can be selected, because these species are highly abundant throughout the LOM-1 borehole thus their classification highly affects the resulting BFOI index. The second important factor is the positioning of *Lenticulina* group due to its positioning as oxic species in Báldi (2006) and $PT_1$ classification. This importance is caused by generally a low abundance of oxic species thus any increase of oxic species affects the resulting BFOI index. However, it seems that with the exceptions (interval 12.0 m to 13.0 m) no significantly different results were achieved by different models.

# 5.3. Paleotemperatures

Based on the above mentioned isotopic data the range of paleotempeartures was calculated. The paleotemperatures were calculated for the isotopic signal of *G. bulloides* and *Orbulina universa* within the range of maximum 1 and minimum -1.5 $\delta^{18}Oc$ values. For *Orbulina universa* the calculation was done within the range of maximum 0 and minimum -1.5 $\delta^{18}Oc$ values. This is caused by the effect of high salinity to the composition of the shell $\delta^{18}O$. The temperature calculation follows Bemis *et al.* (1998). For G. bulloides the following formula was used:

$$T=13.2 - 4.89x(\delta^{18}Oc - \delta^{18}Ow) + 0.27x(\delta^{18}Oc - \delta^{18}Ow)^2$$

where $T$ is temperature in °C, $\delta^{18}Oc$ the composition of the shell carbonate and $\delta^{18}Ow$ is the composition of the water in which the carbonate was precipitated. The species specific vital effects could offset the isotopic composition of the test compared to the surrounding water (Peeters *et al.* 2002). In many species, the influence of vital effects on their shell composition remains poorly understood. Due to this fact, only species with modern equivalents, with known vital effects on the shell composition, were chosen. For *Orbulina universa* the following formula was used:

$$T=16.5 - 4.81x(\delta^{18}Oc - \delta^{18}Ow)$$

where $T$ is temperature in °C, $\delta^{18}Oc$ the composition of the shell carbonate and $\delta^{18}Ow$ is the composition of the water in which the carbonate was precipitated.

Today the sea water mean $\delta^{18}O$ composition is 0 ‰ (SMOW), but this value can vary locally due to evaporation or mixing with fresh water and other aspects. For this calculations globally averaged $\delta^{18}Ow$ of ca. -1‰ for the Early Miocene by Lear *et al.* (2000), based on Mg/Ca ratios of benthic foraminifers, was used. Harzhauser *et al.* (2007) showed that this value is in agreement with Early Miocene mollusc data from the Central Paratethys (Grunert *et al.*, 2010). The results are shown in Fig. 30.

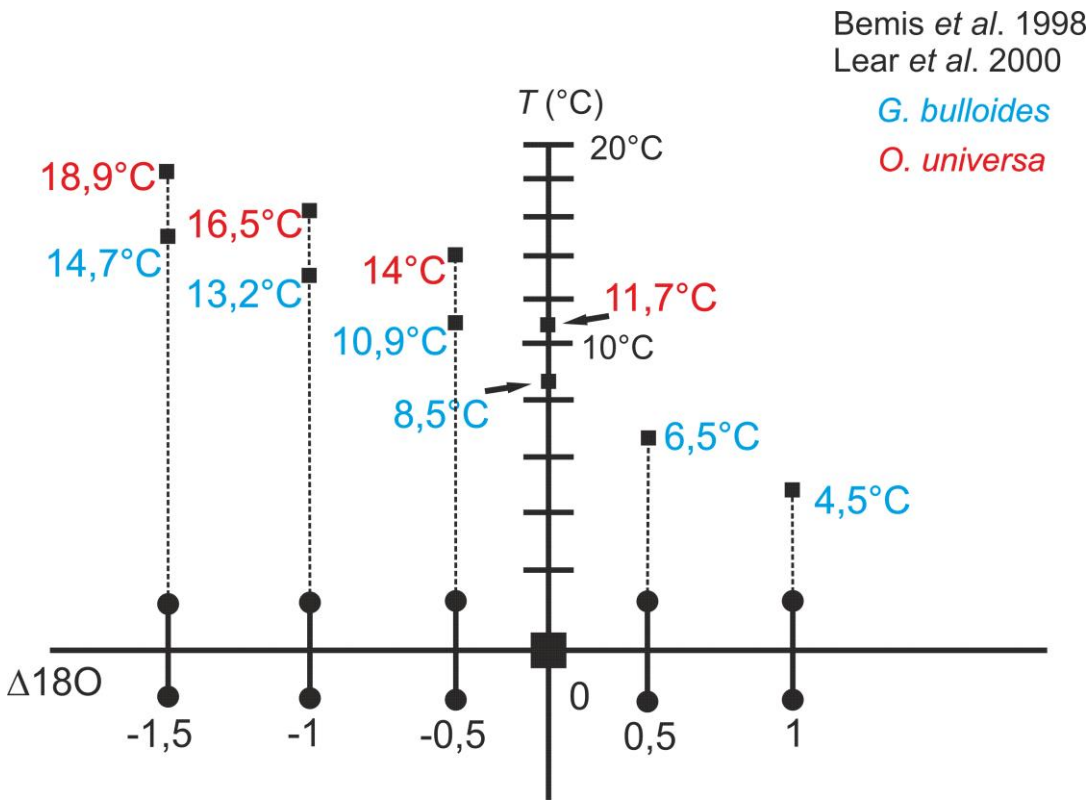


**Figure 30.** Table with calculated temperatures for *G. bulloides* and *Orbulina universa*.

As an example, the sample 8.50 m was chosen (see chapter 5.1.). *Orbulina universa* specimens show the range of values around - 0.5 $\delta^{18}O$. For our purposes consider the value - 0.5 $\delta^{18}O$. Conversely, *G. bulloides* specimens' isotopic values within the red cluster show the range of values slightly above 0 $\delta^{18}O$, consider the 0 $\delta^{18}O$. From this comparison the difference between the temperatures of the warm upper water layer indicated by Orbulina and stratified water column indicated by the red cluster of values for *G. buloides* is 5.5°C. If the red cluster is replaced by the orange cluster of isotopic values for *G. bulloides* (if consider the value - 0.5 $\delta^{18}O$), the difference is only 3.1°C. These differences are relatively small and do not correspond well with oceanological observations (https://www.nodc.noaa.gov/General/temperature.html). Nevertheless, the $\delta^{18}O$ increase with a shell development in *G. bulloides* (Spero and Lea, 1996) has to be taken into account in these calculations. The other important factor is that oxygen isotopic values in *Orbulina universa* are influenced by possible higher salinity, within the warm upper water layer which causes the enrichment in $\delta^{18}O$ (Shiebel and Hemleben, 2005).

# 6. Discussion

The above mentioned results based on the carbon and oxygen isotope analysis show (with exceptions) the two most abundant basic patterns occurring throughout the samples. The first pattern is the reflection of a summer season with high relative abundances of indicative species as *Globigerinoides* spp. or *Orbulina universa*. This pattern provides a quite stable isotopic signal with isotopic values corroborating the habitat of the indicative species. This pattern reflects a stratified water column with an oligotrophic warm upper water layer. The second pattern is an isotopic signal of the various populations of *G. bulloides*. This pattern indicates a well mixed water column and again, it is corroborated by the isotopic values. However, *G. bulloides* shows a progressive $\delta^{18}O$ increase with a shell development (Spero and Lea, 1996). All the specimens of the various species were picked up with respect to the approximately same size, thus this fact should be excluded. Nevertheless, this fact could be present, especially in the positions only marked by one specimen.

The results document a certain similarity compared to the interpretation based on the composition of fossil assemblages proposed by Holcová *et al.* (submitted). However, the hypoxy at the sea floor in interval of 21 – 21.5 m as proposed by Holcová *et al.* (submitted), indicated by the gammaspectrometrical curve, is inconsistent with the BFOI calculations, which indicate a low oxic environment of the bottom water in all three models. The samples 19.25 m and 19.20 m document the presence of at least two different seasons. No significant oscillations at the sea floor are present. According to the BFOI, the oxygen conditions of bottom water are low oxic in both cases. This partly disagrees with the seasonal oscillations of nutrient and oxygen conditions at the sea floor suggested by Holcová *et al.* (submitted). The sample 18.00 m represents no apparent seasonality. The mixed water column and nutrient oscillations at the sea floor are present. The oxygen isotopes point to rather cooler conditions. No equivalent of the summer season is present. This is inconsistent with rapid warming suggested by Holcová *et al.* (submitted), but it could support the deepening of the basin. The samples 16.75 m and 16.5 m again displays at least two different seasons with nutrient oscillations at the sea floor. The proposed seasonal coastal upwelling regime is in agreement with the sample 16.75 m where the upwelling regime cannot be excluded from the isotopic values. However, the cooling and instability within the water column proposed by Holcová *et al.* (submitted) is not confirmed by the isotopic data. The hypoxic conditions at the sea floor suggested by Holcová *et al.* (submitted) partly agree with the BFOI calculations indicating a low oxic and suboxic environment in this interval. The samples 14.50 m and 14.25 m demonstrate no apparent seasonality with the oscillation of nutrient conditions at the sea floor. It points to cooler conditions which corroborate the cooling and instability proposed by Holcová *et al.* (submitted). However, no possible indications of hypoxy at the sea floor proposed by Holcová *et al.* (submitted) such as low carbon values (indicating a high nutrient environment) and an apparent stratification are confirmed by the isotopic signal.

Also no seasonal upwelling regime within this interval, as proposed by Holcová *et al.* (submitted), is reflected. The BFOI documents low oxic conditions in above mentioned samples, however sub oxic conditions are indicated in the interval around 15 m. Throughout the interval 19.25 m – 14.25 m (with exception in the sample 16.50 m), the isotopic response of precipitation or a freshwater input occurs relatively regularly. This documents a certain period with a high rainfall which occurs in a regular pattern. This could indicate stable subtropic climatic conditions within this interval. The sample 12.60 m represents different seasons within the water column and at the sea floor. It points to warm more saline upper water layer throughout the summer season. This is inconsistent with the cooling and decrease of nutrients suggested by Holcová *et al.* (submitted). However, the proposed increase in oxygen conditions corroborates well with the BFOI which documents a low oxic/high oxic environment depending on the used model for this interval. The samples 11.70 m and 11.30 m display seasonality with oscillations of nutrient conditions within the water column and at the sea floor. It points to the instability within the water column and at the sea floor during seasons. It agrees with the cooling proposed by Holcová *et al.* (submitted), but it does not support the decrease in nutrient input. The BFOI documents suboxic conditions which are inconsistent with the increase of oxygen suggested by Holcová *et al.* (submitted). The sample 11.00 m reflects apparent seasonality with relatively stable conditions at the sea floor. This is in agreement with warm, low nutrient conditions proposed by Holcová *et al.* (submitted). The increase in oxygen conditions are well reflected by the BFOI. The sample 10.00 m demonstrates different seasons with no major oscillations of nutrient conditions. It is in agreement with the warm, low nutrient conditions proposed by Holcová *et al.* (submitted). The isotopic signal indicates a catastrophic event of a high rainfall and freshwater input. It could support the periodic high precipitation and freshwater discharge reported by Harzhauser *et al.* (2010). The BFOI documents low oxic conditions within the interval. The sample 9.00 m displays different seasons with oscillations of nutrient conditions at the sea floor. This disagrees with the cooling and stress in superficial layer proposed by Holcová *et al.* (submitted). The BFOI shows low oxic or high oxic conditions depending on the model. The sample 8.50 m documents seasonality with no major oscillations of nutrient conditions. This is inconsistent with the proposed cooling, instability and stress in the superficial layer proposed by Holcová *et al.* (submitted). The possible seasonal upwelling regime is probably reflected by the isotopic signal which is again in disagreement with Holcová *et al.* (submitted). The sample 4.50 m demonstrates seasonality with major oscillations of the nutrient input within the water column and at the sea floor. It confirms the proposed short time oscillations, oscillations in the nutrient input and oxygen at the sea floor proposed by Holcová *et al.* (submitted). Holcová *et al.* (submitted) put the beginning of the basin shallowing and seasonal changes within the water column to the upper parts in interval around 3 m. The isotopic data suggest the beginning of this phase since the interval of 4.50 m. The oscillations in the nutrient input and oxygen is indicated by the BFOI oscillations within this interval.

The BFOI index has been discussed above with the particular samples. As the most suitable model, the $PT_1$ model was chosen. This model was in the best agreement with the isotopic data. However, as mentioned before, the differences between the interpretations by particular models are generally relatively small, thus the other models cannot be put aside. The BFOI provides valuable information about the bottom water conditions especially, when other data (isotopic data; faunal analysis), which can support or refute the interpretations by the BFOI, are present. Nevertheless, it is necessary to consider the specific composition of the assemblages of individual localities and on this basis to choose an appropriate model for the individual locality.

The isotopic analysis revealed a notable relationship between the isotopic signal of *Melonis pompilioides* and *Gyroidinoides* spp. Based on the isotopic signal, the ecologic preference of these particular species could be discussed. *Melonis* shows a shift towards more positive values of carbon isotope than *Gyroidinoides* if present together. *Melonis* is referred as infaunal, dysoxic, cold water (<10°C) species (Murray, 2006). However, the high nutrient input and not the oxygen concentration in the bottom waters seems to control the distribution of *Melonis* (e.g.; Hermelin, 1992; Sjoerdsma and van der Zwaan, 1992; Sen Gupta and Machain-Castillo, 1993; Miao and Thunell, 1993; Rathburn and Corliss, 1994). *Melonis* may then indicate high nutrient but more oxic conditions at the sea floor. Contrary to this Jorissen *et al.* (1995) recorded that with a decreasing organic input and expanding of oxygenated layer under oligotrophic conditions *Melonis* may become very successful. Gyroidinoides spp. ecological preferences are poorly known. According to the isotopic signal it seems that both species occupy the same niche. This above mentioned isotopic shift may be caused by utilization of slightly different organic matter by particular species. However, the different organic matter preferences for *Gyroidinoides* may be due to the pressure of successful taxa as *Melonis*, thus *Gyroidinoides* is forced to utilization of organic matter of variegated quality (Caralp, 1989). It seems that Melonis (if present) is very successful taxa. It could point to the r-selection of *Melonis*. Contrary, *Gyroidinoides* seems to be resilient taxa, which is able to live within various trophic conditions, as shown by the isotopic signal of this species.

This study partly coincides with the isotopic value spans from the Badenian of the Central Paratethys reported by Báldi (2006) and Peryt (2013). However, Báldi (2006) and Peryt (2013) studied a longer interval and they based their observations only on relatively small isotopic datasets which could bring certain inaccuracies. The isotopic values presented in this study show a relatively stable isotopic response of present species, throughout the LOM-1 borehole, with fluctuations according to momentary ecological conditions. No general trend in the isotopic signal is present, thus this disagree with the observations made by Báldi (2006) and Peryt (2013). This is due to a high variability of the environment throughout the LOM-1 borehole, because the global isotopic shifts cannot be traced in such environment. These global isotopic trends are only traceable in long time stable environments.

The paleotemperatures calculated for the various isotopic signals of *G. bulloides* and *Orbulina universa* show a good agreement with the span of temperatures reported by Grunert *et al.* (2010) and Peryt (2013). However, a large span of values is caused by variation in isotopic composition of *G. bulloides* specimens. Nevertheless the $\delta^{18}O$ increase with a shell development in *G. bulloides* (Spero and Lea, 1996) has to be taken into account in these calculations, because it greatly affects the resulting temperature.

# 7. Conclusions

Carbon and oxygen stable isotopic analysis proved to be a convenient tool for reconstructing the paleoecological parameters in the Central Paratethys. However, it is necessary to consider all possible effects influencing isotopic composition in epeiric sea that may affect the resulting interpretations.

The LOM-1 borehole from the Mid Badenian (sensu Hohenegger *et al.* (2014)) of the Carpathian Foredeep represents a variable environment with short time oscillations of paleoecological parameters. The isotopic analysis of carbon and oxygen, presented in this study, allowed distinguishing such short time variations of paleoecological parameters which would otherwise be beclouded.

The lowermost part of the LOM-1 borehole (the samples 19.25 m and 19.20 m) represents an environment with an apparent seasonality with presence of at least two different seasons. No significant oscillations of paleoecological parameters are present. The sample 18.00 m indicates no apparent seasonality. The mixed water column and nutrient oscillations at the sea floor point to rather cooler conditions. This change of paleoecological parameters is followed by the possible seasonal upwelling regime, documented in the sample 16.75 m, and increasing in seasonality and nutrient oscillations at the sea floor as documented by the samples 16.75 m and 16.5 m. The following samples 14.50 m and 14.25 m represent no apparent seasonality with the oscillations of nutrient conditions at the sea floor. It points to cooler conditions and increasing the instability of the paleoecological parameters. Throughout the interval of 19.25 m – 14.25 m (with exceptions) a certain period with high rainfall occurs in remarkably regular pattern. The upper part of the LOM-1 borehole is characterized by rapid changing of the paleoecological conditions. The sample 12.60 m documents the seasonality characterized by warm, more saline upper water layer throughout the summer season. The following samples 11.70 m and 11.30 m also document seasonality, however, the oscillations of nutrient conditions during the seasons are present. The sample 11.00 m documents an apparent seasonality with relatively stable conditions at the sea floor and the sample 10.00 m documents different seasons with no major oscillations of nutrient conditions. A catastrophic event of a high rainfall and freshwater input is reflected here. The following sample 9.00 m documents different seasons with oscillations

of nutrient conditions at the sea floor. Seasonal upwelling regime is possible in this sample. Finally, the uppermost part of the LOM-1 borehole represented by the sample 4.50 m documents the seasonality with major oscillations of a nutrient input within the water column and at the sea floor. The proposed beginning of the basin shallowing and seasonal changes with major oscillations of the paleoecological parameters, are indicating an increase of instability within the environment.

This interpretation documents the large variability and rapid changes of the paleoecological parameters throughout the LOM-1 borehole. It is something that should be expected from the environment at the forefront of the emerging Carpathian mountain chain.

A notable relationship between the isotopic signal of *Melonis pompilioides* and *Gyroidinoides* spp. enabled the discussion about the ecologic preferences of these particular species. It points to a quite similar niche occupied by both species. The difference in the isotopic signal of these species was explained in the terms of different organic matter preferences by particular species if present together. It may be due to the pressure of successful taxa as *Melonis* which seems to be very successful taxa with possible r-selection. On the other hand, *Gyroidinoides* seems to be resilient taxa, as documented by the isotopic signal of this species.

The isotopic values show no global trends as reported by Báldi (2006) and Peryt (2013). These global isotopic shifts cannot be traced in such high variable environment which the LOM-1 borehole represents. However, Báldi (2006) and Peryt (2013) studied a longer interval and based their observations on small isotopic datasets. Nevertheless, the span of the paleotemperatures, based on the isotopic signal of *G. bulloides* and *Orbulina universa,* shows a good agreement with the paleotemperatures reported by Grunert *et al.* (2010) and Peryt (2013).

# 8. References cited

**Abdul Aziz, H.A., Di Stefano, L.M., Foresi, F.J., Hilgen, S.M., Iaccarino, K.F., Kuiper, F., Lirer, G., Salvatorini, A., Turco, E., 2008.** Integrated stratigraphy and $^{40}Ar/^{39}Ar$ chronology of early Middle Miocene sediments from DSDP Leg 42A, Site 372 (Western Mediterranean). *Palaeogeography, Palaeoclimatology, Palaeoecology*, **257**, 123–138.

**Abreu, V.S., Haddad, G.A., 1998.** Glacioeustatic fluctuations: the mechanism linking stable isotope events and sequence stratigraphy from the Early Oligocene to Middle Miocene. In: Graciansky C.-P., Hardenbol, J., Jacquin, T. and Vail, P.R., Eds., *Mesozoic and Cenozoic sequence stratigraphy of European basins.* Tulsa: Society for Sedimentary Geology Special Publication **60**, 245–260.

**Aharon, P., 1983.** 140,000-yr isotope climatic record from raised coral reef in New Guinea. *Nature,* **304**, 720–723.

**Allen, Ph.A., Mange-Rajetzky, M., Matter, A., Homewood, P., 1985.** Dynamic palaeogeography of the open Burdigalian seaway, Swiss Molasse basin. *Eclogae Geologicae Helvetiae,* **78**, 351–381.

**Bąbel M.,** 2004. Badenian evaporite basin of the northern Carpathian Foredeep as a drawdown salina basin. *Acta Geologica Polonica,* **54**, 313-337.

**Báldi, K., 2006.** Paleoceanography and climate of the Badenian (Middle Miocene, 16.4–13.0 Ma) in the Central Paratethys based on foraminifera and stable isotope (δ18O and δ13C) evidence. *International Journal of Earth Sciences (Geologische Rundschau),* **95**, 119–142.

**Báldi, T., 1975.** Holostratotypus: Eger, Wind's brick yard. Hungary (Boundary Stratotype: Kiscellian/Egerian; O/OMa-c). In: Báldi, T., Seneš, J. (Eds.), OM, Egerien. Die Egerer, Pouzdraner, Puchkirchener Schichtgruppe und die Bretkaer Formation. *Chronostratigraphie und Neostratotypen, vol*. **5**, 97–112.

**Báldi, T., 1998.** Paleogene and early Miocene in Hungary. In: Cicha, I., Rögl, F., Rupp, C., Ctyroka, J. (Eds.), Oligocene–Miocene Foraminifera of the Central Paratethys*. Abhandlungen der Senckenbergischen Naturforschenden Gesellschaft*, vol. **549**, 50–53.

**Báldi, T., Seneš, J., 1975.** OM, Egerien. Die Egerer, Pouzdraner, Puchkirchener Schichtgruppe und die Bretkaer Formation. *Chronostratigraphie und Neostratotypen,* **5**, 1–577.

**Báldi, T., 1980.** A korai Paratethys története. *Födtani Köszlöny,* **110**, 456–472.

**Barthelt, D., 1989.** Faziesanalyse und Untersuchungen der Sedimentationsmechanismen in der Unteren Brackwasser-Molasse Oberbayerns. *Münchner Geowissenschaftliche Abhandlungen,* **17**, 1–118.

**Bé, A.W.H., 1980.** Gametogenic calcification in a spinose planktonic foraminifer, *Globigerinoides sacculifer* (Brady). *Marine Micropaleontology,* **5**, 283–310.

**Be, A.W.H., 1977.** An ecological, zoogeographic and taxonomic review of recent planktonic foraminifera. In: *Oceanic Micropaleontology. (ed. A.T.S. Ramsey*). Academic Press, London, 1–100.

**Belanger, P.E., Curry, W.B., Matthews, R.K., 1981.** Core-top evaluation of benthic foraminiferal isotopic ratios for paleo-oceanographic interpretations. *Palaeogeography, Palaeoclimatology, Palaeoecology,* **33**, 205–220.

**Bemis B.E., Spero H.J., Bijma J., Lea D.W., 1998.** Reevaluation of the oxygen isotopic composition of planktonic foraminifers: Experimental results and revised paleotemperature equations. *Paleoceanography,* **13**, 2, 150–160.

**Berger, J.-P., 1996.** Cartes paléogéographiques-palinspastiques du bassin molassique suisse (Oligocène inférieur – Miocène moyen). *Neues Jahrbuch für Geologie und Paläontologie,* **202**, 1–44.

**Berger, W.H., 1971.** Sedimentation of planktonic foraminifera. *Marine Geology,* **11**, 325–358.

**Berger, W.H., Killingley, J.S., Vincent, E., 1978.** Stable isotopes in deep-sea carbonates: box core ERDC–92, West equatorial Pacific. *Oceanologica Acta,* **1**, 203–216.

**Bicchi E., Ferrero E., Gonera M., 2003.** Palaeoclimatic interpretation based on Middle Miocene planktonic Foraminifera: the Silesia Basin (Paratethys) and Monferrato (Tethys) records*. Palaeogeography Palaeoclimatology Palaeoeco*logy, **196**, 265–303.

**Bistricic, A., Jenk, K., 1985.** Area No. 224 b1: Transtethyan Trench “Corridor”. In: Steininger, F.F., Seneš, J., Kleemann, K., Rögl, F. (Eds.), Neogene of the Mediterranean Tethys and Paratethys. *Stratigraphic Correlation Tables and Sediment Distribution Maps, vol*. **1**. University Vienna, Vienna, 72–73.

**Bouvier-Soumagnac, Y., Duplessy, J.C., 1985.** Carbon and oxygen isotopic composition of planktonic foraminifera from laboratory culture, plankton tows and recent sediment: implications for the reconstruction of paleoclimatic conditions and of the global carbon cycle. *Journal of Foraminiferal Research,* **15**, 302–320.

**Brzobohatý, R., 1975.** Otolith fauna of the Moravian Foredeep (in Czech). *Manuscript, Dílčí zpráva Státního úkolu č. II-8 - 1/9.* Univerzita Jana Evangelisty Purkyně Brno.

**Brzobohatý, R., Cicha, I., Kováč, M., Rogl, F. (eds.), 2003.** *The Karpatian. A Lower Miocene Stage of the Central Paratethys. – Masaryk University*, pp. 360. Brno.

**Brzobohatý, R., Nolf, D., Kroupa, O., 2007.** Fisch Otoliths from the Middle Miocene of Kienberg at Mikulov, Czech Republic, Vienna Basin: Their paleoenvironmental and paleogeographic significance. – *Bulletin de l´Institut royal des sciences naturelles de Belgique, Sciences de la Terre*, **77**, 167–196.

**Caralp, M.H., 1989.** Abundance of *Bulimina exilis* and *Melonis barleeanum*: Relationship to the quality of marine organic matter. *Geo-Marine Letters*, **9**, 37-43.

**Chapman, M.R., 2010.** Seasonal production patterns of planktonic foraminifera in the NE Atlantic Ocean: Implications for paleotemperature and hydrographic reconstructions*. Paleoceanography*, **25**, PA1101, doi:10.1029/2008PA001708

**Chira, C., 2000.** Nannoplancton calcaros si molluste Miocene din Transylvania, Romanian. *Editura Carpatica,* Cluy-Napoca (Supergraph Tipo SRL), 1–183.

**Cicha, I., Rögl, F., Ctyroká, J., 2003.** Central Paratethys Karpatian Foraminifera. In: Brzobohatý, R., Cicha, I., Kováč, M., Rögl, F. (Eds.), *The Karpatian — an Early Miocene Stage of the Central Paratethys*. Masaryk University Brno, 169–188.

**Cicha, I., Rögl, F., Rupp, C., Ctyroká, J., 1998.** Oligocene – Miocene foraminifera of the Central Paratethys. *Abhandlungen der Senckenbergischen Naturforschenden Gesellschaft,* **549**, 1–325.

**Cicha, I., Seneš, J., Tejkal, J., 1967.** M3 (Karpatien) Die Karpatische Serie und ihr Stratotypus. *Chronostratigraphie und Neostratotypen, Miozän der Zentralen Paratethys*, **1**, 1–312.

**Coplen, T.B., 1988.** Normalisation of oxygen and hydrogen isotope data. *Chemical Geology (Isotope Geoscience Section),* **72**, 293–297.

**Coplen, T.B., 1994.** Reporting of stable hydrogen, carbon, and oxygen isotopic abundances. *Pure and Applied Chemistry,* **66**, 273–276.

**Ćorić S., Harzhauser M., Hohenegger J., Mandic O., Pervesler P., Roetzel R., Rögl F., Scholger R., Spezzaferri S., Stingl K., Švábenická L., Zorn I., Zuschin M., 2004.** Stratigraphy and correlation of the Grund Formation in the Molasse Basin, northeastern Austria (Middle Miocene, Lower Badenian). *Geologica Carpathica,* **55**, 2, 207–215.

**Craig, H., Gordon, L.I., 1965.** Isotope oceanography: deuterium and oxygen 18 variations in the ocean and the marine atmosphere. *Univeristy of Rhode Island Occasional Publications,* **3**, 277–374.

**Czapowski G., 1994.** The Middle Badenian rock salts in the Carpathian Foredeep – characteristics, origin and economic value. *Geological Quarterly,* **38**, 3, 513-526.

**Dansgaard, W., 1964.** Stable isotopes in precipitation. *Tellus,* **16**, 436–468.

**Deuser, W.G., 1987.** Seasonal variations in isotopic composition and deep-water fluxes of the tests of perennially abundant planktonic foraminifera of the Sargasso Sea: results from sediment-trap collections and their paleoceanographic significance. *Journal of Foraminiferal Research,* **17**, 14–27.

**Di Stefano, A., Foresi, L.M., Lirer, F., Iaccarino, S.M., Turco, E., Amore, F.O., Morabito, S., Salvatorini, G., Mazzei, R., Abdul Aziz, H., 2008.** Calcareous plankton high resolution bio-magnetostratigraphy for the Langhian of the Mediterranean area*. Rivista Italiana di Paleontologia e Stratigrafia,* **114**, 51–76.

**Dullo, W.-C., 1983.** Diagenesis of fossils of the Miocene Leitha Limestone of the Paratethys, Austria: An example for faunal modifications due to changing diagenetic environments. *Facies,* **8**, 1-112.

**Dunbar, R.B., Wefer, G., 1984.** Stable isotope fractionation in benthic foraminifera from the Peruvian continental margin. *Marine Geology,* **59**, 215-225.

**Duplessy, J.C., Blanc, P., Bé, A.W.H., 1981.** Oxygen–18 enrichment of planktonic foraminifera due to gametogenic calcification below the euphotic zone. *Science,* **213**, 1247–1250.

**Duplessy, J.C., Lalou, C., Vinot, A.C., 1970.** Differential isotopic fractionation in benthic foraminifera and paleotemperatures reassessed. *Science,* **168**, 250-251.

**Ehhalt, D., Knott, K., 1965.** Kinetische Isotopentrennung bei der Verdampfung von Wasser. *Tellus,* **17**, 389–397.

**Emiliani, C., 1954.** Depth habitats of some species of pelagic foraminifera as indicated by oxygen isotope ratios. *American Journal of Science,* **252**, 149–158.

**Emiliani, C., 1955.** Pleistocene temperatures. *Journal of Geology,* **63**, 538–578.

**Emiliani, C., 1971.** Depth habitats of growth stages of pelagic foraminifera. *Science,* **173**, 1122–1124.

**Epstein, S., Buchsbaum, R., Lowenstam, H.A., Urey, H.C., 1953.** Revised carbonate-water isotopic temperature scale. *Geological Society of America Bulletin,* **64**, 1315–1325.

**Erez, J., 1978.** Vital effect on stable-isotope composition seen in foraminifera and coral skeletons. *Nature,* **273**, 199–202.

**Erhart, C.W., Piller, W.E., 2004.** Fazies und Geometrie des Leithakalk-Steinbruches Retznei/Rosenberg bei Ehrenhausen (Stmk.). *Berichte des Institutes für Erdwissenschaften, Karl- Franzens-Universität Graz,* **9,** 116.

**Faber, W.W., Anderson, O.R., Lindsey, J.L., Caron, D.A., 1985.** Algal-foraminiferal symbiosis in the planktonic foraminifer *Globigerinella aequilateralis,* I, Occurrence and stability of two mutually exclusive chrysophyte endosymbionts and their ultrastructure. *Journal of Foraminiferal Research,* **18**, 334–343.

**Fairbanks, R.G., 1982.** The origin of continental shelf and slope water in the New York Bight and Gulf of Maine: evidence from $H_2{}^{18}O/H_2{}^{16}O$ ratio measurements. *Journal of Geophysical Research,* **87**, 5796–5808.

**Fairbanks, R.G., 1989.** A 17,000 year glacio-eustatic sea level record: influence of glacial melting rates on the Younger dryas event and deep-ocean circulation. *Nature,* **342**, 637–642.

**Fairbanks, R.G., Wiebe, P.H., 1980.** Foraminifera and chlorophyll maximum: vertical distribution, seasonal succession, and paleoceanographic significance. *Science,* **209**, 1524–1526.

**Fairbanks, R.G., Sverdlove, M., Free, R. *et al.,* 1982.** Vertical distribution and isotopic fractionation of living planktonic foraminifera in the Panama Basin. *Nature,* **298**, 841–844.

**Faupl, P., Roetzel, R., 1990.** Die Phosphoritsande und Fossilreichen Grobsande: Gezeitenbeeinflusste Ablagerunegn der Innviertler Gruppe (Ottnangien) in der oberösterreichischen Molassezone. *Jahrbuch der Geologischen Bundesanstalt,* **133/2**, 157–180.

**Filipescu S., 2001a.** The Miocene from the western border of the Transylvanian Depression. In: Bucur I.I., Filipescu S. & Sasaran E. (Eds.): Algae and carbonate platforms in western part of Romania. *4th Regional Meeting of IFAA Cluj-Napoca 2001, Field Trip Guidebook*, 109–118.

**Flower, B.P., Kennett, J.P., 1993.** Middle Miocene ocean-climate transition: high-resolution oxygen and carbon isotopic records from Deep Sea Drilling Project Site 588A, southwest Pacific. *Paleoceanography,* **8** (4), 811–843.

**Foresi, L.M., Bonomo, S., Caruso, A., Di Stefano, E., Salvatorini, G., Sprovieri, R., 2002a.** Calcareous plankton high resolution biostratigraphy (foraminifera and nannofossils) of the uppermost Langhian - lower Serravallian Ras Il-Pellegrin Section (Malta). *Rivista Italiana di Paleontologia e Stratigrafia,* **108**, 195–210.

**Frew, R.D., Heywood, K.J., Dennis, P.F., 1995.** Oxygen isotope study of water masses in the Princess Elisabeth Trough, Antarctica. *Marine Chemistry,* **49**, 141–153.

**Friebe, J.G., 1993.** Sequence stratigraphy in a mixed carbonate- siliciclastic depositional system (Middle Miocene; Styrian Basin, Austria). *Geologische Rundschau,* **82**, 281–294.

**Friedman, I.,, O'Neil, J.R., 1977.** Compilation of stable isotope fractionation factors of geochemical interest, in Fleischer, M., ed., Data of geochemistry: *U.S. Geological Survey Professional Paper* 440-KK, pp. 12.

**Garlick, G.D., 1974.** The stable isotopes of oxygen, carbon, and hydrogen in the marine environment, in *The Sea,* v. **5**, (ed. E.D. Goldberg), John Wiley & Sons, New York, pp. 393–425.

**Gonfiantini, R., 1986.** Environmental isotopes in lake studies, in *Handbook of Environmental Isotope Geochemistry,* v. **2**, (eds. P. Fritz and J.C. Fontes), Elsevier, Amsterdam, 113–168.

**Gradstein, F.M., Ogg, J.G., 2004.** Geologic Time Scale 2004 - why, how and where next! *Lethaia,* **37**, 175-181.

**Gradstein, F.M., Ogg, J.G., Schmitz, M.D., Ogg, G.M., 2012.** *The Geologic Time Scale 2012 2-Volume Set.* Elsevier, New York, pp. 1144.

**Gradstein, F.M., Ogg, J.G., Smith, A.G., Bleeker, W., Lourens, L.J., 2004.** A new geologic time scale with special reference to Precambrian and Neogene. *Episodes,* **27**, 83-100.

**Grill, R., 1943.** Über mikropaläontologische Gliederungsmöglichkeiten im Miozän des Wiener Becken. *Mitteilungen der Reichsanstalt für Bodenforschung,* **6**, 33-44.

**Grossman, E.L., 1984a.** Stable isotope fractionation in live benthic foraminifera from the Southern California borderland. *Palaeogeography, Palaeoclimatology, Palaeoecology,* **47**, 301–327.

**Grossman, E.L., 1984b.** Carbon isotopic fractionation in live benthic foraminifera – comparison with inorganicprecipitate studies. *Geochimica et Cosmochimica Acta,* **48**, 1505–1512.

**Grossman, E.L., 1987.** Stable isotopes in modern benthic foraminifera: A study of vital effect. *Journal of Foraminiferal Research,* **17**, 48–61.

**Grossman, E.L., Ku, T.L., 1986.** Oxygen and carbon isotope fractionation in biogenic aragonite: temperature effects. *Chemical Geology (Isotope Geoscience Section),* **59**, 59–74.

**Grunert P., Soliman A., Harzhauser M., Müllegger S., Piller W., Roetzel R., Rögl F., 2010.** Upwelling conditions in the Early Miocene Central Paratethys Sea. *Geologica Carpathica*, **61**(2), 129–145.

**Grunert, P., Soliman, A., Ćorić, S., Scholger, R., Harzhauser, M., Piller, W.E., 2010.** Stratigraphic re-evaluation of the stratotype for the regional Ottnangian stage (Central Paratethys, middle Burdigalian). *Newsletters on Stratigraphy,* **44**, 1–16.

**Hamršmíd, B., 1985.** *Helicotaphrichnus commensalis* from lokality Lomnice near Tišnov (in Czech). Manuscript, *Dílčí zpráva Státního úkolu VI-1-13/01.* Univerzita Jana Evangelistu Purkyně Brno, 176–188.

**Haq, B.U., Hardenbol, J., Vail, P.R., 1988.** Mesozoic and Cenozoic chronostratigraphy and cycles of sea level changes. In: Wilgus, C.K. (Ed.), Sea-level changes — an integrated approach. *Society of Economic Paleontologists and Mineralogists, Special Publications,* vol. **42**, 71–108.

**Hardenbol, J., Thierry, J., Farley, M.B., Jacquin, T., Graciansky, P.-C., Vail, P.R., 1998.** Mesozoic and Cenozoic Sequence Chronostratigraphic Framework of European Basins. In: Graciansky, C.-P., Hardenbol, J., Jacquin, T., Vail, P.R. (Eds.), *Mesozoic and Cenozoic Sequence Stratigraphy of European Basins*. *SEPM*, Special Publications, vol. **60**, 3–13.

**Harzhauser M., Piller W., 2007.** Benchmark data of a changing sea – Palaeogeography, palaeobiogeography and events in the Central Paratethys during the Miocene. *Palaeogeography, Palaeoclimatology, Palaeoecology*, **253**, 8–31.

**Harzhauser M., Mandic O., Zuschin M., 2003.** Changes in Paratethyan marine molluscs at the Early/Middle Miocene transition: diversity, palaeogeography and palaeoclimate. *Acta Geologica Polonica,* **53**, 323–339.

**Harzhauser M., Piller W.E., Latal C., 2007.** Geodynamic impact on the stable isotope signatures in a shallow epicontinental sea. *Terra Nova,* **19**, 1–7.

**Harzhauser, M, Piller, W. E., Mulleger, S., Grunert, P., Micheels, A., 2010.** Changing seasonality patterns in Central Europe from Miocene Climate Optimum to Miocene Climate Transition deduced from the Crassostrea isotope archive. *Global Planetary Change*, **76**, 77–84.

**Harzhauser, M., Piller, W.E., Steininger, F.F., 2002.** Circum-Mediterranean Oligo-Miocene biogeographic evolution – the gastropods' point of view. *Palaeogeography, Palaeoclimatology, Palaeoecology,* **183**, 103–133.

**Harzhauser, M., Piller, W.E., 2004a.** The Early Sarmatian—hidden seesaw changes. *Courier Forschungsinstitut Senckenberg,* **246**, 89–112.

**Harzhauser, M., Piller, W.E., 2004b.** Integrated Stratigraphy of the Sarmatian (Upper Middle Miocene) in the western Central Paratethys. *Stratigraphy,* **1**, 65-86.

**Harzhauser, M., Tempfer, P., 2004.** Late Pannonian Wetland Ecology of the Vienna Basin based on Molluscs and Lower Vertebrate Assemblages (Late Miocene, MN 9, Austria). *Courier der Senckenbergischen Naturforschenden Gesellschaft*, Frankfurt/Main, **246**, 55–68.

**Hemleben, C., Spindler, M., Anderson, O.R., 1989.** *Modern Planktonic Foraminifera,* Springer, New York, pp. 363.

**Hermelin, J.O.R., 1992.** Variations in the benthic foraminiferal fauna of the Arabian Sea: a response to changes in upwelling intensity? *Geological Society Special Publications,* **64**, 151–166.

**Hladil, J., 1976.** Badenian Hexacorals (Scleractinia) (in Czech*). Manuscript, Diploma Thesis*, Univerzita Jana Evangelistu Purkyně Brno.

**Hoefs, J., 1997.** *Stable Isotope Geochemistry,* 4th ed., Springer-Verlag, Berlin, pp. 200.

**Hohenegger J., Wagreich M., 2012.** Time calibration of sedimentary sections based on insolation cycles using combined cross— correlation: dating the gone Badenian stratotype (Middle Miocene, Paratethys, Vienna Basin, Austria). *International Journal of Earth Sciences (Geologische Rundschau),* **101**, 339-349.

**Hohenegger, J., Ćorić, S., Wagreich, M., 2014.** Timing of the Middle Miocene Badenian Stage of the Central Paratethys. *Geologica Carpathica*, **65** (1), 55–66.

**Holcová K., Brzobohatý R., Kopecká J., Nehyba S., submitted.** Lomnice/Tišnov denudation relict – exceptional record of the Middle Miocene ecosystem evolution in the Carpathian Foredeep (Czech Republic). *Geological Quarterly*.

**Holcová, K., Hrabovský, J., Nehyba, S., Hladilová, Š., Doláková, N., Demeny, A., 2015.** The Langhian (Middle Badenian) carbonate production event in the Moravian part of the Carpathian Foredeep (Central Paratethys): a multiproxy record. *Facies,* **61**, 1–26.

**Hudáčková, N., Holcová, K., Zlinská, A., Kováč, M., Nagymarosy, A., 2000.** Paleoecology and eustasy: Miocene 3rd order cycles of relative sea-level changes in theWestern Carpathian – North Pannonian basins. *Slovak Geological Magazine,* **6**, 95–100.

**Hudec, P., 1986.** Sytematic and paleoecological analysis of molusca from Badenian locality Lomnice u Tišnova (in Czech). *Manuscript, Diploma Thesis*. Přírodovědecká fakulta Masarykovy univerzity Brno.

**Hüsing, S.K., Cascella, A., Hilgen, F.J., Krijgsman, W., Kuiper, K.F., Turco, E., Winson, D., 2010.** Astrochronology of the Mediterranean Langhian between 15.29 and 14.17 Ma*. Earth and Planetary Science Letters*, **290**, 254–269.

**Imbrie, J., Boyle, E.A., Clemens, S.C. *et al.,* 1992.** On the structure and origin of major glaciation cycles. 1. Linear responses to Milankovitch forcing. *Paleoceanography*, **7***,* 701–738.

**Imbrie, J., Shackleton, N.J., Pisias, N.G. *et al.,* 1984b.** The orbital theory of Pleistocene climate: support from a revised chronology of the marine $\delta^{18}O$ record, in *Milankovitch and Climate,* (eds. A. Berger *et al*.), D. Reidel, Hingham, Massachusetts, 269–305.

**Jiříček R., 1983.** Redefinition of the Oligocene and Neogene Ostracod zonation of the Paratethys. Knihovnička ZPN*, Miscellanous Micropal*eontology, **1**, 195–236.

**Jones, R.W., 1999.** Marine invertebrate (chiefly foraminiferal) evidence for the palaeogeography of the Oligocene-Miocene of western Eurasia and consequences for terrestrial vertebrate migration. In: Agusti, J., Rook, L. and Andrews, P., Eds.,

*Hominid evolution and environmental change in the Neogene of Europe.* Cambridge: Cambridge University Press, 274–308

**Jorissen, F.J., Barmawidjaja, D.M., Puskaric, S., Van der Zwaan, G.J., 1992.** Vertical distribution of benthic Foraminifera in the Northern Adriatic Sea. The relation with high organic flux. *Marine Micropaleontology*, **19**, 131–146.

**Jorissen, F.J., Destinger, H.C., Widmark, J.G.V., 1995.** A conceptual model explaining benthic foraminifera microhabitat. Marine Micropaleontology, **26**, 3-15.

**Jouzel, J., Merlivat, L., Roth, E., 1975.** Isotopic study of hail. *Journal of Geophysical Research,* **80**, 5015–5030.

**Kaiho, K., 1999.** Effect of organic carbon flux and dissolved oxygen on the benthic foraminiferal oxygen index (BFOI). *Marine Micropaleontology,* **37**, 67–76.

**Kaiho, K., 1994.** Benthic foraminiferal dissolved-oxygen index and dissolved oxygen levels in the modern ocean. *Geology*, **22,** 719–722.

**Kaiser, D., Rasser, M., Nebelsick, J.H., Piller, W.E., 2001.** Late Oligocene algal limestones on a mixed carbonate–siliciclastic ramp at the southern margin of the Bohemian Massif (Upper Austria). In: Piller, W.E., Rasser, M. (Eds.), The Paleogene of Austria. *Österreichische Akademie der Wissenschaften, Schriftenreihe der Erdwissenschaftlichen Kommissionen, vol.* **14**, 197–224.

**Kasprzyk, G., 1999.** Sedimentary evolution of the Badenian (Middle Miocene) gypsum deposits in the northern Carpathian Foredeep. *Geological Quarterly,* **43**, 449–654.

**Kelly, E.F., Yonker, C., Marino, B., 1993.** Stable carbon isotope composition of paleosols: an application to Holocene, in *Climate Change in Continental Isotopic Records,* (eds P.K. Swart, K.C. Lohmann, J. McKenzie and S. Savin), Geophysical Monograph Series, v. **78**, American Geophysical Union, Washington D.C., 233–239.

**Kim, S.T., O'Neil, J.R., 1997.** Equilibrium and nonequilibrium oxygen isotope effects in synthetic calcites. *Geochimica et Cosmochimica Acta*, **61**, 3461–3475.

**Kipphut, G.W., 1990.** Glacial meltwater input to the Alaska coastal current: evidence from oxygen isotope measurements. *Journal of Geophysical Research*, **95**, 5177–5181.

**Kopecká, J., 2012.** Foraminifera as environmental proxies of the Middle Miocene (Early Badenian) sediments of the Central Depression (Central Paratethys, Moravian part of the Carpathian Foredeep). *Bulletin of Geosciences*, **87**, 431-442.

**Kouwenhoven, T.J., van der Zwaan, G.J., 2006.** A reconstruction of late Miocene Mediterranean circulation patterns using benthic foraminifera. *Palaeogeography Palaeoclimatology Palaeoecol*ogy, **238**, 373–385.

**Kováč M., Andreyeva-Grigorovich A., Bajraktarević Z., Brzobohatý R., Filipescu S., Fodor L., Harzhauser M., Oszczypko N., Pavelic D., Rögl F., Saftić B., Sliva L., Studencka B., 2007.** Badenian evolution of the Central Parathethys sea: paleogeography, climate and eustatic sea level changes. *Geologica Carpathica,* **58**, 579-606.

**Kováč, M., Andreyeva-Grigorovich, A.S., Brzobohatý, R., Fodor, L., Harzhauser, M., Oszczypko, N., Pavelic, D., Rögl, F., Saftic, B., Sliva, B., Stránik, Z., 2003.** Karpatian paleogeography, tectonics and eustatic changes. In: Brzobohatý, R., Cicha, I., Kováč, M., Rögl, F. (Eds.), *The Karpatian— an Early Miocene Stage of the Central Paratethys*. Masaryk University Brno, 49–72.

**Kováč, M., Baráth, I., Harzhauser, M., Hlavatý, I., Hudáčková, N., 2004.** Miocene depositional systems and sequence stratigraphy of the Vienna Basin. *Courier Forschungsinstitut Senckenberg,* **246**, 187–212.

**Kováč, M., Holcová, K., Nagymarosy, A., 1999.** Paleogeography, paleobathymetry and relative sea-level changes in the Danube Basin and adjacent areas. *Geologica Carpathica,* **50**, 325–338.

**Kováč, M., Nagymarosy, A., Oszczypko, N., Csontos, L., Slaczka, A., Marunteanu, M., Matenco, L., Márton, E., 1998b.** Palinspastic reconstruction of the Carpathian – Pannonian region during the Miocene. In: Rakús, M., Ed., *Geodynamic development of the Western Carpathians.* Bratislava, Mineralia slovaca Monograph, 189–217.

**Kováčová M., Doláková N., Kováč M., 2011.** Miocene vegetation pattern and climate change in the northwestern Central Paratethys domain (Czech and Slovak Republic). *Geologica Carpathica,* **62,** 251–266.

**Kreutzer, N., 1986.** DieAblagerungssequenzen der miozänen Badener Serie im Feld Matzen und im zentralen Wiener Becken. *Erdöl- Erdgas-Kohle,* **102**, 492–503.

**Krézsek, CS., Filipescu, S., 2005.** Middle to Late Miocene sequence stratigraphy of the Transylvanian Basin (Romania). *Tectonophysics,* **410**, 437-463.

**Kroh, A., Harzhauser, M., Piller, W.E., Rögl, F., 2003.** The Lower Badenian (Middle Miocene) Hartl Formation (Eisenstadt- Sopron Basin, Austria). In: Piller, W.E., Ed., *Stratigraphia Austriaca. Österreichische Akademie der Wissenschaften, Schriftenreihe der Erdwissenschaftlichen Kommissionen*, **16,** 87–109.

**Kroon, D., Darling, K., 1995.** Size and upwelling control of the stable isotope composition of *Neogloboquadrina dutertrei* (d'Orbigy), *Globigerinoides ruber* (d'Orbiny) and *Globigerina bulloides* d'Orbigny: examples from the Panama Basin and Arabian Sea. *Journal of Foraminiferal Research,* **25**, 39–52.

**Kroopnick, P.M., 1974.** Correlations between $^{13}C$ and Earth $\Sigma CO_2$ in surface waters and atmospheric $CO_2$. Earth *and Planetary Science Letters,* **22**, 397–403.

**Kroopnick, P.M., 1975.** Respiration, photosynthesis, and oxygen isotope fractionation in oceanic surface water. *Limnology and Oceanography,* **20**, 988-992.

**Kroopnick, P.M., 1985.** The distribution of$^{13}C$ of $\Sigma CO_2$ in the world oceans *Deep-Sea Research*, **32,** 57–84.

**Kroopnick, P.M., Weiss, R.F., Craig, H., 1972.** Total $CO_2$ $^{13}C$ and dissolved oxygen - $^{18}O$ at GEOSECS II in the north Atlantic. *Earth and Planetary Science Letters,* **16**, 103–110.

**Kroopnick, P.M., Margolis, S.V., Wong, C.S., 1977.** $\delta^{13}C$ variations in marine carbonate sediments as indicators of the $CO_2$ balance between the atmosphere and the oceans, in *The Fate of Fosssil Fuel in the Oceans*, (eds N.R. Anderson and A. Malahoff), Plenum Press, New York, 295-321.

**Labeyrie, L.D., Duplessy, J.C., Blanc, P.L., 1987.** Variations in the mode of formation and temperature of oceanic deep waters over the past 125,000 years. *Nature,* **327**, 477–482.

**Latal, C., Piller, W.E., 2003.** Stable Isotope Signatures at the Karpatian/Badenian Boundary in the Styrian Basin. In: Brzobohatý, R., Cicha, I., Kováč, M., Rögl, F. (Eds.), *The Karpatian—an Early Miocene stage of the central Paratethys*. Masaryk University Brno, 37–48.

**Lear C.H., Elderfield H., Wilson P.A., 2000.** Cenozoic deep-sea temperatures and global ice volumes from Mg/Ca in Benthic Foraminiferal Calcite. *Science,* **287**, 269–272.

**Leavitt, S.W., 1993.** Environmental information from $^{13}C/^{12}C$ ratios of wood, in *Climate Change in Continental Isotopic Records,* (eds P.K. Swart, K.C. Lohmann, J. McKenzie and S. Savin), *Geophysical monograph series,* **78**, American Geophysical Union, Washington DC, 325–331.

**Lorius, C., 1983.** Antarctica: survey of near-surface mean isotopic values, in *The Climate Record of the Polar Ice Sheet,* (ed G. de Q. Robin), Cambridge University Press, New York, 52–56.

**Loubere, P., 1997.** Benthic foraminiferal assemblage formation, organic carbon flux and oxygen concentrations on the outer continental shelf and slope. *Journal of Foraminiferal Research,* **27**, 93–100.

**Loubere, P., Meyers, P., Gary, A., 1995.** Benthic foraminiferal microhabitat selection, carbon isotope values, and association with larger animals: A test with *Uvigerina peregrina. Journal of Foraminiferal Research,* **25**, 83–95.

**Lourens, L., Hilgen, F., Shackleton, N.J., Laskar, J., Wilson, D., 2004.** The Neogene Period. In: Gradstein, F.M., Ogg, J.G. and Smith, A.G., Eds., *A Geologic Time Scale 2004*., Cambridge University Press, Cambridge, 409–440.

**Lynch-Steiglitz, J., Fairbanks, R.G., 1994.** A conservative tracer for glacial ocean circulation from carbon isotope and paleo-nutrient measurements in benthic foraminfera. *Nature,* **369**, 308–310.

**Macdonald, R.W., Paton, D.W., Carmack, E.C., Omstedt, A., 1995.** The freshwater budget and under-ice spreading of Mackenzie River water in the Canadian Beaufort Sea based on salinity and $^{18}O/^{16}O$ measurements in water and ice. *Journal of Geophysical Research,* **100C**, 895–919.

**Magyar, I., Geary, D.H., Müller, P., 1999.** Paleogeographic evolution of the Late Miocene Lake Pannon in Central Europe. *Palaeogeography, Palaeoclimatology, Palaeoecology,* **147**, 151–167.

**Majoube, M., 1971.** Fractionnement en oxygene 18 et deuterium entre l'eau et sa vapeur. *Journal de Chimie Physique.,* **10**, 1423–1436.

**Mandic, O., 2004.** Foraminiferal paleoecology of a submarine swell – the Lower Badenian (Middle Miocene) of the Mailberg Formation at the Buchberg in the Eastern Alpine Foredeep: initial report. *Annalen des Naturhistorischen Museums in Wien,* **105A**, 161-174.

**Mandic, O., Harzhauser, M., Spezzaferri, S., Zuschin, M., 2002.** The paleoenvironment of an early Middle Miocene Paratethys sequence in NE Austria with special emphasis on paleoecology of mollusks and foraminifera. *Geobios Mémoire spécial,* **24**, 193-206.

**Martel, A.T., Allen, Ph.A., Slingerland, R., 1994.** Use of tidal circulation modelling in paleogeographical studies: an example from the Tertiary of the Alpine perimeter. *Geology,* **22**, 925–928.

**Martini E., 1971.** Standard Tertiary and Quaternary calcareous nanoplankton zonation. *Proc. of 2nd Planktonic Conference*, Roma 1970, 739–785.

**Márton, E., Drobne, K., Cosovic, V., Moro, A., 2003.** Palaeomagnetic evidence for Tertiary counterclockwise rotation of Adria. *Tectonophysics,* **377,** 143–156.

**Márton, E., Jelen, B., Tomljenovic, B., Pavelic, D., Poljak, M., Márton, P., Avanic, R., Pamic, J., 2006.** Late Neogene counterclockwise rotation in the SW part of the Pannonian Basin. *Geologica Carpathica,* **57**, 41–46.

**McConnaughey, T., 1989a.** $\delta^{13}C$ and $\delta^{18}O$ isotopic disequilibrium in biological carbonates: I. Patterns. *Geochimica et Cosmochimica Acta,* **53**, 151–162.

**McConnaughey, T., 1989b.** $\delta^{13}C$ and $\delta^{18}O$ isotopic disequilibrium in biological carbonates: II. *In vitro* simulation of kinetic isotope effects. *Geochimica et Cosmochimica Acta,* **53**, 163–171.

**McCorkle, D.C., Emerson, S.R., Quay, P.D., 1985.** Stable carbon isotopes in marine porewaters. *Earth and Planetary Science Letters,* **74**, 13–26.

**McCrea, J.M., 1950.** On the isotope chemistry of carbonates and a paleotemperature scale. *Journal of Chemical Physics,* **18**, 849–857.

**Merlivat, L., Jouzel, J., 1979.** Global climatic interpretation of the Deuterium-Oxygen 18 relationship for precipitation. *Journal of Geophysical Research,* **84** (C8), 5029–5033.

**Miao, Q., Thunell, R.C., 1993.** Recent deep-sea benthic foraminiferal distribution in the South China Sea. *Marine Micropaleontology*, **22,** 1–32.

**Miller, K.G., Lohmann, G.P., 1982.** Environmental distribution of recent benthic foraminifera on the northeast United States continental slope*. GSA Bulletin*, **93**, 200–206.

**Mísař, Z., Dudek, A., Havlena, V., Weiss, J., 1983.** *Geologie ČSSR I. – Český masiv*, Státní pedagogické nakladatelství Praha, pp. 336.

**Murray, J.W., 2006.** *Ecology and Applications of Benthic Foraminifera*. Cambridge University Press, Cambridge, pp. 488.

**Nehyba, S., Šikula, J., 2007.** Depositional architecture, sequence stratigraphy and geodynamic development of the Carpathian Foredeep (Czech Republic). *Geologica Carpathica,* **58**, 53–69.

**Nevesskaja, L.A., Goncharova, I.A., Paramonova, N.P., Popov, S.B., Babak, E.B., Bagdasarjan, K.G., Voronina, A.A., 1993.** *Opredelitelj miocenovj ih dvustvorchatjih molljuskov Jugo-Zapadnoi Evrazii.* Moskow: Nauka, pp. 412.

**Novák, Z., 1975.** Lower Badenian Limestones from the Carpathian Foredeep (in Czech). *Manuscript, Kandidátská práce*. Univerzita Jana Evangelisty Purkyně Brno.

**Ortiz, J.D., Mix, A.C., Rugh, W. *et al.,* 1996.** Deep-dwelling planktonic foraminifera of the northeastern Pacific Ocean reveal environmental control of oxygen and carbon isotopic disequilibria. *Geochimica et Cosmochimica Acta,* **60** (22), 4509-4523.

**Papp, A., Cicha, I., 1978.** Definition der Zeiteinheit M [4] – Badenien. In: Papp,A.,Cicha, I., Seneš, J. and Steininger, F., Eds., M4 – Badenien (Moravien, Wielicien, Kosovien). *Chronostratigraphie und Neostratotypen, Miozän der Zentralen Paratethys,* **6**, 47-48.

**Papp, A., 1985a.** Holostratotypus: Vösendorf, Wiener Becken (Österreich). In: Papp, A., Jámbor,Á., Steininger, F.F. (Eds.),M6 Pannonian (Slavonien und Serbien). *Chronostratigraphie und Neostratotypen. Miozän der Zentralen Paratethys, vol.* **7**, 187–198.

**Papp, A., Cicha, I., Seneš, J., Steininger, F., 1978.** M4 – Badenien (Moravien, Wielicien, Kosovien). *Chronostratigraphie und Neostratotypen, Miozän der Zentralen Paratethys,* **6,** 1–594.

**Papp, A., Steininger, F., 1974.** Holostratotypus Nexing N.Ö. In: Papp, A., Marinescu, F., Seneš, J. (Eds.),M5. *Sarmatien.Chronostratigraphie und Neostratotypen,Miozän der Zentralen Paratethys, vol*. **4**, 162–166.

**Paren, J.G., Potter, J.R., 1984.** Isotopic tracers in polar seas and glacier ice. *Journal of Geophysical Research,* **89**, 749–750.

**Peeters F.J.C., Brummer G.-J.A., Ganssen G., 2002.** The effect of upwelling on the distribution and stable isotope composition of *Globigerina bulloides* and *Globigerina ruber* (planktic foraminifers) in modern surface waters of the NW Arabian Sea. *Global and Planetary Change,* **34**, 269-291.

**Peryt D., 2013.** Foraminiferal record of the Mid dle Mio cene climate transition prior to the Badenian salinity crisis in the Polish Carpathian Foredeep Basin (Central Paratethys). *Geological Quarterly*, **57** (1), 141–164.

**Peryt, T.M., 2001.** Gypsum facies transitions in basin-marginal evaporites: middle Miocene (Badenian) of west Ukraine. *Sedimentology,* **48**, 1103-1119.

**Piller W., Harzhauser M., Mandic O. 2007.** Miocene Central Paratethys stratigraphy – current status and future directions. *Stratigraphy,* **4**, 151-168.

**Piller, W.E. and Kleemann, K., 1991.** Middle Miocene Reefs and related facies in Eastern Austria. I) Vienna Basin. *VI. International Symposium on Fossil Cnidaria including Archaeocyatha and Porifera, Excursion-Guidebook, Excursion B4*, 1–28.

**Pisera, A., 1996.** Miocene reefs of the Paratethys: a review. *SEPM **5***, 97–104.

**Popov, S.V., Rögl, F., Rozanov, A.Y., Steininger, F.F., Shcherba, I.G., Kováč, M. Eds., 2004.** Lithologicalpaleogeographic maps of Paratethys. 10 Maps Late Eocene to Pliocene. *Courier Forschungsinstitut Senckenberg,* **250**, 1–46.

**Procházka, V.J., 1892a.** Předběžná zpráva o stratigrafických a faunistických poměrech nejzazší části miocenu západní Moravy. *Věstník královské české společnosti nauk*, 326–368.

**Procházka, V.J., 1892b.** Miocaen moravský. První příspěvek ku poznání rázu zvířeny mořských jílů a slínů severo- západo a středomoravské oblasti. *Věstník královské české společnosti nauk,* 458–471.

**Procházka, V.J., 1893.** Geologický nástin Tišnovska. *V průvodci výstavy okresní v Tišnově,* Tišnov, 19–50.

**Procházka, V.J., 1899.** Miocénové ostrovy v krasu Moravském. *Rozpravy České Akademie*, **2,** 1–37.

**Rathburn, A.E., Corliss, B.H., 1994.** The ecology of deep-sea benthic foraminifera from the Sulu Sea*. Paleoceanography,* **9**, 87–150.

**Ravelo, A.C., Fairbanks, R.G., 1995.** Carbon isotopic fractionation in multiple species of planktonic foraminifera from core-tops in the tropical Atlantic, *Journal of Foraminiferal Research,* **25** (1), 53–74.

**Reichenbacher, B., 2000.** Das brackisch-lakustrische Oligozän und Unter-Miozän im Mainzer Becken und Hanauser Becken: Fischfaunen, Paläoökologie, Biostratigraphie, Paläogeographie. *Courier Forschungsinstitut Senckenberg,* **222**, 1–143.

**Reynolds, L., Thunell, R.C., 1985.** Seasonal succession of planktonic foraminifera in the subpolar North Pacific. *Journal of Foraminiferal Research*, **15,** 282–301.

**Riegl, B., Piller, W.E., 2002.** Reefs and coral carpets in the Miocene Paratethys (Badenian, Leitha Limestone, Austria). *Proceedings 9th International Coral Reef Symposium, Bali,* **1,** 211-216.

**Riegl, B., Piller, W.E., 2000.** Biostromal coral facies –A Miocene example fromthe Leitha Limestone (Austria) and its actualistic interpretation. *Palaios,* **15**, 399–413.

**Rögl F., Brandstätter F., 1993.** The foraminifera genus Amphistegina in the Korytnica Clays (Holy Cross Mts, Central Poland) and its significance in the Miocene of the Paratethys. *Acta Geologica Polonica,* **43**, 122–146.

**Rögl, F., 1998.** Palaeogeographic considerations for Mediterranean and Paratethys seaways (Oligocene to Miocene). *Annalen des Naturhistorischen Museums in Wien,* **99**, 279–310.

**Rögl, F., 1998b.** Paratethys Oligocene-Miocene stratigraphic correlation. In: Cicha, I., Rögl, F., Rupp,C. and Ctyroka, J.,Oligocene –Miocene foraminifera of the Central Paratethys. *Abhandlungen der Senckenbergischen Naturforschenden Gesellschaft,* **549**, 3–7.

**Rögl, F., 1999.** Mediterranean and Paratethys. Facts and hypotheses of an Oligocene to Miocene Paleogeography (short overview). *Geologica Carpathica,* **59**, 339–349.

**Rögl, F., Brzobohatý, R., Cicha, I., Coric, S., Daxner-Höck, G., Doláková, N., Harzhauser, M., 2003.** Paleobiological characterization and definition of the Karpatian stage. In: Brzobohatý, R., Cicha, I., Kováč, M., Rögl, F. (Eds.), *The Karpatian— a Lower Miocene Stage of the Central Paratethys*. Masaryk University, Brno, 357–360.

**Rögl, F., Schultz, O., Hölzl, O., 1973.** Holostratotypus und Faziostratotypen der Innviertler Schichtengruppe. In: Papp, A., Rögl, F., Seneš, J. (Eds.), M2 Ottnangien. Die Innviertler, Salgótarjáner, Bántapusztaer Schichtengruppe und die Rzehakia Formation. *Chronostratigraphie und Neostratotypen, Miozän der Zentralen Paratethys*, vol. **3**, 140–196.

**Rögl, F., Spezzaferri, S., Coric, S., 2002.** Micropaleontology and biostratigraphy of the Karpatian-Badenian transition (Early-Middle Miocene boundary) in Austria (Central Paratethys). *Courier Forschungsinstitut Senckenberg,* **237,** 47–67.

**Rögl, F., 1998a.** Palaeogeographic considerations for Mediterranean and Paratethys seaways (Oligocene to Miocene). *Annalen des Naturhistorischen Museums in Wien,* **99A**, 279–310.

**Rohling, E.J., Bigg, G.R., 1998.** Paleosalinity and a critical assessment. *Journal of Geophysical Research,* **103** (C1), 1307–1318.

**Romanek, C.S., Grossman, E.L., Morse, J.W., 1992.** Carbon isotopic fractionation in synthetic aragonite and calcite: effects of temperature and precipitation rate. *Geochimica et Cosmochimica Acta,* **56**, 419–430.

**Rozanski, K., Araguas-Araguas, L., Gonfiantini, R., 1993.** Isotopic patterns in modern global precipitation, in *Climate Change in Continental Isotopic Records,* (eds P.K. Swart, K.C. Lohmann, J. McKenzie and S. Savin), *Geophysical Monograph Series,* **78**, American Geophysical Union, Washington DC, 1–36.

**Rozanski, K., Sonntag, C., Münnich, K.O., 1982.** Factors controlling stable isotope composition of European precipitation. *Tellus,* **34**, 142–150.

**Schiebel R., Hemleben, C., 2005.** Modern planktic foraminifera. Paläontologische Zeitschrift, **79,** 135–148.

**Schiebel, R., Bijma, J., Hemleben, C., 1997.** Population dynamics of the planktic foraminifer Globigerina bulloides from the eastern North Atlantic. Deep Sea Research Part I: *Oceanographic Research Papers*, **44** (9–10), 1701–1713.

**Schmid, H.P., Harzhauser, M. and Kroh, A., 2001.** Hypoxic events in a Middle Miocene carbonate platform of the Central Paratethys (Austria, Badenian, 14 Ma). *Annalen des Naturhistorischen Museums Wien,* **102A,** 1-50.

**Schweizer M., Pawlowski J., Kouwenhoven T., Van Der Zwaan B., 2009.** Molecular phylogeny of common Cibicidids and relatedrotaliida (foraminifera) based on small subunit rDNA sequences. *Journal of Foraminiferal Research,* **39**, 300–315.

**Seghedi, I., Downes, H., Szakács, A., Mason, P.R.D., Thirlwall, M.F., Rosu, E., Pécskay, Z., Márton, E., Panaiotu, C., 2004.** Neogene-Quaternary magmatism and geodynamics in the Carpathian-Pannonian region: a synthesis. *Lithos,* **72,** 117-146.

**Sen Gupta, B. K., 1999.** *Modern Foraminifera*. Dordrecht, Kluwer Academic Publishers, Netherlands, pp. 371.

**Sen Gupta, B.K., Machain-Castillo, M.L., 1993.** Benthic foraminifera in oxygen-poor habitats. *Marine Micropaleontology*, **20**, 183–201.

**Seneš, J., 1961.** Paläogeographie des Westkarpatischen Raumes in Beziehung zur übrigen Paratethys im Miozän. *Geologické Práce,* **60**, 1–56.

**Shackleton, N.J., 1977a.** $\delta^{13}C$ in Uvigerina: tropical rainforest history and the equatorial Pacific carbonate dissolution cycles, in *Fate of Fossil Fuel $CO_2$ in the Oceans,* (eds N. Anderson and A. Malahof), Plenum, New York, 401–427.

**Shackleton, N.J., 1977b.** The oxygen isotope stratigraphic record of the Late Pleistocene. *Philosophical Transactions of the Royal Society, London,* B, **280**, 169–182.

**Shackleton, N.J., 1987.** Oxygen isotopes, ice volume and sea-level. *Quaternary Science Reviews,* **6**, 183–190.

**Shackleton, N.J., Opdyke, N.D., 1973.** Oxygen isotope and paleomagnetic stratigraphy of equatorial Pacific core V28–238: oxygen isotope temperatures and ice volumes on a $10^5$ and $10^6$ year scale. *Quaternary Research,* **3**, 39–55.

**Shevenell, A.E., Kennett, J.P., Lea, D.W., 2004.** MiddleMiocene Southern Ocean Cooling and Antarctic Cryosphere Expansion. *Science,* **305**, 1766-1770.

**Sjoerdsma, P.G., Van der Zwaan, G.J., 1992.** Simulating the effect of changing organic flux and oxygen content on the distribution of benthic foraminifera. *Marine Micropaleontology*, **19,** 163–180.

**Spero, H.J, Lea, D.W., 1996.** Experimental determination of stable isotope variability in *Globigerina bulloides:* implications for paleoceanographic reconstructions. *Marine Micropaleontology,* **28**, 231–246.

**Spero, H.J., 1992.** Do planktic foraminifera accurately record shifts in the carbon isotopic composition of sea water $\Sigma CO_2$? *Marine Micropaleontology,* **19,** 275-285.

**Spero, H.J., Lea, D.W., 1993.** Intraspecific stable isotope variability in the planktonic foraminifer *Globigerinoides sacculifer:* results from laboratory experiments. *Marine Micropaleontology,* **22**, 221–234.

**Spero, H.J., Parker, S.L., 1985.** Photosynthesis in the symbiotic planktonic foraminifer *Orbulina universa* and its potential contribution to oceanic primary productivity. *Journal of Foraminiferal Research,* **15,** 273–281.

**Spero, H.J., Williams, D.F., 1988.** Extracting environmental information from planktonic foraminiferal $^{13}C$ data. *Nature,* **335**, 717–719.

**Spero, H.J., Bijma, J., Lea, D.W., Bemis, B.E., 1997.** Effect of seawater carbonate concentration on foraminiferal carbon and oxygen isotopes. *Nature*, **390,** 497–500.

**Spero, H.J., Lerche, I., Williams, D.F., 1991.** Opening the carbon isotope 'vital effect' black box, 2, quantitative model for interpreting foraminiferal carbon isotope data. *Paleoceanography,* **6**, 639–655.

**Spezzaferri, S., Coric, S., Hohenegger, J., Rögl, F., 2002.** Basin-scale paleobiogeography and paleoecology: an example from Karpatian (Latest Burdigalian) benthic and planktonic foraminifera and calcareous nannoplankton from the Central Paratethys. *Geobios, Mémoir spécial,* **24,** 241-256.

**Spezzaferri, S., Rögl, F., Coric, S., Hohenegger, J., 2004.** Paleoenvironmental changes and agglutinated foraminifera across the Karpatian/Badenian (Early/Middle Miocene) boundary in the Styrian Basin (Austria, Central Paratethys). In: Bubík, M. and Kaminski, M.A., Eds., *Proceedings of the Sixth International Workshop on Agglutinated Foraminifera*. Grzybowski Foundation Special publication, **8**, 423–459.

**Steininger, F., 1971.** Holostratotypus und Faziostratotypen der Eggenburger Schichtengruppe im Raum von Eggenburg in Niederösterreich (Österreich). In: Steininger, F., Seneš, J. (Eds.), M1 Eggenburgien. Die Eggenburger Schichtengruppe und ihr Stratotypus. *Chronostratigraphie und Neostratotypen, vol. **2***, pp. 104–167.

**Steininger, F., 1973.** Die Molluskenfaunen des Ottnangien. In: Papp, A., Rögl, F., Seneš, J. (Eds.), M2 Ottnangien. Die Innviertler, Salgótarjáner, Bántapusztaer Schichtgruppe und die Rzehakia Formation*. Chronostratigraphie und Neostratotypen, Miozän der zentralen Paratethys, vol*. **3**, pp. 380–615.

**Steininger, F., Rögl, F, Müller, C., 1978.** Geodynamik und paläogeographische Entwicklung des Badenien. In: Papp, A., Cicha, I., Seneš, J. and Steininger, F., Eds., M4 – Badenien (Moravien, Wielicien, Kosovien). *Chronostratigraphie und Neostratotypen, Miozän der Zentralen Paratethys,* **4,** 110–127.

**Steininger, F., Seneš, J., 1971.** M1 Eggenburgien. Die Eggenburger Schichtengruppe und ihr Stratotypus. *Chronostratigraphie und Neostratotypen,* **2**, 1–827.

**Steininger, F., Wessely, G., 2000.** From the Tethyan Ocean to the Paratethys Sea: Oligocene to Neogene Stratigraphy, Paleogeography and Paleobiogeography of the circum-Mediterranean region and the Oligocene to Neogene Basin evolution in Austria. *Mitteilungen der Österreichischen Geologischen Gesellschaft,* **92**, 95–116.

**Stewart, M.K., 1975.** Stable isotope fractionation due to evaporation and isotopic exchange of falling waterdrops: applications to atmospheric processes and evaporation of lakes. *Journal of Geophysical Research,* **80**, 1133–1146.

**Stille, H., 1924.** *Grundfragen der vergleichenden Tektonik.* Gebrüder Bornträger, Berlin, pp. 443.

**Strain, P.M., Tan, F.C., 1993.** Seasonal evolution of oxygen isotope-salinity relationships in high-latitude surface waters. *Journal of Geophysical Research,* **98**, 14589–14598.

**Strauss, P., Harzhauser, M., Hinsch, R., Wagreich, M., 2006.** Sequence stratigraphy in a classic pull-apart basin (Neogene, Vienna Basin). A 3D seismic based integrated approach. *Geologica Carpathica,* **57**, 185–197.

**Studencka B., 1999.** Remarks on Miocene bivalve zonation in the Polish part of the Carpathian Foredeep*. Geological Quarterly,* **43**, 4, 467–477.

**Studencka, B., Gontsharova, I.A., Popov, S.V., 1998.** The bivalve faunas as a basis for reconstruction of the Middle Miocene history of the Paratethys. *Acta Geologica Polonica,* **48**, 285–342.

**Švábenická, L., 2002.** Calcareous nannofossils of the Upper Karpatian and Lower Badenian deposits in the Carpathian Foredeep, Moravia (Czech Republic)*. Geologica Carpathica*, **53**, 197–210.

**Swart, P.K., 1983.** Carbon and oxygen isotope fractionation in scleractinian corals: a review. *Earth-Science Reviews,* **19**, 51–80.

**Swart, P.K., Burns, S.J., Leder, J.J., 1991.** Fractionation of the stable isotopes of oxygen and carbon in carbon dioxide during the reaction of calcite with phosphoric acid as a function of temperature and technique. *Chemical Geology (Isotope Geoscience Section),* **86**, 89–96.

**Szczechura J., 1997.** Bolboforms (Protophyta, incerte sedis) from the Middle Miocene of the Upper Silesia (Carpathian Foredeep, southern Poland). *Bulletin of the Polish Academy of Sciences, Earth Ser*., **45**, 133–144.

**Tan, F.C., 1989.** Stable carbon isotopes in dissolved inorganic carbon in marine and estuarine environments, in *Handbook of environmental isotope geochemistry,* v*.* **3A**, (eds. P. Fritz and J.C. Fontes), Elsevier, Amsterdam, pp. 171–190.

**Tarutani, T., Clayton, R.N., Mayeda, T.K., 1969.** The effect of polymorphism and magnesium substitution on oxygen isotope fractionation between calcium carbonate and water. *Geochimica et Cosmochimica Acta,* **33**, 987–996.

**ter Kuile, B., Erez, J., 1984.** *In situ* growth late experiments on the symbiont-bearing foraminifera Amphis*tegina lobifera* and *Amphisorus hemprichii. Journal of Foraminiferal Research,* **14**, 262–276.

**Usdowski, E., Hoefs, J., 1993.** Oxygen isotope exchange between carbonic acid, bicarbonate, carbonate, and water: a re-examination of the data of McCrea (1950) and an expression for the overall partitioning of oxygen isotopes between the carbonate species and water. *Geochimica et Cosmochimica Acta,* **57**, 3815–3818.

**Vincent, E., Killingley, J.S., Berger, W.H., 1981.** Stable isotope composition of benthic foraminifera from the equatorial Pacific. *Nature,* **289**, 639–643.

**Wade B.S., Pearson P.N., Berggren W.A., Pälike H., 2011.** Review and revision of Cenozoic tropical planktonic foraminiferal biostratigraphy and calibration to the geomagnetic polarity and astronomical time scale. *Earth Science Reviews,* **104**, 111-142.

**Wagner, L.R., 1996.** Stratigraphy and hydrocarbons in Upper Austrian Molasse Foredeep (Active margin). In: Wessely, G., Liebl, W. (Eds.), Oil and Gas in Alpidic Thrustbelts and Basins of Central and Eastern Europe. European Association of Geoscientists and Engineers. Special Publications, vol. **5**, pp. 217–235.

**Wefer, G., Berger, W.H., 1991.** Isotope paleontology: growth and composition of extant calcareous species. *Marine Geology,* **100**, 207–248.

**Wefer, G., Heinze, P.M., Berger, W.H., 1994.** Clues to ancient methane release. *Nature,* **369**, 282.

**Weiss, R.F., Östlund, H.G., Craig, H., 1979.** Geochemical studies of the Weddell Sea. *Deep-Sea Research,* **26A**, 1093–1120.

**Weissenbäck, M., 1996.** Lower to Middle Miocene sedimentation model of the central Vienna Basin. In: Wessely, G. and Liebl, W., Eds., *Oil and Gas in Alpidic Thrustbelts and Basins of the Central and Eastern Europe*. European Association of Geoscientists and Engineers, Special Publications, **5**, 355–363.

**White, W. M., 2013.** *Geochemistry*. Wiley-Blackwell, New York, pp. 668.

**Woodruff, F., Savin, S.M., Douglas, R.G., 1980.** Biological fractionation of oxygen and carbon isotopes by recent benthic foraminifera. *Marine Micropaleontology,* **5***,* 3–11.

**Zahn, R., Winn, K., Sarnthein, M., 1986.** Benthic foraminiferal $^{13}C$ and accumulation rates of organic carbon: *Uvigerina peregrina* group and *Cibicidoides wuellerstorfi. Paleoceanography,* **1**, 27–42.

**Zdražílková N., 1985.** Badenian algal limestones from the Carpathian Foredeep (in Czech). *Manuscript, Diploma Thesis*, Univerzita Jana Evangelistu Purkyně Brno.

# 9. WWW Resources

www.thermoscientific.com

https://www.nodc.noaa.gov/General/temperature.html

# Appendices 1 - 5

# Appendix 1

The examples display the preservation of the inner wall structure. The pictures from the SEM (scanning electron microscope) show the differences between the well-preserved inner wall structure and the recrystallized one. In the left column, there are pictures showing the well-preserved inner wall structure and conversely in the right column, there are pictures showing the recrystallization of the inner wall structure.

| **Well-preserved** | **Recrystallized** |
| --- | --- |
| 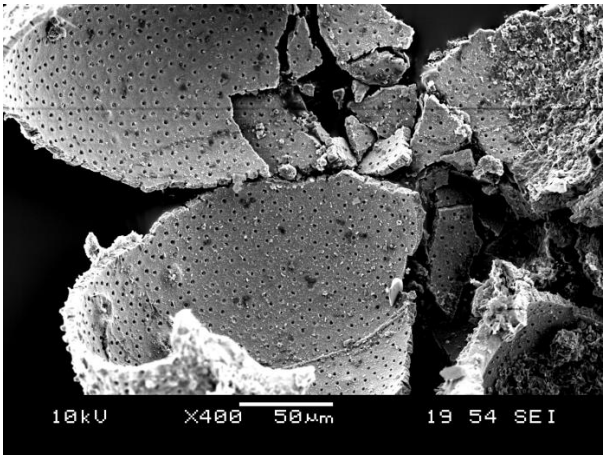  | 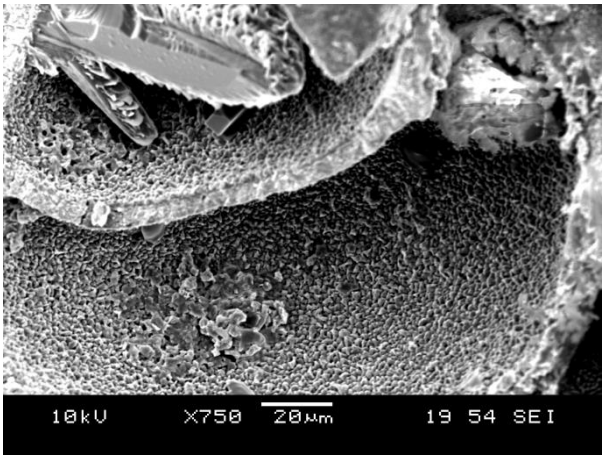  |
| 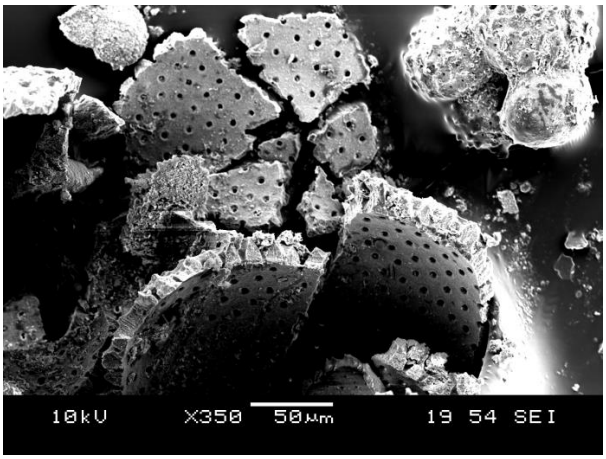  | 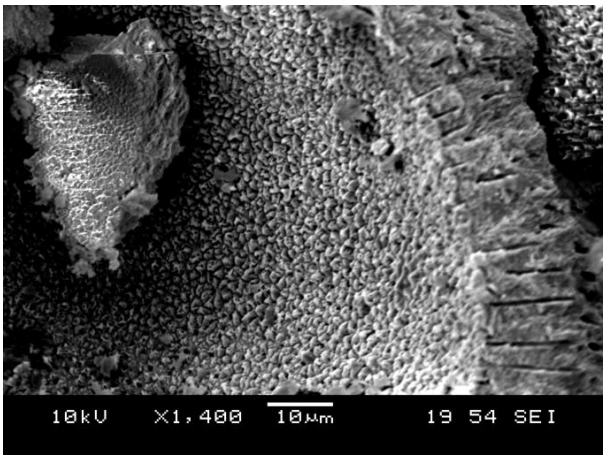  |

# Appendix 1

**Well-preserved** **Recrystallized**

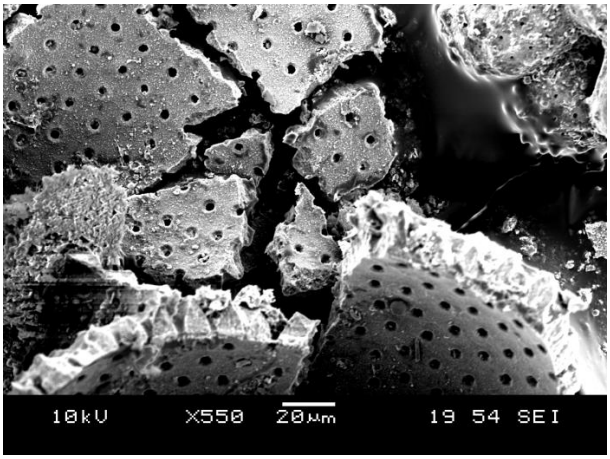


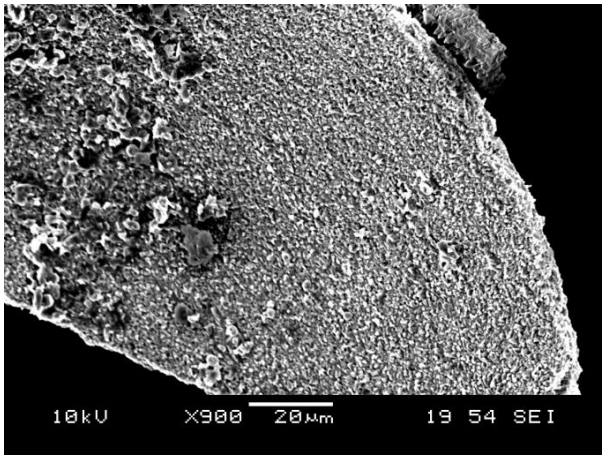


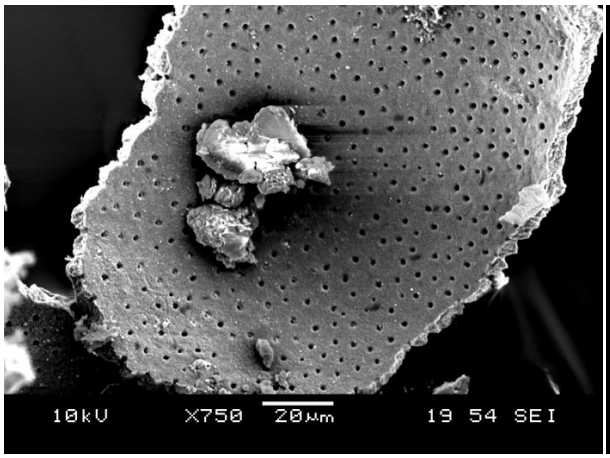


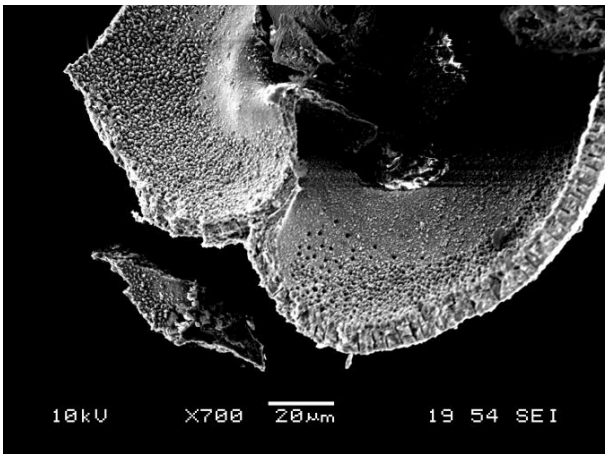


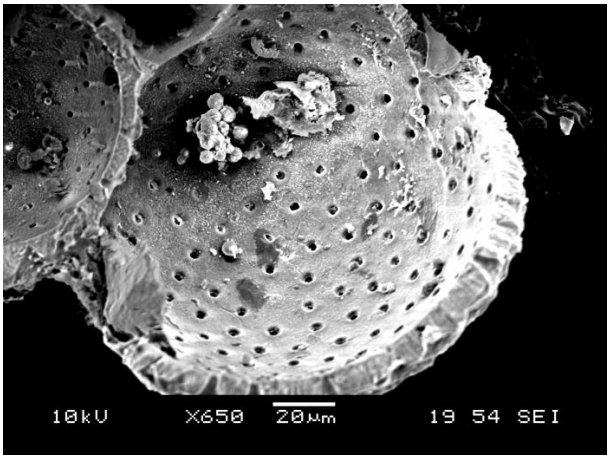


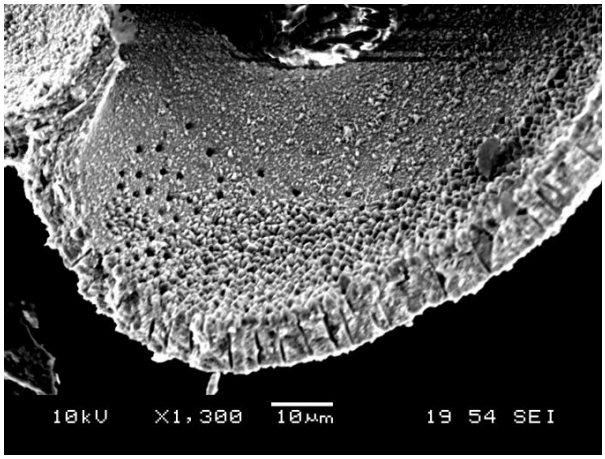

# Appendix 1

**Well-preserved** **Recrystallized**

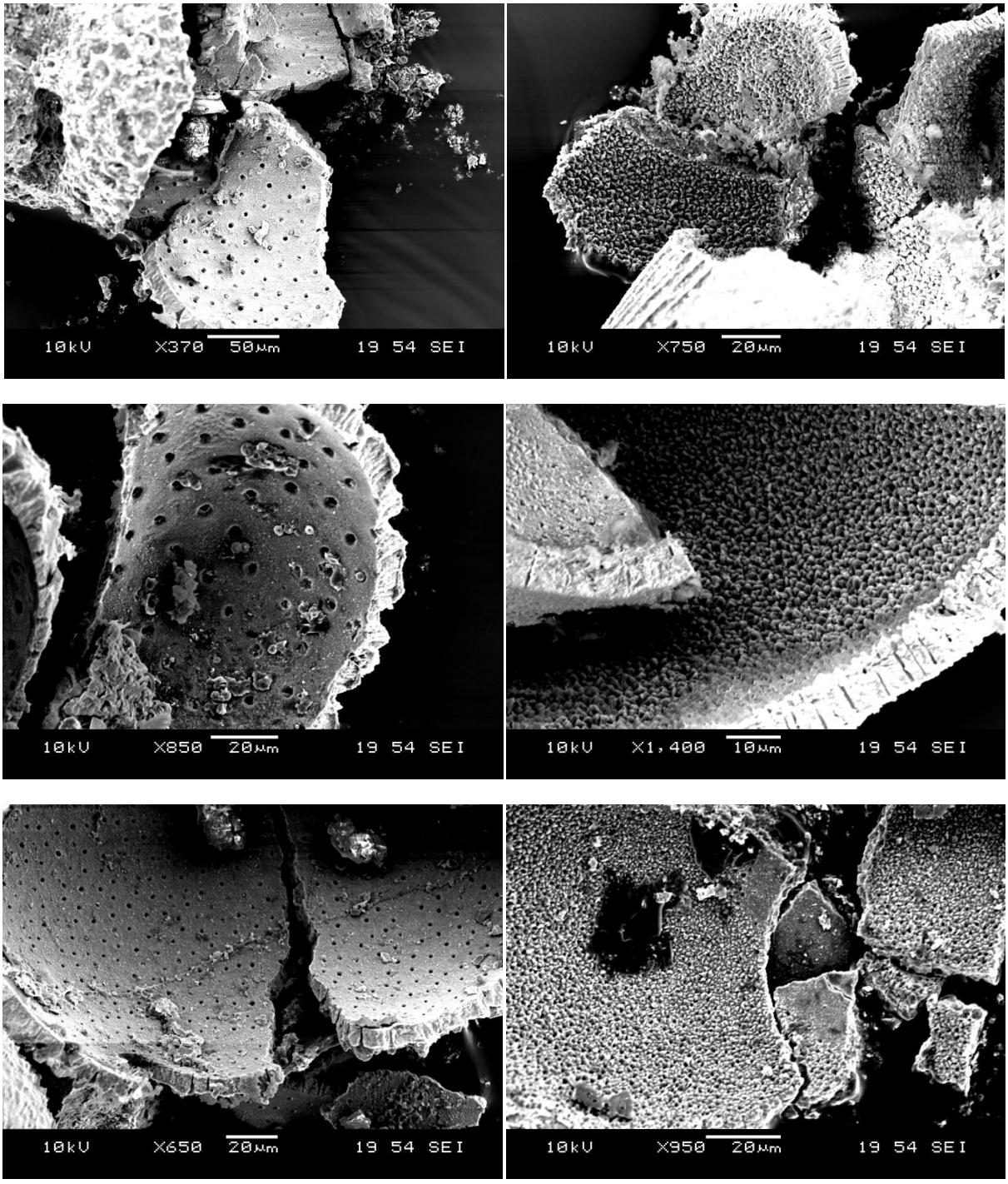

# Appendix 2

The original data of the $\delta^{13}C/^{12}C$ and $\delta^{18}O/^{16}O$ isotope analysis performed by Dr. R. Milovský, Geologický Ústav SAV Banská Bystrica, Slovakia, are shown below.

| Identifier 1 | Identifier 2 | Comment | 1 Cycle Int Samp 44 | δ $^{13}C/^{12}C$ Mean | δ $^{18}O/^{16}O$ Mean | δ $^{13}C$ CORR | δ $^{18}O$ CORR |
|---|---|---|---|---|---|---|---|
| *G. bulloides* | 8.5 m | LOM-1 | 1354,261 | 0,812 | 0,066 | **0,809** | **0,066** |
| *G. bulloides* | 8.5 m | LOM-1 | 1178,18 | 0,742 | -0,315 | **0,736** | **-0,315** |
| *G. bulloides* | 8.5 m | LOM-1 | 1121,167 | 0,251 | -0,835 | **0,243** | **-0,835** |
| *G. bulloides* | 8.5 m | LOM-1 | 1308,496 | 1,062 | 0,113 | **1,058** | **0,113** |
| *G. bulloides* | 8.5 m | LOM-1 | 1191,299 | 0,515 | 0,162 | **0,509** | **0,162** |
| *Orbulina suturalis* | 8.5 m | LOM-1 | 3771,989 | 2,461 | -0,401 | **2,461** | **-0,401** |
| *Orbulina suturalis* | 8.5 m | LOM-1 | 3706,897 | 2,427 | -0,501 | **2,427** | **-0,501** |
| *Orbulina suturalis* | 8.5 m | LOM-1 | 3630,624 | 1,881 | -0,412 | **1,881** | **-0,412** |
| *Orbulina suturalis* | 8.5 m | LOM-1 | 2959,681 | 1,921 | -0,166 | **1,921** | **-0,166** |
| *Orbulina suturalis* | 8.5 m | LOM-1 | 2261,228 | 1,43 | -0,58 | **1,430** | **-0,580** |
| *Uvigerina* spp. | 8.5 m | LOM-1 | 4126,408 | -0,12 | 0,838 | **-0,120** | **0,838** |
| *Uvigerina* spp. | 8.5 m | LOM-1 | 3235,326 | -0,362 | 0,901 | **-0,362** | **0,901** |
| *Uvigerina* spp. | 8.5 m | LOM-1 | 5207,967 | -0,169 | 0,63 | **-0,169** | **0,630** |
| *Uvigerina* spp. | 8.5 m | LOM-1 | 7237,266 | 0,166 | 0,992 | **0,166** | **0,992** |
| *Uvigerina* spp. | 8.5 m | LOM-1 | 4312,224 | -0,059 | 0,917 | **-0,059** | **0,917** |
| *Heterolepa dutemplei* | 8.5 m | LOM-1 | 3269,875 | 0,753 | 0,564 | **0,753** | **0,564** |
| *Heterolepa dutemplei* | 8.5 m | LOM-1 | 1946,02 | 0,706 | 0,437 | **0,706** | **0,437** |
| *Cibicidoides* spp. | 8.5 m | LOM-1 | 2845,913 | 0,182 | 0,46 | **0,182** | **0,460** |
| *Cibicidoides* spp. | 8.5 m | LOM-1 | 2044,334 | 0,151 | 0,21 | **0,151** | **0,210** |
| *Cibicidoides* spp. | 8.5 m | LOM-1 | 2834,892 | 1,018 | 0,677 | **1,018** | **0,677** |
| *Cibicidoides* spp. | 8.5 m | LOM-1 | 3821,304 | 1,068 | 0,415 | **1,068** | **0,415** |
| *Elphidium* spp. | 8.5 m | LOM-1 | 1406,452 | 0,477 | -0,474 | **0,475** | **-0,474** |
| *Elphidium* spp. | 8.5 m | LOM-1 | 2678,182 | 1,166 | -1,631 | **1,166** | **-1,631** |
| *G. bulloides* | 12.6 m | LOM-1 | 852,409 | 0,045 | -1,28 | **0,016** | **-1,295** |
| *G. bulloides* | 12.6 m | LOM-1 | 1251,706 | 0,412 | 0,031 | **0,407** | **0,031** |
| *G. bulloides* | 12.6 m | LOM-1 | 1582,836 | 0,491 | 0,437 | **0,490** | **0,437** |
| *G. bulloides* | 12.6 m | LOM-1 | 1418,787 | 0,178 | -1,051 | **0,176** | **-1,051** |
| *G. bulloides* | 12.6 m | LOM-1 | 1468,326 | 0,333 | -0,464 | **0,331** | **-0,464** |
| *Orbulina suturalis* | 12.6 m | LOM-1 | 4904,413 | 2,258 | -0,203 | **2,258** | **-0,203** |

# Appendix 2

| *Identifier 1* | Identifier 2 | Comment | 1 Cycle Int Samp 44 | δ $^{13}C/^{12}C$ Mean | δ $^{18}O/^{16}O$ Mean | δ $^{13}C$ CORR | δ $^{18}O$ CORR |
|---|---|---|---|---|---|---|---|
| *Orbulina suturalis* | 12.6 m | LOM-1 | 3065,798 | 1,776 | 0,517 | **1,776** | **0,517** |
| *Praeorbulina glomerosa* | 12.6 m | LOM-1 | 4459,167 | 1,838 | -0,053 | **1,838** | **-0,053** |
| *Praeorbulina glomerosa* | 12.6 m | LOM-1 | 3406,642 | 1,439 | -0,729 | **1,439** | **-0,729** |
| *Cibicidoides* spp. | 12.6 m | LOM-1 | 4354,024 | 0,294 | 0,814 | **0,294** | **0,814** |
| *Cibicidoides* spp. | 12.6 m | LOM-1 | 2161,672 | -0,086 | 0,533 | **-0,086** | **0,533** |
| *Cibicidoides* spp. | 12.6 m | LOM-1 | 3041,473 | 0,225 | 0,834 | **0,225** | **0,834** |
| *Cibicidoides* spp. | 12.6 m | LOM-1 | 3388,918 | 0,379 | 0,806 | **0,379** | **0,806** |
| *Heterolepa dutemplei* | 12.6 m | LOM-1 | 5516,266 | 0,755 | 0,87 | **0,755** | **0,870** |
| *Heterolepa dutemplei* | 12.6 m | LOM-1 | 2148,745 | 0,51 | 1,022 | **0,510** | **1,022** |
| *Heterolepa dutemplei* | 12.6 m | LOM-1 (Velka) | 4663,236 | 0,556 | 0,86 | **0,556** | **0,860** |
| *Uvigerina* spp. | 12.6 m | LOM-1 | 3644,378 | -0,095 | 1,098 | **-0,095** | **1,098** |
| *Uvigerina* spp. | 12.6 m | LOM-1 | 3580,152 | -0,16 | 1,317 | **-0,160** | **1,317** |
| *Uvigerina* spp. | 12.6 m | LOM-1 | 2531,849 | -0,222 | 1,059 | **-0,222** | **1,059** |
| *Uvigerina* spp. | 12.6 m | LOM-1 | 2260,637 | -0,122 | 1,379 | **-0,122** | **1,379** |
| *G. bulloides* | 12.6 m | LOM-1 | 1008,169 | 0,118 | -0,602 | **0,104** | **-0,604** |
| *G. bulloides* | 12.6 m | LOM-1 | 1771,119 | 0,143 | -0,301 | **0,143** | **-0,301** |
| *Orbulina suturalis* | 450 | LOM-1 | 1950,975 | 1,094 | -0,986 | **1,094** | **-0,986** |
| *Orbulina suturalis* | 450 | LOM-1 | 1769,557 | 1,78 | -0,815 | **1,780** | **-0,815** |
| *Orbulina suturalis* | 450 | LOM-1 | 1727,79 | 0,51 | -0,864 | **0,509** | **-0,864** |
| *Cibicidoides* spp. | 450 | LOM-1 | 1270,428 | -0,115 | 0,343 | **-0,119** | **0,343** |
| *Cibicidoides* spp. | 450 | LOM-1 | 313,646 | -0,705 | -2,488 | **-0,949** | **-2,998** |
| *Gyroidinoides* spp. | 450 | LOM-1 | 1705,31 | -0,445 | 0,799 | **-0,446** | **0,799** |
| *Gyroidinoides* spp. | 450 | LOM-1 | 2169,794 | -0,318 | 0,765 | **-0,318** | **0,765** |
| *Heterolepa dutemplei* | 450 | LOM-1 | 1751,782 | -0,823 | 0,562 | **-0,823** | **0,562** |
| *Heterolepa dutemplei* | 450 | LOM-1 | 1655,516 | -0,297 | 0,334 | **-0,298** | **0,334** |
| *Orbulina suturalis* | 450 | LOM-1 | 1608,108 | 0,821 | 0,281 | **0,820** | **0,281** |
| *Gyroidinoides* spp. | 450 | LOM-1 | 2514,299 | -0,268 | 0,65 | **-0,268** | **0,650** |
| *Cibicidoides* spp. | 450 | LOM-1 | 725,353 | 0,847 | -0,016 | **0,795** | **-0,096** |
| *Orbulina suturalis* | 450 | LOM-1 | 1503,641 | 0,868 | -0,34 | **0,867** | **-0,340** |

# Appendix 2

| *Identifier 1* | Identifier 2 | Comment | 1 Cycle Int Samp 44 | δ $^{13}C/^{12}C$ Mean | δ $^{18}O/^{16}O$ Mean | δ $^{13}C$ CORR | δ $^{18}O$ CORR |
|---|---|---|---|---|---|---|---|
| *Cibicidoides* spp. | 450 | LOM-1 | 462,52 | -0,204 | 0,274 | **-0,376** | **-0,190** |
| *Gyroidinoides* spp. | 450 | LOM-1 | 1469,133 | -0,161 | 1,022 | **-0,163** | **1,022** |
| *Gyroidinoides* spp. | 450 | LOM-1 | 1428,265 | -0,255 | 0,833 | **-0,257** | **0,833** |
| *G. bulloides* | 450 | LOM-1 | 666,098 | 0,209 | -1,346 | **0,141** | **-1,502** |
| *Cibicidoides* spp. | 450 | LOM-1 | 500,982 | 0,508 | -1,687 | **0,364** | **-2,117** |
| *Globigerinoides* spp. | 450 | LOM-1 | 2296,63 | 1,259 | -0,963 | **1,259** | **-0,963** |
| *G. bulloides* | 450 | LOM-1 | 305,678 | -1,344 | -2,567 | **-1,588** | **-3,078** |
| *Globigerinoides* spp. | 450 | LOM-1 | 2249,544 | 1,253 | -1,392 | **1,253** | **-1,392** |
| *G. bulloides* | 450 | LOM-1 | 405,73 | 0,171 | -1,268 | **-0,052** | **-1,761** |
| *Globigerinoides* spp. | 450 | LOM-1 | 1899,375 | 0,967 | -0,876 | **0,967** | **-0,876** |
| *Paragloborotalia* spp. | 450 | LOM-1 | 304,459 | -1,229 | -1,822 | **-1,473** | **-2,333** |
| *Cibicidoides* spp. | 1130 | LOM-1 | 1071,953 | -0,236 | 0,284 | **-0,247** | **0,283** |
| *Gyroidinoides* spp. | 1130 | LOM-1 | 643,724 | 0,243 | 1,506 | **0,168** | **1,313** |
| *Gyroidinoides* spp. | 1130 | LOM-1 | 477,58 | -0,701 | 0,902 | **-0,862** | **0,449** |
| *Orbulina suturalis* | 1130 | LOM-1 | 1310,599 | 1,394 | -0,818 | **1,390** | **-0,818** |
| *Cibicidoides* spp. | 1130 | LOM-1 | 330,721 | -0,46 | -1,734 | **-0,704** | **-2,243** |
| *Cibicidoides* spp. | 1130 | LOM-1 | 817,374 | 0,577 | 0,244 | **0,543** | **0,220** |
| *Praeorbulina glomerosa* | 1130 | LOM-1 | 2272,647 | -0,017 | -1,537 | **-0,017** | **-1,537** |
| *Praeorbulina glomerosa* | 1130 | LOM-1 | 1614,757 | 0,463 | -0,721 | **0,462** | **-0,721** |
| *Paragloborotalia* spp. | 1130 | LOM-1 | 123,765 | -3,927 | -6,794 | **-3,767** | **-6,575** |
| *Paragloborotalia* spp. | 1130 | LOM-1 | 262,123 | -1,271 | -2,547 | **-1,505** | **-3,024** |
| *G. bulloides* | 1130 | LOM-1 | 514,442 | 0,317 | -0,371 | **0,181** | **-0,786** |
| *Globigerinoides* spp. | 1130 | LOM-1 | 765,341 | 1,405 | -0,988 | **1,362** | **-1,036** |
| *G. bulloides* | 1130 | LOM-1 | 853,707 | 0,946 | -1,1 | **0,917** | **-1,115** |
| *G. bulloides* | 1130 | LOM-1 | 1100,774 | 0,651 | -3,948 | **0,642** | **-3,948** |
| *Globigerinoides* spp. | 1130 | LOM-1 | 1538,146 | 1,255 | -1,811 | **1,254** | **-1,811** |
| *G. bulloides* | 1130 | LOM-1 | 898,501 | 0,854 | -1,423 | **0,831** | **-1,431** |
| *Gyroidinoides* spp. | 1100 | LOM-1 | 735,585 | -0,431 | 0,359 | **-0,480** | **0,289** |
| *Heterolepa dutemplei* | 1100 | LOM-1 | 1462,305 | -1,37 | -1,451 | **-1,372** | **-1,451** |

# Appendix 2

| *Identifier 1* | Identifier 2 | Comment | 1 Cycle Int Samp 44 | δ $^{13}C/^{12}C$ Mean | δ $^{18}O/^{16}O$ Mean | δ $^{13}C$ CORR | δ $^{18}O$ CORR |
|---|---|---|---|---|---|---|---|
| *Paragloborotalia* spp. | 1100 | LOM-1 | 1468,479 | 0,33 | 1,36 | **0,328** | **1,360** |
| *Melonis pompilioides* | 1100 | LOM-1 | 721,387 | 0,033 | 0,611 | **-0,020** | **0,527** |
| *Melonis pompilioides* | 1100 | LOM-1 | 914,885 | 0,093 | 0,961 | **0,071** | **0,955** |
| *Melonis pompilioides* | 1100 | LOM-1 | 1488,016 | -0,161 | 0,862 | **-0,163** | **0,862** |
| *Gyroidinoides* spp. | 1100 | LOM-1 | 1952,53 | -0,036 | 1,046 | **-0,036** | **1,046** |
| *Melonis pompilioides* | 1100 | LOM-1 | 1140,269 | 0,149 | 0,764 | **0,141** | **0,764** |
| *Melonis pompilioides* | 1100 | LOM-1 | 887,092 | 0,039 | 0,828 | **0,014** | **0,819** |
| *Melonis pompilioides* | 1100 | LOM-1 | 1179,808 | -0,384 | 0,52 | **-0,390** | **0,520** |
| *Melonis pompilioides* | 1100 | LOM-1 | 1459,484 | -0,322 | 0,304 | **-0,324** | **0,304** |
| *Globigerinoides* spp. | 1100 | LOM-1 | 926,379 | 2,34 | -0,071 | **2,320** | **-0,076** |
| *Paragloborotalia* spp. | 1100 | LOM-1 | 404,459 | 0,406 | 0,093 | **0,182** | **-0,400** |
| *Gyroidinoides* spp. | 1100 | LOM-1 | 868,488 | 0,005 | 0,885 | **-0,022** | **0,873** |
| *G. bulloides* | 1100 | LOM-1 | 813,832 | 0,585 | 0,438 | **0,551** | **0,413** |
| *Orbulina suturalis* | 1100 | LOM-1 | 2149,805 | 2,154 | -0,728 | **2,154** | **-0,728** |
| *G. bulloides* | 1800 | LOM-1 | 896,643 | 0,088 | -1,313 | **0,065** | **-1,321** |
| *G. bulloides* | 1800 | LOM-1 | 669,349 | 0,237 | -0,956 | **0,170** | **-1,107** |
| *G. bulloides* | 1800 | LOM-1 | 726,742 | 0,442 | 0,025 | **0,391** | **-0,054** |
| *G. bulloides* | 1800 | LOM-1 | 569,45 | 0,869 | 1,356 | **0,764** | **1,025** |
| *G. bulloides* | 1800 | LOM-1 | 1451,475 | 0,3 | -0,386 | **0,298** | **-0,386** |
| *Gyroidinoides* spp. | 1800 | LOM-1 | 488,236 | -4,732 | -11,365 | **-4,885** | **-11,808** |
| *Gyroidinoides* spp. | 1800 | LOM-1 | 667,842 | -0,611 | 1,393 | **-0,678** | **1,240** |
| *G. bulloides* | 1800 | LOM-1 | 1262,386 | 0,374 | -0,448 | **0,370** | **-0,448** |
| *Melonis pompilioides* | 1800 | LOM-1 | 957,464 | -0,409 | 0,591 | **-0,427** | **0,587** |
| *G. bulloides* | 1800 | LOM-1 | 443,609 | 0,127 | 0,311 | **-0,061** | **-0,165** |
| *Gyroidinoides* spp. | 1800 | LOM-1 | 746,675 | -0,496 | 0,86 | **-0,543** | **0,799** |
| *Gyroidinoides* spp. | 1800 | LOM-1 | 554,203 | -0,754 | 0,642 | **-0,867** | **0,285** |
| *Melonis pompilioides* | 1800 | LOM-1 | 986,002 | -0,593 | 0,005 | **-0,609** | **0,003** |
| *Gyroidinoides* spp. | 1800 | LOM-1 | 1373,345 | -0,16 | 0,823 | **-0,163** | **0,823** |
| *Melonis pompilioides* | 1800 | LOM-1 | 883,544 | -0,127 | 0,873 | **-0,152** | **0,863** |
| *G. bulloides* | 1170 | LOM-1 | 711,018 | 0,483 | -0,248 | **0,428** | **-0,343** |

# Appendix 2

| *Identifier 1* | Identifier 2 | Comment | 1 Cycle Int Samp 44 | δ $^{13}C/^{12}C$ Mean | δ $^{18}O/^{16}O$ Mean | δ $^{13}C$ CORR | δ $^{18}O$ CORR |
|---|---|---|---|---|---|---|---|
| *Cibicidoides* spp. | 1170 | LOM-1 | 1129,016 | 0,786 | 0,242 | **0,778** | **0,242** |
| *G. bulloides* | 1170 | LOM-1 | 307,947 | -3,279 | -2,619 | **-3,523** | **-3,130** |
| *Cibicidoides* spp. | 1170 | LOM-1 | 642,066 | 1,486 | 1,612 | **1,410** | **1,416** |
| *Heterolepa dutemplei* | 1170 | LOM-1 | 735,396 | 0,801 | 1,174 | **0,752** | **1,103** |
| *Cibicidoides* spp. | 1170 | LOM-1 | 354,599 | 0,296 | -0,865 | **0,052** | **-1,370** |
| *G. bulloides* | 1170 | LOM-1 | 490,613 | 0,162 | 0,529 | **0,011** | **0,088** |
| *G. bulloides* | 1170 | LOM-1 | 219,833 | -2,028 | -4,222 | **-2,185** | **-4,511** |
| *G. bulloides* | 1170 | LOM-1 | 608,419 | 0,192 | -0,287 | **0,104** | **-0,546** |
| *Cibicidoides* spp. | 1170 | LOM-1 | 1402,318 | -0,051 | 0,06 | **-0,053** | **0,060** |
| *Melonis pompilioides* | 1170 | LOM-1 | 1987,211 | 0,005 | 0,91 | **0,005** | **0,910** |
| *Melonis pompilioides* | 1170 | LOM-1 | 3,705 | -13,675 | -12,615 | **-13,236** | **-12,619** |
| *Cibicidoides* spp. | 1170 | LOM-1 | 987,06 | 0,338 | 1,123 | **0,322** | **1,121** |
| *Melonis pompilioides* | 1170 | LOM-1 | 1753,762 | -0,285 | 0,707 | **-0,285** | **0,707** |
| *Melonis pompilioides* | 1170 | LOM-1 | 1252,694 | -0,08 | 0,708 | **-0,085** | **0,708** |
| *Melonis pompilioides* | 1170 | LOM-1 | 1420,341 | -0,101 | 0,763 | **-0,103** | **0,763** |
| *Gyroidinoides* spp. | 1170 | LOM-1 | 1201,703 | -0,66 | 1,016 | **-0,666** | **1,016** |
| *Gyroidinoides* spp. | 1170 | LOM-1 | 934,968 | -0,086 | 1,247 | **-0,106** | **1,242** |
| *Gyroidinoides* spp. | 1170 | LOM-1 | 338,823 | -0,757 | 0,531 | **-1,001** | **0,023** |
| *Gyroidinoides* spp. | 1170 | LOM-1 | 789,828 | -0,775 | 0,865 | **-0,813** | **0,830** |
| *Uvigerina* spp. | 1170 | LOM-1 | 1123,56 | 0,077 | 1,611 | **0,069** | **1,611** |
| *Uvigerina* spp. | 1170 | LOM-1 | 1308,851 | -0,128 | 1,712 | **-0,132** | **1,712** |
| *Orbulina suturalis* | 1170 | LOM-1 | 998,383 | 2,002 | 0,019 | **1,987** | **0,017** |
| *Uvigerina* spp. | 1170 | LOM-1 | 2188,729 | 0,408 | 1,327 | **0,408** | **1,327** |
| *Globigerinoides* spp. | 1170 | LOM-1 | 1832,091 | 0,22 | 1,101 | **0,220** | **1,101** |
| *Praeorbulina glomerosa* | 1425 | LOM-1 | 1384,293 | 1,248 | 0,632 | **1,245** | **0,632** |
| *Cibicidoides* spp. | 1425 | LOM-1 | 868,726 | 0,448 | 1,054 | **0,421** | **1,042** |
| *Heterolepa dutemplei* | 1425 | LOM-1 | 876,55 | 0,925 | 1,041 | **0,899** | **1,030** |
| *Heterolepa dutemplei* | 1425 | LOM-1 | 941,845 | 0,454 | 0,767 | **0,435** | **0,763** |
| *Heterolepa dutemplei* | 1425 | LOM-1 | 1081,914 | 0,299 | 0,816 | **0,289** | **0,815** |

# Appendix 2

| *Identifier 1* | Identifier 2 | Comment | 1 Cycle Int Samp 44 | δ $^{13}C/^{12}C$ Mean | δ $^{18}O/^{16}O$ Mean | δ $^{13}C$ CORR | δ $^{18}O$ CORR |
|---|---|---|---|---|---|---|---|
| *Gyroidinoides* spp. | 1425 | LOM-1 | 725,317 | -0,577 | 0,848 | **-0,629** | **0,768** |
| *Heterolepa dutemplei* | 1425 | LOM-1 | 965,495 | 0,786 | 0,948 | **0,769** | **0,945** |
| *Gyroidinoides* spp. | 1425 | LOM-1 | 713,615 | -0,322 | 1,464 | **-0,376** | **1,372** |
| *G. bulloides* | 1425 | LOM-1 | 879,032 | 0,497 | -1,222 | **0,472** | **-1,232** |
| *G. bulloides* | 1425 | LOM-1 | 907,769 | 0,63 | -0,597 | **0,608** | **-0,604** |
| *G. bulloides* | 1425 | LOM-1 | 461,238 | 0,376 | 0,355 | **0,203** | **-0,110** |
| *G. bulloides* | 1425 | LOM-1 | 412,13 | 0,099 | -0,439 | **-0,118** | **-0,930** |
| *Cibicidoides* spp. | 1425 | LOM-1 | 436,378 | -0,011 | 0,954 | **-0,205** | **0,474** |
| *Melonis pompilioides* | 1425 | LOM-1 | 406,055 | 0,135 | 1,276 | **-0,087** | **0,783** |
| *Melonis pompilioides* | 1425 | LOM-1 | 364,069 | 0,39 | 1,39 | **0,146** | **0,886** |
| *G. bulloides* | 1425 | LOM-1 | 325,441 | 1,118 | 0,441 | **0,874** | **-0,068** |
| *Melonis pompilioides* | 1425 | LOM-1 | 300,366 | 0,813 | 1,904 | **0,569** | **1,393** |
| *G. bulloides* | 1425 | LOM-1 | 808,053 | 1,082 | -0,381 | **1,047** | **-0,408** |
| *G. bulloides* | 1425 | LOM-1 | 921,449 | 0,366 | 0,115 | **0,345** | **0,109** |
| *Heterolepa dutemplei* | 1425 | LOM-1 | 871,731 | 0,687 | 0,45 | **0,661** | **0,438** |
| *G. bulloides* | 1425 | LOM-1 | 725,113 | 0,653 | 0,389 | **0,601** | **0,309** |
| *Melonis pompilioides* | 1425 | LOM-1 | 818,485 | -0,008 | 0,672 | **-0,042** | **0,648** |
| *Cibicidoides* spp. | 1450 | LOM-1 | 231,132 | -0,357 | -2,875 | **-0,540** | **-3,222** |
| *G. bulloides* | 1450 | LOM-1 | 428,45 | -0,391 | -0,535 | **-0,592** | **-1,019** |
| *G. bulloides* | 1450 | LOM-1 | 445,788 | 0,617 | 0,795 | **0,431** | **0,320** |
| *Melonis pompilioides* | 1450 | LOM-1 | 400,995 | 0,268 | 1,112 | **0,041** | **0,618** |
| *Melonis pompilioides* | 1450 | LOM-1 | 361,473 | 0,338 | 1,134 | **0,094** | **0,630** |
| *G. bulloides* | 1450 | LOM-1 | 560,698 | 0,037 | -0,428 | **-0,073** | **-0,775** |
| *G. bulloides* | 1450 | LOM-1 | 754,227 | 0,411 | -1,099 | **0,366** | **-1,155** |
| *G. bulloides* | 1450 | LOM-1 | 867,644 | 0,126 | -1,458 | **0,099** | **-1,470** |
| *Gyroidinoides* spp. | 1450 | LOM-1 | 616,672 | 0,243 | 1,881 | **0,158** | **1,638** |
| *G. bulloides* | 1450 | LOM-1 | 1068,295 | 0,204 | -0,157 | **0,193** | **-0,158** |
| *G. bulloides* | 1450 | LOM-1 | 671,275 | 1,309 | 1,175 | **1,243** | **1,027** |
| *Melonis pompilioides* | 1450 | LOM-1 | 699,71 | -0,02 | 0,993 | **-0,078** | **0,885** |
| *Uvigerina* spp. | 1450 | LOM-1 | 882,867 | -0,144 | 0,642 | **-0,169** | **0,632** |
| *Gyroidinoides* spp. | 1450 | LOM-1 | 979,671 | 0,323 | 1,711 | **0,307** | **1,708** |
| *Cibicidoides* spp. | 1450 | LOM-1 | 983,324 | 0,381 | 1,08 | **0,365** | **1,078** |

# Appendix 2

| *Identifier 1* | Identifier 2 | Comment | 1 Cycle Int Samp 44 | δ $^{13}C/^{12}C$ Mean | δ $^{18}O/^{16}O$ Mean | δ $^{13}C$ CORR | δ $^{18}O$ CORR |
|---|---|---|---|---|---|---|---|
| *Gyroidinoides* spp. | 1450 | LOM-1 | 1549,387 | 0,209 | 1,077 | **0,208** | **1,077** |
| *Gyroidinoides* spp. | 1450 | LOM-1 | 1367,81 | 0,074 | 1,132 | **0,071** | **1,132** |
| *Uvigerina* spp. | 1450 | LOM-1 | 1576,414 | 0,009 | 1,319 | **0,008** | **1,319** |
| *Gyroidinoides* spp. | 1450 | LOM-1 | 2340,734 | 0,621 | 0,847 | **0,621** | **0,847** |
| *Uvigerina* spp. | 1450 | LOM-1 | 2068,234 | -0,175 | 0,927 | **-0,175** | **0,927** |
| *Gyroidinoides* spp. | 1650 | LOM-1 | 2283,004 | -0,87 | 0,19 | **-0,870** | **0,190** |
| *Globigerinoides* spp | 1650 | LOM-1 | 826,106 | 1,709 | -0,601 | **1,677** | **-0,623** |
| *Gyroidinoides* spp. | 1650 | LOM-1 | 843,278 | -0,15 | 1,346 | **-0,180** | **1,329** |
| *Globigerinoides* spp | 1650 | LOM-1 | 1470,248 | 1,361 | -0,964 | **1,359** | **-0,964** |
| *G. bulloides* | 1650 | LOM-1 | 1384,721 | -0,24 | -0,592 | **-0,243** | **-0,592** |
| *G. bulloides* | 1650 | LOM-1 | 1360,818 | -0,053 | -0,447 | **-0,056** | **-0,447** |
| *Globigerinoides* spp | 1650 | LOM-1 | 571,003 | 1,4 | -1,247 | **1,295** | **-1,576** |
| *Melonis pompilioides* | 1650 | LOM-1 | 640,673 | -0,725 | 0,038 | **-0,801** | **-0,161** |
| *G. bulloides* | 1650 | LOM-1 | 716,132 | -0,028 | -0,334 | **-0,082** | **-0,423** |
| *Gyroidinoides* spp. | 1650 | LOM-1 | 793,272 | -0,617 | 0,623 | **-0,655** | **0,590** |
| *Melonis pompilioides* | 1650 | LOM-1 | 623,48 | 0,072 | 0,951 | **-0,010** | **0,721** |
| *G. bulloides* | 1650 | LOM-1 | 731,959 | -0,425 | -1,031 | **-0,475** | **-1,105** |
| *Melonis pompilioides* | 1650 | LOM-1 | 1024,236 | -0,766 | 0,006 | **-0,779** | **0,005** |
| *G. bulloides* | 1650 | LOM-1 | 875,921 | -0,175 | -0,768 | **-0,201** | **-0,779** |
| *Heterolepa dutemplei* | 1650 | LOM-1 | 3960,007 | 0,265 | 0,736 | **0,265** | **0,736** |
| *Gyroidinoides* spp. | 1650 | LOM-1 | 1015,433 | 0,048 | 1,1 | **0,034** | **1,098** |
| *Gyroidinoides* spp. | 1650 | LOM-1 | 1533,86 | -0,35 | 0,785 | **-0,351** | **0,785** |
| *Gyroidinoides* spp. | 1650 | LOM-1 | 914,432 | -0,537 | 1,05 | **-0,559** | **1,044** |
| *Globigerinoides* spp. | 1920 | LOM-1 | 1499,457 | 2,17 | -0,712 | **2,169** | **-0,712** |
| *Heterolepa dutemplei* | 1920 | LOM-1 | 1489,623 | 0,346 | 0,755 | **0,344** | **0,755** |
| *Gyroidinoides* spp. | 1675 | LOM-1 | 3161,928 | -0,272 | 1,028 | **-0,272** | **1,028** |
| *Melonis pompilioides* | 1920 | LOM-1 | 3075,107 | -0,436 | 0,65 | **-0,436** | **0,650** |
| *Globigerinoides* spp. | 1920 | LOM-1 | 2591,259 | 1,722 | -0,465 | **1,722** | **-0,465** |
| *Globigerinoides* spp. | 1920 | LOM-1 | 1163,951 | 2,006 | -0,367 | **1,999** | **-0,367** |

# Appendix 2

| *Identifier 1* | Identifier 2 | Comment | 1 Cycle Int Samp 44 | δ $^{13}C/^{12}C$ Mean | δ $^{18}O/^{16}O$ Mean | δ $^{13}C$ CORR | δ $^{18}O$ CORR |
|---|---|---|---|---|---|---|---|
| *Heterolepa dutemplei* | 1675 | LOM-1 | 1124,325 | 0,773 | 0,967 | **0,765** | **0,967** |
| *Globigerinoides* spp. | 1675 | LOM-1 | 2508,243 | 1,442 | -1,07 | **1,442** | **-1,070** |
| *Globigerinoides* spp. | 1675 | LOM-1 | 2856,058 | 1,772 | -1,078 | **1,772** | **-1,078** |
| *Globigerinoides* spp. | 1675 | LOM-1 | 2637,704 | 0,891 | -1,78 | **0,891** | **-1,780** |
| *Cibicidoides* spp. | 1920 | LOM-1 | 2319,626 | 0,578 | 0,728 | **0,578** | **0,728** |
| *Gyroidinoides* spp. | 1920 | LOM-1 | 2270,958 | -0,22 | 1,096 | **-0,220** | **1,096** |
| *Gyroidinoides* spp. | 1675 | LOM-1 | 1743,697 | -0,279 | 0,988 | **-0,279** | **0,988** |
| *Melonis pompilioides* | 1675 | LOM-1 | 1811,783 | -0,326 | 0,432 | **-0,326** | **0,432** |
| *Globigerinoides* spp. | 1675 | LOM-1 | 1495,411 | 0,285 | -0,18 | **0,283** | **-0,180** |
| *G. bulloides* | 1675 | LOM-1 | 1436,022 | 0,286 | 0,084 | **0,284** | **0,084** |
| *Heterolepa dutemplei* | 1920 | LOM-1 | 1611,976 | 0,278 | 0,354 | **0,277** | **0,354** |
| *G. bulloides* | 1675 | LOM-1 | 1503,512 | 0,582 | -1,1 | **0,581** | **-1,100** |
| *G. bulloides* | 1675 | LOM-1 | 1597,418 | 0,302 | -0,566 | **0,301** | **-0,566** |
| *G. bulloides* | 1675 | LOM-1 | 1045,204 | 0,312 | -0,635 | **0,300** | **-0,636** |
| *G. bulloides* | 1675 | LOM-1 | 1111,691 | -0,38 | -0,552 | **-0,389** | **-0,552** |
| *Melonis pompilioides* | 1675 | LOM-1 | 1634,552 | 0,184 | 0,208 | **0,183** | **0,208** |
| *Melonis pompilioides* | 1675 | LOM-1 | 1521,868 | -0,361 | 0,357 | **-0,362** | **0,357** |
| *Melonis pompilioides* | 1675 | LOM-1 | 1510,651 | -0,279 | 0,443 | **-0,280** | **0,443** |
| *G. bulloides* | 1675 | LOM-1 | 1375,099 | -0,102 | -0,073 | **-0,105** | **-0,073** |
| *Gyroidinoides* spp. | 1920 | LOM-1 | 1475,534 | 0,103 | 1,146 | **0,101** | **1,146** |
| *G. bulloides* | 1675 | LOM-1 | 1068,834 | 0,154 | -0,791 | **0,143** | **-0,792** |
| *Gyroidinoides* spp. | 1920 | LOM-1 | 1203,776 | -0,411 | 0,705 | **-0,417** | **0,705** |
| *Melonis pompilioides* | 1920 | LOM-1 | 1244,692 | -0,715 | 0,115 | **-0,720** | **0,115** |
| *Melonis pompilioides* | 1920 | LOM-1 | 1204,837 | -0,482 | 0,54 | **-0,488** | **0,540** |
| *Gyroidinoides* spp. | 1675 | LOM-1 | 937,632 | -0,405 | 0,969 | **-0,424** | **0,964** |
| *G. bulloides* | 1675 | LOM-1 | 728,144 | 0,422 | -1,735 | **0,371** | **-1,812** |
| *Melonis pompilioides* | 1675 | LOM-1 | 872,292 | -0,69 | 0,242 | **-0,716** | **0,231** |
| *Gyroidinoides* spp. | 1920 | LOM-1 | 473,049 | -0,556 | 0,669 | **-0,720** | **0,213** |
| *Gyroidinoides* spp. | 1920 | LOM-1 | 693,334 | -0,632 | 0,713 | **-0,692** | **0,597** |

# Appendix 2

| *Identifier 1* | Identifier 2 | Comment | 1 Cycle Int Samp 44 | δ $^{13}C/^{12}C$ Mean | δ $^{18}O/^{16}O$ Mean | δ $^{13}C$ CORR | δ $^{18}O$ CORR |
|---|---|---|---|---|---|---|---|
| *Heterolepa dutemplei* | 1675 | LOM-1 | 844,681 | -0,013 | 0,104 | **-0,043** | **0,087** |
| *Gyroidinoides* spp. | 1675 | LOM-1 | 624,63 | -0,43 | 0,68 | **-0,512** | **0,452** |
| *Heterolepa dutemplei* | 1675 | LOM-1 | 624,41 | -0,531 | 0,06 | **-0,613** | **-0,169** |
| *Gyroidinoides* spp. | 1920 | LOM-1 | 608,846 | -0,54 | 0,948 | **-0,628** | **0,690** |
| *G. bulloides* | 1675 | LOM-1 | 475,78 | 1,052 | -0,227 | **0,890** | **-0,681** |
| *Globigerinoides* spp | 1650 | LOM-1 | 993,862 | 1,827 | -1,169 | **1,812** | **-1,171** |
| *Cibicidoides* spp. | 1920 | LOM-1 | 4771,681 | 0,119 | 0,905 | **0,119** | **0,905** |
| *Uvigerina* spp. | 1920 | LOM-1 | 2200,987 | 0,715 | 0,821 | **0,715** | **0,821** |
| *Uvigerina* spp. | 1920 | LOM-1 | 1228,37 | -0,308 | 1,184 | **-0,313** | **1,184** |
| *Globigerinoides* spp. | 1920 | LOM-1 | 2330,397 | 1,372 | -0,805 | **1,372** | **-0,805** |
| *Melonis pompilioides* | 1920 | LOM-1 | 2884,509 | -0,238 | 0,647 | **-0,238** | **0,647** |
| *Gyroidinoides* spp. | 1925 | LOM-1 | 2832,976 | -0,075 | 1,012 | **-0,075** | **1,012** |
| *Heterolepa dutemplei* | 1920 | LOM-1 | 2081,286 | 0,379 | 0,886 | **0,379** | **0,886** |
| *Cibicidoides* spp. | 1920 | LOM-1 | 2647,398 | 0,555 | -0,962 | **0,555** | **-0,962** |
| *Heterolepa dutemplei* | 1925 | LOM-1 | 2285,787 | 0,36 | 0,685 | **0,360** | **0,685** |
| *Cibicidoides* spp. | 1925 | LOM-1 | 890,557 | 1,071 | 1,066 | **1,047** | **1,057** |
| *Cibicidoides* spp. | 1925 | LOM-1 | 885,958 | 0,725 | 0,915 | **0,700** | **0,906** |
| *Cibicidoides* spp. | 1925 | LOM-1 | 1969,555 | 0,39 | 0,535 | **0,390** | **0,535** |
| *Globigerinoides* spp. | 1925 | LOM-1 | 1809,283 | 1,771 | -0,914 | **1,771** | **-0,914** |
| *G. bulloides* | 1925 | LOM-1 | 1487,305 | 0,724 | 0,467 | **0,722** | **0,467** |
| *G. bulloides* | 1925 | LOM-1 | 1189,888 | 1,087 | -1,309 | **1,081** | **-1,309** |
| *G. bulloides* | 1925 | LOM-1 | 845,36 | 0,703 | 0,235 | **0,673** | **0,218** |
| *Gyroidinoides* spp. | 1925 | LOM-1 | 673,369 | 0,199 | 1,269 | **0,134** | **1,125** |
| *Gyroidinoides* spp. | 1925 | LOM-1 | 644,197 | 0,331 | 1,46 | **0,256** | **1,268** |
| *Globigerinoides* spp. | 1925 | LOM-1 | 1191,55 | 1,376 | -0,985 | **1,370** | **-0,985** |
| *Globigerinoides* spp. | 1920 | LOM-1 | 1293,431 | 1,244 | -1,244 | **1,240** | **-1,244** |
| *Heterolepa dutemplei* | 1925 | LOM-1 | 1193,5 | 0,354 | 0,427 | **0,348** | **0,427** |
| *G. bulloides* | 1925 | LOM-1 | 1092,025 | 0,906 | -1,397 | **0,896** | **-1,398** |
| *Gyroidinoides* spp. | 1925 | LOM-1 | 898,997 | -0,782 | 0,992 | **-0,805** | **0,984** |

# Appendix 2

| *Identifier 1* | Identifier 2 | Comment | 1 Cycle Int Samp 44 | δ $^{13}C/^{12}C$ Mean | δ $^{18}O/^{16}O$ Mean | δ $^{13}C$ CORR | δ $^{18}O$ CORR |
|---|---|---|---|---|---|---|---|
| *G. bulloides* | 1925 | LOM-1 | 934,277 | 1,034 | 0,724 | **1,014** | **0,719** |
| *G. bulloides* | 1925 | LOM-1 | 624,46 | 0,053 | -0,131 | **-0,029** | **-0,359** |
| *Gyroidinoides* spp. | 1925 | LOM-1 | 757,775 | -0,18 | 0,791 | **-0,224** | **0,738** |
| Lobatula spp. | 1925 | LOM-1 | 671,93 | 0,638 | 0,323 | **0,572** | **0,176** |
| *G. bulloides* | 1925 | LOM-1 | 607,503 | 0,425 | -0,528 | **0,336** | **-0,789** |
| *G. bulloides* | 1925 | LOM-1 | 444,399 | 0,304 | 0,645 | **0,117** | **0,169** |
| *G. bulloides* | 1925 | LOM-1 | 392,286 | 0,035 | -0,812 | **-0,199** | **-1,309** |
| *Gyroidinoides* spp. | 900 | LOM-1 | 2291,048 | 0,071 | 0,883 | **0,071** | **0,883** |
| *Gyroidinoides* spp. | 1000 | LOM-1 | 898,897 | -0,283 | 0,323 | **-0,306** | **0,315** |
| *Heterolepa dutemplei* | 900 | LOM-1 | 823,619 | 0,806 | 0,569 | **0,773** | **0,547** |
| *Melonis pompilioides* | 900 | LOM-1 | 813,621 | 0,338 | 0,698 | **0,304** | **0,672** |
| *Orbulina suturalis* | 1000 | LOM-1 | 1371,139 | 0,688 | -1,792 | **0,685** | **-1,792** |
| *Globigerinoides* spp. | 1000 | LOM-1 | 1506,852 | 1,246 | -1,358 | **1,245** | **-1,358** |
| *Heterolepa dutemplei* | 900 | LOM-1 | 1779,7 | 0,416 | 0,266 | **0,416** | **0,266** |
| *Cibicidoides* spp. | 900 | LOM-1 | 1391,173 | 0,306 | 0,26 | **0,304** | **0,260** |
| *Cibicidoides* spp. | 900 | LOM-1 | 1500,904 | 0,198 | 0,298 | **0,197** | **0,298** |
| *Cibicidoides* spp. | 900 | LOM-1 | 625,338 | 0,512 | 0,642 | **0,430** | **0,415** |
| *Cibicidoides* spp. | 1000 | LOM-1 | 646,774 | 0,311 | 0,296 | **0,237** | **0,108** |
| *Melonis pompilioides* | 900 | LOM-1 | 1064,151 | -0,375 | -0,196 | **-0,386** | **-0,197** |
| *Melonis pompilioides* | 900 | LOM-1 | 1099,413 | -0,221 | 0,043 | **-0,230** | **0,043** |
| *Praeorbulina glomerosa* | 1000 | LOM-1 | 1069,369 | 0,613 | -1,388 | **0,602** | **-1,389** |
| *Globigerinoides* spp. | 1000 | LOM-1 | 909,421 | 1,473 | -1,727 | **1,451** | **-1,734** |
| *G. bulloides* | 900 | LOM-1 | 854,142 | 0,656 | -0,866 | **0,627** | **-0,881** |
| *Melonis pompilioides* | 900 | LOM-1 | 846,155 | -0,134 | -0,197 | **-0,164** | **-0,213** |
| *Globigerinoides* spp. | 900 | LOM-1 | 1033,109 | 0,851 | -1,198 | **0,838** | **-1,199** |
| *Orbulina suturalis* | 1000 | LOM-1 | 438,291 | -0,268 | -2,705 | **-0,460** | **-3,184** |
| *Globigerinoides* spp. | 1000 | LOM-1 | 486,386 | -0,029 | -3,552 | **-0,183** | **-3,997** |
| *Globigerinoides* spp. | 1000 | LOM-1 | 455,596 | 0,196 | -3,343 | **0,018** | **-3,812** |
| *Globigerinoides* spp. | 900 | LOM-1 | 553,76 | 1,431 | -1,777 | **1,318** | **-2,135** |

# Appendix 2

| *Identifier 1* | Identifier 2 | Comment | 1 Cycle Int Samp 44 | δ $^{13}C/^{12}C$ Mean | δ $^{18}O/^{16}O$ Mean | δ $^{13}C$ CORR | δ $^{18}O$ CORR |
|---|---|---|---|---|---|---|---|
| *Cibicidoides* spp. | 900 | LOM-1 | 627,011 | 1,156 | -1,411 | **1,075** | **-1,635** |
| *Praeorbulina glomerosa* | 1000 | LOM-1 | 605,888 | 0,362 | -0,567 | **0,273** | **-0,831** |
| *Cibicidoides* spp. | 1000 | LOM-1 | 171,571 | -0,463 | -1,378 | **-0,473** | **-1,395** |
| *Cibicidoides* spp. | 1000 | LOM-1 | 166,813 | -1,243 | -3,906 | **-1,237** | **-3,896** |
| *Cibicidoides* spp. | 1000 | LOM-1 | 224,403 | -1,73 | -3,242 | **-1,898** | **-3,555** |
| *Gyroidinoides* spp. | 1000 | LOM-1 | 2548,15 | 0,213 | 0,249 | **0,213** | **0,249** |
| *Globigerinoides* spp. | 1000 | LOM-1 | 2807,301 | 1,944 | -1,533 | **1,944** | **-1,533** |
| *Orbulina suturalis* | 1000 | LOM-1 | 2465,447 | 2,032 | -1,861 | **2,032** | **-1,861** |
| *Gyroidinoides* spp. | 900 | LOM-1 | 1561,936 | 0,393 | 0,943 | **0,392** | **0,943** |
| *Praeorbulina glomerosa* | 900 | LOM-1 | 1606,344 | 2,284 | -0,575 | **2,283** | **-0,575** |
| *Orbulina suturalis* | 900 | LOM-1 | 3719,68 | 1,915 | -0,289 | **1,915** | **-0,289** |
| *Orbulina suturalis* | 900 | LOM-1 | 3994,413 | 1,674 | -1,112 | **1,674** | **-1,112** |
| *Praeorbulina glomerosa* | 1000 | LOM-1 | 2087,693 | 1,351 | -1,316 | **1,351** | **-1,316** |
| *Orbulina suturalis* | 900 | LOM-1 | 1206,656 | 2,716 | -0,666 | **2,710** | **-0,666** |
| *Cibicidoides* spp. | 900 | LOM-1 | 3167,988 | 0,044 | 0,094 | **0,044** | **0,094** |
| *Globigerinoides* spp. | 900 | LOM-1 | 2356,712 | 1,968 | -1,018 | **1,968** | **-1,018** |
| *Gyroidinoides* spp. | 900 | LOM-1 | 2341,523 | -0,593 | 0,482 | **-0,593** | **0,482** |
| *Gyroidinoides* spp. | 900 | LOM-1 | 1070,697 | 0,427 | 0,974 | **0,416** | **0,973** |
| *Praeorbulina glomerosa* | 1000 | LOM-1 | 1665,411 | 0,69 | -1,404 | **0,689** | **-1,404** |
| *Heterolepa dutemplei* | 900 | LOM-1 | 2035,764 | -0,279 | 0,03 | **-0,279** | **0,030** |
| *Praeorbulina glomerosa* | 1000 | LOM-1 | 1321,308 | 1,066 | -0,667 | **1,063** | **-0,667** |
| *G. bulloides* | 1000 | LOM-1 | 505,446 | -0,056 | -1,504 | **-0,197** | **-1,929** |
| *G. bulloides* | 1000 | LOM-1 | 470,16 | 0,21 | -0,465 | **0,044** | **-0,924** |
| *Praeorbulina glomerosa* | 450 | LOM-1 | 2939,207 | 1,405 | -0,729 | **1,405** | **-0,729** |
| *Orbulina suturalis* | 380 | OV-1 | 1577,68 | 0,273 | -1,054 | **0,272** | **-1,054** |
| *Globigerinoides* spp. | 380 | OV-1 | 1622,5 | 1,942 | -1,57 | **1,941** | **-1,570** |
| *Globigerinoides* spp. | 380 | OV-1 | 1875,522 | 2,356 | -1,764 | **2,356** | **-1,764** |

# Appendix 2

| *Identifier 1* | Identifier 2 | Comment | 1 Cycle Int Samp 44 | δ $^{13}C/^{12}C$ Mean | δ $^{18}O/^{16}O$ Mean | δ $^{13}C$ CORR | δ $^{18}O$ CORR |
|---|---|---|---|---|---|---|---|
| *Globigerinoides* spp. | 380 | OV-1 | 2057,795 | 1,772 | -1,361 | **1,772** | **-1,361** |
| *Praeorbulina glomerosa* | 450 | LOM-1 | 2392,93 | 1,234 | -0,023 | **1,234** | **-0,023** |
| *Globigerinoides* spp. | 1170 | LOM-1 | 2574,941 | 1,981 | -1,525 | **1,981** | **-1,525** |
| *Orbulina suturalis* | 380 | OV-1 | 2843,946 | 0,568 | -0,551 | **0,568** | **-0,551** |
| *G. bulloides* | 1100 | LOM-1 | 1404,32 | 0,803 | -0,297 | **0,801** | **-0,297** |
| *Globigerinoides* spp. | 1100 | LOM-1 | 1568,35 | 2,085 | -0,915 | **2,084** | **-0,915** |
| *Orbulina suturalis* | 1170 | LOM-1 | 555,798 | 0,701 | -0,523 | **0,589** | **-0,878** |
| *Globigerinoides* spp. | 1100 | LOM-1 | 1828,577 | 2,375 | -1,098 | **2,375** | **-1,098** |
| *Globigerinoides* spp. | 380 | OV-1 | 2056,557 | 1,94 | -1,547 | **1,940** | **-1,547** |
| *Melonis pompilioides* | 380 | OV-1 | 2267,253 | -0,393 | 0,546 | **-0,393** | **0,546** |
| *Cibicidoides* spp. | 380 | OV-1 | 1154,069 | 0,564 | 0,134 | **0,557** | **0,134** |
| *G. bulloides* | 380 | OV-1 | 1215,893 | -0,172 | -2,225 | **-0,177** | **-2,225** |
| *G. bulloides* | 1100 | LOM-1 | 1312,353 | 0,213 | -0,557 | **0,210** | **-0,557** |
| *G. bulloides* | 1100 | LOM-1 | 1786,494 | 0,744 | -0,498 | **0,744** | **-0,498** |
| *Globigerinoides* spp. | 1100 | LOM-1 | 1951,684 | 1,809 | -0,809 | **1,809** | **-0,809** |
| *Orbulina suturalis* | 1100 | LOM-1 | 2214,385 | 1,587 | -0,467 | **1,587** | **-0,467** |
| *G. bulloides* | 450 | LOM-1 | 1019,247 | 0,251 | -1,324 | **0,238** | **-1,325** |
| *Globigerinoides* spp. | 380 | OV-1 | 1126,972 | 1,565 | -2,237 | **1,557** | **-2,237** |
| *Melonis pompilioides* | 380 | OV-1 | 1238,607 | -0,984 | 0,032 | **-0,989** | **0,032** |
| *G. bulloides* | 1100 | LOM-1 | 1346,688 | 0,684 | -0,785 | **0,681** | **-0,785** |
| *Cibicidoides* spp. | 450 | LOM-1 | 1496,959 | -0,074 | -0,183 | **-0,075** | **-0,183** |
| *Globigerinoides* spp. | 1100 | LOM-1 | 1694,264 | 1,914 | -0,998 | **1,913** | **-0,998** |
| *G. bulloides* | 1100 | LOM-1 | 709,85 | 0,949 | 0,343 | **0,894** | **0,247** |
| Meloni s pompilioides | 380 | OV-1 | 805,737 | -1,922 | -0,447 | **-1,958** | **-0,475** |
| *Cibicidoides* spp. | 1170 | LOM-1 | 910,642 | 1,384 | 0,948 | **1,362** | **0,941** |
| *Melonis pompilioides* | 1170 | LOM-1 | 980,036 | -0,071 | 0,592 | **-0,087** | **0,589** |
| *Cibicidoides* spp. | 450 | LOM-1 | 1091,74 | -0,073 | -0,401 | **-0,083** | **-0,402** |
| *G. bulloides* | 1100 | LOM-1 | 1191,171 | 1,001 | -1,399 | **0,995** | **-1,399** |
| *G. bulloides* | 450 | LOM-1 | 6,042 | -3,229 | -5,148 | **-2,790** | **-5,129** |
| *Heterolepa dutemplei* | 1100 | LOM-1 | 536,887 | 1,342 | -1,617 | **1,220** | **-2,001** |

# Appendix 2

| *Identifier 1* | Identifier 2 | Comment | 1 Cycle Int Samp 44 | δ $^{13}C/^{12}C$ Mean | δ $^{18}O/^{16}O$ Mean | δ $^{13}C$ CORR | δ $^{18}O$ CORR |
|---|---|---|---|---|---|---|---|
| *Heterolepa dutemplei* | 1170 | LOM-1 | 606,851 | 0,67 | 0,821 | **0,581** | **0,559** |
| *G. bulloides* | 1170 | LOM-1 | 377,148 | -0,227 | -1,901 | **-0,469** | **-2,402** |
| *Globigerinoides* spp. | 560 | OV-1 | 2247,646 | 1,499 | -1,424 | **1,499** | **-1,424** |
| *Globigerinoides* spp. | 450 | OV-1 | 2438,458 | 1,629 | -1,482 | **1,629** | **-1,482** |
| *Praeorbulina glomerosa* | 450 | OV-1 | 1018,996 | 0,659 | -1,686 | **0,646** | **-1,687** |
| *Melonis pompilioides* | 560 | OV-1 | 1202,654 | -1,713 | -1,284 | **-1,719** | **-1,284** |
| *Melonis pompilioides* | 560 | OV-1 | 1338,461 | -0,881 | -0,659 | **-0,884** | **-0,659** |
| *Praeorbulina glomerosa* | 560 | OV-1 | 2085,143 | 0,449 | -0,129 | **0,449** | **-0,129** |
| *Orbulina suturalis* | 380 | OV-1 | 1584,868 | 2,203 | -1,129 | **2,202** | **-1,129** |
| *Orbulina suturalis* | 450 | LOM-1 | 1896,157 | 1,387 | -0,42 | **1,387** | **-0,420** |
| *Orbulina suturalis* | 380 | OV-1 | 2167,835 | 1,763 | -1,38 | **1,763** | **-1,380** |
| *Heterolepa dutemplei* | 380 | OV-1 | 2631,938 | 0,543 | 0,388 | **0,543** | **0,388** |
| *Praeorbulina glomerosa* | 380 | OV-1 | 2828,131 | 1,58 | -0,76 | **1,580** | **-0,760** |

The regression curve (used for data conversion) parameters are shown below. The calculation was done by Dr. R. Milovský, Geologický Ústav SAV Banská Bystrica, Slovakia.

**δ $^{13}C$**

| <275 | | >275 | | | |
|---|---|---|---|---|---|
| y0 | -0,44 | a | 0,2445 | <275 | f=y0+a*x+b*x^2+c*x^3 |
| a | 0,0001 | b | -8,3679 | 275-2000 | f=y0+a/(1+exp(-(x-x0)/b))^c |
| b | 2,47E-05 | c | 0,0384 | >2000 | without correction |
| c | -5,83E-08 | x0 | 386,1962 | | |

**δ $^{18}O$**

| <275 | | >275 | | | |
|---|---|---|---|---|---|
| y0 | 0,041 | a | 0,5164 | <275 | |
| a | -0,0104 | b | -66,1045 | 275-2000 | f=y0+a/(1+exp(-(x-x0)/b))^c |
| b | 8,59E-05 | c | 0,9271 | >2000 | without correction |
| c | -1,52E-07 | x0 | 601,7585 | | |

# Appendix 3

The separate data for each sample with the plotted graphs are displayed below the tables. The order is: 4.5m; 8.5m; 9m; 10m; 11m; 11.3m; 11.7m; 12.6m; 14.25m; 14.5m; 16.5m; 16.75m; 18m; 19.2m; 19.25m. The X – axis represents $\delta^{18}O/^{16}O$, while the Y – axis represents $\delta^{13}C/^{12}C$. All isotopic data are reported in ‰ relative to VPDB related to the ATC1 standard.

# Appendix 3

## LOM-1: 4.50 m

| Identifier 1 | Identifier 2 | Comment | 1 Cycle Int Samp 44 | δ $^{13}C/^{12}C$ Mean | δ $^{18}O/^{16}O$ Mean | δ $^{13}C$ CORR | δ $^{18}O$ CORR |
|---|---|---|---|---|---|---|---|
| *Cibicidoides* spp. | 450 | LOM-1 | 1270,428 | -0,115 | 0,343 | **-0,119** | **0,343** |
| *Cibicidoides* spp. | 450 | LOM-1 | 725,353 | 0,847 | -0,016 | **0,795** | **-0,096** |
| *Cibicidoides* spp. | 450 | LOM-1 | 500,982 | 0,508 | -1,687 | **0,364** | **-2,117** |
| *Cibicidoides* spp. | 450 | LOM-1 | 1496,959 | -0,074 | -0,183 | **-0,075** | **-0,183** |
| *Cibicidoides* spp. | 450 | LOM-1 | 1091,74 | -0,073 | -0,401 | **-0,083** | **-0,402** |
| *G. bulloides* | 450 | LOM-1 | 666,098 | 0,209 | -1,346 | **0,141** | **-1,502** |
| *G. bulloides* | 450 | LOM-1 | 1019,247 | 0,251 | -1,324 | **0,238** | **-1,325** |
| *Globigerinoides* spp. | 450 | LOM-1 | 2296,63 | 1,259 | -0,963 | **1,259** | **-0,963** |
| *Globigerinoides* spp. | 450 | LOM-1 | 2249,544 | 1,253 | -1,392 | **1,253** | **-1,392** |
| *Globigerinoides* spp. | 450 | LOM-1 | 1899,375 | 0,967 | -0,876 | **0,967** | **-0,876** |
| *Gyroidinoides* spp. | 450 | LOM-1 | 1705,31 | -0,445 | 0,799 | **-0,446** | **0,799** |
| *Gyroidinoides* spp. | 450 | LOM-1 | 2169,794 | -0,318 | 0,765 | **-0,318** | **0,765** |
| *Gyroidinoides* spp. | 450 | LOM-1 | 2514,299 | -0,268 | 0,65 | **-0,268** | **0,650** |
| *Gyroidinoides* spp. | 450 | LOM-1 | 1469,133 | -0,161 | 1,022 | **-0,163** | **1,022** |
| *Gyroidinoides* spp. | 450 | LOM-1 | 1428,265 | -0,255 | 0,833 | **-0,257** | **0,833** |
| *Heterolepa dutemplei* | 450 | LOM-1 | 1751,782 | -0,823 | 0,562 | **-0,823** | **0,562** |
| *Heterolepa dutemplei* | 450 | LOM-1 | 1655,516 | -0,297 | 0,334 | **-0,298** | **0,334** |
| *Orbulina suturalis* | 450 | LOM-1 | 1608,108 | 0,821 | 0,281 | **0,820** | **0,281** |
| *Orbulina suturalis* | 450 | LOM-1 | 1503,641 | 0,868 | -0,34 | **0,867** | **-0,340** |
| *Orbulina suturalis* | 450 | LOM-1 | 1950,975 | 1,094 | -0,986 | **1,094** | **-0,986** |
| *Orbulina suturalis* | 450 | LOM-1 | 1769,557 | 1,78 | -0,815 | **1,780** | **-0,815** |
| *Orbulina suturalis* | 450 | LOM-1 | 1727,79 | 0,51 | -0,864 | **0,509** | **-0,864** |
| *Orbulina suturalis* | 450 | LOM-1 | 1896,157 | 1,387 | -0,42 | **1,387** | **-0,420** |
| *Cibicidoides* spp. | 450 | LOM-1 | 462,52 | -0,204 | 0,274 | **-0,376** | **-0,190** |

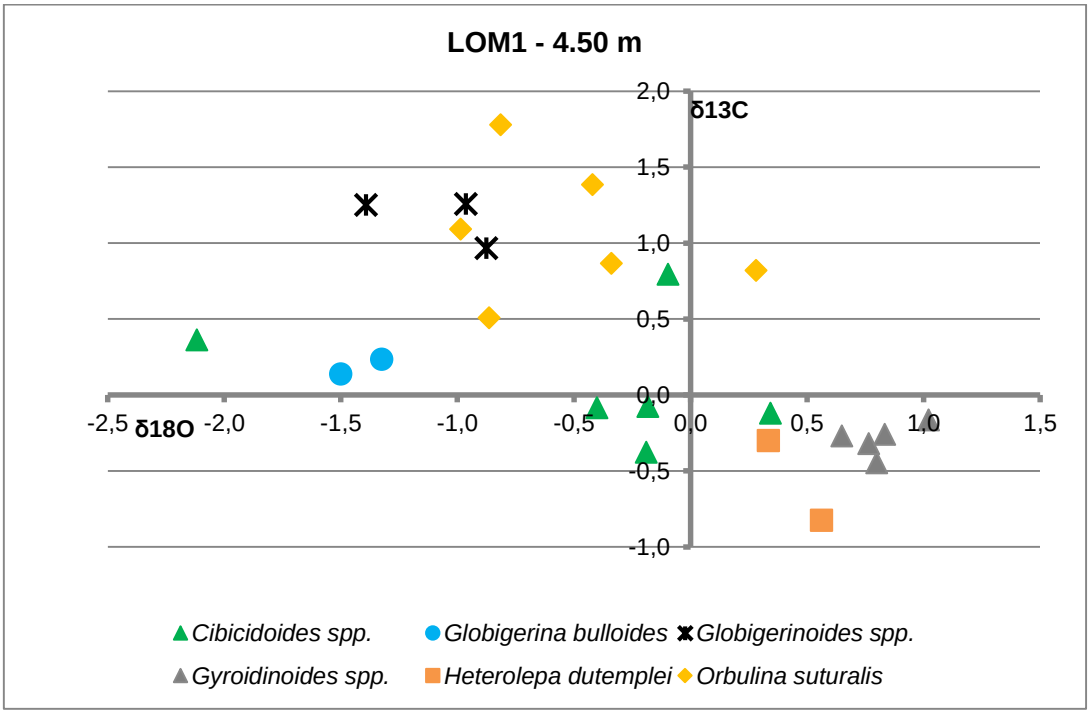

# Appendix 3

## LOM-1: 8.50 m

| Identifier 1 | Identifier 2 | Comment | 1 Cycle Int Samp 44 | δ $^{13}C/^{12}C$ Mean | δ $^{18}O/^{16}O$ Mean | δ $^{13}C$ CORR | δ $^{18}O$ CORR |
|---|---|---|---|---|---|---|---|
| *Cibicidoides* spp. | 850 | LOM-1 | 2845,913 | 0,182 | 0,46 | **0,182** | **0,460** |
| *Cibicidoides* spp. | 850 | LOM-1 | 2044,334 | 0,151 | 0,21 | **0,151** | **0,210** |
| *Cibicidoides* spp. | 850 | LOM-1 | 2834,892 | 1,018 | 0,677 | **1,018** | **0,677** |
| *Cibicidoides* spp. | 850 | LOM-1 | 3821,304 | 1,068 | 0,415 | **1,068** | **0,415** |
| Elphidium spp. | 850 | LOM-1 | 1406,452 | 0,477 | -0,474 | **0,475** | **-0,474** |
| Elphidium spp. | 850 | LOM-1 | 2678,182 | 1,166 | -1,631 | **1,166** | **-1,631** |
| *G. bulloides* | 850 | LOM-1 | 1354,261 | 0,812 | 0,066 | **0,809** | **0,066** |
| *G. bulloides* | 850 | LOM-1 | 1308,496 | 1,062 | 0,113 | **1,058** | **0,113** |
| *G. bulloides* | 850 | LOM-1 | 1191,299 | 0,515 | 0,162 | **0,509** | **0,162** |
| *Heterolepa dutemplei* | 850 | LOM-1 | 3269,875 | 0,753 | 0,564 | **0,753** | **0,564** |
| *Heterolepa dutemplei* | 850 | LOM-1 | 1946,02 | 0,706 | 0,437 | **0,706** | **0,437** |
| *Orbulina suturalis* | 850 | LOM-1 | 3771,989 | 2,461 | -0,401 | **2,461** | **-0,401** |
| *Orbulina suturalis* | 850 | LOM-1 | 3706,897 | 2,427 | -0,501 | **2,427** | **-0,501** |
| *Orbulina suturalis* | 850 | LOM-1 | 3630,624 | 1,881 | -0,412 | **1,881** | **-0,412** |
| *Orbulina suturalis* | 850 | LOM-1 | 2959,681 | 1,921 | -0,166 | **1,921** | **-0,166** |
| *Orbulina suturalis* | 850 | LOM-1 | 2261,228 | 1,43 | -0,58 | **1,430** | **-0,580** |
| *Uvigerina* spp. | 850 | LOM-1 | 4126,408 | -0,12 | 0,838 | **-0,120** | **0,838** |
| *Uvigerina* spp. | 850 | LOM-1 | 3235,326 | -0,362 | 0,901 | **-0,362** | **0,901** |
| *Uvigerina* spp. | 850 | LOM-1 | 5207,967 | -0,169 | 0,63 | **-0,169** | **0,630** |
| *Uvigerina* spp. | 850 | LOM-1 | 7237,266 | 0,166 | 0,992 | **0,166** | **0,992** |
| *Uvigerina* spp. | 850 | LOM-1 | 4312,224 | -0,059 | 0,917 | **-0,059** | **0,917** |
| *G. bulloides* | 850 | LOM-1 | 1178,18 | 0,742 | -0,315 | **0,736** | **-0,315** |
| *G. bulloides* | 850 | LOM-1 | 1121,167 | 0,251 | -0,835 | **0,243** | **-0,835** |

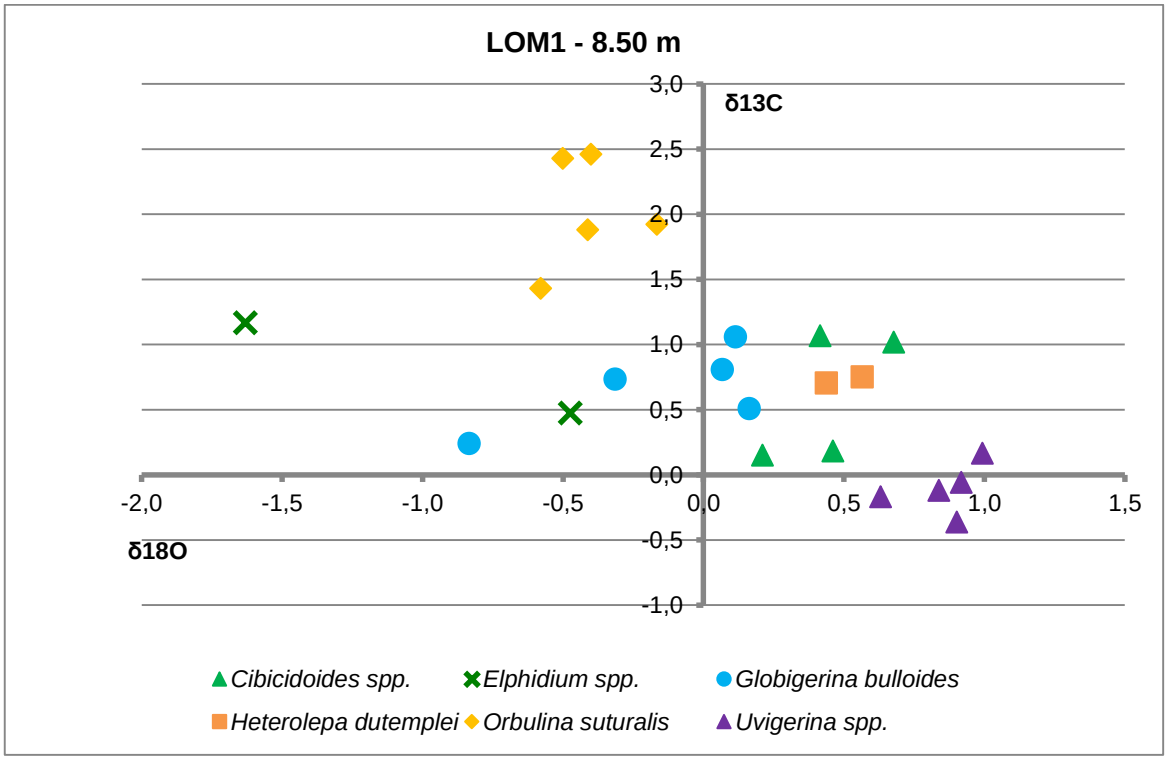

# Appendix 3

## LOM-1: 9.00 m

| Identifier 1 | Identifier 2 | Comment | 1 Cycle Int Samp 44 | δ $^{13}C/^{12}C$ Mean | δ $^{18}O/^{16}O$ Mean | δ $^{13}C$ CORR | δ $^{18}O$ CORR |
|---|---|---|---|---|---|---|---|
| *Cibicidoides* spp. | 900 | LOM-1 | 3167,988 | 0,044 | 0,094 | **0,044** | **0,094** |
| *G. bulloides* | 900 | LOM-1 | 854,142 | 0,656 | -0,866 | **0,627** | **-0,881** |
| *Globigerinoides* spp. | 900 | LOM-1 | 1033,109 | 0,851 | -1,198 | **0,838** | **-1,199** |
| *Globigerinoides* spp. | 900 | LOM-1 | 553,76 | 1,431 | -1,777 | **1,318** | **-2,135** |
| *Globigerinoides* spp. | 900 | LOM-1 | 2356,712 | 1,968 | -1,018 | **1,968** | **-1,018** |
| *Gyroidinoides* spp. | 900 | LOM-1 | 2291,048 | 0,071 | 0,883 | **0,071** | **0,883** |
| *Gyroidinoides* spp. | 900 | LOM-1 | 1561,936 | 0,393 | 0,943 | **0,392** | **0,943** |
| *Gyroidinoides* spp. | 900 | LOM-1 | 2341,523 | -0,593 | 0,482 | **-0,593** | **0,482** |
| *Gyroidinoides* spp. | 900 | LOM-1 | 1070,697 | 0,427 | 0,974 | **0,416** | **0,973** |
| *Heterolepa dutemplei* | 900 | LOM-1 | 1779,7 | 0,416 | 0,266 | **0,416** | **0,266** |
| *Heterolepa dutemplei* | 900 | LOM-1 | 2035,764 | -0,279 | 0,03 | **-0,279** | **0,030** |
| *Melonis pompilioides* | 900 | LOM-1 | 813,621 | 0,338 | 0,698 | **0,304** | **0,672** |
| *Melonis pompilioides* | 900 | LOM-1 | 1064,151 | -0,375 | -0,196 | **-0,386** | **-0,197** |
| *Melonis pompilioides* | 900 | LOM-1 | 1099,413 | -0,221 | 0,043 | **-0,230** | **0,043** |
| *Melonis pompilioides* | 900 | LOM-1 | 846,155 | -0,134 | -0,197 | **-0,164** | **-0,213** |
| *Orbulina suturalis* | 900 | LOM-1 | 3719,68 | 1,915 | -0,289 | **1,915** | **-0,289** |
| *Orbulina suturalis* | 900 | LOM-1 | 3994,413 | 1,674 | -1,112 | **1,674** | **-1,112** |
| *Orbulina suturalis* | 900 | LOM-1 | 1206,656 | 2,716 | -0,666 | **2,710** | **-0,666** |
| *Praeorbulina glomerosa* | 900 | LOM-1 | 1606,344 | 2,284 | -0,575 | **2,283** | **-0,575** |
| *Heterolepa dutemplei* | 900 | LOM-1 | 823,619 | 0,806 | 0,569 | **0,773** | **0,547** |

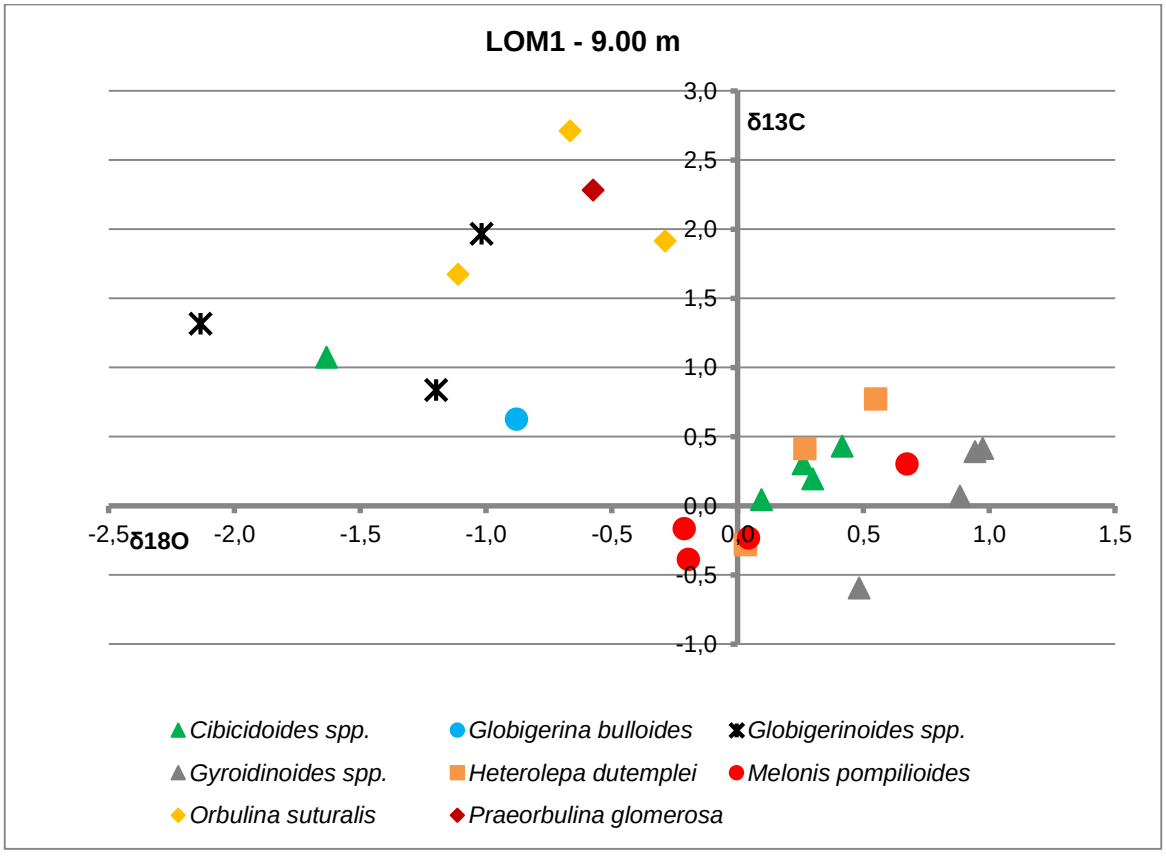

# Appendix 3

## LOM-1: 10.00 m

| Identifier 1 | Identifier 2 | Comment | 1 Cycle Int Samp 44 | δ $^{13}C/^{12}C$ Mean | δ $^{18}O/^{16}O$ Mean | δ $^{13}C$ CORR | δ $^{18}O$ CORR |
|---|---|---|---|---|---|---|---|
| *Cibicidoides* spp. | 1000 | LOM-1 | 646,774 | 0,311 | 0,296 | 0,237 | 0,108 |
| *G. bulloides* | 1000 | LOM-1 | 505,446 | -0,056 | -1,504 | -0,197 | -1,929 |
| *G. bulloides* | 1000 | LOM-1 | 470,16 | 0,21 | -0,465 | 0,044 | -0,924 |
| *Globigerinoides* spp. | 1000 | LOM-1 | 1506,852 | 1,246 | -1,358 | 1,245 | -1,358 |
| *Globigerinoides* spp. | 1000 | LOM-1 | 909,421 | 1,473 | -1,727 | 1,451 | -1,734 |
| *Globigerinoides* spp. | 1000 | LOM-1 | 486,386 | -0,029 | -3,552 | -0,183 | -3,997 |
| *Globigerinoides* spp. | 1000 | LOM-1 | 2807,301 | 1,944 | -1,533 | 1,944 | -1,533 |
| *Gyroidinoides* spp. | 1000 | LOM-1 | 898,897 | -0,283 | 0,323 | -0,306 | 0,315 |
| *Gyroidinoides* spp. | 1000 | LOM-1 | 2548,15 | 0,213 | 0,249 | 0,213 | 0,249 |
| *Orbulina suturalis* | 1000 | LOM-1 | 1371,139 | 0,688 | -1,792 | 0,685 | -1,792 |
| *Orbulina suturalis* | 1000 | LOM-1 | 438,291 | -0,268 | -2,705 | -0,460 | -3,184 |
| *Orbulina suturalis* | 1000 | LOM-1 | 2465,447 | 2,032 | -1,861 | 2,032 | -1,861 |
| *Praeorbulina glomerosa* | 1000 | LOM-1 | 1069,369 | 0,613 | -1,388 | 0,602 | -1,389 |
| *Praeorbulina glomerosa* | 1000 | LOM-1 | 605,888 | 0,362 | -0,567 | 0,273 | -0,831 |
| *Praeorbulina glomerosa* | 1000 | LOM-1 | 2087,693 | 1,351 | -1,316 | 1,351 | -1,316 |
| *Praeorbulina glomerosa* | 1000 | LOM-1 | 1665,411 | 0,69 | -1,404 | 0,689 | -1,404 |
| *Praeorbulina glomerosa* | 1000 | LOM-1 | 1321,308 | 1,066 | -0,667 | 1,063 | -0,667 |

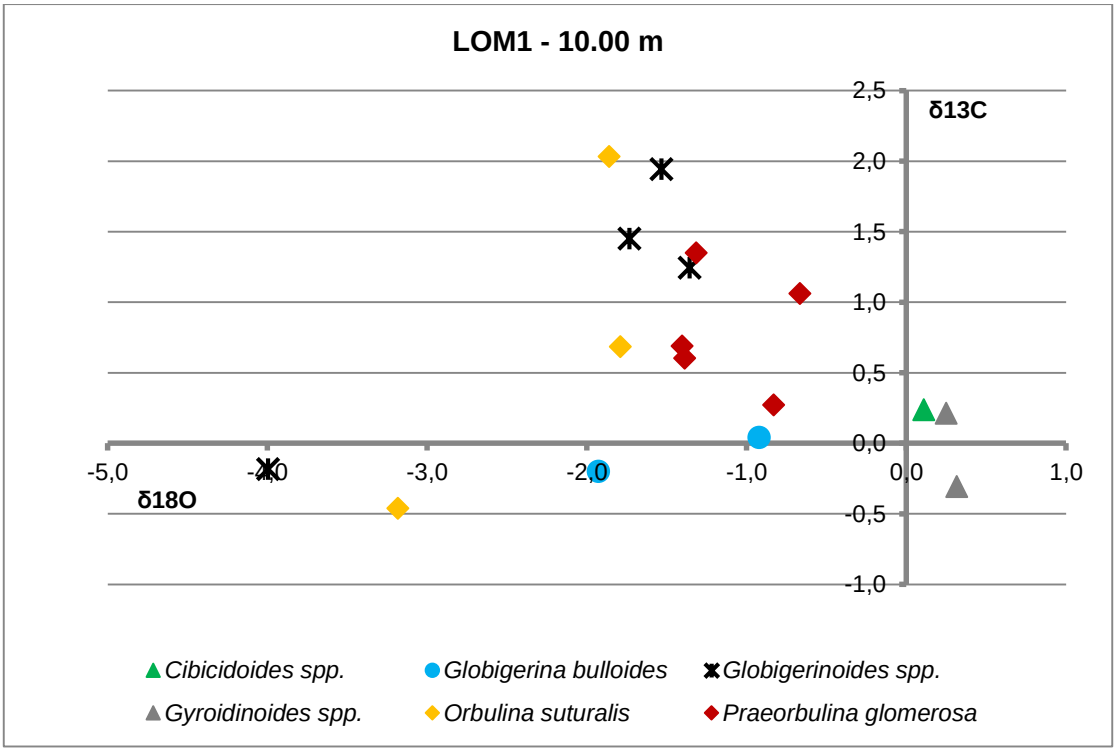

# Appendix 3

## LOM-1: 11.00 m

| Identifier 1 | Identifier 2 | Comment | 1 Cycle Int Samp 44 | δ $^{13}C/^{12}C$ Mean | δ $^{18}O/^{16}O$ Mean | δ $^{13}C$ CORR | δ $^{18}O$ CORR |
|---|---|---|---|---|---|---|---|
| *G. bulloides* | 1100 | LOM-1 | 1191,171 | 1,001 | -1,399 | **0,995** | **-1,399** |
| *Globigerinoides* spp. | 1100 | LOM-1 | 926,379 | 2,34 | -0,071 | **2,320** | **-0,076** |
| *Globigerinoides* spp. | 1100 | LOM-1 | 1568,35 | 2,085 | -0,915 | **2,084** | **-0,915** |
| *Globigerinoides* spp. | 1100 | LOM-1 | 1828,577 | 2,375 | -1,098 | **2,375** | **-1,098** |
| *Globigerinoides* spp. | 1100 | LOM-1 | 1951,684 | 1,809 | -0,809 | **1,809** | **-0,809** |
| *Globigerinoides* spp. | 1100 | LOM-1 | 1694,264 | 1,914 | -0,998 | **1,913** | **-0,998** |
| *Gyroidinoides* spp. | 1100 | LOM-1 | 735,585 | -0,431 | 0,359 | **-0,480** | **0,289** |
| *Gyroidinoides* spp. | 1100 | LOM-1 | 1952,53 | -0,036 | 1,046 | **-0,036** | **1,046** |
| *Gyroidinoides* spp. | 1100 | LOM-1 | 868,488 | 0,005 | 0,885 | **-0,022** | **0,873** |
| *Heterolepa dutemplei* | 1100 | LOM-1 | 1462,305 | -1,37 | -1,451 | **-1,372** | **-1,451** |
| *Heterolepa dutemplei* | 1100 | LOM-1 | 536,887 | 1,342 | -1,617 | **1,220** | **-2,001** |
| *Melonis pompilioides* | 1100 | LOM-1 | 721,387 | 0,033 | 0,611 | **-0,020** | **0,527** |
| *Melonis pompilioides* | 1100 | LOM-1 | 914,885 | 0,093 | 0,961 | **0,071** | **0,955** |
| *Melonis pompilioides* | 1100 | LOM-1 | 1488,016 | -0,161 | 0,862 | **-0,163** | **0,862** |
| *Melonis pompilioides* | 1100 | LOM-1 | 1140,269 | 0,149 | 0,764 | **0,141** | **0,764** |
| *Melonis pompilioides* | 1100 | LOM-1 | 887,092 | 0,039 | 0,828 | **0,014** | **0,819** |
| *Melonis pompilioides* | 1100 | LOM-1 | 1179,808 | -0,384 | 0,52 | **-0,390** | **0,520** |
| *Melonis pompilioides* | 1100 | LOM-1 | 1459,484 | -0,322 | 0,304 | **-0,324** | **0,304** |
| *Orbulina suturalis* | 1100 | LOM-1 | 2214,385 | 1,587 | -0,467 | **1,587** | **-0,467** |
| *Orbulina suturalis* | 1100 | LOM-1 | 2149,805 | 2,154 | -0,728 | **2,154** | **-0,728** |
| Paragloborotalia spp. | 1100 | LOM-1 | 1468,479 | 0,33 | 1,36 | **0,328** | **1,360** |
| Paragloborotalia spp. | 1100 | LOM-1 | 404,459 | 0,406 | 0,093 | **0,182** | **-0,400** |

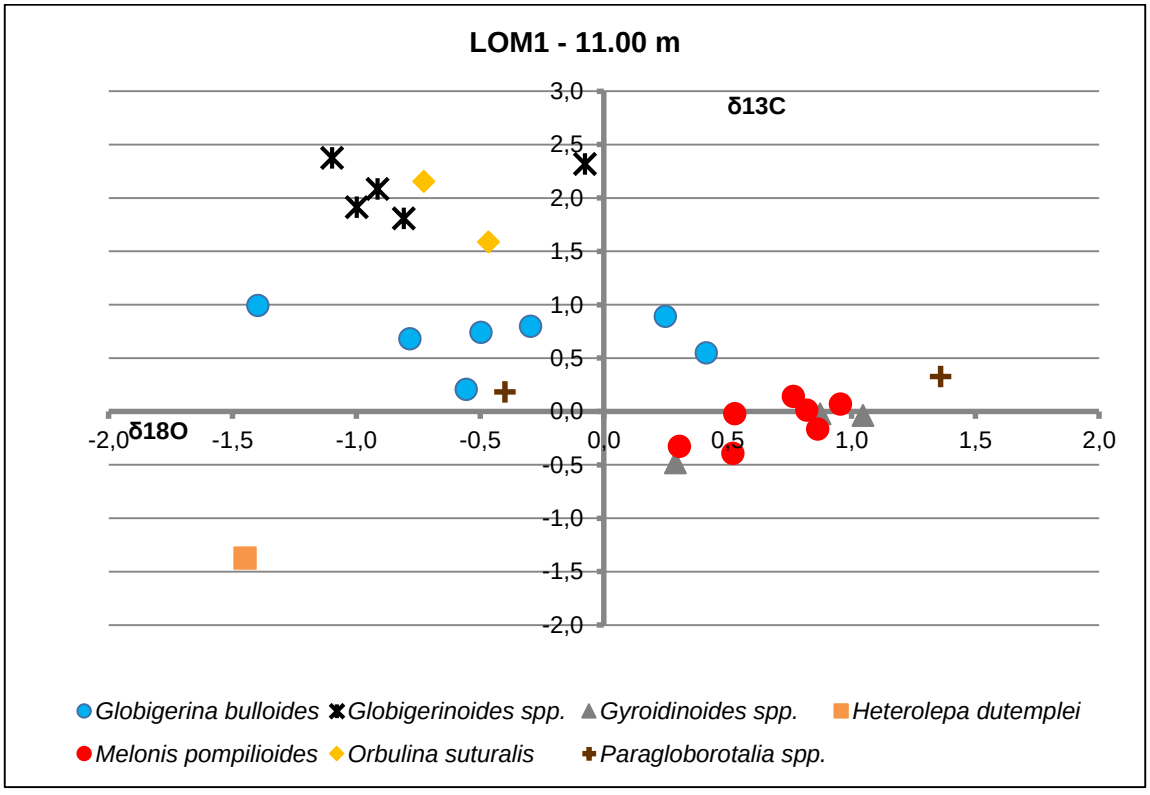

# Appendix 3

## LOM-1: 11.30 m

| Identifier 1 | Identifier 2 | Comment | 1 Cycle Int Samp 44 | δ $^{13}C/^{12}C$ Mean | δ $^{18}O/^{16}O$ Mean | δ $^{13}C$ CORR | δ $^{18}O$ CORR |
|---|---|---|---|---|---|---|---|
| *Cibicidoides* spp. | 1130 | LOM-1 | 1071,953 | -0,236 | 0,284 | **-0,247** | **0,283** |
| *Cibicidoides* spp. | 1130 | LOM-1 | 817,374 | 0,577 | 0,244 | **0,543** | **0,220** |
| *G. bulloides* | 1130 | LOM-1 | 514,442 | 0,317 | -0,371 | **0,181** | **-0,786** |
| *G. bulloides* | 1130 | LOM-1 | 853,707 | 0,946 | -1,1 | **0,917** | **-1,115** |
| *G. bulloides* | 1130 | LOM-1 | 1100,774 | 0,651 | -3,948 | **0,642** | **-3,948** |
| *G. bulloides* | 1130 | LOM-1 | 898,501 | 0,854 | -1,423 | **0,831** | **-1,431** |
| *Globigerinoides* spp. | 1130 | LOM-1 | 765,341 | 1,405 | -0,988 | **1,362** | **-1,036** |
| *Globigerinoides* spp. | 1130 | LOM-1 | 1538,146 | 1,255 | -1,811 | **1,254** | **-1,811** |
| *Gyroidinoides* spp. | 1130 | LOM-1 | 643,724 | 0,243 | 1,506 | **0,168** | **1,313** |
| *Orbulina suturalis* | 1130 | LOM-1 | 1310,599 | 1,394 | -0,818 | **1,390** | **-0,818** |
| *Praeorbulina glomerosa* | 1130 | LOM-1 | 2272,647 | -0,017 | -1,537 | **-0,017** | **-1,537** |
| *Praeorbulina glomerosa* | 1130 | LOM-1 | 1614,757 | 0,463 | -0,721 | **0,462** | **-0,721** |
| *Gyroidinoides* spp. | 1130 | LOM-1 | 477,58 | -0,701 | 0,902 | **-0,862** | **0,449** |

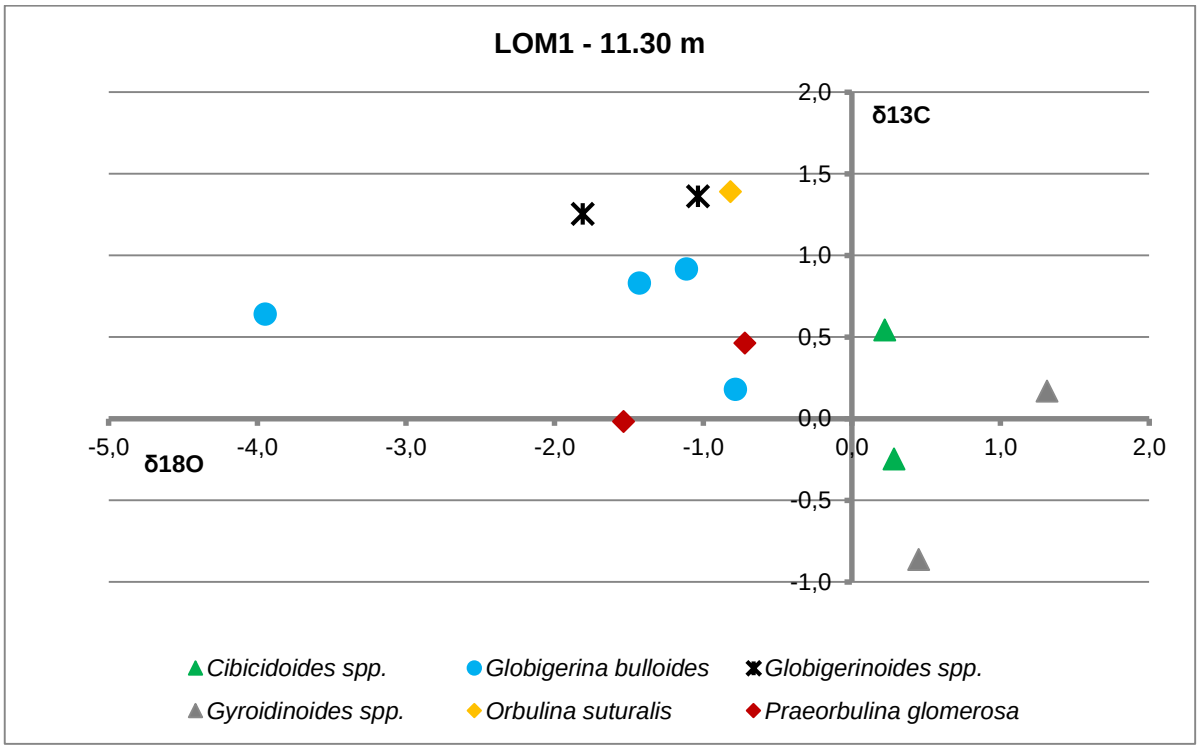

# Appendix 3

## LOM-1: 11.70 m

| Identifier 1 | Identifier 2 | Comment | 1 Cycle Int Samp 44 | δ $^{13}C/^{12}C$ Mean | δ $^{18}O/^{16}O$ Mean | δ $^{13}C$ CORR | δ $^{18}O$ CORR |
|---|---|---|---|---|---|---|---|
| *Cibicidoides* spp. | 1170 | LOM-1 | 1129,016 | 0,786 | 0,242 | **0,778** | **0,242** |
| *Cibicidoides* spp. | 1170 | LOM-1 | 642,066 | 1,486 | 1,612 | **1,410** | **1,416** |
| *Cibicidoides* spp. | 1170 | LOM-1 | 1402,318 | -0,051 | 0,06 | **-0,053** | **0,060** |
| *Cibicidoides* spp. | 1170 | LOM-1 | 987,06 | 0,338 | 1,123 | **0,322** | **1,121** |
| *Cibicidoides* spp. | 1170 | LOM-1 | 910,642 | 1,384 | 0,948 | **1,362** | **0,941** |
| *G. bulloides* | 1170 | LOM-1 | 711,018 | 0,483 | -0,248 | **0,428** | **-0,343** |
| *G. bulloides* | 1170 | LOM-1 | 490,613 | 0,162 | 0,529 | **0,011** | **0,088** |
| *G. bulloides* | 1170 | LOM-1 | 608,419 | 0,192 | -0,287 | **0,104** | **-0,546** |
| *Globigerinoides* spp. | 1170 | LOM-1 | 1832,091 | 0,22 | 1,101 | **0,220** | **1,101** |
| *Globigerinoides* spp. | 1170 | LOM-1 | 2574,941 | 1,981 | -1,525 | **1,981** | **-1,525** |
| *Gyroidinoides* spp. | 1170 | LOM-1 | 1201,703 | -0,66 | 1,016 | **-0,666** | **1,016** |
| *Gyroidinoides* spp. | 1170 | LOM-1 | 934,968 | -0,086 | 1,247 | **-0,106** | **1,242** |
| *Gyroidinoides* spp. | 1170 | LOM-1 | 789,828 | -0,775 | 0,865 | **-0,813** | **0,830** |
| *Heterolepa dutemplei* | 1170 | LOM-1 | 735,396 | 0,801 | 1,174 | **0,752** | **1,103** |
| *Heterolepa dutemplei* | 1170 | LOM-1 | 606,851 | 0,67 | 0,821 | **0,581** | **0,559** |
| Meloni s pompilioides | 1170 | LOM-1 | 980,036 | -0,071 | 0,592 | **-0,087** | **0,589** |
| *Melonis pompilioides* | 1170 | LOM-1 | 1987,211 | 0,005 | 0,91 | **0,005** | **0,910** |
| *Melonis pompilioides* | 1170 | LOM-1 | 1753,762 | -0,285 | 0,707 | **-0,285** | **0,707** |
| *Melonis pompilioides* | 1170 | LOM-1 | 1252,694 | -0,08 | 0,708 | **-0,085** | **0,708** |
| *Melonis pompilioides* | 1170 | LOM-1 | 1420,341 | -0,101 | 0,763 | **-0,103** | **0,763** |
| *Orbulina suturalis* | 1170 | LOM-1 | 555,798 | 0,701 | -0,523 | **0,589** | **-0,878** |
| *Orbulina suturalis* | 1170 | LOM-1 | 998,383 | 2,002 | 0,019 | **1,987** | **0,017** |
| *Uvigerina* spp. | 1170 | LOM-1 | 1123,56 | 0,077 | 1,611 | **0,069** | **1,611** |
| *Uvigerina* spp. | 1170 | LOM-1 | 1308,851 | -0,128 | 1,712 | **-0,132** | **1,712** |
| *Uvigerina* spp. | 1170 | LOM-1 | 2188,729 | 0,408 | 1,327 | **0,408** | **1,327** |

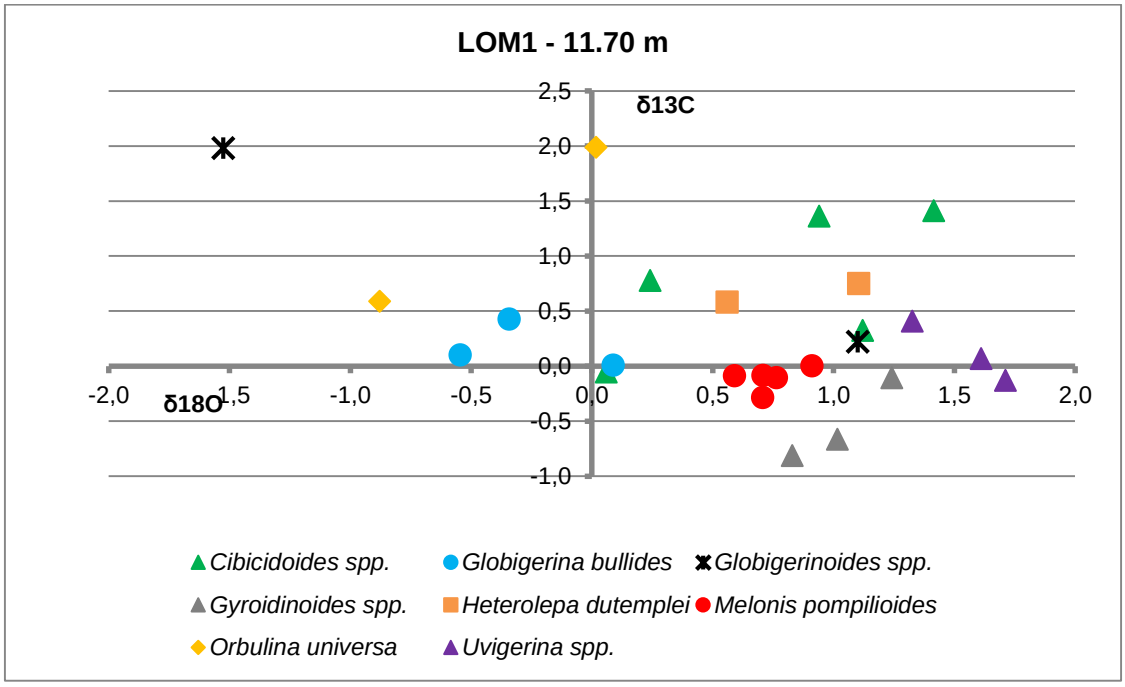

# Appendix 3

## LOM-1: 12.60 m

| Identifier 1 | Identifier 2 | Comment | 1 Cycle Int Samp 44 | δ $^{13}C/^{12}C$ Mean | δ $^{18}O/^{16}O$ Mean | δ $^{13}C$ CORR | δ $^{18}O$ CORR |
|---|---|---|---|---|---|---|---|
| *Cibicidoides* spp. | 126 | LOM-1 | 4354,024 | 0,294 | 0,814 | **0,294** | **0,814** |
| *Cibicidoides* spp. | 126 | LOM-1 | 2161,672 | -0,086 | 0,533 | **-0,086** | **0,533** |
| *Cibicidoides* spp. | 126 | LOM-1 | 3041,473 | 0,225 | 0,834 | **0,225** | **0,834** |
| *Cibicidoides* spp. | 126 | LOM-1 | 3388,918 | 0,379 | 0,806 | **0,379** | **0,806** |
| *G. bulloides* | 126 | LOM-1 | 1251,706 | 0,412 | 0,031 | **0,407** | **0,031** |
| *G. bulloides* | 126 | LOM-1 | 1582,836 | 0,491 | 0,437 | **0,490** | **0,437** |
| *G. bulloides* | 126 | LOM-1 | 1418,787 | 0,178 | -1,051 | **0,176** | **-1,051** |
| *G. bulloides* | 126 | LOM-1 | 1468,326 | 0,333 | -0,464 | **0,331** | **-0,464** |
| *G. bulloides* | 126 | LOM-1 | 1771,119 | 0,143 | -0,301 | **0,143** | **-0,301** |
| *Heterolepa dutemplei* | 126 | LOM-1 | 5516,266 | 0,755 | 0,87 | **0,755** | **0,870** |
| *Heterolepa dutemplei* | 126 | LOM-1 | 2148,745 | 0,51 | 1,022 | **0,510** | **1,022** |
| *Heterolepa dutemplei* | 126 | LOM-1 (Velka) | 4663,236 | 0,556 | 0,86 | **0,556** | **0,860** |
| *Orbulina suturalis* | 126 | LOM-1 | 4904,413 | 2,258 | -0,203 | **2,258** | **-0,203** |
| *Orbulina suturalis* | 126 | LOM-1 | 3065,798 | 1,776 | 0,517 | **1,776** | **0,517** |
| *Praeorbulina glomerosa* | 126 | LOM-1 | 4459,167 | 1,838 | -0,053 | **1,838** | **-0,053** |
| *Praeorbulina glomerosa* | 126 | LOM-1 | 3406,642 | 1,439 | -0,729 | **1,439** | **-0,729** |
| *Uvigerina* spp. | 126 | LOM-1 | 3644,378 | -0,095 | 1,098 | **-0,095** | **1,098** |
| *Uvigerina* spp. | 126 | LOM-1 | 3580,152 | -0,16 | 1,317 | **-0,160** | **1,317** |
| *Uvigerina* spp. | 126 | LOM-1 | 2531,849 | -0,222 | 1,059 | **-0,222** | **1,059** |
| *Uvigerina* spp. | 126 | LOM-1 | 2260,637 | -0,122 | 1,379 | **-0,122** | **1,379** |

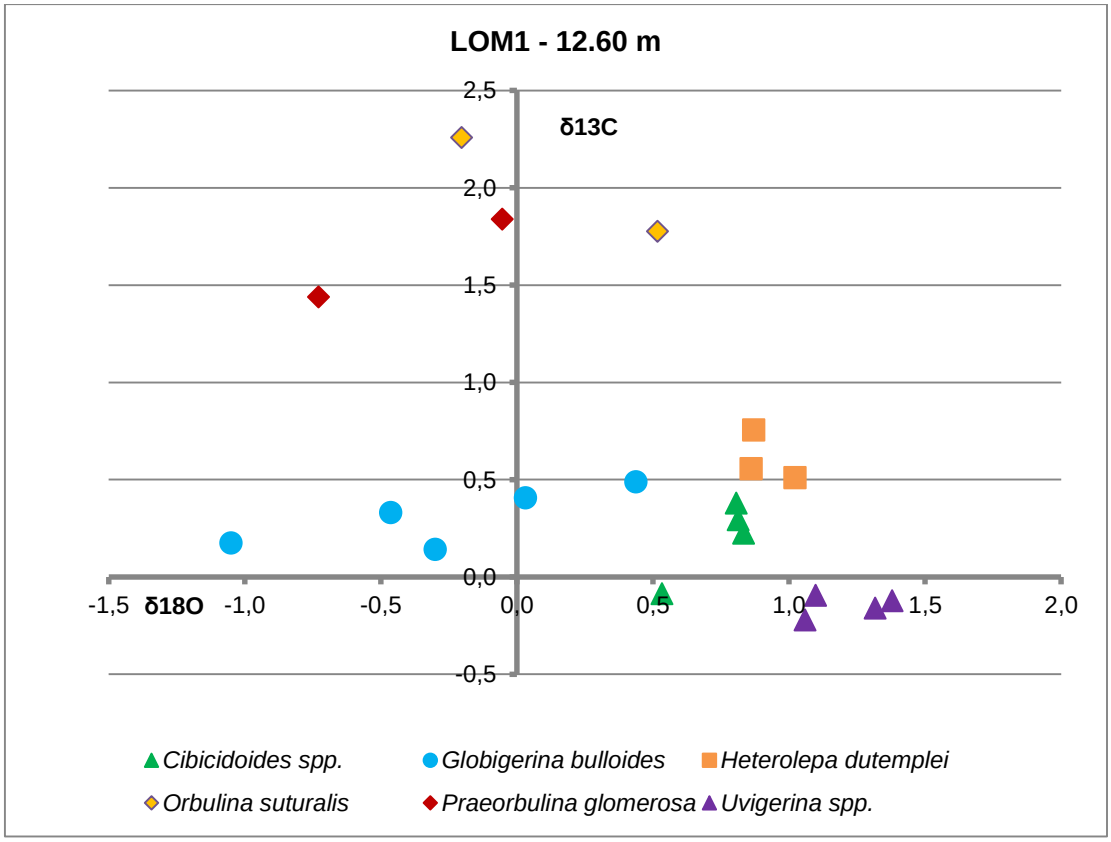

# Appendix 3

## LOM-1: 14.25 m

| Identifier 1 | Identifier 2 | Comment | 1 Cycle Int Samp 44 | δ $^{13}C/^{12}C$ Mean | δ $^{18}O/^{16}O$ Mean | δ $^{13}C$ CORR | δ $^{18}O$ CORR |
|---|---|---|---|---|---|---|---|
| *Cibicidoides* spp. | 1425 | LOM-1 | 868,726 | 0,448 | 1,054 | **0,421** | **1,042** |
| *Cibicidoides* spp. | 1425 | LOM-1 | 436,378 | -0,011 | 0,954 | **-0,205** | **0,474** |
| *G. bulloides* | 1425 | LOM-1 | 879,032 | 0,497 | -1,222 | **0,472** | **-1,232** |
| *G. bulloides* | 1425 | LOM-1 | 907,769 | 0,63 | -0,597 | **0,608** | **-0,604** |
| *G. bulloides* | 1425 | LOM-1 | 325,441 | 1,118 | 0,441 | **0,874** | **-0,068** |
| *G. bulloides* | 1425 | LOM-1 | 808,053 | 1,082 | -0,381 | **1,047** | **-0,408** |
| *G. bulloides* | 1425 | LOM-1 | 921,449 | 0,366 | 0,115 | **0,345** | **0,109** |
| *G. bulloides* | 1425 | LOM-1 | 725,113 | 0,653 | 0,389 | **0,601** | **0,309** |
| *Gyroidinoides* spp. | 1425 | LOM-1 | 725,317 | -0,577 | 0,848 | **-0,629** | **0,768** |
| *Gyroidinoides* spp. | 1425 | LOM-1 | 713,615 | -0,322 | 1,464 | **-0,376** | **1,372** |
| *Heterolepa dutemplei* | 1425 | LOM-1 | 876,55 | 0,925 | 1,041 | **0,899** | **1,030** |
| *Heterolepa dutemplei* | 1425 | LOM-1 | 941,845 | 0,454 | 0,767 | **0,435** | **0,763** |
| *Heterolepa dutemplei* | 1425 | LOM-1 | 1081,914 | 0,299 | 0,816 | **0,289** | **0,815** |
| *Heterolepa dutemplei* | 1425 | LOM-1 | 965,495 | 0,786 | 0,948 | **0,769** | **0,945** |
| *Heterolepa dutemplei* | 1425 | LOM-1 | 871,731 | 0,687 | 0,45 | **0,661** | **0,438** |
| *Melonis pompilioides* | 1425 | LOM-1 | 406,055 | 0,135 | 1,276 | **-0,087** | **0,783** |
| *Melonis pompilioides* | 1425 | LOM-1 | 364,069 | 0,39 | 1,39 | **0,146** | **0,886** |
| *Melonis pompilioides* | 1425 | LOM-1 | 300,366 | 0,813 | 1,904 | **0,569** | **1,393** |
| *Melonis pompilioides* | 1425 | LOM-1 | 818,485 | -0,008 | 0,672 | **-0,042** | **0,648** |
| *Praeorbulina glomerosa* | 1425 | LOM-1 | 1384,293 | 1,248 | 0,632 | **1,245** | **0,632** |
| *G. bulloides* | 1425 | LOM-1 | 461,238 | 0,376 | 0,355 | **0,203** | **-0,110** |
| *G. bulloides* | 1425 | LOM-1 | 412,13 | 0,099 | -0,439 | **-0,118** | **-0,930** |

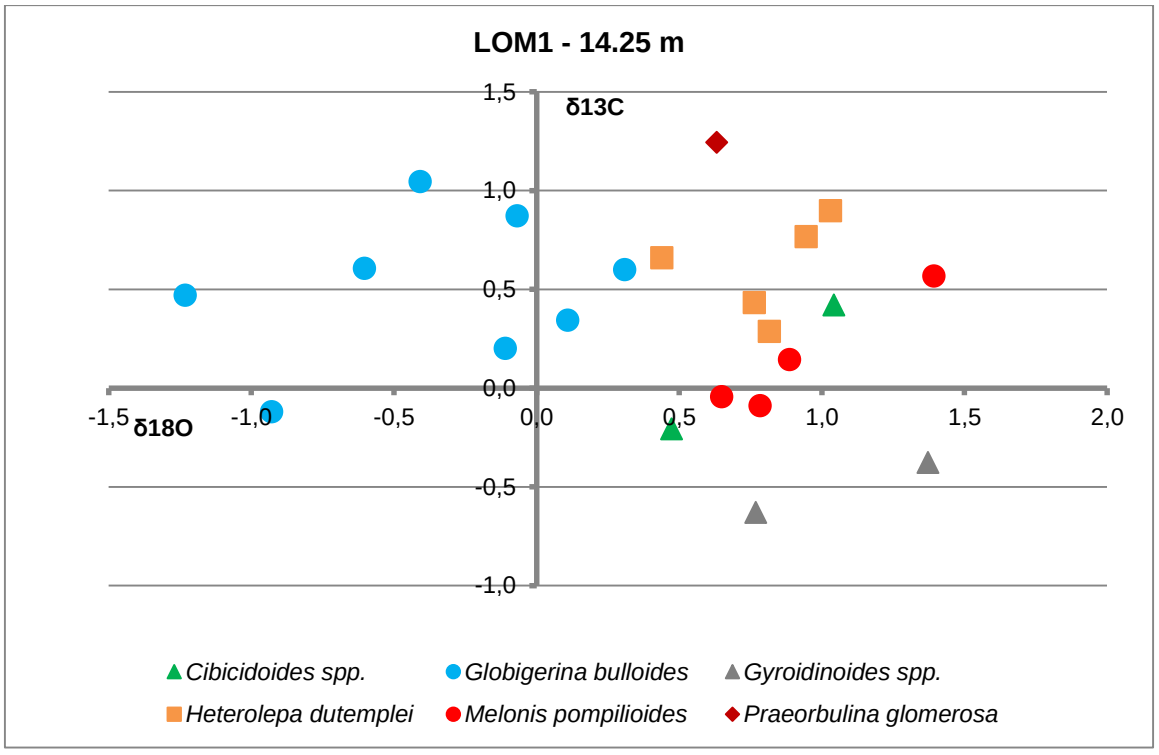

# Appendix 3

## LOM-1: 14.50 m

| Identifier 1 | Identifier 2 | Comment | 1 Cycle Int Samp 44 | δ $^{13}C/^{12}C$ Mean | δ $^{18}O/^{16}O$ Mean | δ $^{13}C$ CORR | δ $^{18}O$ CORR |
|---|---|---|---|---|---|---|---|
| *G. bulloides* | 1450 | LOM-1 | 428,45 | -0,391 | -0,535 | **-0,592** | **-1,019** |
| *Cibicidoides* spp. | 1450 | LOM-1 | 983,324 | 0,381 | 1,08 | **0,365** | **1,078** |
| *G. bulloides* | 1450 | LOM-1 | 445,788 | 0,617 | 0,795 | **0,431** | **0,320** |
| *G. bulloides* | 1450 | LOM-1 | 560,698 | 0,037 | -0,428 | **-0,073** | **-0,775** |
| *G. bulloides* | 1450 | LOM-1 | 754,227 | 0,411 | -1,099 | **0,366** | **-1,155** |
| *G. bulloides* | 1450 | LOM-1 | 867,644 | 0,126 | -1,458 | **0,099** | **-1,470** |
| *G. bulloides* | 1450 | LOM-1 | 1068,295 | 0,204 | -0,157 | **0,193** | **-0,158** |
| *G. bulloides* | 1450 | LOM-1 | 671,275 | 1,309 | 1,175 | **1,243** | **1,027** |
| *Gyroidinoides* spp. | 1450 | LOM-1 | 616,672 | 0,243 | 1,881 | **0,158** | **1,638** |
| *Gyroidinoides* spp. | 1450 | LOM-1 | 979,671 | 0,323 | 1,711 | **0,307** | **1,708** |
| *Gyroidinoides* spp. | 1450 | LOM-1 | 1549,387 | 0,209 | 1,077 | **0,208** | **1,077** |
| *Gyroidinoides* spp. | 1450 | LOM-1 | 1367,81 | 0,074 | 1,132 | **0,071** | **1,132** |
| *Gyroidinoides* spp. | 1450 | LOM-1 | 2340,734 | 0,621 | 0,847 | **0,621** | **0,847** |
| *Melonis pompilioides* | 1450 | LOM-1 | 400,995 | 0,268 | 1,112 | **0,041** | **0,618** |
| *Melonis pompilioides* | 1450 | LOM-1 | 361,473 | 0,338 | 1,134 | **0,094** | **0,630** |
| *Melonis pompilioides* | 1450 | LOM-1 | 699,71 | -0,02 | 0,993 | **-0,078** | **0,885** |
| *Uvigerina* spp. | 1450 | LOM-1 | 882,867 | -0,144 | 0,642 | **-0,169** | **0,632** |
| *Uvigerina* spp. | 1450 | LOM-1 | 1576,414 | 0,009 | 1,319 | **0,008** | **1,319** |
| *Uvigerina* spp. | 1450 | LOM-1 | 2068,234 | -0,175 | 0,927 | **-0,175** | **0,927** |

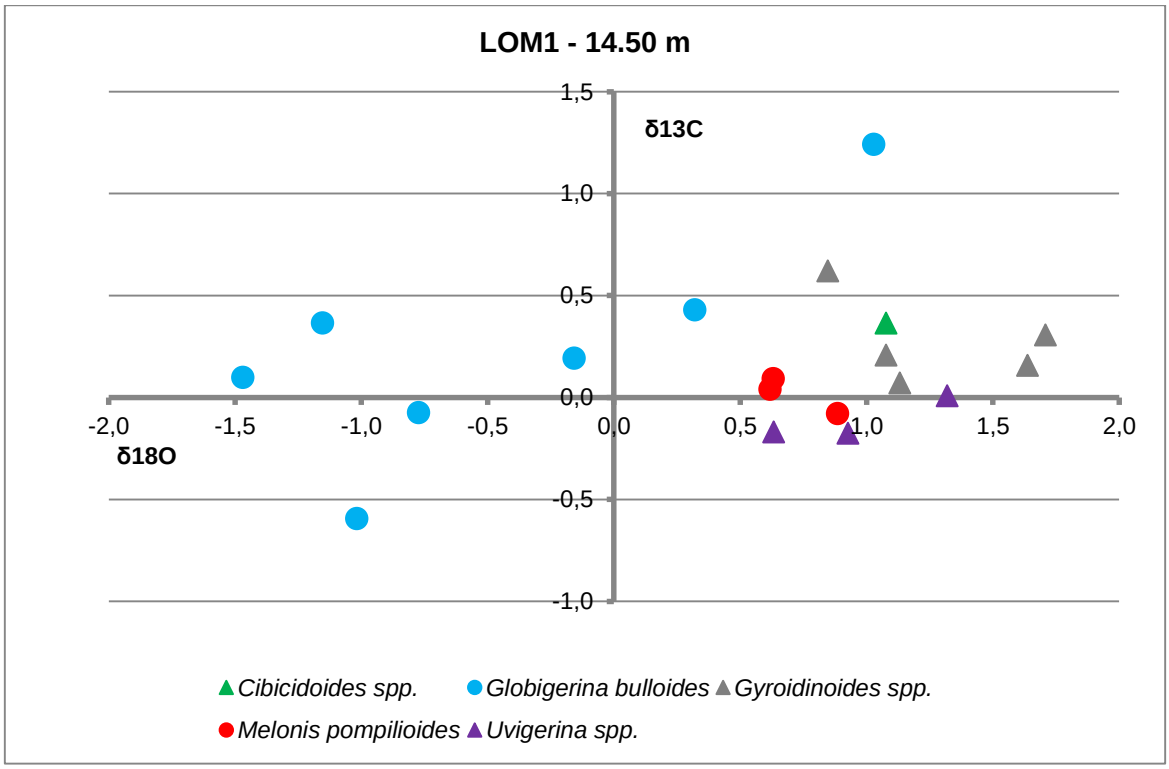

# Appendix 3

## LOM-1: 16.50 m

| Identifier 1 | Identifier 2 | Comment | 1 Cycle Int Samp 44 | δ $^{13}C/^{12}C$ Mean | δ $^{18}O/^{16}O$ Mean | δ $^{13}C$ CORR | δ $^{18}O$ CORR |
|---|---|---|---|---|---|---|---|
| *G. bulloides* | 1650 | LOM-1 | 1384,721 | -0,24 | -0,592 | **-0,243** | **-0,592** |
| *G. bulloides* | 1650 | LOM-1 | 1360,818 | -0,053 | -0,447 | **-0,056** | **-0,447** |
| *G. bulloides* | 1650 | LOM-1 | 716,132 | -0,028 | -0,334 | **-0,082** | **-0,423** |
| *G. bulloides* | 1650 | LOM-1 | 731,959 | -0,425 | -1,031 | **-0,475** | **-1,105** |
| *G. bulloides* | 1650 | LOM-1 | 875,921 | -0,175 | -0,768 | **-0,201** | **-0,779** |
| *Globigerinoides* spp | 1650 | LOM-1 | 826,106 | 1,709 | -0,601 | **1,677** | **-0,623** |
| *Globigerinoides* spp | 1650 | LOM-1 | 1470,248 | 1,361 | -0,964 | **1,359** | **-0,964** |
| *Globigerinoides* spp | 1650 | LOM-1 | 571,003 | 1,4 | -1,247 | **1,295** | **-1,576** |
| *Globigerinoides* spp | 1650 | LOM-1 | 993,862 | 1,827 | -1,169 | **1,812** | **-1,171** |
| *Gyroidinoides* spp. | 1650 | LOM-1 | 2283,004 | -0,87 | 0,19 | **-0,870** | **0,190** |
| *Gyroidinoides* spp. | 1650 | LOM-1 | 843,278 | -0,15 | 1,346 | **-0,180** | **1,329** |
| *Gyroidinoides* spp. | 1650 | LOM-1 | 793,272 | -0,617 | 0,623 | **-0,655** | **0,590** |
| *Gyroidinoides* spp. | 1650 | LOM-1 | 1015,433 | 0,048 | 1,1 | **0,034** | **1,098** |
| *Gyroidinoides* spp. | 1650 | LOM-1 | 1533,86 | -0,35 | 0,785 | **-0,351** | **0,785** |
| *Gyroidinoides* spp. | 1650 | LOM-1 | 914,432 | -0,537 | 1,05 | **-0,559** | **1,044** |
| *Heterolepa dutemplei* | 1650 | LOM-1 | 3960,007 | 0,265 | 0,736 | **0,265** | **0,736** |
| *Melonis pompilioides* | 1650 | LOM-1 | 640,673 | -0,725 | 0,038 | **-0,801** | **-0,161** |
| *Melonis pompilioides* | 1650 | LOM-1 | 623,48 | 0,072 | 0,951 | **-0,010** | **0,721** |
| *Melonis pompilioides* | 1650 | LOM-1 | 1024,236 | -0,766 | 0,006 | **-0,779** | **0,005** |

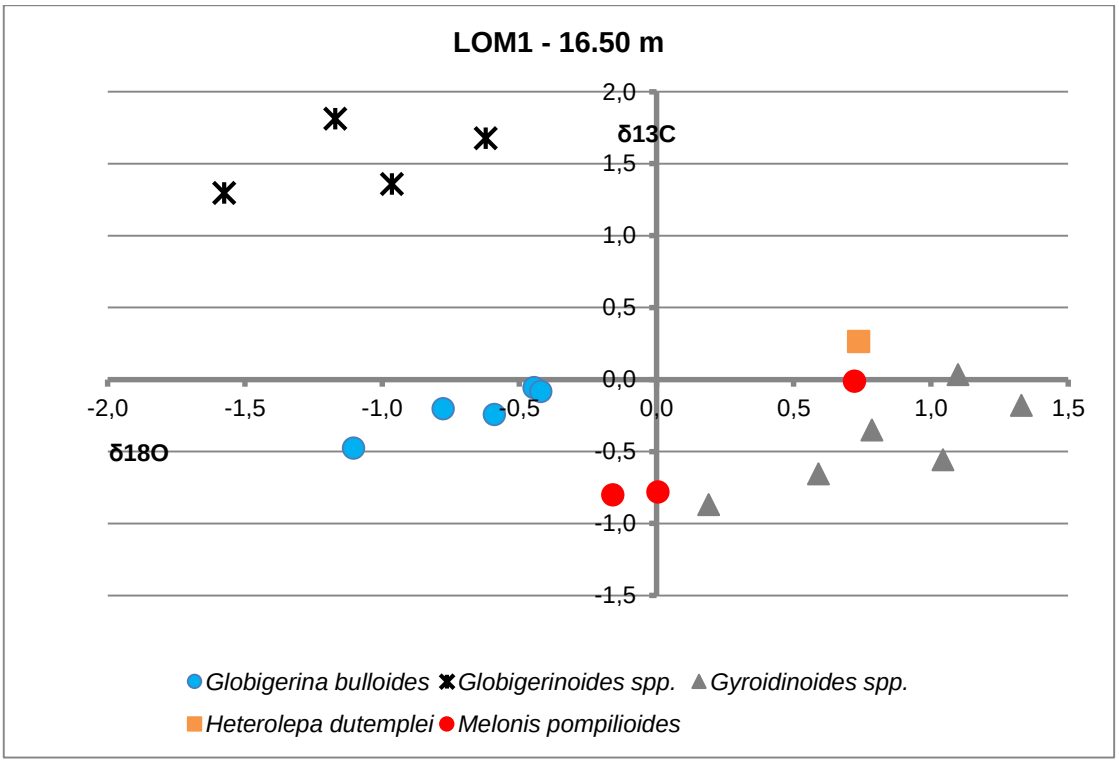

# Appendix 3

## LOM-1: 16.75 m

| Identifier 1 | Identifier 2 | Comment | 1 Cycle Int Samp 44 | δ $^{13}C/^{12}C$ Mean | δ $^{18}O/^{16}O$ Mean | δ $^{13}C$ CORR | δ $^{18}O$ CORR |
|---|---|---|---|---|---|---|---|
| *G. bulloides* | 1675 | LOM-1 | 1436,022 | 0,286 | 0,084 | **0,284** | **0,084** |
| *G. bulloides* | 1675 | LOM-1 | 1503,512 | 0,582 | -1,1 | **0,581** | **-1,100** |
| *G. bulloides* | 1675 | LOM-1 | 1597,418 | 0,302 | -0,566 | **0,301** | **-0,566** |
| *G. bulloides* | 1675 | LOM-1 | 1045,204 | 0,312 | -0,635 | **0,300** | **-0,636** |
| *G. bulloides* | 1675 | LOM-1 | 1111,691 | -0,38 | -0,552 | **-0,389** | **-0,552** |
| *G. bulloides* | 1675 | LOM-1 | 1375,099 | -0,102 | -0,073 | **-0,105** | **-0,073** |
| *G. bulloides* | 1675 | LOM-1 | 1068,834 | 0,154 | -0,791 | **0,143** | **-0,792** |
| *G. bulloides* | 1675 | LOM-1 | 728,144 | 0,422 | -1,735 | **0,371** | **-1,812** |
| *G. bulloides* | 1675 | LOM-1 | 475,78 | 1,052 | -0,227 | **0,890** | **-0,681** |
| *Globigerinoides* spp. | 1675 | LOM-1 | 2508,243 | 1,442 | -1,07 | **1,442** | **-1,070** |
| *Globigerinoides* spp. | 1675 | LOM-1 | 2856,058 | 1,772 | -1,078 | **1,772** | **-1,078** |
| *Globigerinoides* spp. | 1675 | LOM-1 | 2637,704 | 0,891 | -1,78 | **0,891** | **-1,780** |
| *Globigerinoides* spp. | 1675 | LOM-1 | 1495,411 | 0,285 | -0,18 | **0,283** | **-0,180** |
| *Gyroidinoides* spp. | 1675 | LOM-1 | 3161,928 | -0,272 | 1,028 | **-0,272** | **1,028** |
| *Gyroidinoides* spp. | 1675 | LOM-1 | 1743,697 | -0,279 | 0,988 | **-0,279** | **0,988** |
| *Gyroidinoides* spp. | 1675 | LOM-1 | 937,632 | -0,405 | 0,969 | **-0,424** | **0,964** |
| *Gyroidinoides* spp. | 1675 | LOM-1 | 624,63 | -0,43 | 0,68 | **-0,512** | **0,452** |
| *Heterolepa dutemplei* | 1675 | LOM-1 | 1124,325 | 0,773 | 0,967 | **0,765** | **0,967** |
| *Heterolepa dutemplei* | 1675 | LOM-1 | 844,681 | -0,013 | 0,104 | **-0,043** | **0,087** |
| *Heterolepa dutemplei* | 1675 | LOM-1 | 624,41 | -0,531 | 0,06 | **-0,613** | **-0,169** |
| *Melonis pompilioides* | 1675 | LOM-1 | 1811,783 | -0,326 | 0,432 | **-0,326** | **0,432** |
| *Melonis pompilioides* | 1675 | LOM-1 | 1634,552 | 0,184 | 0,208 | **0,183** | **0,208** |
| *Melonis pompilioides* | 1675 | LOM-1 | 1521,868 | -0,361 | 0,357 | **-0,362** | **0,357** |
| *Melonis pompilioides* | 1675 | LOM-1 | 1510,651 | -0,279 | 0,443 | **-0,280** | **0,443** |
| *Melonis pompilioides* | 1675 | LOM-1 | 872,292 | -0,69 | 0,242 | **-0,716** | **0,231** |

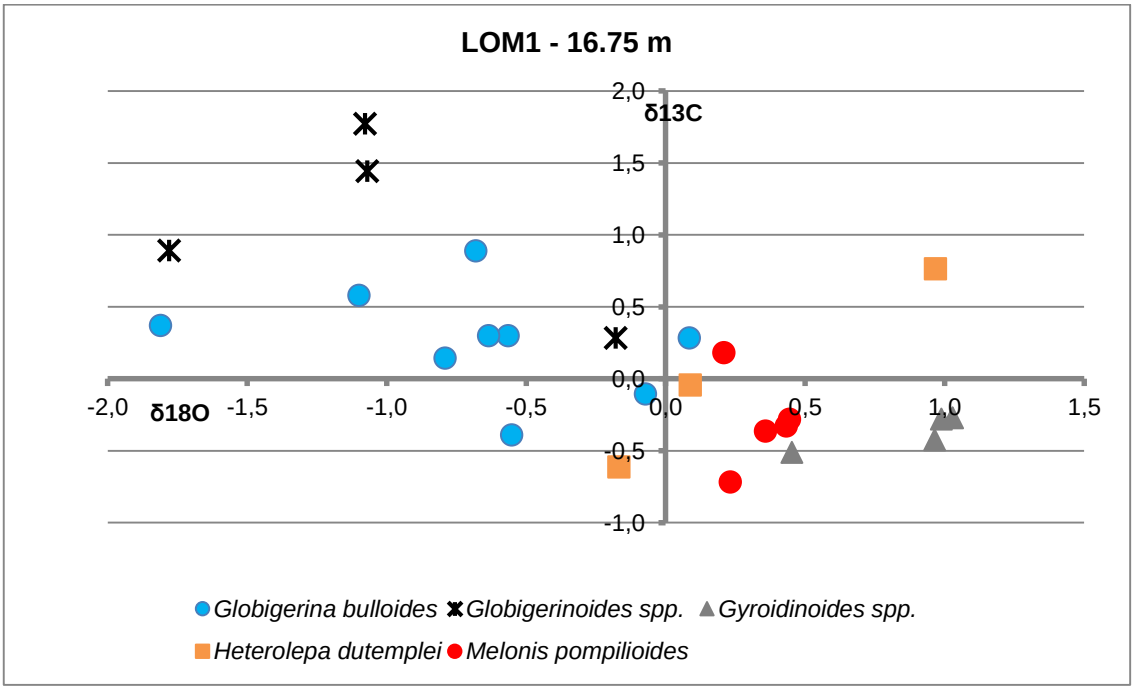

# Appendix 3

## LOM-1: 18.00 m

| Identifier 1 | Identifier 2 | Comment | 1 Cycle Int Samp 44 | δ $^{13}C/^{12}C$ Mean | δ $^{18}O/^{16}O$ Mean | δ $^{13}C$ CORR | δ $^{18}O$ CORR |
|---|---|---|---|---|---|---|---|
| *G. bulloides* | 1800 | LOM-1 | 896,643 | 0,088 | -1,313 | **0,065** | **-1,321** |
| *G. bulloides* | 1800 | LOM-1 | 669,349 | 0,237 | -0,956 | **0,170** | **-1,107** |
| *G. bulloides* | 1800 | LOM-1 | 726,742 | 0,442 | 0,025 | **0,391** | **-0,054** |
| *G. bulloides* | 1800 | LOM-1 | 569,45 | 0,869 | 1,356 | **0,764** | **1,025** |
| *G. bulloides* | 1800 | LOM-1 | 1451,475 | 0,3 | -0,386 | **0,298** | **-0,386** |
| *G. bulloides* | 1800 | LOM-1 | 1262,386 | 0,374 | -0,448 | **0,370** | **-0,448** |
| *G. bulloides* | 1800 | LOM-1 | 443,609 | 0,127 | 0,311 | **-0,061** | **-0,165** |
| *Gyroidinoides* spp. | 1800 | LOM-1 | 488,236 | -4,732 | -11,365 | **-4,885** | **-11,808** |
| *Gyroidinoides* spp. | 1800 | LOM-1 | 667,842 | -0,611 | 1,393 | **-0,678** | **1,240** |
| *Gyroidinoides* spp. | 1800 | LOM-1 | 746,675 | -0,496 | 0,86 | **-0,543** | **0,799** |
| *Gyroidinoides* spp. | 1800 | LOM-1 | 554,203 | -0,754 | 0,642 | **-0,867** | **0,285** |
| *Gyroidinoides* spp. | 1800 | LOM-1 | 1373,345 | -0,16 | 0,823 | **-0,163** | **0,823** |
| *Melonis pompilioides* | 1800 | LOM-1 | 957,464 | -0,409 | 0,591 | **-0,427** | **0,587** |
| *Melonis pompilioides* | 1800 | LOM-1 | 986,002 | -0,593 | 0,005 | **-0,609** | **0,003** |
| *Melonis pompilioides* | 1800 | LOM-1 | 883,544 | -0,127 | 0,873 | **-0,152** | **0,863** |

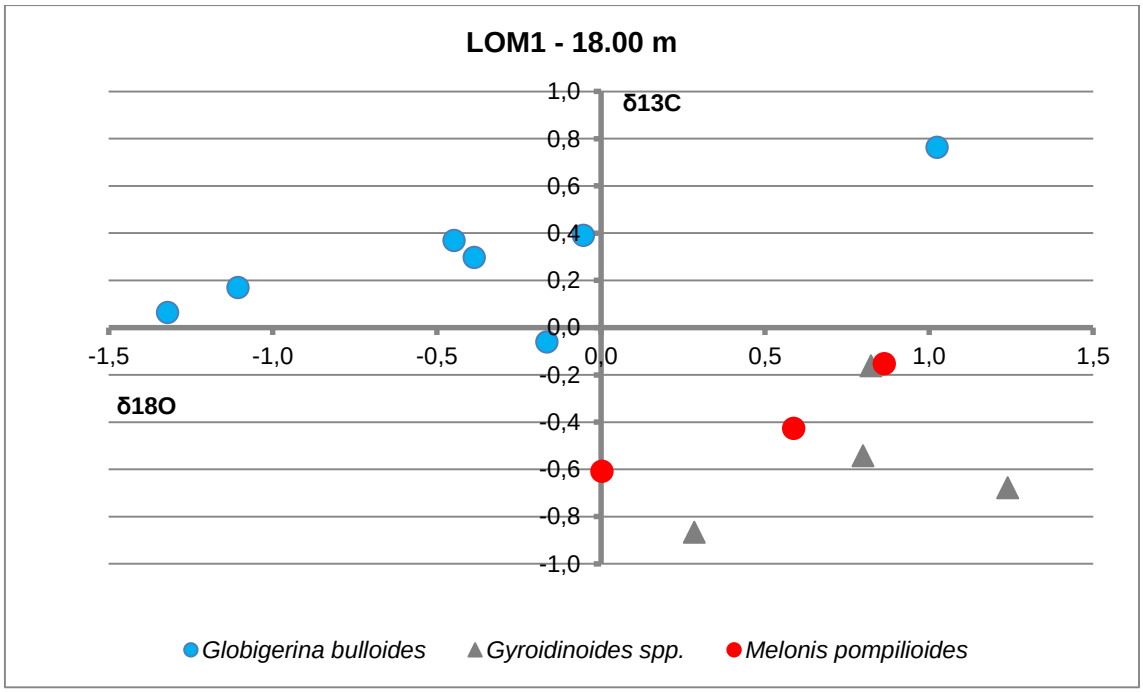

# Appendix 3

## LOM-1: 19.20 m

| Identifier 1 | Identifier 2 | Comment | 1 Cycle Int Samp 44 | δ $^{13}C/^{12}C$ Mean | δ $^{18}O/^{16}O$ Mean | δ $^{13}C$ CORR | δ $^{18}O$ CORR |
|---|---|---|---|---|---|---|---|
| *Cibicidoides* spp. | 1920 | LOM-1 | 2319,626 | 0,578 | 0,728 | **0,578** | **0,728** |
| *Cibicidoides* spp. | 1920 | LOM-1 | 4771,681 | 0,119 | 0,905 | **0,119** | **0,905** |
| *Cibicidoides* spp. | 1920 | LOM-1 | 2647,398 | 0,555 | -0,962 | **0,555** | **-0,962** |
| *Globigerinoides* spp. | 1920 | LOM-1 | 1499,457 | 2,17 | -0,712 | **2,169** | **-0,712** |
| *Globigerinoides* spp. | 1920 | LOM-1 | 2591,259 | 1,722 | -0,465 | **1,722** | **-0,465** |
| *Globigerinoides* spp. | 1920 | LOM-1 | 1163,951 | 2,006 | -0,367 | **1,999** | **-0,367** |
| *Globigerinoides* spp. | 1920 | LOM-1 | 2330,397 | 1,372 | -0,805 | **1,372** | **-0,805** |
| *Globigerinoides* spp. | 1920 | LOM-1 | 1293,431 | 1,244 | -1,244 | **1,240** | **-1,244** |
| *Gyroidinoides* spp. | 1920 | LOM-1 | 2270,958 | -0,22 | 1,096 | **-0,220** | **1,096** |
| *Gyroidinoides* spp. | 1920 | LOM-1 | 1475,534 | 0,103 | 1,146 | **0,101** | **1,146** |
| *Gyroidinoides* spp. | 1920 | LOM-1 | 1203,776 | -0,411 | 0,705 | **-0,417** | **0,705** |
| *Gyroidinoides* spp. | 1920 | LOM-1 | 693,334 | -0,632 | 0,713 | **-0,692** | **0,597** |
| *Gyroidinoides* spp. | 1920 | LOM-1 | 608,846 | -0,54 | 0,948 | **-0,628** | **0,690** |
| *Heterolepa dutemplei* | 1920 | LOM-1 | 1489,623 | 0,346 | 0,755 | **0,344** | **0,755** |
| *Heterolepa dutemplei* | 1920 | LOM-1 | 1611,976 | 0,278 | 0,354 | **0,277** | **0,354** |
| *Heterolepa dutemplei* | 1920 | LOM-1 | 2081,286 | 0,379 | 0,886 | **0,379** | **0,886** |
| *Melonis pompilioides* | 1920 | LOM-1 | 3075,107 | -0,436 | 0,65 | **-0,436** | **0,650** |
| *Melonis pompilioides* | 1920 | LOM-1 | 1244,692 | -0,715 | 0,115 | **-0,720** | **0,115** |
| *Melonis pompilioides* | 1920 | LOM-1 | 1204,837 | -0,482 | 0,54 | **-0,488** | **0,540** |
| *Melonis pompilioides* | 1920 | LOM-1 | 2884,509 | -0,238 | 0,647 | **-0,238** | **0,647** |
| *Uvigerina* spp. | 1920 | LOM-1 | 2200,987 | 0,715 | 0,821 | **0,715** | **0,821** |
| *Uvigerina* spp. | 1920 | LOM-1 | 1228,37 | -0,308 | 1,184 | **-0,313** | **1,184** |
| *Gyroidinoides* spp. | 1920 | LOM-1 | 473,049 | -0,556 | 0,669 | **-0,720** | **0,213** |

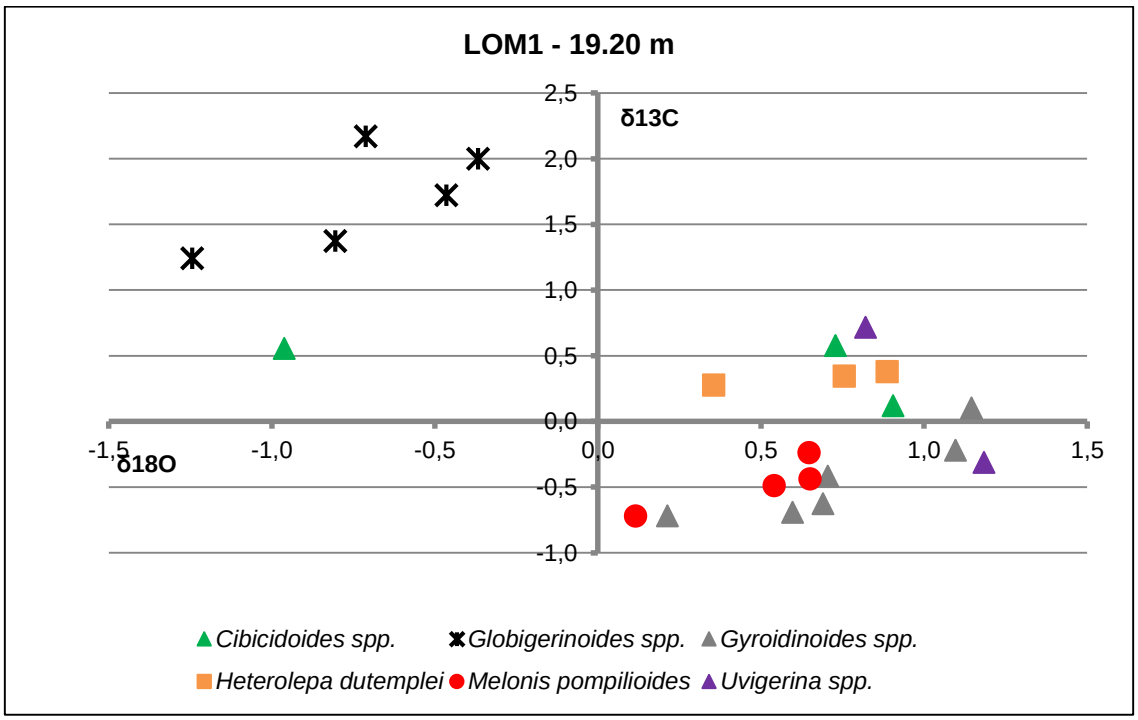

# Appendix 3

## LOM-1: 19.25 m

| Identifier 1 | Identifier 2 | Comm-ent | 1 Cycle Int Samp 44 | δ $^{13}C/^{12}C$ Mean | δ $^{18}O/^{16}O$ Mean | δ $^{13}C$ CORR | δ $^{18}O$ CORR |
|---|---|---|---|---|---|---|---|
| *Cibicidoides* spp. | 1925 | LOM-1 | 890,557 | 1,071 | 1,066 | **1,047** | **1,057** |
| *Cibicidoides* spp. | 1925 | LOM-1 | 1969,555 | 0,39 | 0,535 | **0,390** | **0,535** |
| *G. bulloides* | 1925 | LOM-1 | 1487,305 | 0,724 | 0,467 | **0,722** | **0,467** |
| *G. bulloides* | 1925 | LOM-1 | 1189,888 | 1,087 | -1,309 | **1,081** | **-1,309** |
| *G. bulloides* | 1925 | LOM-1 | 845,36 | 0,703 | 0,235 | **0,673** | **0,218** |
| *G. bulloides* | 1925 | LOM-1 | 1092,025 | 0,906 | -1,397 | **0,896** | **-1,398** |
| *G. bulloides* | 1925 | LOM-1 | 934,277 | 1,034 | 0,724 | **1,014** | **0,719** |
| *G. bulloides* | 1925 | LOM-1 | 624,46 | 0,053 | -0,131 | **-0,029** | **-0,359** |
| *G. bulloides* | 1925 | LOM-1 | 607,503 | 0,425 | -0,528 | **0,336** | **-0,789** |
| *G. bulloides* | 1925 | LOM-1 | 444,399 | 0,304 | 0,645 | **0,117** | **0,169** |
| *Globigerinoides* spp. | 1925 | LOM-1 | 1809,283 | 1,771 | -0,914 | **1,771** | **-0,914** |
| *Globigerinoides* spp. | 1925 | LOM-1 | 1191,55 | 1,376 | -0,985 | **1,370** | **-0,985** |
| *Gyroidinoides* spp. | 1925 | LOM-1 | 2832,976 | -0,075 | 1,012 | **-0,075** | **1,012** |
| *Gyroidinoides* spp. | 1925 | LOM-1 | 673,369 | 0,199 | 1,269 | **0,134** | **1,125** |
| *Gyroidinoides* spp. | 1925 | LOM-1 | 644,197 | 0,331 | 1,46 | **0,256** | **1,268** |
| *Gyroidinoides* spp. | 1925 | LOM-1 | 898,997 | -0,782 | 0,992 | **-0,805** | **0,984** |
| *Gyroidinoides* spp. | 1925 | LOM-1 | 757,775 | -0,18 | 0,791 | **-0,224** | **0,738** |
| *Heterolepa dutemplei* | 1925 | LOM-1 | 2285,787 | 0,36 | 0,685 | **0,360** | **0,685** |
| *Heterolepa dutemplei* | 1925 | LOM-1 | 1193,5 | 0,354 | 0,427 | **0,348** | **0,427** |
| Lobatula spp. | 1925 | LOM-1 | 671,93 | 0,638 | 0,323 | **0,572** | **0,176** |
| *Cibicidoides* spp. | 1925 | LOM-1 | 885,958 | 0,725 | 0,915 | **0,700** | **0,906** |

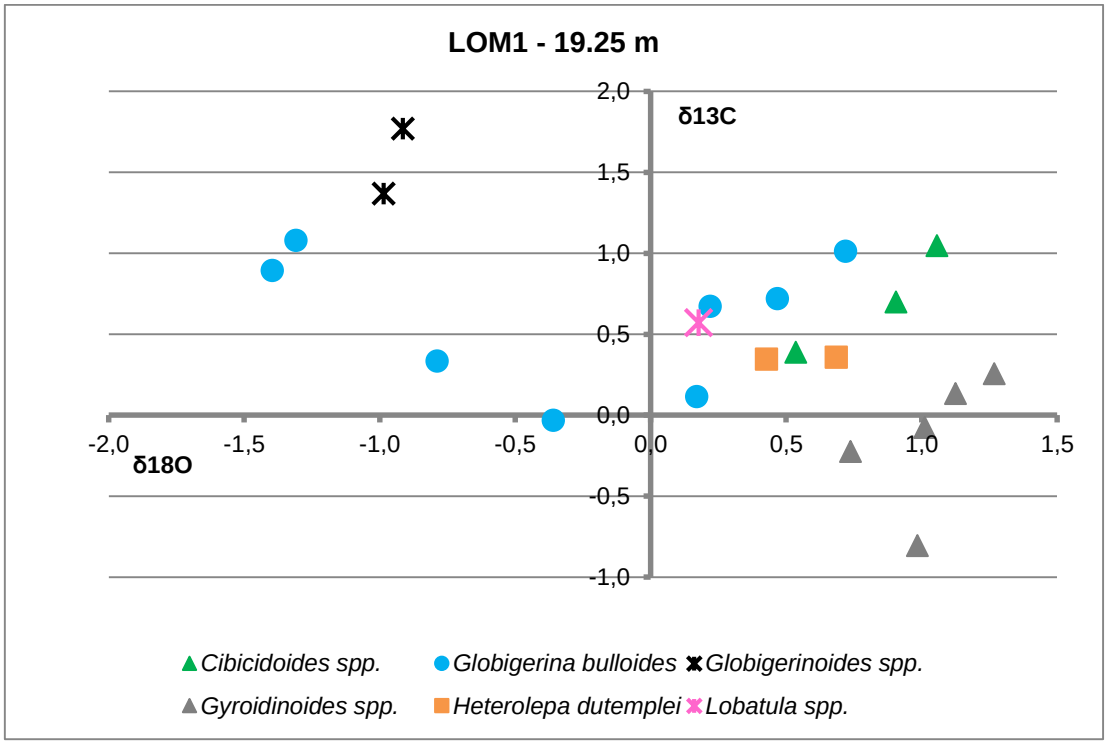

# Appendix 4

The tables show the positioning of various foraminiferal species in particular BFOI calculations (see explanations). A plotted graph for each model is shown below each table. The list of species was composed by Dr. J. Kopecká.

## LOM-1 BFOI Kaiho (1994)

| EXPLANATIONS |
|---|
| Infaunal/Dysoxic |
| Oxyphilic |
| Suboxic |

| LIST OF SPECIES | |
|---|---|
| *Allomorphina trigona* REUSS | *Hoeglundina elegans* (D´ORBIGNY) |
| *Amphicoryna badenensis* (D´ORBIGNY) | *Karreriella chilostoma* (REUSS) |
| *Amphimorphina haueriana* NEUGEBORGEN | *Laevidentalina badenensis* (D´ORBIGNY) |
| *Amphicoryna hispida (*D´ORBIGNY) | *Laevidentalina elegans* (D´ORBIGNY) |
| *Asterigerinata planorbis (*D´ORBIGNY) | *Lagena striata* (D´ORBIGNY) |
| *Bathysiphon* spp. | *Lenticulina americana* (CUSMAN) |
| *Bathysiphon taurinensis* SACCO | *Lenticulina austriaca* (D´ORBIGNY) |
| *Bigenerina aglutinans* D´ORBIGNY | *Lenticulina inornata (*D´ORBIGNY) |
| *Bolivina cf. lowmani* PHLEGER & PARKER | *Lenticulina intermedia* (D´ORBIGNY) |
| *Bolivina dilatata dilatata REUSS* | *Martinottiella communis* (D´ORBIGNY) |
| *Bolivina hebes* MACFADYEN | *Martinottiella karreri* (CUSHMANN) |
| *Bolivina sagittula* DIDKOVSKYI | *Myllostomella advena* (CUSHMAN & LAMING) |
| *Bolivina simplex* PHLEGER & PARKER | *Myllostomella recta* (PALMER & BERMUDEZ) |
| *Bulimina cf. aculeata* (D´ORBIGNY) | *Melonis pompilioides* (FICHTEL & MOLL) |
| *Bulimina elongata* (D´ORBIGNY) | *Neoeponides schreibersi* (D´ORBIGNY) |
| *Bulimina schischkinskayae* SAMOYLOVA | *Neugeborina irregularis* (D´ORBIGNY) |
| *Bulimina* spp. | *Nonion communne* (D´ORBIGNY) |
| *Bulimina subulata* CUSHMAN & PARKER | *Nonionoides karaganicus* (KRASHENINNIKOV) |
| *Bulimina striata* (D´ORBIGNY) | *Oridorsalis umbonatus* (REUSS) |
| *Cibicidoides austracus* (D´ORBIGNY) | *Ortomorphina* spp. |
| *Cibicidoides ornarus* (CICHA & ZAPLETALOVA) | *Pseudosolenia lateralis* (BUCHNER) |
| *Cibicidoides ungerianus* (d´ORBIGNY) | *Pullenia bulloides* (D´ORBIGNY) |
| *Colominella paalzowi* (CUSHMAN) | *Pygmaeoseistron hispidum* REUSS |
| *Cribrorobulina clericii (*FORNASINI) | *Pyramidulina continuicosta* (SCHUBERT) |
| *Cycloforina contorta* (D´ORBIGNY) | *Siphonodosaria consobrina* (D´ORBIGNY) |
| *Dentalina acuta* D´ORBIGNY | *Siphonodosaria scripta* (D´ORBIGNY) |
| *Dentalina beyrichana* NEUGEBORGEN | *Sphaeroidina bulloides* D´ORBIGNY |
| *Dimorphina akneriana (NEUGEBORGEN)* | *Spiroloculina canaliculata* D´ORBIGNY |
| *Elphidium fichtelianum* (D´ORBIGNY) | *Spirorutilus carinatus* (D´ORBIGNY) |
| *Elphidium rugosum* (D´ORBIGNY) | *Stilostomella adolphina* (D´ORBIGNY) |
| *Fontbotia wuellerstorfi* (SCHWAGER) | *Stilostomella cf. consobrina* (D´ORBIGNY) |
| *Fursenkoina acuta* (D´ORBIGNY) | *Textularia gramen* D´ORBIGNY |
| *Gaudryinopsis beregoviensis* (VENGLINSKYI) | *Uvigerina aculeata* D´ORBIGNY |
| *Globobulimina pupoides* (D´ORBIGNY) | *Uvigerina acuminata* HOSIUS |
| *Globulina gibba D´ORBIGNY* | *Uvigerina graciliformis* PAPP &TURNOVSKY |
| *Gyroidinoides octocameratus* (CUSHMAN & HANNA) | *Uvigerina macrocarinata* (PAPP&TURNOVSKY) |
| *Gyroidinoides umbonatus* (SILVESTRI) | *Uvigerina semiornata* D´ORBIGNY |
| *Hansenisca soldanii* (D´ORBIGNY) | *Vaginulinopsis pedum* (D´ORBIGNY) |
| *Hanzawaia boueana* (D´ORBIGNY) | *Valvulineria complanata* (D´ORBIGNY) |
| *Heterolepa dutemplei* (D´ORBIGNY) | |

# Appendix 4

## LOM-1 BFOI Kaiho (1994)

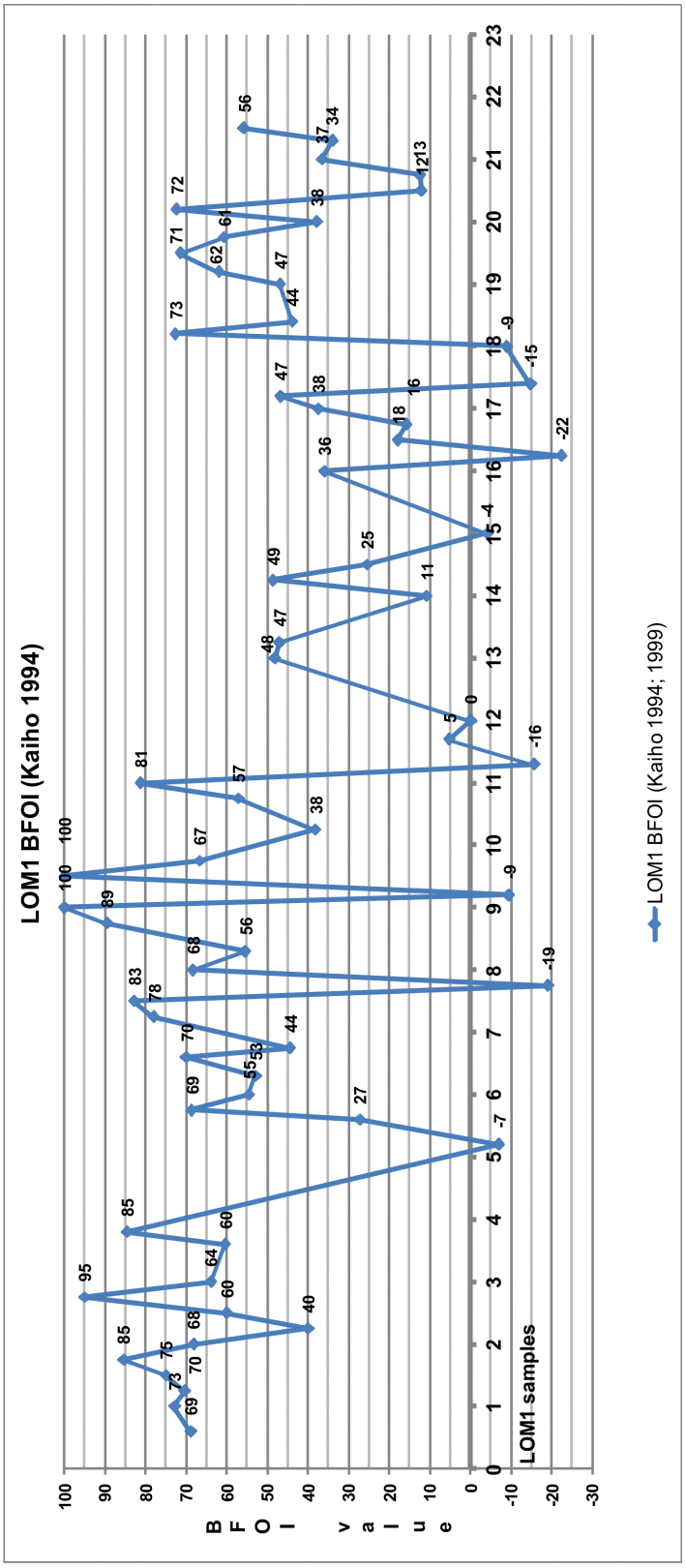


The BFOI Kaiho (1994) graph is shown here.

# Appendix 4

## LOM-1 BFOI Báldi (2006)

| EXPLANATIONS |
|---|
| Infaunal/Dysoxic |
| Oxyphilic |
| Suboxic |

| LIST OF SPECIES | |
|---|---|
| *Allomorphina trigona* REUSS | *Hoeglundina elegans* (D´ORBIGNY) |
| *Amphicoryna badenensis* (D´ORBIGNY) | *Karreriella chilostoma* (REUSS) |
| *Amphimorphina haueriana* NEUGEBORGEN | *Laevidentalina badenensis* (D´ORBIGNY) |
| *Amphicoryna hispida (*D´ORBIGNY) | *Laevidentalina elegans* (D´ORBIGNY) |
| *Asterigerinata planorbis (*D´ORBIGNY) | *Lagena striata* (D´ORBIGNY) |
| *Bathysiphon* spp. | *Lenticulina americana* (CUSMAN) |
| *Bathysiphon taurinensis* SACCO | *Lenticulina austriaca* (D´ORBIGNY) |
| *Bigenerina aglutinans* D´ORBIGNY | *Lenticulina inornata (*D´ORBIGNY) |
| *Bolivina cf. lowmani* PHLEGER & PARKER | *Lenticulina intermedia* (D´ORBIGNY) |
| *Bolivina dilatata dilatata REUSS* | *Martinottiella communis* (D´ORBIGNY) |
| *Bolivina hebes* MACFADYEN | *Martinottiella karreri* (CUSHMANN) |
| *Bolivina sagittula* DIDKOVSKYI | *Myllostomella advena* (CUSHMAN & LAMING) |
| *Bolivina simplex* PHLEGER & PARKER | *Myllostomella recta* (PALMER & BERMUDEZ) |
| *Bulimina cf. aculeata* (D´ORBIGNY) | *Melonis pompilioides* (FICHTEL & MOLL) |
| *Bulimina elongata* (D´ORBIGNY) | *Neoeponides schreibersi* (D´ORBIGNY) |
| *Bulimina schischkinskayae* SAMOYLOVA | *Neugeborina irregularis* (D´ORBIGNY) |
| *Bulimina* spp. | *Nonion communne* (D´ORBIGNY) |
| *Bulimina subulata* CUSHMAN & PARKER | *Nonionoides karaganicus* (KRASHENINNIKOV) |
| *Bulimina striata* (D´ORBIGNY) | *Oridorsalis umbonatus* (REUSS) |
| *Cibicidoides austracus* (D´ORBIGNY) | *Ortomorphina* spp. |
| *Cibicidoides ornarus* (CICHA & ZAPLETALOVA) | *Pseudosolenia lateralis* (BUCHNER) |
| *Cibicidoides ungerianus* (d´ORBIGNY) | *Pullenia bulloides (*D´ORBIGNY) |
| *Colominella paalzowi* (CUSHMAN) | *Pygmaeoseistron hispidum* REUSS |
| *Cribrorobulina clericii (*FORNASINI) | *Pyramidulina continuicosta* (SCHUBERT) |
| *Cycloforina contorta* (D´ORBIGNY) | *Siphonodosaria consobrina* (D´ORBIGNY) |
| *Dentalina acuta* D´ORBIGNY | *Siphonodosaria scripta* (D´ORBIGNY) |
| *Dentalina beyrichana* NEUGEBORGEN | *Sphaeroidina bulloides* D´ORBIGNY |
| *Dimorphina akneriana (NEUGEBORGEN)* | *Spiroloculina canaliculata* D´ORBIGNY |
| *Elphidium fichtelianum* (D´ORBIGNY) | *Spirorutilus carinatus*(D´ORBIGNY) |
| *Elphidium rugosum* (D´ORBIGNY) | *Stilostomella adolphina* (D´ORBIGNY) |
| *Fontbotia wuellerstorfi* (SCHWAGER) | *Stilostomella cf. consobrina* (D´ORBIGNY) |
| *Fursenkoina acuta* (D´ORBIGNY) | *Textularia gramen* D´ORBIGNY |
| *Gaudryinopsis beregoviensis* (VENGLINSKYI) | *Uvigerina aculeata* D´ORBIGNY |
| *Globobulimina pupoides* (D´ORBIGNY) | *Uvigerina acuminata* HOSIUS |
| *Globulina gibba D´ORBIGNY* | *Uvigerina graciliformis* PAPP &TURNOVSKY |
| *Gyroidinoides octocameratus* (CUSHMAN & HANNA) | *Uvigerina macrocarinata* (PAPP&TURNOVSKY) |
| *Gyroidinoides umbonatus* (SILVESTRI) | *Uvigerina semiornata* D´ORBIGNY |
| *Hansenisca soldanii* (D´ORBIGNY) | *Vaginulinopsis pedum* (D´ORBIGNY) |
| *Hanzawaia boueana* (D´ORBIGNY) | *Valvulineria complanata* (D´ORBIGNY) |
| *Heterolepa dutemplei* (D´ORBIGNY) | |

# Appendix 4

## LOM-1 BFOI Báldi (2006)

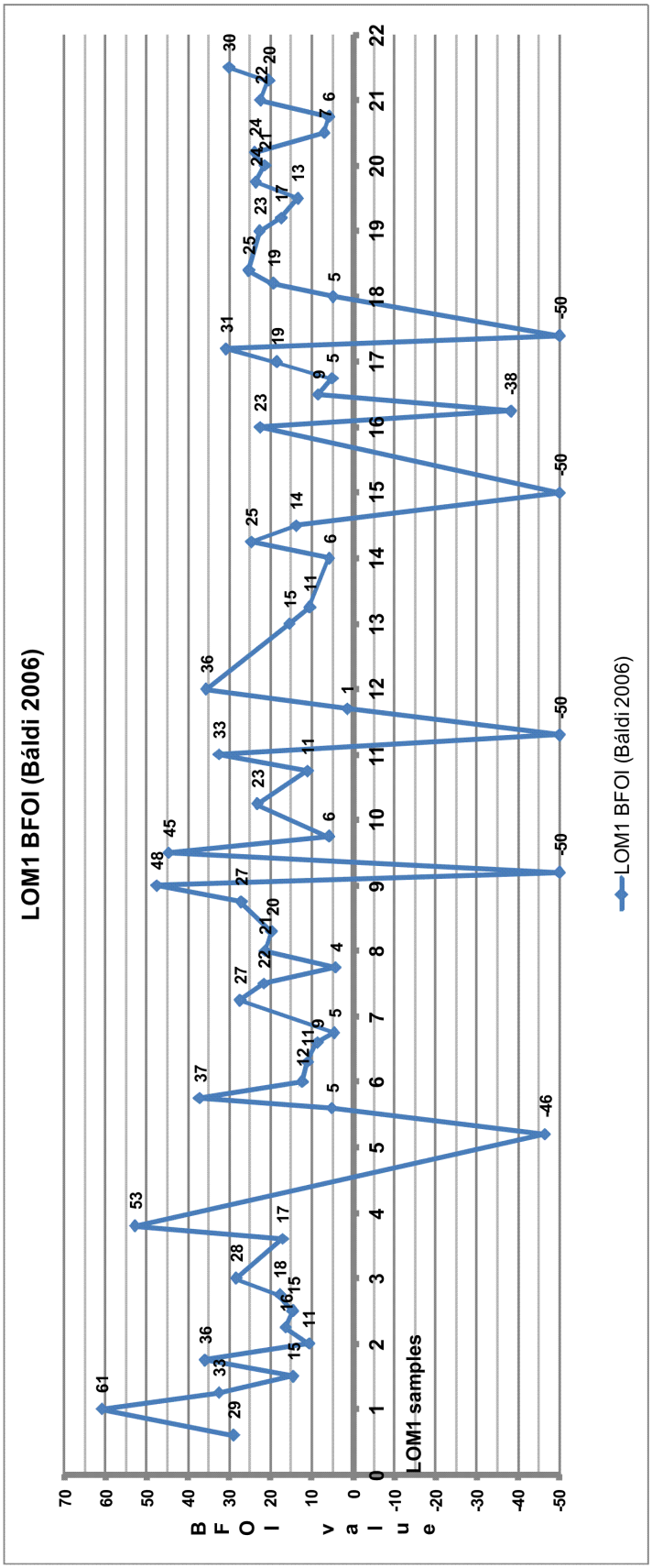


The BFOI Báldi (2006) graph is shown here.

# Appendix 4

## LOM-1 BFOI $PT_1$ (my own proposal)

| EXPLANATIONS |
|---|
| Infaunal/Dysoxic |
| Oxyphilic |
| Suboxic |

| LIST OF SPECIES | |
|---|---|
| *Allomorphina trigona* REUSS | *Hoeglundina elegans* (D´ORBIGNY) |
| *Amphicoryna badenensis* (D´ORBIGNY) | *Karreriella chilostoma* (REUSS) |
| *Amphimorphina haueriana* NEUGEBORGEN | *Laevidentalina badenensis* (D´ORBIGNY) |
| *Amphicoryna hispida (*D´ORBIGNY) | *Laevidentalina elegans* (D´ORBIGNY) |
| *Asterigerinata planorbis (*D´ORBIGNY) | *Lagena striata* (D´ORBIGNY) |
| *Bathysiphon* spp. | *Lenticulina americana* (CUSMAN) |
| *Bathysiphon taurinensis* SACCO | *Lenticulina austriaca* (D´ORBIGNY) |
| *Bigenerina aglutinans* D´ORBIGNY | *Lenticulina inornata (*D´ORBIGNY) |
| *Bolivina cf. lowmani* PHLEGER & PARKER | *Lenticulina intermedia* (D´ORBIGNY) |
| *Bolivina dilatata dilatata REUSS* | *Martinottiella communis* (D´ORBIGNY) |
| *Bolivina hebes* MACFADYEN | *Martinottiella karreri* (CUSHMANN) |
| *Bolivina sagittula* DIDKOVSKYI | *Myllostomella advena* (CUSHMAN & LAMING) |
| *Bolivina simplex* PHLEGER & PARKER | *Myllostomella recta* (PALMER & BERMUDEZ) |
| *Bulimina cf. aculeata* (D´ORBIGNY) | *Melonis pompilioides* (FICHTEL & MOLL) |
| *Bulimina elongata* (D´ORBIGNY) | *Neoeponides schreibersi* (D´ORBIGNY) |
| *Bulimina schischkinskayae* SAMOYLOVA | *Neugeborina irregularis* (D´ORBIGNY) |
| *Bulimina* spp. | *Nonion communne* (D´ORBIGNY) |
| *Bulimina subulata* CUSHMAN & PARKER | *Nonionoides karaganicus*(KRASHENINNIKOV) |
| *Bulimina striata* (D´ORBIGNY) | *Oridorsalis umbonatus* (REUSS) |
| *Cibicidoides austracus* (D´ORBIGNY) | *Ortomorphina* spp. |
| *Cibicidoides ornarus* (CICHA & ZAPLETALOVA) | *Pseudosolenia lateralis* (BUCHNER) |
| *Cibicidoides ungerianus* (d´ORBIGNY) | *Pullenia bulloides (*D´ORBIGNY) |
| *Colominella paalzowi* (CUSHMAN) | *Pygmaeoseistron hispidum* REUSS |
| *Cribrorobulina clericii (*FORNASINI) | *Pyramidulina continuicosta* (SCHUBERT) |
| *Cycloforina contorta* (D´ORBIGNY) | *Siphonodosaria consobrina* (D´ORBIGNY) |
| *Dentalina acuta* D´ORBIGNY | *Siphonodosaria scripta* (D´ORBIGNY) |
| *Dentalina beyrichana* NEUGEBORGEN | *Sphaeroidina bulloides* D´ORBIGNY |
| *Dimorphina akneriana (NEUGEBORGEN)* | *Spiroloculina canaliculata* D´ORBIGNY |
| *Elphidium fichtelianum* (D´ORBIGNY) | *Spirorutilus carinatus* (D´ORBIGNY) |
| *Elphidium rugosum* (D´ORBIGNY) | *Stilostomella adolphina* (D´ORBIGNY) |
| *Fontbotia wuellerstorfi* (SCHWAGER) | *Stilostomella cf. consobrina* (D´ORBIGNY) |
| *Fursenkoina acuta* (D´ORBIGNY) | *Textularia gramen*D´ORBIGNY |
| *Gaudryinopsis beregoviensis*(VENGLINSKYI) | *Uvigerina aculeata* D´ORBIGNY |
| *Globobulimina pupoides* (D´ORBIGNY) | *Uvigerina acuminata* HOSIUS |
| *Globulina gibba D´ORBIGNY* | *Uvigerina graciliformis* PAPP &TURNOVSKY |
| *Gyroidinoides octocameratus* (CUSHMAN & HANNA) | *Uvigerina macrocarinata* (PAPP&TURNOVSKY) |
| *Gyroidinoides umbonatus* (SILVESTRI) | *Uvigerina semiornata* D´ORBIGNY |
| *Hansenisca soldanii* (D´ORBIGNY) | *Vaginulinopsis pedum* (D´ORBIGNY) |
| *Hanzawaia boueana* (D´ORBIGNY) | *Valvulineria complanata* (D´ORBIGNY) |
| *Heterolepa dutemplei* (D´ORBIGNY) | |

# Appendix 4

## LOM-1 BFOI $PT_1$ (my own proposal)

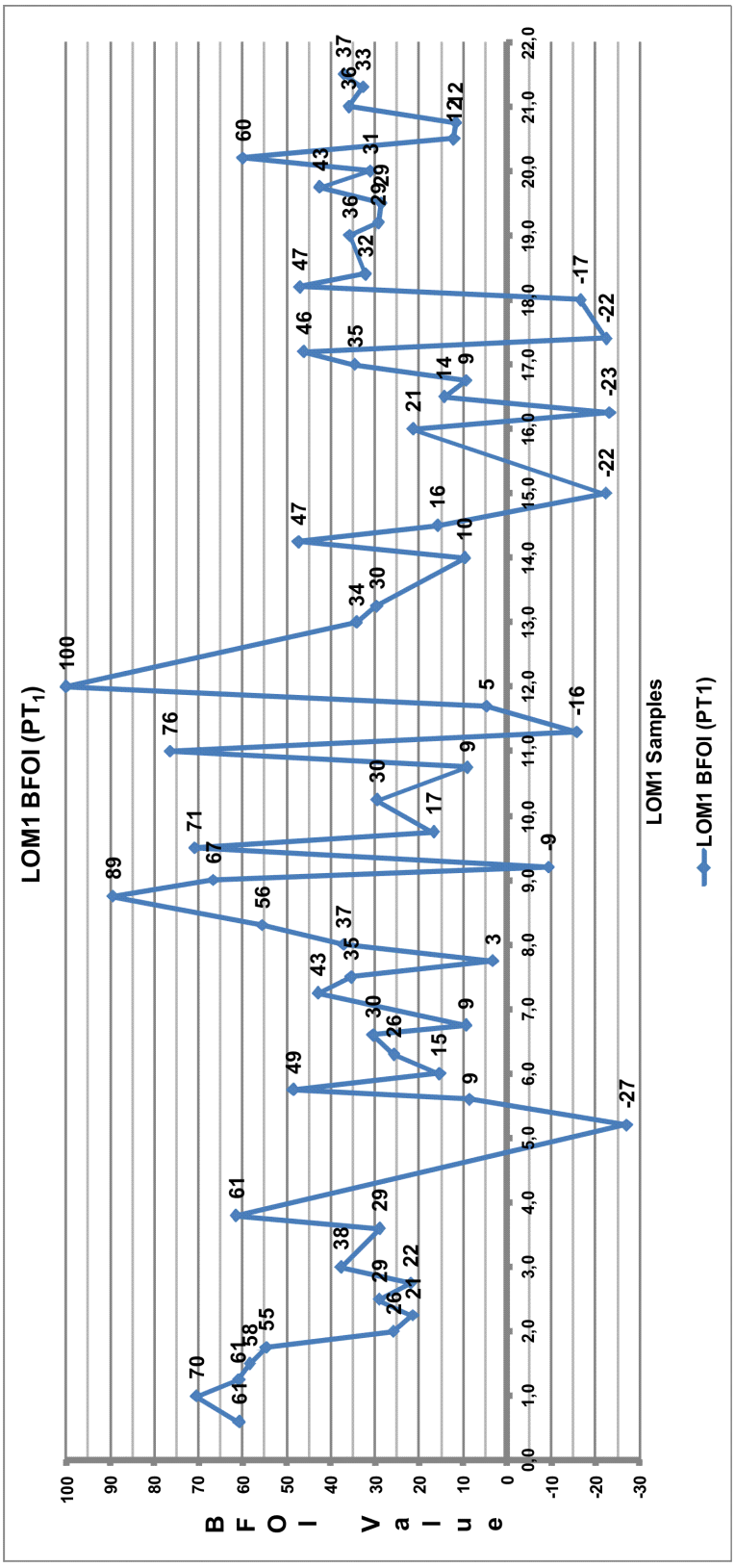


The BFOI $PT_1$ graph is shown here.

# Appendix 5

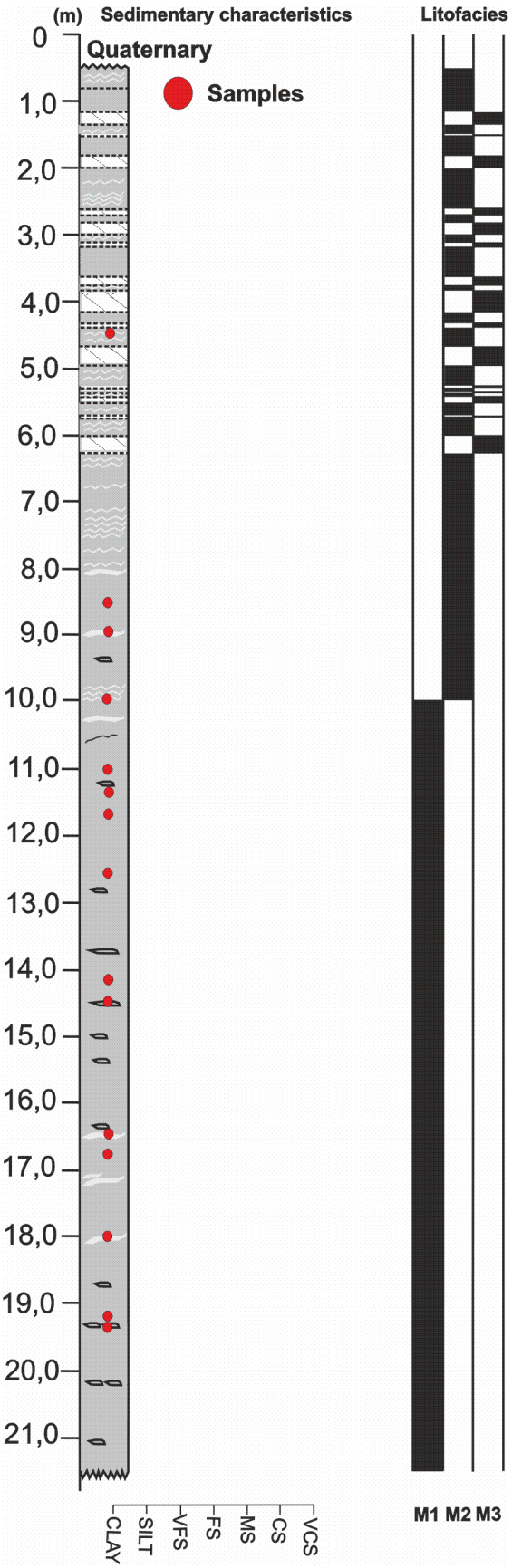


The sedimentary and litofacial profile of the LOM-1 borehole composed by Dr. S. Nehyba is shown here. The red dots represent the positions of the samples used for the stable isotopic analysis.